Morpho-anatomie crânienne chez les rongeurs murinés : aspects fonctionnels, génétiques et écologiques

Samuel Ginot

THÈSE POUR OBTENIR LE GRADE DE DOCTEUR DE L'UNIVERSITÉ DE MONTPELLIER

En Biologie de l'Évolution

École doctorale GAIA

Unité de recherche : Institut des Sciences de l'Évolution de Montpellier

Morpho-anatomie crânienne chez les rongeurs murinés : aspects fonctionnels, génétiques et écologiques.

Présentée par Samuel GINOT
Le 30 Novembre 2017

Sous la direction de Julien CLAUDE

Rapporteurs

Christiane DENYS, Professeur, Muséum National d'Histoire Naturelle, Paris
Leandro MONTEIRO, Associate Professor, Universidade Estadual do Norte Fluminense, Rio de Janeiro

Devant le jury composé de

Julien CLAUDE, Maître de Conférences, Institut des Sciences de l'Évolution de Montpellier	**Directeur de thèse**
Anthony HERREL, Directeur de Recherche, Muséum National d'Histoire Naturelle, Paris	**Examinateur**
Alexandra HOUSSAYE, Chargé de Recherche, Muséum National d'Histoire Naturelle, Paris	**Examinateur**
Leandro MONTEIRO, Associate Professor, Universidade Estadual do Norte Fluminense, Rio de Janeiro	**Rapporteur**
Sabrina RENAUD, Directeur de Recherche, Laboratoire de Biométrie et Biologie Évolutive, Lyon	**Examinateur et Président du jury**

UNIVERSITÉ DE MONTPELLIER

SOMMAIRE

INTRODUCTION

La variation phénotypique, notamment morphologique, a été à l'origine de l'étude de l'évolution des organismes, et reste aujourd'hui au centre des préoccupations de la biologie évolutive (e.g. Darwin 1859, Simpson 1939, Gould 1966, Schluter 2000). Depuis l'apparition des notions de sélection et d'adaptation des organismes à leur environnement, l'étude des liens entre les traits phénotypiques et les fonctions qu'ils exercent (i.e. morphologie fonctionnelle et biomécanique ; Arnold 1983, Kingslover et Huey 2003), s'est superposée à l'étude de la variation phénotypique en regard de la sélection naturelle. Le concept de performance est ainsi apparu afin de quantifier la variation d'une fonction biologique par rapport à la variation d'un ou plusieurs traits lui étant liés (par exemple, longueur des jambes et vitesse de course). La performance a des conséquences sur les interactions d'un individu avec son environnement (son habitat, ses prédateurs, ses proies et ses conspécifiques), et sur ses capacités de survie et de reproduction, donc sa valeur sélective. Arnold (1983) a proposé une approche (Fig. 1) pour intégrer la morphologie fonctionnelle et la biomécanique dans le cadre plus large de l'étude de l'évolution des organismes par sélection naturelle. Il a ainsi formalisé la relation qui existe entre les traits (notamment morphologiques) et la performance, et entre cette dernière et la valeur sélective des individus (*fitness*). Ce modèle considère que les traits (et leurs interconnexions) influencent la performance et que cette performance influence à son tour la valeur sélective, puisqu'elle intervient directement dans la capacité d'un organisme à survivre.

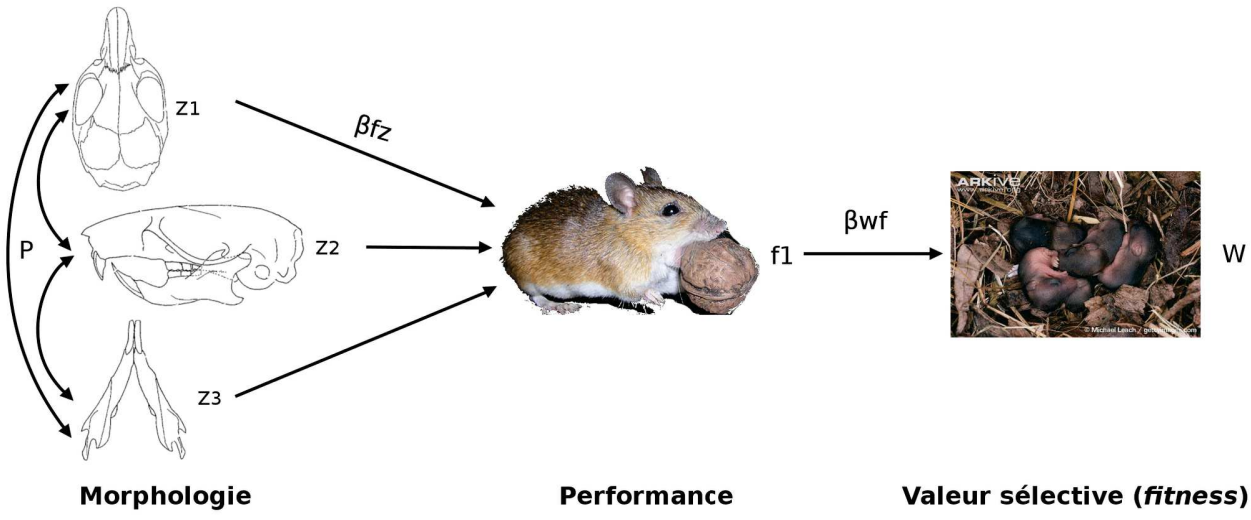

Figure 1. Diagramme des chemins illustrant le cadre théorique "Morphologie-Performance-*Fitness*" proposé par Arnold (1983), avec un exemple lié à cette thèse chez une espèce de muriné. Z : traits morphologiques ; P : interactions entre les traits morphologiques intégrés ; β_{fz} : gradient de performance ; β_{wf} : gradient de valeur sélective. Modifié d'après Arnold (1983) et Satoh (1997). Images : Wikimedia et Michael Leach.

Si ce modèle fait aujourd'hui consensus, il s'est aussi complexifié suite à de nombreuses études en laboratoire et en milieux naturels (Kingslover et Huey 2003). Il est notamment apparu que la performance ne dépend pas uniquement des traits intrinsèques d'un individu (morphologie, comportement, sexe, génétique), mais aussi de variables externes, environnementales par exemple. De plus, bien que la sélection s'exerce au niveau de l'organisme complet à travers l'ensemble de ses performances, les modalités de l'évolution de ces dernières sont encore mal comprises (Irschick 2008). Les études des gradients de sélections s'appliquant sur la performance, ainsi que les approches de génétique quantitative permettent de mieux cerner ces modalités. En effet, si le lien entre morphologie, performance et *fitness* est aujourd'hui établi chez de nombreuses espèces et dans diverses conditions, les études d'héritabilité et d'évolvabilité couplant traits morphologiques et performance restent rares. Bien que la proposition d'Arnold (1983) ne contienne pas cet axe de recherche, son inclusion est l'une des voies proposée (Irschick 2008) pour permettre la prédiction des effets de la sélection sur l'évolution et l'adaptation des organismes, via le lien entre morphologie et fonction. Si le modèle d'Arnold a permis la jonction entre vision mécanistique et adaptationiste, l'ajout de facteurs génétiques et environnementaux à ce cadre constitue l'une des clés pour comprendre l'influence de la morphologie fonctionnelle sur l'évolution adaptative et l'écologie des populations et des espèces de manière fonctionnelle.

Le crâne des vertébrés est l'une des structures concentrant le plus de fonctions, tout en étant contraint en termes développementaux (Gans et Northcutt 1983, Emerson et Bramble 1993, Hanken et Thorogood 1993). Les fonctions du crâne incluent par exemple le support des structures sensorielles (e.g., yeux, oreilles, narines, bouche et vibrisses), les vocalisations, la récolte de nourriture et la mastication, ainsi que l'attaque ou la défense contre les prédateurs, proies ou concurrents conspécifiques. Les changements de l'anatomie crânienne sont donc un reflet des phénomènes de diversification et d'adaptation chez les vertébrés (Hanken et Thorogood 1993). Par conséquent, le crâne est un sujet de choix pour les études de biomécanique, de morphologie fonctionnelle et des contraintes développementales, en raison de ses nombreuses fonctions (Emerson et Bramble 1993). Le rôle fonctionnel et la mécanique de la musculature masticatrice en est un des aspects les plus importants car elle joue un rôle primordial dans la survie d'un animal en assurant sa capacité à se nourrir (capture, incision, et mastication des aliments ; Brandt 1855, Wood 1965, Turnbull 1970, Druzinsky et al. 2011). Son anatomie est donc liée au régime alimentaire et à l'écologie des organismes. La musculature

masticatrice doit notamment produire une force de morsure suffisante pour réduire les aliments en morceaux et permettre leur ingestion.

Les rongeurs forment un groupe particulier et spécialisé au niveau de la morphologie de leur crâne, de leur dentition et de leur musculature masticatrice (Wood 1965, Turnbull 1970, Druzinsky et al. 2011). Leur capacité à se nourrir d'aliments durs ou coriaces et à ronger toutes sortes de matériaux est à l'origine du nom et de la réputation du groupe. Parmi les rongeurs, la variation morpho-anatomique du crâne est généralement mise en relation avec des formes de spécialisations, notamment dans les capacités d'incision *versus* mastication (Cox et Jeffery 2011).

L'étude de la morphologie et de l'anatomie crânienne chez les muridés, en lien avec leur performance de morsure, est ici appréhendée dans le cadre "Morphologie-Performance-*Fitness*" proposé par Arnold (1983). La famille des muridés permet en outre l'utilisation d'animaux de laboratoire afin de combiner ce cadre à des approches de génétique quantitative. Cette famille présente une grande diversité d'espèces aux écologies variées qui permet de s'intéresser aux problématiques de sélection et d'adaptation locale des organismes.

Objectifs de la thèse

Les effets de la morphologie sur la performance ont été démontrés chez de nombreux groupes et dans des contextes variés. Chez les rongeurs, la littérature mettant en lien la performance *in vivo* et la morphologie reste toutefois peu développée, au niveau inter- comme intra-spécifique (voir cependant les études de Nies et Ro 2004, Freeman et Lemen 2008a,b, Van Daele et al. 2008, Becerra et al. 2011, Cox et al. 2012). De même, les études concernant l'influence des gènes sur la morphologie existent (Gendron-Maguire et al. 1993, Matsuo et al. 1995, Klingenberg et Leamy 2001, Klingenberg et al. 2001), bien qu'elles restent rares chez les rongeurs sauvages, mais la génétique de la performance masticatrice n'a jamais été étudiée chez ce groupe (Irschick et al. 2008). Il en va de même pour la variation de la performance due à d'autres facteurs tels que l'environnement, le développement, le stress ou les hormones. En résumé, cette thèse a pour objectif majeur de décrire la variation (inter et intra-espèce) morpho-anatomique du crâne chez les murinés (Rodentia:Muridae), et de relier celle-ci à la variation de performance de morsure, tout en prenant en compte de nombreux autres facteurs biologiques pouvant en principe influencer la morphologie, la performance, et leur relation.

Plan de la thèse

Cette thèse débute donc par une description et une comparaison de la variation morpho-anatomique interspécifique parmi un échantillon d'espèces sauvages de murinés, qui reste aujourd'hui peu connue. Par la suite, elle se concentrera sur les conséquences fonctionnelles de cette variation, et leur lien avec l'écologie de ces espèces.

Dans le contexte plus large des muridés, le lien entre forme et fonction du crâne est relativement bien connu au niveau osseux mais peu étudié du point de vue de la musculature, et les données de force de morsures *in vivo* sont rares. Une étude de la variation morpho-fonctionnelle intraspécifique permettra notamment de cibler les variables morphologiques, anatomiques ou développementales qui expliquent le mieux la force de morsure individuelle. Si la performance (telle que la force de morsure) fait le lien entre l'environnement d'un individu et sa valeur sélective, les parties de l'anatomie crânienne qui sont le plus liées à la force de morsure doivent être une source importante d'adaptation, notamment aux variations de régime alimentaire. Il est également possible que d'autres facteurs intrinsèques aux individus tels que le sexe ou la variation génétique puissent influencer la performance. Malgré leur

importance potentielle, ces effets sont rarement étudiés.

La seconde partie cherche donc à mieux comprendre le rôle de ces facteurs, leur relation avec la performance, ainsi qu'avec la morphologie. Pour accéder à ces relations, il est possible d'utiliser des populations en laboratoire, chez lesquelles les génotypes ou les pedigrees sont connus et les conditions environnementales contrôlées. À ce niveau, l'influence du déterminisme sexuel, associé à des différences comportementales, sur la force de morsure sera étudiée. Puis ce travail se focalisera sur le lien entre la diversité génétique (consanguinité), la force de morsure et la morphologie, ainsi que sur l'héritabilité de la performance et des paramètres anatomiques qui la régissent.

Enfin, la troisième partie de la thèse est consacrée aux liens entre performance, morphologie et niche écologique dans le cadre de populations sauvages où des espèces peuvent interagir. Cette partie étudiera d'abord le rôle de la compétition pour la nourriture et du partage de niche chez deux murinés du Sud de la France en se basant sur leur force de morsure. Puis le dernier article de la thèse s'intéressera, à plus large échelle, aux effets du commensalisme et du degré de spécialisation sur la variation morphologique et fonctionnelle dans des communautés de murinés d'Asie du Sud-Est. Ce dernier volet a pour objectif de mieux comprendre comment, d'un point de vue macroévolutif, des populations peuvent diverger, ou converger, dans leur morphologie et dans leur performance, en fonction de la niche écologique qu'elles occupent.

Cette thèse se compose donc d'un large spectre d'approches sur l'anatomie crânienne et ses fonctions, leur évolution et leur rôle écologique. Elle commence par l'étude détaillée de la variation anatomique, et de son lien avec la fonction, puis tente d'élucider l'influence potentielle de la variation génétique sur la morphologie et la fonction. Ceci permet de faire le lien entre les différences écologiques et ces sources de variabilité de manière à mieux appréhender les relations entre niche et variation morpho-fonctionnelle.

Cadre systématique de la thèse

Les rongeurs constituent le plus grand ordre de mammifères actuel avec plus de 2000 espèces (Carleton and Musser 2005). Ils ont aujourd'hui une répartition mondiale (Fig. 2), et ont colonisé tous les continents (excepté l'Antarctique), mais aussi certaines des îles les plus isolées (Macquarie, Georgie du Sud, île de Pâques). Cette extraordinaire aire de répartition s'explique à la fois par des migrations, mais aussi par la relation qu'entretiennent certaines espèces de rongeurs avec l'homme. Parmi ces dernières, les plus connues font partie de la sous-famille des murinés, et incluent le rat noir (*Rattus rattus*), le rat brun (*Rattus norvegicus*) et la souris domestique (*Mus musculus*). Cependant, la majorité des rongeurs ne sont pas commensaux de l'homme, et ont souvent des aires de répartition bien plus réduites. Qu'ils soient commensaux ou non, les rongeurs subissent ou profitent de l'impact environnemental de l'homme. Leur présence dans la plupart des écosystèmes terrestres, leur grande capacité d'adaptation et leur polyvalence en terme d'alimentation font des murinés un groupe très approprié pour mieux comprendre les changements évolutifs, adaptatifs et écologiques dans des environnements variables et sur des échelles de temps courtes.

Au sein des rongeurs, les muridés constituent la famille la plus diversifiée avec plus de 700 espèces (Fig. 2, Carleton and Musser 2005). Les Cricetidae forment la famille la plus proche, à la fois phylogénétiquement et en nombre d'espèces (681). Ces deux groupes sont rassemblés, avec d'autres familles, dans le clade des Myodonta (Fabre et al. 2012, Steppan et Schenk 2017). Ce clade est aujourd'hui rapproché par les données moléculaires des Castorimorpha (Geomyidae, Heteromyidae et Castoridae) et des Anomaluromorpha (Anomaluridae et Pedetidae), avec lesquels il constitue un groupe monophylétique apparenté à la souris (*mouse related clade* en anglais ; Fabre et al. 2012, 2015).

Les relations phylogénétiques au sein des Myodonta sont actuellement bien résolues et consensuelles. Les gerboises (Dipodoidea) forment le groupe frère des Muroidea, qui contiennent six familles dont les Platacanthomyidae, les Nesomyidae, les Calomyscidae, les Cricetidae (hamsters, lemmings, campagnols, rats et souris du Nouveau Monde), les Spalacidae (rats taupes Eurasiatiques) et les Muridae (Fabre et al. 2012, Steppan et Schenk 2017).

Les espèces étudiées dans cette thèse appartiennent à la famille des muridés, et plus particulièrement sur la sous-famille des murinés. Ce groupe monophylétique contient aujourd'hui plus de 600 espèces (Carleton and Musser 2005), réparties dans toute l'Eurasie, l'Afrique, l'Océanie et

l'Australie. De plus, certaines espèces ayant adopté des modes de vie commensaux sont parvenus jusqu'aux Amériques en profitant des déplacements humains récents (e.g. Jones et al. 2012). La sous-famille des murinés est, à elle seule, plus diversifiée que n'importe quel ordre de mammifères, à l'exception des chauves-souris.

L'origine géographique des murinés se situe probablement en Asie du Sud. Elle est soutenue à la fois par les données moléculaires (Steppan et al. 2005, Rowe et al. 2008, Schenk et al. 2013, Fabre et al. 2013), et par les plus vieux fossiles connus (Jacobs and Downs 1994, Patnaik 2000, Sehgal et Patnaik 2012, Patnaik 2013, Kimura et al. 2015). Le registre fossile des murinés commence dans la région du Siwalik (Himalaya). Le premier genre de muriné fossile attesté est *Antemus*, vieux d'environ 14-16 Ma (Jacobs and Downs 1994, Wessels 2009, Patnaik 2014), puis apparaît le genre *Progonomys* (à partir de -12Ma, Jacobs and Downs 1994), qui est considéré comme le groupe frère du genre *Mus*, dont la première apparition dans le registre fossile date de 7.3Ma (Jacobs and Flynn 2005). Le genre *Progonomys* est certainement le premier à avoir migré hors d'Asie, puisqu'on le trouve en Afrique (Ameur 1984, Jacobs and Downs 1994) et en Europe (Van De Weerd 1976, Aguilar 1982). Le genre *Karnimata* se distingue de *Progonomys* vers 11 Ma. Cette séparation de lignées a souvent été considérée comme l'origine des genres *Rattus* et *Mus* respectivement. Cependant cette interprétation est aujourd'hui discutée sur la base de la morphologie et des données moléculaires (Patnaik 2014, Kimura et al. 2015, Fabre et al. 2015). Notamment, la correspondance de *Karnimata* avec un ancêtre de la lignée des *Rattus* est très incertaine (Schenk et al. 2013, Patnaik 2014, Kimura et al. 2015, Fabre et al. 2015). Cette discussion est importante puisque la séparation des lignées de *Mus* et de *Rattus* est très fréquemment utilisée pour calibrer les phylogénies moléculaires. Certains auteurs suggèrent que ces genres fossiles correspondent à un nœud plus tardif (Kimura et al. 2015), tandis que d'autres placent cette séparation plus précocement dans la phylogénie (Fabre et al. 2013, Patnaik 2014).

Quoi qu'il en soit, le registre fossile des murinés semble toujours largement lacunaire. En effet, les données moléculaires (Fabre et al. 2013, Schenk et al. 2013, Kimura et al. 2015) montrent que le clade de murinés le plus basal est celui des genres endémiques philippins *Phloeomys*, *Carpomys*, *Crateromys*, *Musseromys* et *Batomys* (qui composent la "division *Phloeomys*", ou tribu des Phloeomyini). La séparation de ce clade est généralement estimée à plus de 12Ma, mais pourrait être bien antérieure (-15Ma selon Jansa et al. 2006, -14Ma selon Kimura et al. 2015). Cependant, le registre fossile des Phloeomyini est quasi inexistant et se limite à la fin du Pléistocène, entre -50 000 et -68 000 ans (Heaney et al. 2011). Ainsi, si l'on considère les murinés fossiles des dépôts des Siwaliks comme

les plus proches parents fossiles des lignées *Mus* et *Rattus* (ou d'une séparation plus récente ; Fabre et al. 2015, Kimura et al. 2015), il apparaît qu'une grande partie du registre fossile des murinés reste méconnue.

La tribu des Rattini est la suivante à diverger (après celle des Phloeomyini). Elle contient 35 genres pour 167 espèces (Pagès et al. 2010), dont plusieurs étaient auparavant rapprochées dans le groupe *Rattus sensu lato* (Verneau et al. 1998, Pagès et al. 2010). Le groupe-frère de tous les autres Rattini est le genre Eurasiatique *Micromys* (Schenk et al. 2013, Fabre et al. 2013). Les genres du groupe *Rattus sensu lato* (*Maxomys*, *Niviventer*, *Leopoldamys*, *Sundamys*, *Berylmys*, *Bandicota* et *Rattus*) sont tous originaires d'Asie du Sud-Est et se repartissent actuellement en Asie du Sud-Est et sur le plateau du Sahul (Australie et Nouvelle-Guinée ; Fabre et al. 2012). Le registre fossile de ces rats est connu en Thaïlande et au Sud de la Chine à partir d'environ 2 à 3Ma avec notamment *Maxomys*, *Leopoldamys* et *Rattus* (Chaimanee and Jaeger 2001). L'ancienneté réelle du registre est toutefois limitée par le manque d'études détaillées des sites antérieurs à 3Ma. Les données moléculaires semblent suggérer une origine plus ancienne autour de 8Ma (Ruedas and Kirsch 1997, Fabre et al. 2013, Kimura et al. 2015) et donc une lacune dans le registre fossile. Malgré cela, la diversité fossile retrouvée en Thaïlande et en Chine entre 2 et 3Ma reste en accord avec les données moléculaires qui montrent une diversification de ces rats commençant avec la séparation du genre *Maxomys* autour de -7Ma, puis plus tardivement des autres genres durant le Pliocène (Ruedas and Kirsche 1997, Fabre et al. 2013). Cette diversification ne se limite pas à l'Asie du Sud-Est continentale, puisque de nombreuses colonisations des îles Indo-Pacifiques (au moins six ; Fabre et al. 2013) se sont produites au cours du Pliocène et du Pléistocène, donnant naissance à de nombreuses espèces et genres endémiques de rats. La grande diversité de rats sud-est asiatiques a fait l'objet d'études de phylogénie moléculaire (e.g. Singleton et al. 2003, Pagès et al. 2010, Aplin et al. 2011, Fabre et al. 2013). Mieux connaître l'évolution de ces rongeurs, dans une région qui s'anthropise rapidement, est important car ils constituent des réservoirs pour les parasites et maladies émergentes (Singleton et al. 2003).

La tribu des Hydromyini, phylogénétiquement plus proche des autres murinés que des Rattini (Fabre et al. 2013, Schenk et al. 2013), est elle aussi originaire d'Asie du Sud-Est. Ce groupe s'est diversifié dans les Philippines et en Australie / Papouasie-Nouvelle-Guinée. Il a la particularité d'avoir produit plusieurs lignées de rongeurs aux régimes alimentaires spécialisés, se nourrissant notamment de

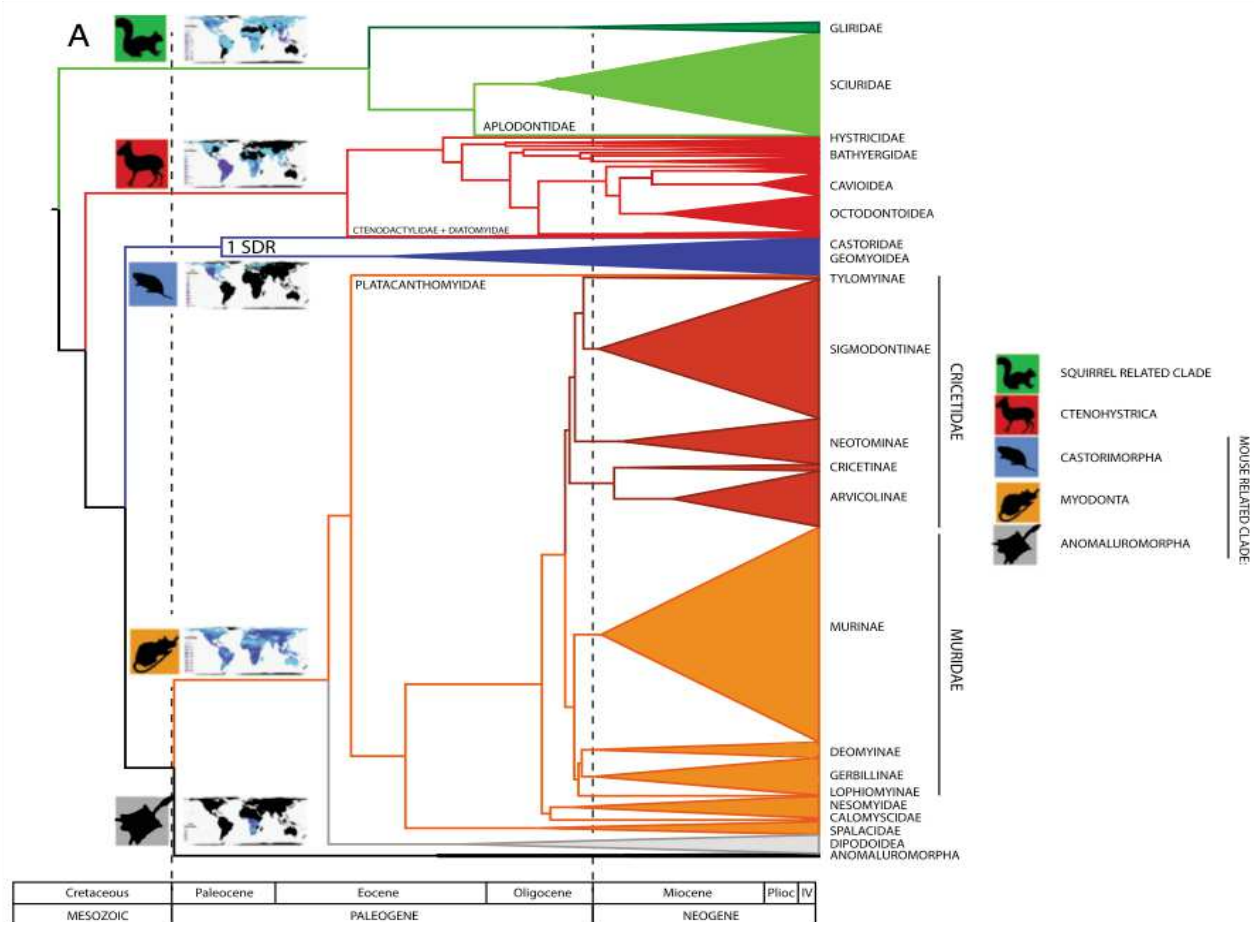

Figure 2. Phylogénie des rongeurs, représentant également les temps de divergence des groupes, leur diversité, et leur répartition mondiale. Modifiée à partir de Fabre et al. 2012.

vers, d'invertébrés aquatiques et d'insectes (Rowe et al. 2016, Fabre et al. 2017).

Au moins deux colonisations indépendantes de l'Australie et de la Papouasie-Nouvelle-Guinée (Sahul) ont été identifiées chez les murinés. La première a donné naissance à un groupe monophylétique dits des "Anciens Endémiques" entre 4 et 6 Mya (selon les estimations moléculaires, en accord avec les premiers fossiles), et plus récemment par le genre *Rattus* qui s'est diversifié en un groupe dit des "Nouveaux Endémiques" (Rowe et al. 2008, Schenk et al. 2013, Fabre et al. 2013). Les "Anciens Endémiques" sont donc issus de la tribu de Hydromyini, et leur groupe-frère est formé par les espèces endémiques des Philippines (Rowe et al. 2008, Schenk et al. 2013, Fabre et al. 2013). De leur côté, les rats "Nouveaux Endémiques" sont aujourd'hui rapprochés des espèces de *Rattus* d'Asie du Sud-Est, notamment le rat noir (*Rattus rattus*) et le rat polynésien (*Rattus exulans*) (Rowe et al. 2008,

Schenk et al. 2013, Fabre et al. 2013). Enfin, une nouvelle colonisation très récente a eu lieu avec l'arrivée des Européens en Australie (Aplin et al. 2011).

Les lignées restantes parmi les murinés se retrouvent principalement en Afrique et en Eurasie. Les principaux groupes sont les Arvicanthini, les Otomyini et les Praomyini africains d'un côté, et les Murini (souris) et Apodemurini (mulots) eurasiatiques de l'autre. Bien que probablement originaires d'Asie, les murinés endémiques d'Afrique sont très diversifiés, représentant un quart des espèces (Lecompte et al. 2008). De plus, les données moléculaires et fossiles suggèrent plusieurs épisodes de colonisations, voire des échanges fréquents entre l'Afrique et l'Asie via la péninsule arabique. La cladogénèse des Arvicanthini, des Otomyini et des Praomyini aurait eu lieu il y a 10Ma, avec une diversification des lignées actuelles autour de -8Ma (Chevret et al. 1994, Lecompte et al. 2008). L'arrivée du genre *Mus* en Afrique serait plus tardive, et sa diversification avec le sous-genre *Nannomys* est estimée entre -6 et -8Ma (Chevret et al. 2005). Ces estimations moléculaires sont en accord avec le registre fossile, mais sont très largement dépendantes de la calibration utilisée par les différentes études (Lecompte et al. 2008). Les premiers fossiles de murinés Africains sont connus entre 10 et 11Ma (Ameur 1984) et sont généralement considérés comme appartenant au genre asiatique *Progonomys*, arrivé d'Asie. D'autres rongeurs fossiles basaux plus récents (entre 9 et 10Ma) pourraient être à l'origine d'une diversification intra-Afrique des Praomyini et des Arvicanthini, bien que Lecompte et al. (2008) suggèrent plutôt une origine plus ancienne de ces lignées qui auraient ensuite migré vers l'Afrique et s'y seraient diversifiées.

La souris pygmée africaine (*Nannomys*), n'est connue qu'à partir de -3Ma en Afrique de l'Est (Auffray et al. 1990), bien que Chevret et al. (2005) indiquent une diversification du groupe entre -6 et -3Ma. Ce sous-genre occupe aujourd'hui une grande partie de l'Afrique sub-saharienne et compte de nombreuses espèces (entre 5 et 30 selon les estimations), assez proches morphologiquement, mais présentant une grande diversité de karyotypes (Veyrunes et al. 2005).

Outre *Nannomys*, *Mus* contient trois autres sous-genres : *Coelomys* et *Pyromys*, retrouvés en Inde et en Asie du Sud-Est, et *Mus*, dont la zone de répartition naturelle est l'Eurasie et l'Afrique du Nord, mais qui a aujourd'hui colonisé tous les continents via l'intermédiaire de *Mus musculus*, qui a accompagné les migrations humaines (Suzuki et al. 2004, Chevret et al. 2005, Siahsarvie et al. 2012, Suzuki et Aplin 2012).

Coelomys et *Pyromys* contiennent quatre et cinq espèces respectivement (Chevret et al. 2003) mais restent à ce jour assez peu étudiés en comparaison de *Nannomys* et *Mus*. *Coelomys* est généralement considéré comme le groupe-frère du clade formé par le reste des souris (Veyrunes et al. 2005, Auffray and Britton-Davidian 2012, Suzuki et Aplin 2012). Ce sous-genre est très insectivore et présente certaines convergences morphologiques crâniennes (museau allongé, petits yeux) avec les musaraignes. *Nannomys* constitue le groupe-frère du clade *Mus+Pyromys*, et a probablement divergé lors de son arrivée en Afrique (Chevret et al. 2005).

Le sous-genre *Mus* contient 14 espèces, réparties dans quatre complexes d'espèces (Auffray and Britton-Davidian 2012, Suzuki et Aplin 2012). Il a été très étudié en raison de l'utilisation de la souris domestique (*Mus (Mus) musculus*) en temps qu'animal modèle. Les complexes d'espèces de *Mus* correspondent grossièrement à leur répartition géographique :

- Le complexe d'espèces *M. cervicolor*, présent en Asie du Sud-Est, contient trois espèces, *M. cervicolor*, *M. caroli* et *M. cookii*. Ces espèces sont très proches morphologiquement, partiellement commensales et fréquemment trouvées en sympatrie.
- Le complexe *M. booduga*, dont trois espèces sont présentes sur le sous-continent Indien (*M. booduga*, *M. terricolor* et *M. famulus*) et deux en Asie du Sud-Est (*M. fragilicauda*, *M. nitidulus*). *M. fragilicauda* est également retrouvée en sympatrie avec les espèces du complexe *M. cervicolor* (Auffray et al. 2003).
- *M. lepidoides* qui forme un clade monospécifique, trouvé uniquement au Myanmar.
- Le complexe *M. musculus*, à la répartition paléarctique, contenant *M. musculus*, *M. spretus*, *M. spicilegus*, *M. macedonicus* et *M. cypriacus*. *Mus musculus* est présente de l'Europe au Moyen-Orient et sur le pourtour méditerranéen d'Afrique, en sympatrie avec la plupart des autres espèces de son sous-genre : autour de la Méditerranée avec *M. spretus*, dans les balkans avec *M. spicilegus*, et avec *M. cypriacus* sur la côte nord de Chypre. Bien que *M. musculus* soit trouvée dans les mêmes zones géographiques que *M. macedonicus*, il apparaît qu'elles s'excluent mutuellement de leurs territoires respectifs.

Les murinés représentent donc un groupe très divers et présent mondialement. Cette grande diversité d'espèces, leur vaste aire de répartition, les niches écologiques variées qu'ils occupent, ainsi que leurs relations avec l'homme font des murinés un groupe unique pour l'étude de l'évolution et de l'adaptation notamment face aux changements rapides liés à l'anthropisation des milieux. L'anatomie

crânio-mandibulaire constitue l'un des aspects majeurs de cette évolution car elle joue un rôle primordial dans l'alimentation, mais aussi dans l'agression, la défense et la compétition. De manière à mieux comprendre ces interactions, cette thèse s'est appuyée sur l'étude de différentes espèces de Rattini et Murini, aux modes de vies, écologies et origines géographiques variées : les communautés de rats et de souris de Thaïlande (genres *Mus*, *Rattus*, *Maxomys*, *Niviventer*, *Bandicota*, *Berylmys*), la souris à queue courte (*Mus spretus*) du Sud de la France, vivant en sympatrie avec le mulot sylvestre (*Apodemus sylvaticus*), mais aussi des souches de souris élevées laboratoire issues de populations écossaises (*Mus musculus*) et d'Afrique du Sud (*Mus minutoides*, *Mus mattheyi*). Ces espèces ont été choisies en partie pour des raison pratiques (*e.g.* colonies de laboratoires pré-existantes, collections de rongeurs d'Asie de Sud-Est), mais aussi pour des raisons biologiques, puisque ce sont des espèces aux caractéristiques bien particulières. Outre qu'elles représentent une grande partie de l'aire de répartition native des murinés (Asie, Afrique, Europe), ce sont des espèces aux écologies variées, et avec différents niveaux de commensalisme. Les rats et souris d'Asie du Sud-Est forment des communautés diverses, avec de nombreux cas de sympatrie, et de syntopie, et ont un intérêt particulier, puisqu'elles sont souvent associées à l'homme. La syntopie est également d'intérêt pour le couple *M. spretus* / *A. sylvaticus*, dont la première est pourtant une espèce plutôt endémique, tandis que la seconde jouit d'une très large aire de répartition. Les espèces élevées en animalerie, outre les aspects de gestion des lignées et des conditions environnementales, sont elles aussi des cas particuliers. *M. minutoides* et *M. mattheyi* sont des espèces naines au détermininsme sexuel unique au sein des Mammifères, ce qui en fait un modèle d'étude important. Enfin les souches de *M. musculus* étudiées dans cette thèse sont issus d'ancêtres sauvages insulaires des Orcades, et séparées en trois lignées correspondantes au îles d'origines, de tailles et d'écologies différentes (notamment par l'accessibilité à l'homme et l'agriculture).

Anatomie cranio-mandibulaire chez les muridés

Au cours du XIXème et du XXème siècle, le crâne a été fréquemment utilisé comme outil de classification (Waterhouse 1839, Tullberg 1899, Simpson 1945, Wood 1965). De plus, la morphologie crânienne des rongeurs a été considérée comme un élément clé dans leur succès évolutif (Landry 1970), en leur permettant d'accéder à une grande variété de ressources alimentaires. Historiquement, quatre groupes de rongeurs, considérés alors comme des clades, furent distingués sur la base de leur morphologie crânienne : les protrogomorphes, les sciuromorphes, les hystricomorphes et les myomorphes (Wood 1965). Ces groupes furent séparés en fonction de la taille du foramen infra-orbitaire et de la plaque massétérique, correspondant à des différences d'insertions musculaires (Wood 1965, Cox et al. 2012). Cette classification fut définitivement abandonnée lorsque les premières études moléculaires confirmèrent de nombreux cas de convergences morphologiques précédemment établies (Nedbal et al. 1996, Huchon et al. 2002). Actuellement, les groupes sciuromorphes, hystricomorphes et myomorphes sont encore utilisés en tant que morphotypes avec des implications fonctionnelles différentes (Samuels 2009, Cox et al. 2012). Les rongeurs sciuromorphes et hystricomorphes sont considérés comme spécialistes dans la morsure au niveau des incisives pour les premiers, et dans la mastication au niveau des molaires pour les seconds. Les myomorphes, dont font partie les muridés, sont quant à eux considérés comme des généralistes (Cox et al. 2012).

Description de l'anatomie du crâne chez les muridés

Parmi les muridés, l'anatomie cranio-mandibulaire osseuse (Fig. 3) et musculaire (Fig. 4) a été décrite de manière détaillée dans seulement quelques cas : le rat brun (Greene 1955, Hiimae et Houston 1971), le rat noir (Satoh 2008), la souris domestique (Cook 1965, Patel 1978, Baverstock et al. 2013) pour les mieux connus, mais aussi chez *Apodemus speciosus* (Satoh 1997, 1998, 1999). De manière générale, le crâne des muridés est similaire au sein de la famille, avec un morphotype myomorphe chez toutes les espèces. Cependant, des différences notables peuvent exister entre certains groupes en fonction de leurs distances phylogénétiques ou de leurs écologies spécialisées (e.g. Satoh et Iwaku 2006, Fabre et al. 2017).

La littérature actuelle chez les rongeurs, ainsi que pour la majorité des mammifères reconnaît quatre groupes de muscles associés à l'adduction de la mandibule (Cox et Jeffery 2011, Druzinsky et al.

2011, Baverstock 2013) : le groupe masséterique, le groupe temporal, le groupe zygomaticomandibulaire et le groupe ptérygoïde. Chez les rongeurs, ces groupes sont séparés en différentes sous-parties selon les études et les données de dissections (Cox et Jeffery 2011, Baverstock

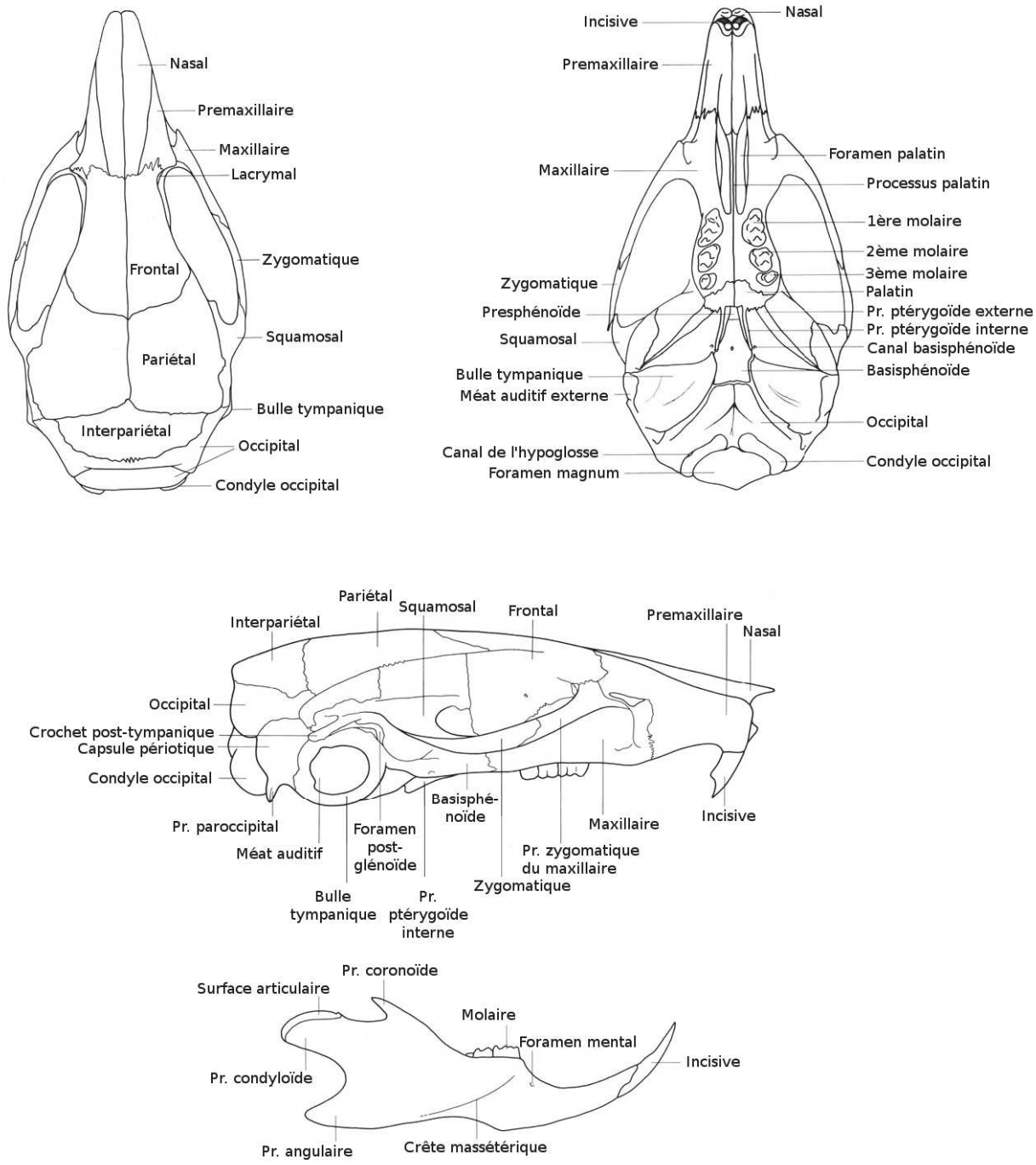

Figure 3. Dessin du crâne et de la mandibule d'une souris, indiquant les différentes structures les composant. Adapté de Cook (1965). Abréviation : Pr., processus.

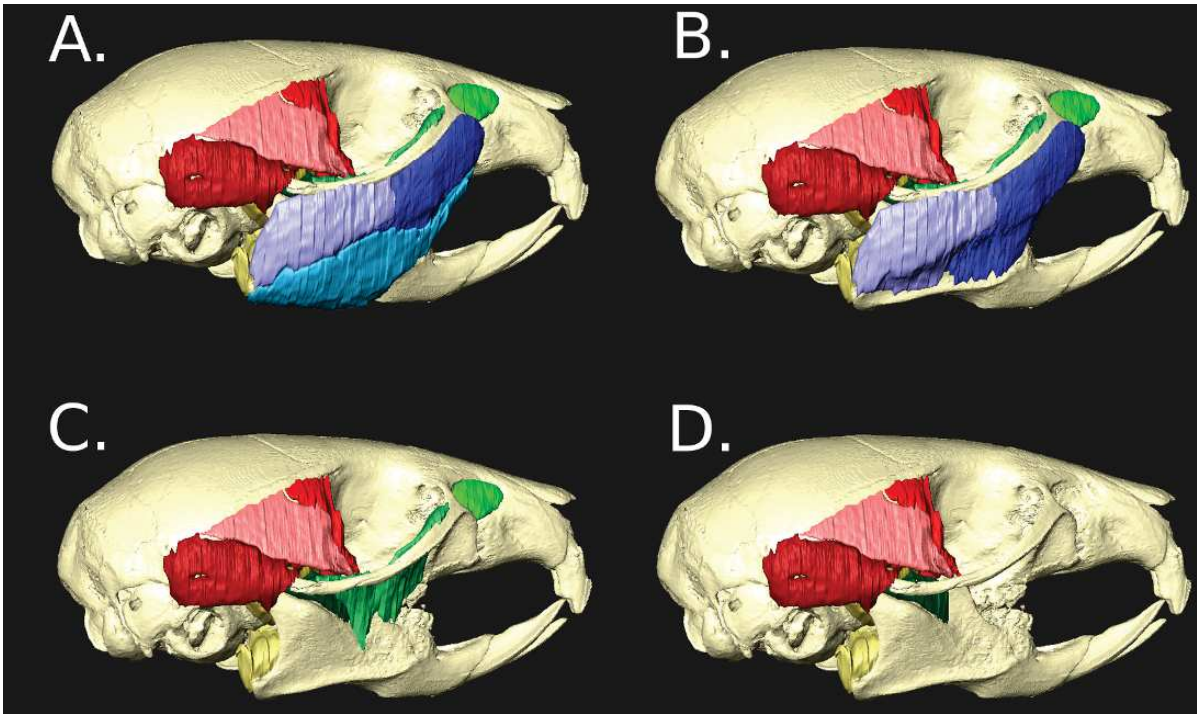

Figure 4. Reconstruction en trois dimensions de la musculature d'une souris thaïlandaise, *M. caroli*. Les muscles en bleu forment le groupe masséter, en rouge le groupe temporal en vert le groupe zygomaticomandibulaire et en jaune le groupe ptérygoïde. (A) Tous les muscles représentés ; (B) sans le masseter superficiel ; (C) sans les muscles du groupe masseter ; (D) sans le zygomaticomndibularis antérieur et infra-orbital.

2013 ; Figure 4). Dans la présente thèse, la nomenclature suivante sera utilisée :

- Le muscle masséter est séparé en deux parties, le masséter superficiel et le masséter profond. Le premier prend son origine sur le crâne, antérieurement à la rangée dentaire, au niveau d'un petit processus à la limite ventrale et antérieure de la plaque massétérique. Il s'insère autour du bord du processus angulaire de la mandibule, en développant parfois une *pars reflexa* sur la face médiale de la mandibule. Le masséter profond occupe une position médiale par rapport au masséter superficiel. Il est séparé en deux parties, l'une antérieure et l'autre postérieure. La partie antérieure a pour origine la plaque massétérique et la partie antéro-ventrale de l'arcade zygomatique. La partie postérieure prend son origine sur la partie médio-ventrale de l'arcade zygomatique. Les deux parties du masséter profond s'insèrent le long de la crête massétérique, située sur la partie ventrale du corps de la mandibule.
- Le muscle temporal est séparé en deux parties, le temporal latéral et le temporal médial. Une troisième partie est parfois décrite (Druzinsky et al. 2011), le temporal intra-orbitaire, qui est

reliée au temporal médial ou latéral selon les espèces. La partie intra-orbitaire prend son origine sur la partie antérieure de l'arête temporale et se développe verticalement pour s'insérer antérieurement sur le bord supérieur du processus coronoïde de la mandibule. Elle est parfois difficile à séparer du temporal latéral, dont l'origine est directement postérieure et qui s'insère aussi sur le bord supérieur du processus coronoïde, cependant plus latéralement. Enfin la partie médiale du temporal est la plus ventrale et postérieure des trois. Elle s'insère entre la limite postérieure de l'arête temporale et l'arête située au-dessus de la bulle auditive. La partie médiale se développe parfois par-dessus la partie postérieure de l'arcade zygomatique et peut la recouvrir. Elle s'insère sur le côté médial du processus coronoïde.

- Le muscle zygomaticomandibulaire est situé médialement par rapport au masséter. Il est également séparé en trois parties : infra-orbitaire, antérieure et postérieure. La partie infra-orbitaire a pour origine la fosse située antérieurement au foramen infra-orbitaire, ainsi que la partie antéro-médiale de l'arcade zygomatique. Elle traverse le foramen et s'insère sur la face latérale de la mandibule, ventralement aux premières et deuxièmes molaires. La partie antérieure se situe directement postérieurement à la partie infra-orbitaire, prenant son origine sur le bord médial de la partie médiane de l'arcade zygomatique, et s'insérant aussi le long de la rangée dentaire, postérieurement à la partie infra-orbitaire. Enfin, la partie postérieure, généralement plus petite que les deux autres, prend son origine sur le bord médial de la partie postérieure de l'arcade zygomatique au niveau de la cavité glénoïde. Les origines des parties antérieure et postérieure sont généralement séparées, et leurs fibres sont orientées très différemment (antéro-ventralement pour la partie postérieure, et postéro-ventralement pour la partie antérieure). Le zygomaticomandibulaire postérieur s'insère sur la mandibule au niveau du ramus, dans la fosse produite par le relief formé par l'alvéole de l'incisive.
- Le muscle ptérygoïde se situe entre la face palatine du crâne et la face médiale de la mandibule. Il comprend deux parties, l'une interne et l'autre externe. La première prend son origine sur le processus ptérygoïde et dans la fosse ptérygoïde ; elle s'insère sur la face médiale du processus angulaire de la mandibule. La seconde est en position plus dorsale, et a pour origine une fosse, située latéralement au processus ptérygoïde. Elle s'insère sur la face médiale du processus condyloïde de la mandibule.

En plus de ces muscles adducteurs de la mandibule, le cycle masticatoire nécessite l'activité des

muscles hyoïdes et digastriques qui jouent un rôle primordial dans l'ouverture de la bouche, la stabilisation de la mandibule et le transport des aliments (Weijs et Dantuma 1975). Ces muscles ne seront cependant pas détaillés dans la thèse, puisque qu'elle se focalise sur l'adduction de la mandibule et la force de morsure.

Aspects fonctionnels du crâne

De par sa morphologie particulière, le système masticateur des rongeurs est très spécialisé d'un point de vue fonctionnel. En effet, lorsque les molaires sont en occlusion, les incisives ne sont pas en contact. La mastication et l'incision sont donc deux processus distincts et exclusifs chez les rongeurs. Le fonctionnement mécanique de la morsure et de la mastication a été étudié de manière détaillée, notamment chez le rat brun, mais aussi dans quelques autres cas (Hiiemae 1971, Hiiemae et Houston 1971, Weijs et Dantuma 1975, Satoh 1997, 1998, 1999, Satoh et Iwaku 2006).

Lors de l'incision, la mandibule peut-être considérée comme un levier de type 3 (Hiiemae 1971, Satoh 1997), dans lequel le fulcrum (ici le condyle), l'effort (ici les forces musculaires) et la résistance (ici la réaction des aliments au niveau des incisives) sont alignés dans cet ordre. Lors de cette phase d'incision, les muscles adducteurs sont tous actifs (Weijs et Dantuma 1975) et la force résultante est dirigée dorsalement et antérieurement (Fig. 5).

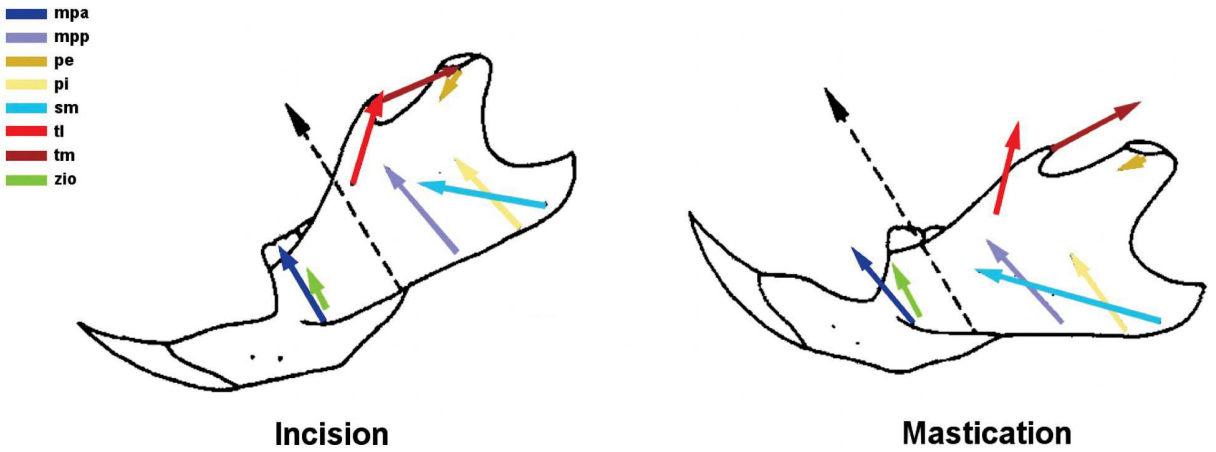

Figure 5. Les deux positions de la mandibule lors de l'incision ou de la mastication chez un rongeur muridé. Les flèches représentent les vecteurs des forces des muscles durant les deux processus. En bleu les muscles du masséter, en vert du zygomaticomandibularis, en rouge du temporal et en jaune du ptérygoïde. La flèche en pointillés représente la résultante de tous les vecteurs. Modifiée de Weijs et Dantuma (1975). Abréviations : mpa, masseter profond antérieur ; mpp, masseter profond postérieur ; pe, ptérygoïde externe ; pi, ptérygoïde interne ; sm, masseter superficiel ; tl, temporal latéral ; tm, temporal médial ; zio, zygomaticomandibularis infra-orbitaire.

Lors de la mastication au niveau des molaires, la mandibule est d'abord ramenée postérieurement et dorsalement avant l'occlusion par l'action des muscles temporaux et hyoïdes. Puis lors de l'écrasement des aliments à proprement parler, tous les muscles adducteurs sont activés, et la force résultante est dirigée antérieurement et dorsalement (Fig. 5). Contrairement à l'incision, lors de la mastication la mandibule ne peut pas être assimilée à un levier de type 3 (Fig. 6A) car le condyle ne subit pas de stress (Hiiemae 1971, mais voir Cox et Jeffery 2011). Elle peut en revanche se comporter

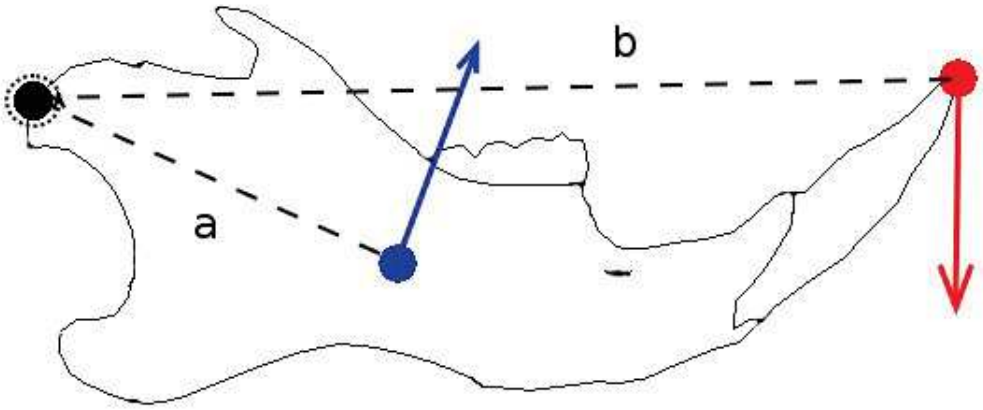

Levier type III (incision) :
- Pivot, force, résistance
- Avantage mécanique : a/b < 1

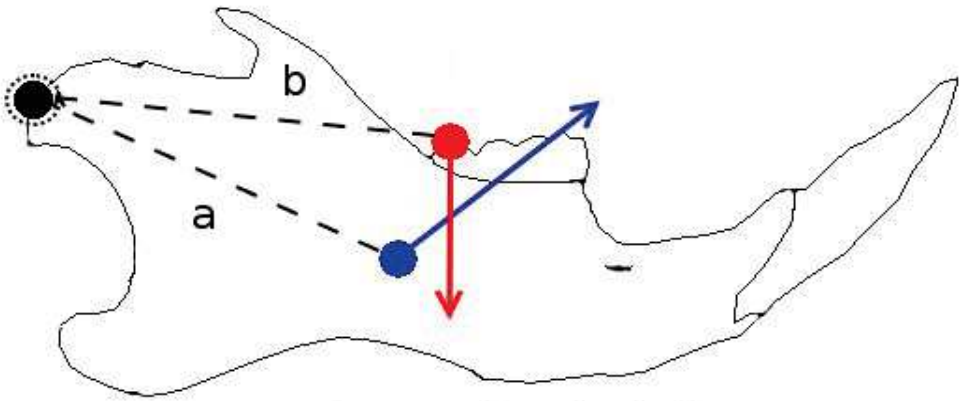

Levier type II (mastication) :
- Pivot, résistance, force
- Avantage mécanique : a/b >= 1

Figure 6. Les deux types de leviers que peut représenter la mandibule, selon qu'elle agit en mastication ou en incision. En fonction de la position de la nourriture et des lignes d'action des muscles, la mandibule peut se comporter comme un levier de type II ou III.

comme un levier de type 2 (Fig. 6B), plus efficace puisque ayant un plus grand avantage mécanique (Turnbull 1970, Samuels 2009). Le niveau d'activité du groupe temporal est similaire entre l'incision et la mastication. En revanche, les muscles ptérygoïdes sont plus actifs lors de l'incision, tandis que les muscles massétériques se contractent plus lors de la mastication (Weijs et Dantuma 1975).

Plusieurs études biomécaniques (Weijs et Dantuma 1975, Satoh 1998, Satoh et Iwaku 2006, Cox et Jeffery 2011) ont permis de réaliser des estimations des avantages mécaniques des muscles, des angles possibles d'ouverture de la bouche, mais aussi des forces de morsure et de mastication. Cependant, des mesures de forces de morsure *in vivo* n'ont été réalisées que récemment sur les rongeurs (Nies et Ro 2004, Freeman et Lemen 2008a, b, Van Daele et al. 2009, Becerra et al. 2011, Cox et al. 2012).

Adaptation et évolution de l'anatomie crânienne

Au sein des rongeurs, la morphologie hystricomorphe est considérée comme spécialisée pour la mastication, tandis que la morphologie sciuromorphe serait spécialisée pour l'incision. De leurs côtés, les myomorphes seraient plus généralistes (Cox et al. 2012, Maestri et al. 2016). Toutefois, ces études suggèrent que les rongeurs myomorphes soient capables de meilleures performances que les groupes "spécialistes" dans leurs domaines respectifs. Ces performances pourraient en partie expliquer la relative stabilité morphologique crânienne du groupe (Maestri et al. 2016, Rowe et al. 2011). La morphologie et la musculature crânienne des myomorphes permettraient donc de maximiser les forces de morsures tant au niveau des molaires que des incisives.

Bien que cette morphologie particulière leur confère un accès à des ressources variées sans nécessiter de modifications morphologiques importantes (Maestri et al. 2016), certains rongeurs myomorphes montrent des degrés et des modes variables de spécialisations (Michaux et al. 2007, Samuels 2009, Maestri et al. 2016, Fabre et al. 2017). Ces spécialisations entraînent des changements anatomiques parfois spectaculaires, et d'autres plus subtils. L'adaptation à un régime insectivore, par exemple, est corrélée à l'allongement du rostre, de la mandibule, à la réduction des rangées dentaires voire des incisives (Michaux et al. 2007, Samuels 2009, Maestri et al. 2016). D'un point de vue fonctionnel, ces changements se traduisent par une plus faible force de morsure, mais aussi par un gain de vitesse de rotation de la mandibule et un museau permettant d'accéder plus aisément aux proies. Les herbivores quant à eux se caractérisent par un crâne et un rostre larges et hauts, de larges et courtes

incisives et des rangées dentaires allongées et élargies. En parallèle, leur mandibule est également haute et robuste, avec un processus angulaire développé, produisant des forces importantes au niveau des molaires, tout en maintenant les deux hémimandibules entre elles (Michaux et al. 2007, Samuels 2009, Maestri et al. 2016).

Bien que relativement peu d'études se soient intéressées au lien entre écologie et musculature, elles semblent aussi indiquer des changements interprétables en termes adaptatifs chez les rongeurs (e.g. Satoh 1997, 1999, Satoh et Iwaku 2006). Les herbivores les plus extrêmes parmi les myomorphes montrent des changements importants dans l'orientation des lignes d'action de leurs muscles masticateurs (Satoh 1997). Chez les Arvicolinae, par exemple, les orientations des lignes d'actions du temporal devient plus verticale, tandis que celles des masséters et ptérygoïdes deviennent plus horizontales, permettant d'importants mouvements propalinaux (antéro-postérieurs) de la mandibule (Kesner 1980). Chez *Neotoma mexicana*, le temporal montre une aponeurose importante, suggérant de grandes forces occlusales, tandis que les masséters et ptérygoïdes sont plus inclinés antéro-postérieurement que chez une espèce proche non spécialiste (*Peromyscus maniculatus*) (Satoh et Iwaku, 2009). Ces changements musculaires induisent des mouvements propalinaux important permettant de broyer les aliments. Les rongeurs carnivores quant à eux, semblent favoriser une plus grande ouverture de la bouche grâce à un allongement des fibres, et une réduction des aponeuroses du masséter profond (Fabre et al. 2017). De plus, la réduction du masséter profond (et de ses aponeuroses) chez les formes carnivores est compensée par un accroissement des muscles temporaux et/ou par un changement d'inclinaison des fibres du masséter profond, augmentant l'avantage mécanique. Ces derniers changements permettent aux rongeurs carnivores spécialistes de produire une force de morsure importante au niveau des incisives, au détriment des forces occlusales au niveau des molaires (Satoh et Iwaku 2006, Fabre et al. 2017). À l’échelle de la sous-famille des murinés cependant, cette variation musculaire et ses conséquences bio-mécaniques ne sont pas étudiées.

Dans les exemples précédents, les changements morphologiques sont interprétés en termes fonctionnels par leur influence sur l'angle d'ouverture de la bouche, les mouvements de la mandibule et la force de morsure. Cependant les liens fonctionnels entre ces caractères, liés à l'écologie et à la valeur sélective des individus, et l'anatomie crânienne sont rarement testés de manière directe.

Dans cette thèse, la force de morsure *in vivo*, mesurée au niveau des incisives grâce à un transducteur de force (Fig. 7), est utilisée en tant que mesure de performance pour les rongeurs. La relation entre la force de morsure et l'anatomie des animaux est établie pour mieux comprendre

l'évolution du crâne en lien avec les différentes spécialisations écologiques de ces animaux. La force de morsure est un trait phénotypique pouvant être influencé par de nombreuse variables systémiques (e.g. morphologie, physiologie, développement, stress et âge) et environnementales (dominance, compétition, température et parasitisme ; Herrel et al. 2001, 2004, 2005, 2010, Verwaijen et al. 2002, Lailvaux et al. 2004, Huyghe et al. 2005, Anderson et al. 2008, Santana et al. 2010). Il est donc nécessaire de tester quels effets sont les plus importants. En contrepartie, les différences de forces de morsures permettent de tester des hypothèses en termes d'écologie, d'adaptation et de compétition intra et interspécifique. La majorité des espèces de murinés sont aujourd'hui omnivores et utilisent différentes ressources alimentaires. Il semble que la radiation et le succès des murinés aient été en partie permis par l’acquisition d’un appareil masticateur polyvalent et puissant (Landry 1970, Cox et al. 2012) qui leur a permis d'occuper des niches et des habitats variés. Par la suite, l'occupation de niches plus spécialisées a pu produire des morphologies plus variables, notamment via des processus d’isolement et évoluer vers une diversité de formes, tout en conservant le plan d'organisation myomorphe.

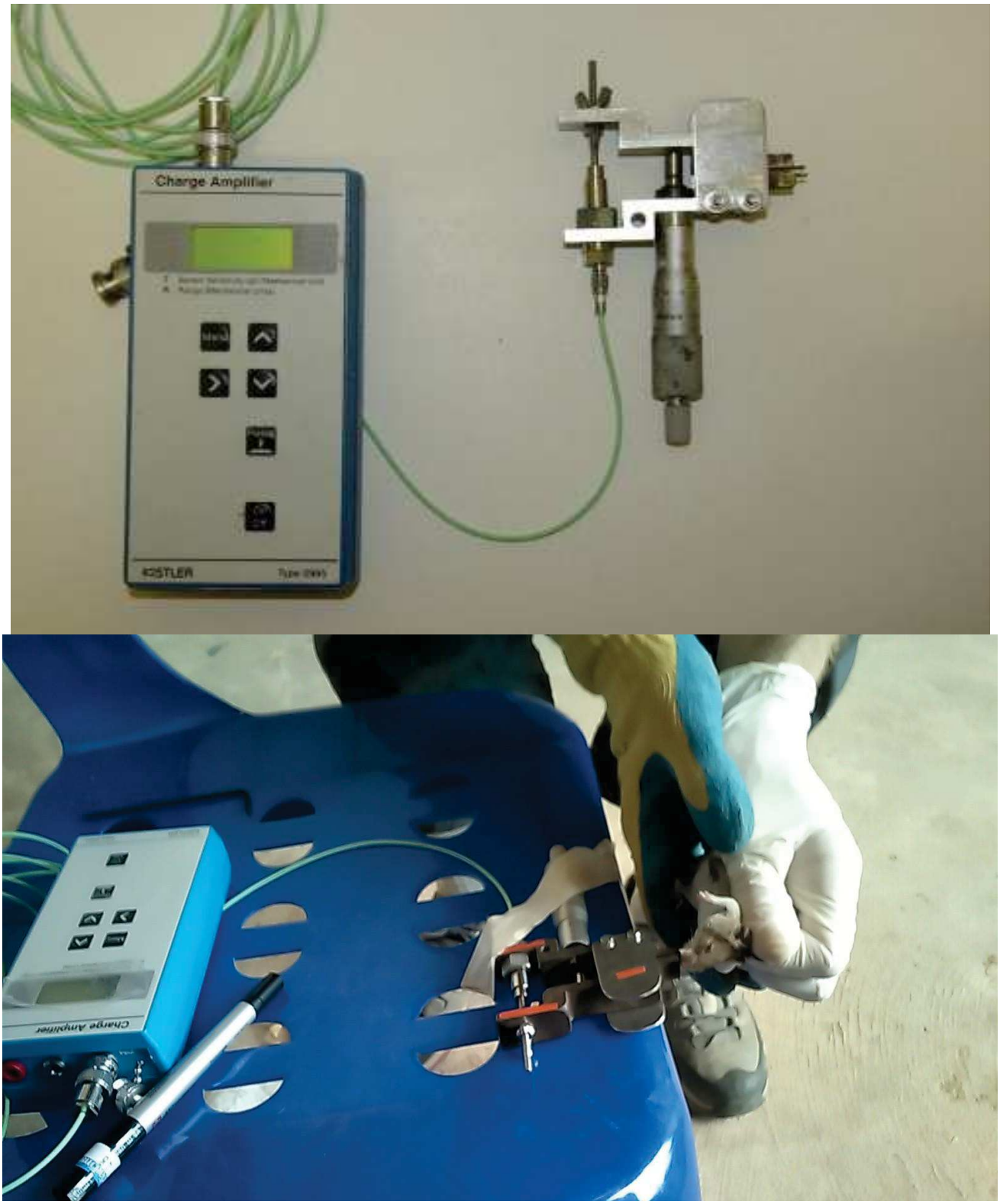

Figure 7. A) Le transducteur de force utilisé pour mesurer les forces de morsures des rongeurs. Les plaques métalliques à droite de l'image permettent à l'animal de mordre et transmettent par levier une force de tension au piézomètre relié par un câble à l'amplificateur situé à gauche. B) Une souris mordant sur le transducteur de force lors d'une mission de terrain en Thaïlande.

Cadre méthodologique

Cette section synthétise les différentes méthodes et protocoles utilisés au cours de la thèse, et donne des précisions sur les animaux utilisés durant la thèse. Des détails supplémentaires sont donnés dans les articles correspondants.

Matériel biologique utilisé

Les animaux utilisés dans cette thèse sont des rongeurs murinés soit sauvages, soit élevés en animalerie. Les souris d'animalerie (*Mus musculus*) étudiées dans cette thèse forment trois lignées, qui descendent d'ancêtres sauvages, ayant pour origine respective l'île de Mainland (lignée ML), l'île de Papa Westray (lignée PW) et l'île de South Ronaldsay (lignée SR), se situant toutes dans l'archipel des Orcades (Écosse). Parmi ces trois lignées, la première constitue une lignée destinée à rester non-consanguine, en effectuant des croisements entre individus non apparentés. Les deux autres lignées ont été systématiquement sélectionnées pour la fixation (PW) ou l'absence (SR) d'un caractère dentaire : la présence d'une cuspide supplémentaire, ou préstyle. Les individus de ces deux dernières lignées ont été croisés entre apparentés, ce qui a augmenté leur taux de consanguinité de manière drastique. Ces trois lignées ont été maintenues en captivité à l'animalerie de la Faculté des Sciences de Montpellier (CECEMA) notamment par Rohollah Siahsarvie, Sylvie Agret et moi-même. Parmi ces souris, l'âge et le sexe sont précisément connus, et pris en compte dans les études les concernant. Ces souris d'animalerie ont été principalement utilisées dans les parties 1.2.3, 1.2.4, 2.2 et 2.3.

Les souris naines utilisées dans la partie 2.1 sont également maintenues en captivité à la Faculté des Sciences de Montpellier (CECEMA), notamment par Frédéric Veyrunes, pour étudier leur déterminisme du sexe unique chez les Mammifères (trois types de chromosomes : X, Y et X*). Les individus croisés ne sont généralement pas apparentés, et le pedigree utilisé a pour but de permettre l'identification des chromosomes sexuels portés par certains individus. Là aussi, l'âge et le sexe est systématiquement noté, et pris en compte dans l'étude de la partie 2.1.

Le reste des rongeurs utilisés dans cette thèse est composé de rongeurs sauvages, soit directement piégés dans la nature, soit issus de collections, en particulier celles accumulées dans le cadre des projets ANR CERoPath et BiodivHealthSEA. Ces animaux proviennent pour la plupart d'Asie du Sud-Est, et notamment de Thaïlande, pour ceux ayant été capturés vivants tout au long de

cette thèse. En outre, deux espèces européennes (*Mus spretus* et *Apodemus sylvaticus*) ont été capturées dans Montpellier et ses alentours (Hérault, France). Pour tous ces rongeurs sauvages, l'âge n'a pas pu être contrôlé de manière précise, bien que les individus adultes et juvéniles aient généralement été distingués. Le sexe des individus a été noté, mais n'est pas toujours pris en compte dans les études de cette thèse, généralement pour garder des tailles d'échantillons appropriées. Les rongeurs Asiatiques ont été utilisés dans les parties 1.1, 1.2.1 et 3.2. Les rongeurs capturés dans l'Hérault sont étudiés dans la partie 3.1.

Mesure de la force de morsure in vivo

La force de morsure *in vivo* est obtenue grâce à l'appareil présenté dans la figure 7. Les plaques métalliques, sur lesquelles mordent les rongeurs (Fig. 7B), forment un levier qui pivote au niveau de la tête d'un micromètre. Celui-ci permet aussi de régler l'espacement des plaques. Le levier transmet une force de tension à un capteur pour petites forces (piézomètre) de marque Kistler, type 9203. Ce dernier est ensuite relié par un câble Kistler de type 1631C à un amplificateur de charge (Kistler type 5995A) sur lequel s'affiche la force mesurée instantanée, minimum (tension) ou maximum (pression). A cause de l'avantage mécanique produit par le levier, toutes les forces mesurées brutes sont multipliées par 0.7 (ratio de la distance des plaques à la tête du micromètre, sur la distance de la tête du micromètre au piézomètre) pour obtenir la force de morsure au niveau des plaques.

Pour faire mordre le rongeur, l'utilisateur le maintient par la peau du cou au niveau des oreilles, si possible en tenant aussi la queue pour éviter les mouvements des pattes arrières. Le rongeur est ensuite rapproché des plaques, et mord généralement spontanément. La valeur affichée sur l'amplificateur est notée, le rongeur est éloigné puis à nouveau rapproché des plaques pour répéter la mesure, et une troisième répétition est ensuite effectuée si possible. La plus grande des trois forces obtenues est celle qui est utilisée dans les analyses. La mesure obtenue est donc considérée comme la force maximale pouvant être produite au niveau des incisives par l'animal. Bien que la morsure, dans la manière dont elle est mesurée ici, soit en elle-même un réflexe défensif, de nombreuses études montrent cependant qu'elle est une mesure répétable, et corrélée au régime alimentaire et à l'efficacité avec laquelle les animaux peuvent se nourrir (voir notamment Verwaijen et al. 2002, Anderson et al. 2008, Santana et al. 2010).

ERRATUM : Une erreur dans les réglages de l'appareil permettant de mesurer les forces de morsures a causé plusieurs biais dans les données obtenues. Ce problème a été détecté tardivement, entre le dépôt du premier manuscrit de thèse et la soutenance, grâce à l'aide de A. Herrel, S. Renaud et J. Claude notamment. La sensibilité du capteur ayant été modifiée, les mesures brutes obtenues étaient surestimées 2.4 fois (e.g. une force affichée à 30N représentait en fait une force de 12.5N). De plus, la gamme de valeurs du capteur n'étant plus adaptée à sa sensibilité, une absence artefactuelle de données a été produite entre 30.9 et 32N. Pour corriger ces biais, nous avons repéré le moment auquel le changement de réglage est arrivé (un seul événement, au début de la thèse), et divisé toutes les valeurs obtenues postérieurement par un facteur de 2.4. De plus, les forces valant 30.9N ont été écartées des analyses, car il est impossible de savoir leur valeur réelle (comprise entre 30.9 et 31.9N). Les valeurs données dans cette version finale de la thèse sont donc corrigées, avec cependant deux avertissements à prendre en compte : 1) les données ayant été divisée par un facteur de 2.4, certaines ont dû être arrondies ; et 2) l'absence de données entre 30.9 et 32N ne peut pas être corrigée en elle-même, bien que peu d'individus soient concernés (~5 % de toutes les mesures).

Tous les chapitres de la thèse ont été affectés par ces biais, cependant l'application des corrections n'a eu que peu d'impact sur les résultat des analyses. Seul l'article du chapitre 2.1 de ce manuscrit contient encore des données non corrigées, car il était déjà publié au moment de la découverte du biais. Un erratum est en préparation pour le journal concerné. Les autres articles, publiés, sous presse ou en préparation ont pu être corrigés durant le stade d'écriture, des relectures ou des preuves.

Dissections

Les musculatures de diverses espèces de souris sont décrites en détail dans la première partie de la thèse. Les descriptions sont accompagnées de reconstructions 3D. Ces données furent acquises à partir d'un protocole combinant dissections conventionnelles et digitales. Les spécimens (crânes de souris sauvages capturés en Asie du Sud-Est, ou souris élevée en laboratoire) sont initialement conservés en alcool. Ils sont ensuite rincés, et dépecés, avant d'être fixés au formol (4%) durant deux à trois jours (selon la taille du spécimen). Afin d'éviter les problèmes liés à la toxicité du formol, les spécimens sont ensuite replongés dans l'alcool (70%) jusqu'à la dissection.

La dissection manuelle est effectuée du côté gauche. Chaque muscle est individuellement

conservé en alcool (90%). Après avoir disséqué tous les muscles du côté gauche, le spécimen est rincé puis scanné par microtomographie à rayon X (CT scan), à une résolution de 18 µm dans notre cas pour permettre la reconstruction aisée des os du crâne et de la mandibule. Le crâne est ensuite placé dans une solution iodée (I2KI). Cette solution nécessite, pour 1L : 33g d'iodure de potassium (KI), et 16g de diiode (I2), mis en solution dans un tampon phosphate salin (PBS 1x). Le spécimen est ensuite laissé dans la solution iodée pendant deux semaines. Il est alors à nouveau scanné, en utilisant la même résolution. La diffusion de l'iode dans les tissus mous les rend opaques aux rayons X, ce qui permet ensuite de les visualiser sur les images scannées. Il devient donc possible de reconstruire en 3D la musculature en place. Dans cette thèse les reconstructions sont toutes effectuées à l'aide du logiciel Avizo 9.x. Pour finir le crâne est replacé dans une solution de PBS 1x sans iode (afin d'extraire la solution iodée), puis rincé et nettoyé pour être conservé en collection sous forme de crâne sec.

Ce protocole permet donc d'obtenir 1) des données sur les insertions et origines des muscles ainsi que sur l'orientation de leurs fibres par dissection manuelle ; 2) les masses musculaires, longueurs de fibres et PCSA (*Physiological cross-sectional area* : aire de section physiologique) grâce aux muscles prélevés (voir section suivante) ; 3) une reconstruction des os du crâne grâce au premier scan ; 4) une reconstruction des muscles masticateurs complets et en place grâce au second scan, qui vient compléter les données de dissections manuelles.

Estimation de la force de morsure à partir de données musculaires

La force de morsure peut être estimée à partir de la somme des forces théoriques de chaque muscle impliqué dans l'adduction de la mandibule. Ces forces peuvent être estimées à partir des données obtenues pour les muscles individuels disséqués (voir section précédente). Chaque muscle est d'abord tamponné pour enlever l'excédent d'alcool, avant d'être pesé à l'aide d'une balance de précision. Une fois les masses musculaires obtenues, les muscles sont transférés dans un bain d'acide nitrique (HNO3) à 30% pendant 20 à 24h sous hotte et à température ambiante. Cet acide a pour effet de digérer les tissus conjonctifs qui maintiennent les fibres musculaires les unes avec les autres. Cependant, si on laisse trop longtemps un muscle dans le bain, les fibres qui le constituent seront également digérées. Lorsque les fibres musculaires peuvent être séparées facilement, l'acide est remplacé par une solution de glycérol (C3H8O3) à 50% pour stopper la digestion. Il est ensuite possible d'observer les fibres à la

loupe binoculaire (dans le glycérol), et de les photographier ou de les dessiner sous loupe binoculaire grâce à une chambre claire. On mesure ensuite les longueurs d'un échantillon de dix à vingt fibres sélectionnées au hasard, pour calculer la longueur de fibre moyenne de chaque muscle.
On peut ensuite calculer la PCSA des muscles par la formule suivante :

$$PCSA = \frac{Masse}{densité \times longueur\ de\ fibre}$$

La densité d'un muscle étant de 1.06 g.cm^{-3} (Mendez and Keys 1960).

La force pouvant être produite par un muscle est proportionnelle à sa PCSA selon la formule :

$$\vec{F} = PCSA \times 30 \times \cos(\alpha)$$

Où 30 N.cm^{-1} représente une estimation conservatrice (Herzog 1994) de la force pouvant être produite par unité de PCSA, et α représente l'angle entre le vecteur de la force du muscle et le vecteur de la force de réaction.

On obtient l'estimation de force de morsure en additionnant les forces individuelles des muscles et en multipliant par deux (on suppose donc que les deux côtés sont actifs en même temps et avec la même intensité).

Morphométrie géométrique

Toutes les analyses de morphométrie géométrique présentées dans cette thèse ont été effectuées selon le même protocole. Les mandibules ou les crânes sont d'abord photographiés sous différentes vues à l'aide d'un appareil photo Pentax K200, avec un objectif Pentax SMC DA (focale 45mm) et positionné à une distance fixe (11 cm) des spécimens grâce à un banc photo. Les photos sont ensuite importées dans le logiciel tpsDig2.x (Rohlf 2010) afin de digitaliser les points homologues. Ces points peuvent varier selon les études, mais ils représentent toujours des structures d'intérêt morphologique, facilement et systématiquement reconnaissables chez tous les individus (par exemple, les extrémités des processus, des crêtes d'insertions musculaires, ou divers foramens). Le logiciel permet de placer ces points sur les photos et traduit leurs position en coordonnées dans un repère x/y. Les fichiers de coordonnées obtenus au format texte sont ensuite lus dans R (R Core Team 2017) grâce au fonctions de bases. Les formes obtenues par l'ensemble des coordonnées des points sont centrées, mises à l'échelle et

superposées grâce aux fonctions d'analyses Procustes décrites dans Claude (2008). Ce processus est aujourd'hui largement utilisé dans le domaine de la morphométrie géométrique, et permet d'obtenir les différences de positions des points (donc les différences de formes), indépendamment de l'orientation, de la position ou du grossissement de l'objet étudié sur la photo. De plus, il permet aussi d'extraire l'information de la taille de l'objet, afin de se concentrer sur les différences de forme uniquement.

Différentes analyses multivariées, comme l'analyse en composante principale (ACP), l'analyse discriminante (LDA), la régression linéaire, ou les analyses de variance (ANOVA, MANOVA) peuvent ensuite être utilisées pour décrire et tester la variation de forme et de taille et leur covariation avec d'autres facteurs. Parmi ces analyses, l'ACP est fréquemment utilisée pour réduire le nombre de variables, ce qui est particulièrement souhaitable dans le cas où la forme d'un objet est représentée par de nombreux points, chacun ayant deux coordonnées (par exemple pour un objet représenté par 14 points, on obtiendra 28 variables). L'utilisation de l'ACP permet de réduire le nombre de dimensions étudiées, en combinant sur des axes (composantes principales) la variation de plusieurs variables corrélées entre elles. Les différentes composantes principales peuvent être ensuite utilisées dans les analyses précédemment citées, à la place des coordonnées elles-mêmes. Les analyses utilisées sont bien sûr dépendantes du but recherché, mais de manière générale, les analyses discriminantes permettent de différencier des groupes (espèces, populations différentes, etc.) et de visualiser ces différences. Les analyses de variance sont utilisées pour tester des différences inter-groupes, bien que dans certains cas elles aient également été utilisées pour quantifier l'asymétrie, qui constitue une variance intra-individuelle (cf. partie 2.2), ou encore pour mesurer l'héritabilité de certains traits en comparant les variances au sein des portées à celles entre les portées (cf. partie 2.3). Enfin les régressions linéaires sont utilisées pour tester et visualiser les relations entre des variables, mais sont également utilisées dans l'estimation statistique des valeurs de forces de morsures à partir d'autres traits, notamment la taille (cf. parties 1.2.2 et 3.2, et paragraphe suivant).

Estimation de la force de morsure à partir de données morphométriques

Outre le modèle biomécanique présenté précédemment, il est possible de faire des estimations sur la base de la morphologie osseuse uniquement. Ces estimations sont basées sur la corrélation entre la force de morsure et la forme ou les ratios des bras de leviers de la mandibule. Ces approches sont testées dans cette thèse au moyen d'une validation croisée *leave-one-out*. Le principe est de construire

un modèle linéaire de la force de morsure *in vivo* par la morphologie (bras de levier ou forme) à partir d'un échantillons de n individus. On réalise le modèle sur les n individus, moins le premier. A partir du modèle, on estime la force de morsure de l'individu exclu (ici le premier). On réalise ensuite la même procédure en excluant seulement le second, puis seulement le troisième individu, etc. Ceci est répété n fois, jusqu'à obtenir une estimation pour chaque individu. On peut ensuite tester la corrélation entre valeurs estimées et valeurs *in vivo* pour connaître la précision des estimations fournies par le modèle. Si ces estimations s'avèrent bonnes, on peut alors estimer les valeurs chez des individus dont on ne connaît pas la force de morsure *in vivo*.

Génétique quantitative

Afin d'estimer la part de variation phénotypique (force de morsure et morphologie) expliquée par de la variation génétique, un protocole de croisement en animalerie a été réalisé (Fig. 8). Les souris concernées sont des *M. musculus* issues de fondateurs capturés dans la nature sur l'île de Mainland (archipel des Orcades). La lignée issue de ces fondateurs a été maintenue dans la mesure du possible sans réaliser de croisements consanguins.

Le protocole appliqué durant ma thèse a été lancé à partir de souris de la deuxième génération de captivité, et leurs descendants représentent donc la troisième génération de captivité. Il s'agit d'un protocole de croisements frère-demi-frère, dans lequel un mâle est croisé avec plusieurs femelles, choisies pour être inapparentées au mâle, et dont les ancêtres sauvages ont été capturés à la plus grande distance possible des ancêtres du mâle, pour éviter de potentiel apparentements non-contrôlés chez les ancêtres. Cette sélection des femelles a pour but de limiter au maximum le niveau de consanguinité des descendants, afin de préserver la variance génétique dans la lignée et entre les descendants.

Le protocole de croisements a pour but de pouvoir partitionner la variance phénotypique de leurs descendants en variance génétique additive (différences attendues entres les portées de différents pères), variance due à des effets liés à la mère (différences entre portées d'un même père), et variance résiduelle (effets aléatoires parmi les individus d'une même portée). Les différents termes de variance sont décomposés dans une analyse de variance, selon le principe des moindres carrés, en corrigeant pour les tailles inégales des échantillons (Sahai et Ojeda, 2005).

Au total 18 mâles ont été croisés avec 3 femelles chacun, ce qui a permis d'obtenir 54 portées soit environ 350 descendants (Fig. 8). Chaque individu impliqué a vu sa force de morsure mesurée, son

crâne et sa mandibule nettoyés et séchés, afin de pouvoir mesurer la variation phénotypique (pour les traits morphologiques, et pour la force de morsure), et de la décomposer en termes de variances précédemment cités.

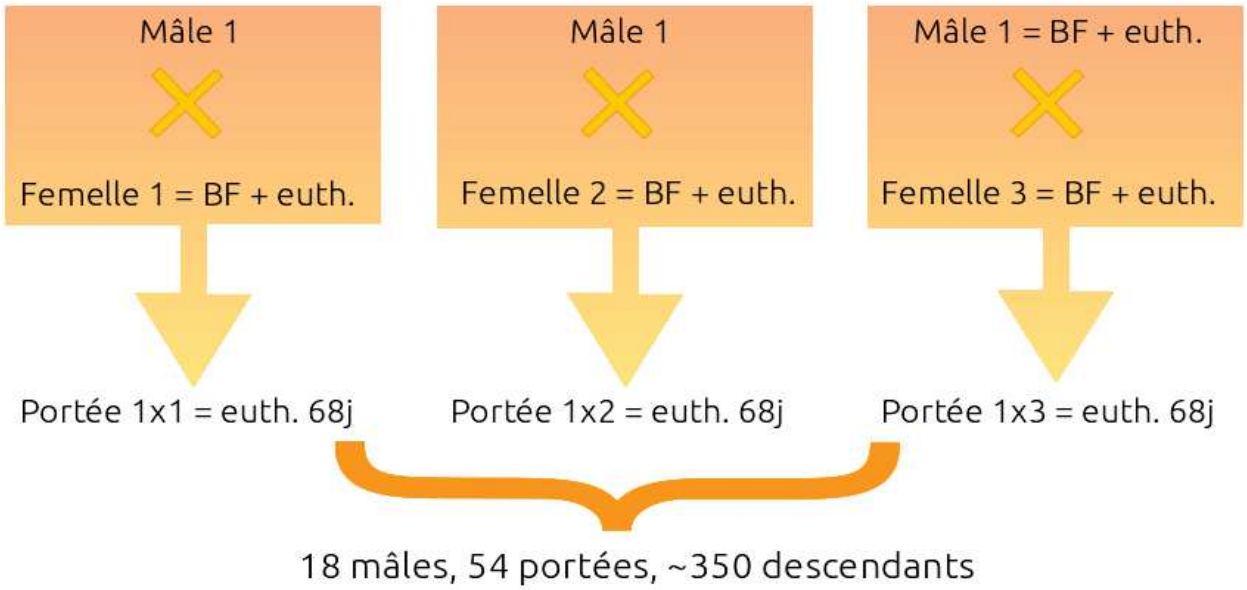

Figure 8. Protocole de croisements réalisé dans le cadre de la thèse, dans l'objectif d'utiliser des approches de génétique quantitative. Chaque mâle (ici par exemple le mâle 1) est croisé avec trois femelles n'ayant pas de lien génétique entre elles, ni avec le mâle (femelles 1, 2, 3), ce qui produit trois portées de descendants pour chaque mâle, et une portée par femelle. Les descendants voient leurs forces de morsures mesurées et sont euthanasiés à l'âge adulte (68 jours). Les forces de morsures des mères sont mesurées après qu'une mère ait produit une portée, c'est à dire après le sevrage, puis elle est euthanasiée. Enfin les forces de morsures des pères sont mesurées après qu'ils aient effectués leurs trois croisements, puis ils sont euthanasiés. Les âges des parents lors de l'euthanasie sont donc variables. Abréviation : euth., euthanasie ; BF, mesure de la force de morsure.

Partie 1 – Variation morpho-anatomique et fonctionnelle chez les Murinae

Cette partie se focalise sur la variation morpho-anatomique du crâne des Murinae. La variation interspécifique de la morphologie crânienne chez ces rongeurs est déjà bien étudiée, pourtant il n'existe que peu de descriptions et de comparaisons de la musculature adductrice de la mandibule. La première section de cette partie est donc une étude d'anatomie comparée de cette musculature chez plusieurs espèces de souris (genre *Mus*), afin de mieux cerner sa variabilité, en tenant compte des écologies et tailles variées des espèces étudiées. La seconde section de cette partie concerne la relation morpho-fonctionnelle unissant la morphologie du crâne et des muscles masticateurs avec la force morsure inférée ou mesurée *in vivo*.

1.1 – Anatomie comparée du crâne de plusieurs espèces de souris (article soumis dans *Journal of Morphology*).

Au sein des rongeurs, les murinés constituent la sous-famille la plus diversifiée en terme de nombre d'espèces. Leur diversité écologique est non moins importante, et la morphologie osseuse de leur mandibule et de leur crâne a été étudiée d'un point de vue éco-morphologique (e.g. Maestri et al. 2016, Michaux et al. 2007, Renaud et Auffray 2010, Renaud et Michaux 2007, Rowe et al. 2011, Samuels 2009). Pourtant, les descriptions de leur musculature masticatrice ainsi que les études d'anatomie comparée restent rares. Curieusement (et bien que l'utilisation du rat et de la souris comme organismes modèles soit relativement ancienne), la majorité de la littérature s'intéressant à la myologie et à l'anatomie comparée du crâne des rongeurs ne s'est pas focalisée sur les murinés. D'autres groupes de rongeurs ont été décrits (notamment parmi les hystricognathes / Ctenohystrica, voir par exemple Woods 1972, Hautier et Saksiri 2009, Hautier et al. 2012), tandis que parmi les Muridae, ce sont les Cricetinae qui semblent avoir reçu le plus d'intérêt (Rinker 1954, Satoh et Iwaku 2004). Parmi les murinés, seul le rat (Greene 1955, Hiiemae et Houston 1971, Cox et Jeffery 2011), et plus récemment la souris (Patel 1978, Baverstock et al. 2013) ont été décrits de manière exhaustive.

La variabilité musculaire et osseuse du crâne entre diverses espèces de murinés reste donc peu explorée. Dans cette section, la musculature masticatrice de quelques espèces de souris est décrite, sur la base de dissections digitales et conventionnelles (voir Introduction - Cadre méthodologique et les *Material and Methods* de l'article). Cette méthode connaît actuellement un essor (cf. Cox et Jeffery 2011, Hautier et al. 2012, Baverstock et al. 2013) qui relance en même temps l'intérêt pour des études comparées de la musculature. L'utilisation d'agents de contraste en microtomographie est non-destructive, réversible, et a l'avantage par rapport aux dissections manuelles de permettre de visualiser tous les muscles en place, liés au crâne (y compris chez des espèces de petite taille).

La description de nouvelles espèces permet à la fois d'élargir notre vision de la variabilité au sein des murinés, mais aussi de comparer la lignée des rats à celle des souris, ainsi que de s'intéresser aux différences liées à la taille et à des variation de régimes alimentaires.

One skull to rule them all? Descriptive and comparative anatomy of the masticatory apparatus in five mice species based on traditional and digital dissections.

Authors:

Samuel Ginot[1], Julien Claude[1], Lionel Hautier[1]

Institutional addresses:

[1] Institut des Sciences de l'Evolution de Montpellier, Université Montpellier, CNRS, IRD, EPHE, Cc 064; place Eugène Bataillon, 34095 Montpellier Cedex 5, France.

Abstract. Murine rodents display a unique cranial morphology and masticatory musculature. Yet detailed myological descriptions are scarce, especially considering the great diversity of the subfamily and the use of the house mouse and brown rat as model organisms. The masticatory musculature in these two species has been thoroughly described, which allows comparisons with other wild species. Description and comparison of a wide range of species constitutes a necessary step to fully understand how ecological factors may influence the morphology and myology of the skull in the Murinae and *vice versa*. In this study, we describe the masticatory musculature of five mice species: *Mus caroli*, *Mus cervicolor*, *Mus pahari*, *Mus fragilicauda*, and *Mus minutoides*. For each species, one to five specimens were dissected, and their muscle weights and volumes calculated. One specimen was selected for iodine-enhanced CT-scanning, which allowed us to digitally reconstruct the musculature. We then compared the different masticatory arrangements between these species, as well as with the previous descriptions of the house mouse and brown rat. We showed that interspecific differences especially involved the temporalis muscle and zygomatico-mandibularis muscular groups, although

some differences were also seen in the pterygoid muscle and masseter muscle groups. We then proposed some ecological interpretations for these differences, by interpreting them in terms of functional differences.

Keywords. Murinae, masticatory musculature, dissection, iodine-enhanced CT-scan, skull myology.

Introduction

Skull morphology and its associated masticatory musculature are unique in rodents, particularly within the Murinae. In the latter, the skull is said to be myomorphous, displaying both a zygomatic plate and a large infraorbital foramen (Wood 1965, Cox et al. 2012, Hautier et al. 2015). Both these bony structures are linked to the attachment of the adductor muscles on the mandible. Because of this unique association of anatomical features, the skull myology of murines (Murinae, Muridae) has attracted a lot of attention, especially in the morpho-functional and ecomorphological domains (e.g. Hiiemae 1971, Hiiemae and Houston 1971, Weijs and Dantuma 1975, Satoh 1997, 1998, 1999, Satoh and Iwaku 2006, 2009, Fabre et al. 2017). Since the house mouse has been intensively used as a model organism, cranio-facial developmental studies enable to link changes in skull morphology with variations in muscular constraints (e.g. Byron 2004, Willmore et al. 2006, Hallgrimsson and Lieberman 2006). In a study comparing the rat to the squirrel and guinea pig, Cox and Jeffery (2011) proposed that myomorphous rodents, more particularly murids, should be considered as "high-performance generalists", which may explain their great evolutionary success. However, what may apply to the brown rat (*Rattus norvegicus*), or the house mouse (*Mus musculus*), may not be applicable to the rest of the tremendous diversity of the Muridae. The tendency to extrapolate patterns seen in these two model species to the rest of murine or even murid rodents raises the possibility that a larger morphological diversity has been overlooked.

So far, studies have only focused on a handful of species, and detailed descriptions of the masticatory apparatus among murine rodents are rare. Indeed, only the house mouse (e.g. Baverstock et al. 2013), the brown rat (e.g. Greene 1955, Cox and Jeffery 2011), the large Japanese field mouse (*Apodemus speciosus*), and *Hydromys chyrogaster,* an Australasian carnivorous water-rat (Satoh 1997, 1998, 1999, Satoh and Iwaku 2006, 2009, Fabre et al. 2017), have been thoroughly described. When comparing to the diversity of the group (i.e., over 600 murine species, Musser and Carleton 2005), our

knowledge of their muscular interspecific variation appears rather limited. In some cases, only laboratory mice were used (e.g. Baverstock et al. 2013), while controlled conditions may bias muscular development, notably due to the use of uniform pellets that deviate from what animals usually eat in the wild (Ginot et al. 2018).

Biomechanical models generally provide precise estimations of functional outputs such as bite force or gape angle (e.g. Satoh and Iwaku 2006, Fabre et al. 2017, Ginot et al. 2018), which in turn are often related to the ecology and diet. Yet, the lack of knowledge about how masticatory musculature actually varies among species may hinder proper characterizations of the evolutionary constraints acting on this complex and integrated system. Descriptive and comparative anatomy of the murine masticatory apparatus is therefore a prerequisite for improving our understanding of how it may function and evolve.

In this study, we describe the masticatory muscles in five species of mice, including three of the five *Mus* subgenera. These include one species of lab-reared African pygmy mouse, *Mus (Nannomys) minutoides*. The four remaining species are represented by wild-caught specimens from Southeast Asia: *Mus (Coelomys) pahari*, *Mus (Mus) cervicolor*, *Mus (Mus) caroli*, and *Mus (Mus) fragilicauda*. To do so, we combined traditional dissections to obtain the masses and volumes of the muscles, and virtual dissections with iodine-enhanced CT-scanning to perform 3D reconstruction of soft tissues (see for example Cox and Jeffery 2011, Baverstock et al. 2013). While they represent only a very small fraction of murine diversity, these five species include one dwarf species (*M. minutoides*), one insectivorous species (*M. pahari*), and three generalist omnivores often found in sympatry or syntopy in Southeast Asia (Auffray et al. 2003; field observations). Variations in muscular arrangement may be found due to size constraints (*M. minutoides*), specialized diet (*M. pahari*), character displacement in the syntopic species, and/or may reflect phylogenetic divergence among the taxa. These five species will also be compared to *Mus musculus* (Baverstock et al. 2013), *Rattus norvegicus* (Cox and Jeffery 2011), and

Hydromys chrysogaster (Fabre et al. 2017). This study will represent one of the first attempts to broaden the amount of thorough descriptions of the murine masticatory complex, and the first to look at variation within a genus, which we hope will stimulate interest in the variation of myology at a fine phylogenetic scale and future functional and ecological studies.

Materials and Methods

Specimens

Wild specimens were caught by live traps during two field campaigns in Thailand. After measuring bite force (see Ginot et al. 2018), the mice were euthanized by CO2 inhalation and dissected for collecting parasitological and genomic samples. The heads were then cut off and stored in 70% ethanol until further treatment. The same protocol was used on lab-reared specimens of *M. minutoides* from a colony kept at the animal facilities at the University of Montpellier. The species studied include, by order of increasing size: *M. minutoides, M. caroli, M. cervicolor, M. fragilicauda and M. pahari*. Wild rodent specimens included in the study are neither on the CITES list, nor the Red List (IUCN). Animals were treated in accordance with the guidelines of the American Society of Mammalogists, and within the European Union legislation guidelines (Directive 86/609/EEC). Approval notices for trapping and investigation of rodents were provided by the Ethical Committee of Mahidol University, Bangkok, Thailand, number 0517.1116/661.

Dissections and muscular data

We dissected as many specimens as were available for each species: *M. caroli* n=4; *M. cervicolor* n=10; *M. fragilicauda* n =2; *M. minutoides* n=2; *M. pahari* n=2. Because of the small size of the skulls, dissections were usually done under a binocular microscope. Only one side was dissected, to allow for

iodine-enhanced CT-scanning of the other side. Muscle insertions and origins were noted, and each muscle was kept in an individual tube of 70% ethanol for weighing. We blotted the muscles dry and weighed them with a 0.01mg Sartorius A 120 S precision scale. Muscular volumes were obtained based on their mass and a density of 1.06 $g.cm^{-3}$ (Mendez and Keys 1960), to be compared with 3D reconstructed volumes (see next section).

Iodine-enhanced CT-scanning

For each species, one specimen was selected based on approximate age (obtained via reproductive status and tooth wear for wild specimens, exact age was available for the lab specimens) and state of conservation. In all cases, we tried to use representative adult individuals with undamaged skulls. However, some damage occurred during dissections, especially with very delicate skulls in *M. minutoides*. We therefore used the best preserved specimen. Before staining, we ran a first scan on each specimen so the bones could be more easily reconstructed by 3-D image analysis.

We then stained our specimens following the protocol described in Cox and Jeffery (2011) and Baverstock et al. (2013). We first fixed the heads in a 4% formaldehyde solution, and placed them in a 3.75% I2KI solution dissolved in 1x PBS (phosphate buffered saline). The specimens were left in this contrast agent for 14 days, checking regularly for satisfactory contrasts in the soft tissues. After CT-scanning, the specimens were placed in PBS to remove the iodine staining, they were then skeletonized for conservation. All skulls are now stored at the Institut des Sciences de l'Evolution, University of Montpellier.

The heads were scanned at resolution of 18 µm using a Skyscan 1076 micro-CT scan with parameters optimizing the contrast. The CT images were then reconstructed using the software Nrecon, and imported in ImageJ 1.48k, to create raw files. The raw files were imported in Avizo 9.3.0 and segmented manually using the segmentation function. To improve the speed of the manual

segmentation, we used the interpolation function every 10 slices. After doing so for the first scan (to segment bones) and for the second (for the muscles), we used the "register" function of Avizo to match bones and muscles 3D reconstructions. All surfaces created were smoothed at an intermediate level, which preserves details but does not completely erase the "blocky" look of the muscles (contrary to Cox and Jeffery 2011 and Baverstock et al. 2013). It should also be noted that our iodine-enhanced scans did not allow us to reconstruct all tendons and aponeuroses (contrary to Baverstock et al. 2013), which explains why some muscles may appear detached from the bones in the reconstructions (notable in the zygomaticomandibularis muscle groups in particular). The reconstructed volumes therefore represent only the muscular part of the muscles. Volumes for each muscle (mm^3) were estimated with built-in functions from Avizo 9.x, and compared with volumes obtained from the dissections to control for the impact of potential shrinkage due to iodine staining. 3D reconstructions of the specimens were deposited in MorphoMuseum (http://www.morphomuseum.com/; M3#XXx).

Nomenclature

We followed the muscular nomenclature used in several recent papers (e.g. Cox and Jeffery 2011, Baverstock et al. 2013, but see Druzinsky et al. 2011 for correspondence with other nomenclature), which separates the masticatory musculature in three groups, each divided in several parts. The masseter muscle complex is composed of a superficial layer (superficial masseter muscle), a median layer (anterior and posterior deep masseter muscle), and a medial layer (the zygomaticomandibularis muscle) separated in three parts (infraorbital, anterior and posterior). The temporalis muscle is separated between its lateral and medial parts. The latter part is composed of two units (one orbital and one posterior), which are always continuous but will be often described individually since they display very different fiber orientations. Finally, the pterygoid muscle is composed of an internal and an external part, referring to their respective origin on the skull. This nomenclature was chosen to match

150 the one used by Cox and Jeffery (2011) and Baverstock et al. (2013), but also because it is consistent
151 with the nomenclature commonly used in other groups of mammals (Druzinsky et al. 2011).
152
153 *Comparison with previously described species*
154 All quantitative data (*i.e.* muscular masses or percentages of total mass) on *Rattus norvegicus*, *Mus*
155 *musculus*, and *Hydromys chrysogaster* were taken from the literature (Cox and Jeffery 2011;
156 Baverstock et al. 2013; Fabre et al. 2017). All qualitative characters (*e.g.* insertions and origins of
157 muscles) were assessed from figures or descriptions presented in these articles. *Melomys obiensis* could
158 also be included in the quantitative comparison of muscle proportions, but was not described in details
159 or figured in Fabre et al.'s (2017) article, and therefore it was not included in the qualitative
160 comparisons. *Apodemus speciosus* was left out of all comparisons due to the use of a different
161 nomenclature and dissection protocol (Satoh 1997).
162
163 **Results**
164 Table 1 shows the average weights and volumes of muscles obtained from dissections for each
165 species. Figure 1 represents the average percentages of total muscular mass for each muscle in all
166 species studied here. Both are derived from the manual dissections of several specimens. Table 2 shows
167 volumes obtained for the 3D reconstructions from Avizo. Muscular volumes from dissections and 3D
168 reconstructions are correlated (slope = 0.94, $t = 8.4$, $df = 47$, $P < 0.001$), but 3D volumes are generally
169 larger than dissection volumes (median dissection/3D volume ratio = 0.58). Table 3 synthesizes the
170 differences between species in the anatomical characters that vary the most. Below are detailed
171 qualitative descriptions of the masticatory muscles for each species, based on dissections as well as 3D
172 reconstructions.
173

Muscle mass in mg													
species	specimen	DM.ant	DM.pos	M.sup	Pt.ext	Pt.int	Tp.l-O	Tp.lat	Tp.med	Zyg.ant	Zyg.l-O	Zyg.pos	Total mass
Mus caroli	7195	8,8	7,9	8,6	1,2	4,3	2,2	1,6	4,9	1,5	1,5	1	43,5
Mus caroli	7225	10,4	9,7	12	2,2	4,9	2,9	2,8	6,1	1	2,7	1,3	56
Mus caroli	7236	9,1	7,3	7,8	2,4	3,5	1,5	1	7,2	NA	2,2	0,8	42,8
Mus caroli	7264	8,6	9,4	7,1	2,6	2,2	1,3	0,8	5,5	2,7	NA	0,8	41
Mus cervicolor	7255	5,2	6,9	7,3	3	6,2	1,63	1,63	1,63	NA	2,1	2,1	37,69
Mus cervicolor	7258	4,1	4,6	6,3	1	1	1,2	NA	2,6	NA	1,1	1,1	23
Mus cervicolor	7259	5,5	6,7	7,6	3,6	5	1,6	1,4	4,4	1,3	1,1	0,2	38,4
Mus cervicolor	7262	7,8	5,7	8,1	2,3	5,3	2,6	0,1	5,2	1,7	2,2	0,7	41,7
Mus cervicolor	7263	6,4	3,9	6,3	0,9	3,4	0,1	0,1	3,7	3,2	NA	0,1	28,1
Mus cervicolor	7286	6	7,9	7,4	1,4	2,4	0,8	1,2	3,9	1,2	NA	1,2	33,4
Mus cervicolor	7304	7,3	6,4	9,2	5,4	6	2,1	0,1	9	2,1	2,1	0,1	49,8
Mus cervicolor	7313	6,3	6,7	9,2	1,6	5,6	1,6	1,1	3,8	1,2	0,9	0,7	38,7
Mus cervicolor	7314	12,8	10	15,2	4,4	10,3	4,2	2,4	9,3	1,6	3,9	0,9	75
Mus cervicolor	7315	7,4	9,5	11,5	1,8	4,7	2,8	2,3	6,5	NA	3,2	0,6	50,3
Mus fragilicauda	7254	5,6	16,6	15,3	4,1	4	2,3	NA	12,7	NA	5,6	0,8	67
Mus fragilicauda	7261	3,7	5,5	6,4	0,1	1,9	0,2	1,4	2,6	NA	1,5	0,6	23,9
Mus minutoides	minut1	3	3,4	3,3	2	3	NA	2,4	2,4	1,6	1,6	1,6	24,3
Mus minutoides	minut2	3,6	4,4	5,2	1,5	3,1	NA	0,1	4	1,3	1,3	0,1	24,6
Mus pahari	7226	9,1	16,7	16,1	4	13,5	7,8	3,7	5,4	NA	4,1	0,8	81,2
Mus pahari	7235	11,4	12	13,5	0,8	3,5	1,2	0,7	7	NA	5,6	0,7	56,4
Av. *Mus caroli*		9,23	8,58	8,88	2,1	3,73	1,98	1,55	5,93	1,73	2,13	0,98	46,82
Av. *Mus cervicolor*		6,88	6,83	8,81	2,54	4,99	1,86	1,15	5	1,76	2,08	0,77	42,67
Av. *Mus fragilicauda*		4,65	11,05	10,85	2,1	2,95	1,25	1,4	7,65	NA	3,55	0,7	46,15
Av. *Mus minutoides*		3,3	3,9	4,25	1,75	3,05	NA	1,25	3,2	1,45	1,45	0,85	24,45
Av. *Mus pahari*		10,25	14,35	14,8	2,4	8,5	4,5	2,2	6,2	NA	4,85	0,75	68,8
Muscle mass in percentage of total muscle mass													
% *Mus caroli*		19,71	18,33	18,97	4,49	7,97	4,23	3,31	12,67	3,7	4,55	2,09	100
% *Mus cervicolor*		16,12	16,01	20,65	5,95	11,69	4,36	2,7	11,72	4,12	4,87	1,8	100
% *Mus fragilicauda*		10,08	23,94	23,51	4,55	6,39	2,71	3,03	16,58	NA	7,69	1,52	100
% *Mus minutoides*		13,5	15,95	17,38	7,16	12,47	NA	5,11	13,09	5,93	5,93	3,48	100
% *Mus pahari*		14,9	20,86	21,51	3,49	12,35	6,54	3,2	9,01	NA	7,05	1,09	100
% *Hydromys chrysogaster*		12	7,2	25,1	8,4	4,2	NA	16,2	9	4,2	2,4	4,8	100
% *Melomys obiensis*		20,2	10,7	19	8,2	3,8	NA	14,5	6,6	5,6	2,7	3,2	100
% *Rattus norvegicus*		14,91	19,43	20,42	3,33	8,29	NA	7,73	19,14	1,59	4,24	0,94	100
% *Mus musculus*		33,32	NA	19,13	4,74	11,56	NA	5,22	17,22	4,72	2,15	1,06	100

Table 1. Individual specimen and species average (Av.) masses of the masticatory muscles dissected, and average percentages (%) of total muscular mass represented by each muscle (also including data from Cox and Jeffery 2011, Baverstock et al. 2013 and Fabre et al. 2017). Abbreviations : DM.ant, anterior deep masseter muscle ; DM.post, posterior deep masseter muscle ; M.sup, superficial masseter muscle ; Pt.ext, external pterygoid muscle ; Pt.int, internal pterygoid muscle ; Tp.o, orbital part of the medial temporalis muscle ; Tp.med, medial temporalis muscle ; Tp.lat, lateral temporalis muscle ; Zyg.ant, anterior zygomaticomandibularis muscle ; Zyg.io, infraorbital zygomaticomandibularis muscle ; Zyg.pos, posterior zygomaticomandibularis muscle.

Species	Specimen	DM.ant	DM.pos	M.sup	Pt.ext	Pt.int	Tp.l-O	Tp.lat	Tp.med	Zyg.ant	Zyg.l-O	Zyg.pos
Mus caroli	7264	13,639	9,371	10,496	8,555	5,017	7,957	3,540	4,619	5,026	1,862	1,413
Mus pahari	7226	17,863	16,134	19,159	19,737	8,219	12,780	5,371	8,024	4,655	7,033	1,922
Mus fragilicauda	7261	8,895	7,384	7,761	4,788	7,638	NA	1,724	10,882	1,063	3,471	1,320
Mus cervicolor	7314	17,547	11,710	14,369	7,359	13,860	NA	5,293	19,399	1,796	6,797	1,854
Mus minutoides	minut1	6,311	5,602	8,008	3,214	6,185	NA	1,199	7,166	3,014	1,242	0,488

Table 2. Individual muscle volumes (mm3) obtained from 3D reconstructions in Avizo 9.x. Abbreviations : DM.ant, anterior deep masseter muscle ; DM.post, posterior deep masseter muscle ; M.sup, superficial masseter muscle ; Pt.ext, external pterygoid muscle ; Pt.int, internal pterygoid muscle ; Tp.o, orbital part of the medial temporalis muscle ; Tp.med, medial temporalis muscle ; Tp.lat, lateral temporalis muscle ; Zyg.ant, anterior zygomaticomandibularis muscle ; Zyg.io, infraorbital zygomaticomandibularis muscle ; Zyg.pos, posterior zygomaticomandibularis muscle.

	Mus caroli	*Mus cervicolor*	*Mus fragilicauda*	*Mus minutoides*	*Mus pahari*	*Mus musculus*	*Rattus norvegicus*	*Hydromys chrysogaster*
Anterior development of muscular fibers of superficial masseter	++	0	+	0	+	+	+	+
Length of anterior deep masster	+	++	+	0	+	NA	+	+
Orientation of anterior deep masseter	Vertical	Oblique (anterodorsal-posteroventral)	Oblique (anterodorsal-posteroventral)	Oblique (anterodorsal-posteroventral)	Oblique (anterodorsal-posteroventral)	NA	Oblique (anterodorsal-posteroventral)	Oblique (anterodorsal-posteroventral)
Shape of posterior deep masseter	Short rectangle	Oval	Long parallelogram	Long parallelogram	Long parallelogram	NA	Oval (with straight anterior edge)	Short oval
Extension of muscular fibers of anterior zygomaticomandibularis	Ventral : 0 Posterior : ++	Ventral : 0 Posterior : ++	Ventral : + Posterior : 0	Ventral : + Posterior : +	Ventral : + Posterior : ++	Ventral : ++ Posterior : ++	Ventral : 0 Posterior : ++	Ventral : ++ Posterior : ++
Insertion of anterior zygomaticomandibularis	Short aponeurosis	Short aponeurosis	Long aponeurosis	Long aponeurosis	Long aponeurosis	Long aponeurosis	NA	Short aponeurosis
Extension of infraobrital zygomaticomandibularis	Ventral : 0 Posterior : 0	Ventral : ++ Posterior : +	Ventral : ++ Posterior : +	Ventral : 0 Posterior : 0	Ventral : + Posterior : +	Ventral : 0 Posterior : +	Ventral : ++ Posterior : +	Ventral : ++ Posterior : +
Insertion of infraobrbital zygomaticomandibularis	Long and thin tendon	Short tendon	Short tendon	Long and thin tendon	Short tendon	Long and thin tendon	NA	Short aponeurosis
Length of posterior zygomaticomandibularis	+	++	+	++	0	++	0	++
Dorsal extension of lateral temporal	++	+	0	0	++	0	++	++
Insertion area of lateral temporal	+	++	+	+	+	0	++	++
Development of medial temporal (posterior part)	++	++	++	0	+	+	++	++
Development of medial temporal (orbital part)	+	++	++	+	++	+	0	+
Attachement on zygomatic process of squamosal bone	+	+	+	0	+	+	++	++
Development of internal pterygoid compared to external pterygoid	+	+	0	+	++	++	NA	NA
Concavity of ventral side of internal pterygoid	+	++	+	++	0	+	NA	NA

Table 3. Synthetic view of interspecific differences in the most variable anatomical characters found in this study, including species from this study, as well as Cox and Jeffery 2011, Baverstock et al. 2013 and Fabre et al. 2017. Character codes are the following: 0 = reduced, + = developed, ++ = very developed.

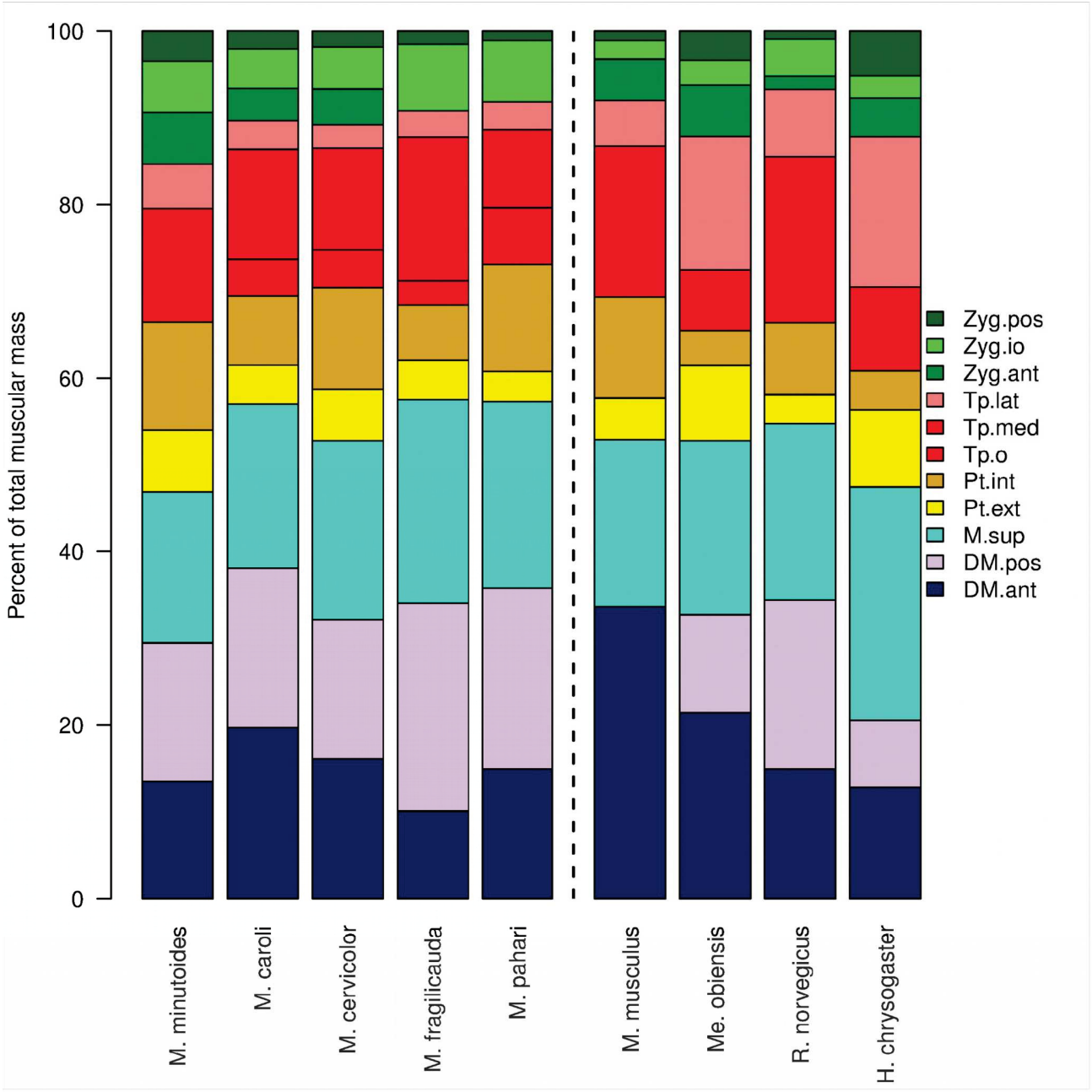

Figure 1. Barplot showing the percentage of total muscular mass for each individual muscle in the five species studied. Abbreviations : DM.ant, anterior deep masseter muscle ; DM.post, posterior deep masseter muscle ; M.sup, superficial masseter muscle ; Pt.ext, external pterygoid muscle ; Pt.int, internal pterygoid muscle ; Tp.o, orbital part of the medial temporalis muscle ; Tp.med, medial temporalis muscle ; Tp.lat, lateral temporalis muscle ; Zyg.ant, anterior zygomaticomandibularis muscle ; Zyg.io, infraorbital zygomaticomandibularis muscle ; Zyg.pos, posterior zygomaticomandibularis muscle.

In all species, we were able to separate the anterior and posterior part of the deep masseter muscle using both traditional and virtual dissections. Although the orbital and posterior parts of the medial

182 temporalis muscle are linked, they could generally be separated in the dissections except in *M.*
183 *minutoide*s (Tab. 1, Fig. 1). In 3D reconstructions, the location of their separation was often unclear.
184 The lateral temporalis muscle could always be separated from the medial temporalis muscle in
185 traditional dissections, although the iodine-enhanced scans also revealed some interconnections with
186 the medial temporalis muscle. The three parts of the zygomaticomandibularis muscle were generally
187 easy to tell apart in both traditional and virtual dissections. In *M. pahari* and *M. fragilicauda*, we were
188 not able not separate the anterior and infraorbital parts during the dissections (both parts are therefore
189 combined in Fig. 1 and Tab. 1), although we found some separations in the 3D reconstructions. Finally,
190 the internal and external pterygoid muscles were easily separated in the traditional dissections.
191 However, the latter was often difficult to dissect in its entirety due to its internal position in the skull,
192 and was therefore more precisely characterized using the 3D reconstructions.
193
194 *Mus caroli* (Fig. 2)
195 Superficial masseter muscle
196 The superficial masseter muscle represents an important part of the masseteric complex (Fig. 2A
197 and Table 1). It is very long with muscle fibers present even in the most anterior part (Fig. 2A),
198 underlying the strong tendon and almost reaching the origin. It takes its origin on a small rounded
199 process located on the antero-ventral angle of the zygomatic plate, just ventrally to the origin of the
200 anterior deep masseter muscle. The superficial masseter muscle then runs obliquely, and overlies both
201 the posterior and anterior parts of the deep masseter muscle. Its insertion is muscular and runs along the
202 ventral border of the posterior half of the horizontal ramus to the ventral part of the angular process. It
203 also inserts on the medial side of the mandible via a developed *pars reflexa*, which is attached
204 posteriorly to a ridge circumscribed by the incisor alveolus.
205

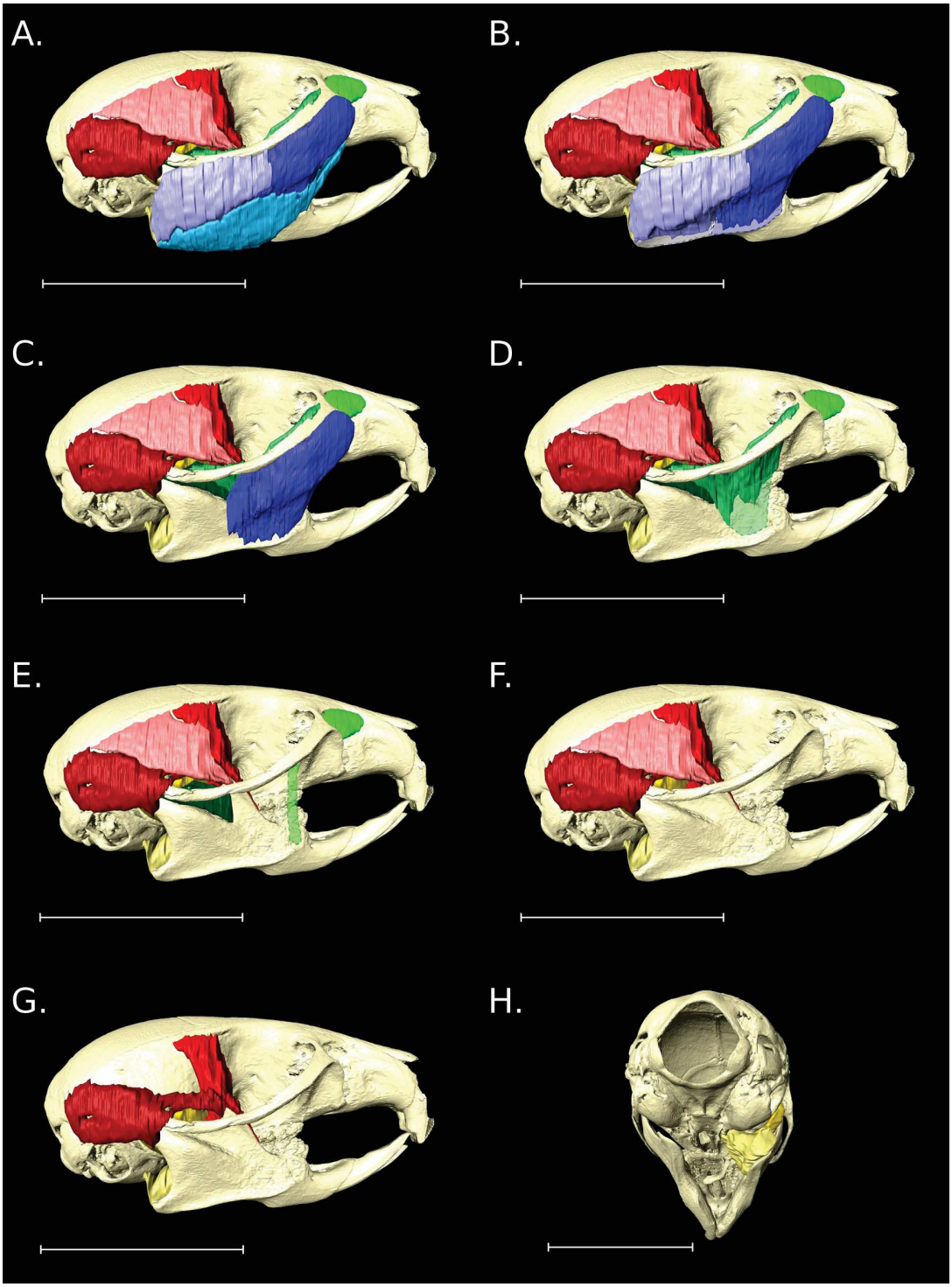

Figure 2. Three-dimensional reconstruction of the masticatory muscles of *Mus caroli*. Colors for the muscles are the same as in Fig. 1, with sky blue: superficial masseter; dark blue: anterior deep masseter; light purple: posterior deep masseter; pink: lateral temporalis; red: medial temporalis; sea green infraorbital zygomaticomandibularis; green: anterior zygomaticomandibularis; dark green: posterior zygomaticomandibularis; yellow: external pterygoid; golden yellow: internal pterygoid. The separation between the orbital and posterior parts of the medial temporalis was often unclear, therefore they were represented by the same color (red) in Fig. 2 to 6. Coloured areas outlined by dashes represent aponeuroses and tendons that were described in the dissections, but could not be segmented in 3D reconstructions. Scale bar = 1cm.

207

208 Anterior deep masseter muscle

209 The anterior part of the deep masseter muscle is also important in size (Fig. 2B-C and Table 1), and
210 can be easily separated from the posterior part, except posteriorly where there appears to be some
211 connexions between the two parts. The anterior part of the muscle is thick and directly originates on the
212 whole surface of the zygomatic plate, as well as along the anterior half of the zygomatic arch. The
213 posterior limit of the origin lies just anteriorly to the suture between the maxillary zygomatic process
214 and the jugal bone (Fig. 2C). The ventral part of the muscle thins down where it underlies the
215 superficial masseter muscle. The muscle inserts on the mandible via a strong and short aponeurosis,
216 which extends from the anterior limit of the masseteric ridge, just ventrally to the first lower molar, to
217 approximately half of the ridge, just dorsally to the maximum curvature of the ramus.

218

219 Posterior deep masseter muscle

220 The posterior part of the deep masseter muscle is also large, and roughly parallelogram-shaped
221 with an extended antero-dorsal part (Fig. 2B). As such, the anterior extremity of its origin laterally
222 overlies the posterior part of the anterior deep masseter muscle. This origin is muscular and runs along
223 the zygomatic arch from a point just anterior to the suture between the maxillary zygomatic process and
224 the jugal to the ventral side of the suture between the jugal bone and the zygomatic process of the
225 squamosal bone, in lateral view. It inserts on the mandible with an aponeurosis running along the dorsal
226 edge of the posterior half of the masseteric ridge.

227

228 Infraorbital zygomaticomandibularis muscle

229 Although it is thick within the infraorbital foramen, and developed along the rostrum, the
230 infraorbital part of the zygomaticomandibularis muscle is rather short, and undeveloped posteriorly

(Fig. 2D-E). It inserts on the mandible by a long aponeurosis, which attaches anteriorly to that of the anterior zygomaticomandibularis muscle, ventrally to the first lower molar.

Anterior zygomaticomandibularis muscle

The anterior zygomaticomandibularis muscle is the longest of the three parts of the zygomaticomandibularis muscle, but is rather thin (Fig. 2D-E). Its origin extends along the medial side of the zygomatic plate, from the posterior border of the zygomatic plate, to the medio-ventral side of the suture between the jugal bone and the zygomatic process of the squamosal bone. Its insertion is comparatively shorter. It attaches dorsally to the anterior masseteric ridge by an aponeurosis, just medially and dorsally to the anterior part of the insertion of the anterior deep masseter muscle.

Posterior zygomaticomandibularis muscle

The posterior zygomaticomandibularis muscle is comparatively smaller than the two other parts. It originates from the medial side of the zygomatic process of the squamosal bone, posteriorly to its suture with the jugal bone (Fig. 2E). It is oriented obliquely and inserts on the mandible in the fossa located between the posterior part of the incisor alveolus and the postero-ventral part of the coronoid process.

Lateral temporalis muscle

The lateral part of the temporalis muscle is wide and long, but thin (Fig. 2E-F). Its origin extends along most of the temporal crest. From this origin, the muscle runs obliquely and overlies the medial temporalis muscle. Its insertions area is limited to the most dorsal part of the lateral side of the coronoid process.

Medial temporalis muscle

The medial temporalis muscle is much more developed than its lateral counterpart (Fig 2F-G). It is particularly developed posteriorly and extends to the suture between the parietal and occipital bones. Its origin covers most of the lateral side of the parietal and squamosal bones. This posterior part is also developed ventrally, overlying the post-tympanic hook of the squamosal and the dorsal border of the tympanic bulla. More anteriorly, it also overlies the zygomatic process of the squamosal bone, and likely covers the posterior edge of the condylar process (Fig 2C-G). It is linked to the orbital part by a thin strip of muscle, which extends anteriorly and ventrally. The orbital part of the medial temporalis muscle is also important. Its origin extends from the anterior part of the parietal crest to the frontal crest of the posterior part of the orbit (Fig. 2G). It then extends deep into the orbit, where it joins with the extension of the posterior part of the muscle. The fibers insert on a large area that covers the medial side of the coronoid process and extends ventrally to the back of the teeth row.

Internal pterygoid muscle

The internal pterygoid muscle is comparatively more developed than its external counterpart, especially in its posterior half (Fig. 2G-H). It originates muscularly from a fossa located posteriorly to the upper tooth row, between the external and internal pterygoid processes. The muscle thickens posteriorly; its ventral side is slightly concave. It inserts on the mandible on the medial side of the angular process and extends anteriorly and almost reaches the *pars reflexa* of the superficial masseter muscle.

External pterygoid muscle

Although less voluminous than the internal pterygoid muscle, the external pterygoid muscle is longer and extends from the mandibular condyle to the posterior end of the upper tooth row (Fig 2G-

H). It originates muscularly posteriorly and laterally to the upper third molar, and covers the lateral and ventral (delimited by the external pterygoid process) sides of the basisphenoid bone and the ventralmost part of the squamosal. Its insertion is also muscular and located on the medial side of the condylar process of the mandible.

Mus cervicolor (Fig. 3)

Superficial masseter muscle

In *M. cervicolor*, the superficial masseter muscle represents an important part of the masseteric complex. Its muscular part is short (Fig. 3A), linked by a strong tendon to its origin. This tendon is attached on a marked process located on the ventral edge of the zygomatic plate, slightly posteriorly to the anterior edge of the plate. The superficial masseter muscle then runs obliquely, overlying the posterior part of the anterior deep masseter muscle and the ventralmost border of the posterior deep masseter muscle. Its insertion is muscular and runs along the ventral border of the posterior half of the ramus to cover the ventral and posterior part of the angular process. It also inserts on the medial side of the mandible with a small *pars reflexa*, which is attached posteriorly to the ventral part of the ridge formed by the incisor alveolus.

Anterior deep masseter muscle

The anterior part of the deep masseter muscle is also well-developed (Fig. 3B-C) and can be easily separated from the posterior part, although there appears to be some connexions between the two parts posteriorly. The muscle is thick and directly originates on the whole surface of the zygomatic plate, and along the anterior half of the zygomatic arch. The posterior part of the origin extends much posteriorly (Fig. 3C). The ventral part does not thin down strongly as in *M. caroli*. The muscle inserts by a strong and short aponeurosis on the mandible from the anterior limit of the masseteric ridge, just ventrally to

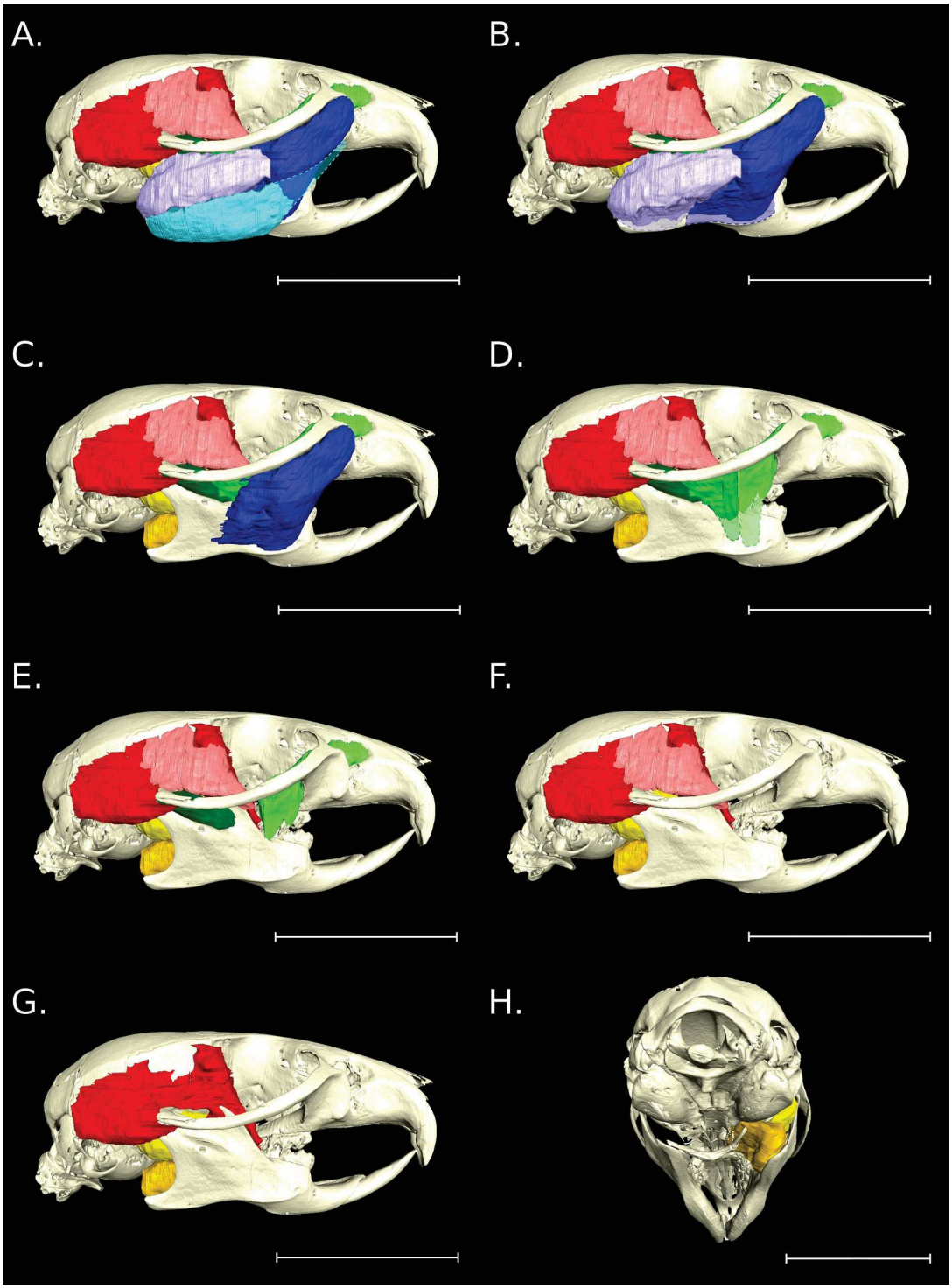

Figure 3. Three-dimensional reconstruction of the masticatory muscles of *Mus cervicolor*. Colors for the muscles are the same as in Fig. 1, with sky blue: superficial masseter; dark blue: anterior deep masseter; light purple: posterior deep masseter; pink: lateral temporalis; red: medial temporalis; sea green infraorbital zygomaticomandibularis; green: anterior zygomaticomandibularis; dark green: posterior zygomaticomandibularis; yellow: external pterygoid; golden yellow: internal pterygoid. The separation between the orbital and posterior parts of the medial temporalis was often unclear, therefore they were represented by the same color (red) in Fig. 2 to 6. Coloured areas outlined by dashes represent aponeuroses and tendons that were described in the dissections, but could not be segmented in 3D reconstructions. Scale bar = 1cm.

304 the first lower molar, and extends more posteriorly than its area of origin.

305

306 Posterior deep masseter muscle

307 The posterior part of the deep masseter muscle appears narrower than the superficial and anterior
308 parts of the masseter muscle. It is oval-shaped and oriented parallel to the superficial masseter muscle
309 (Fig. 3A-B). The anterior extremity of the origin laterally overlies the posterior part of the anterior deep
310 masseter muscle. This origin is muscular and runs along the zygomatic arch from a point ventral to the
311 suture between the maxillary zygomatic process and the jugal bone to a point anterior and ventral to the
312 suture between the jugal bone and the zygomatic process of the squamosal bone. It inserts on the
313 mandible via an aponeurosis that runs along the posterior half of the masseteric ridge, but covers only
314 the dorsal edge of the angular process.

315

316 Infraorbital zygomaticomandibularis muscle

317 The infraorbital zygomaticomandibularis muscle is larger than its anterior counterpart (Fig. 3D-E).
318 Its origin extends from the rostrum, through the infraorbital foramen, as well as on the medial side of
319 the zygomatic plate and the medial side of the maxillary zygomatic process. It inserts by a strong
320 aponeurosis, anteriorly and ventrally to the insertion of the anterior zygomaticomandibularis muscle.

321

322 Anterior zygomaticomandibularis muscle

323 The anterior zygomaticomandibularis muscle is the shortest of the three parts of the
324 zygomaticomandibularis muscle. However, its separation with the infraorbital part is unclear (Fig. 3D-
325 E). Its origin extends along the middle part of the zygomatic arch, and appears limited to the jugal
326 bone. Its insertion lies ventrally to the second lower molar, medially and dorsally to the insertion of the
327 anterior deep masseter muscle.

328

329 Posterior zygomaticomandibularis muscle

330 The posterior zygomaticomandibularis muscle originates from the medial side of the zygomatic
331 process of the squamosal bone, and extends to the posterior tip of the jugal bone (Fig. 3E). It is oriented
332 obliquely and inserts on the mandible in the fossa between the posterior part of the incisor alveolus, and
333 the postero-ventral part of the coronoid process.

334

335 Lateral temporalis muscle

336 The lateral part of the temporalis muscle is developed posteriorly and dorsally, but thin in its
337 postero-dorsal part (Fig. 3E-F). Its origin extends along the anterior half of the parietal crest, but does
338 not reach the orbit. The muscle then runs obliquely and ventrally, overlying the medial temporalis
339 muscle, and thickening towards its insertion. Its long insertion area covers the dorsal part of the lateral
340 side of the coronoid process and runs ventrally along the anterior border of the process.

341

342 Medial temporalis muscle

343 The medial temporalis muscle is much more developed than its lateral counter part (Fig 3F-G). It is
344 developed posteriorly and extends to the suture between the parietal and occipital bones. The origin of
345 the muscle covers most of the lateral side of the parietal and squamosal bones. The posterior part is also
346 developed ventrally; it overlies the post-tympanic hook of the squamosal, the dorsal border of the
347 tympanic bulla, and the dorsal edge of the tympanic meatus. More anteriorly, it laterally overlies most
348 of the zygomatic process of the squamosal bone, and projects ventrally and overlies part of the
349 condylar process. The posterior and orbital parts are closely associated with a wide and thick link
350 between them. The orbital part of the medial temporalis muscle is very thick, and oriented slightly
351 anteriorly. Its origin extends from the anterior part of the temporal crest to the back of the orbit (Fig.

352 3G). Both parts join to form an even thicker array of muscular fibers, which runs deep into the orbit
353 and inserts on a wide area on the medial side of the coronoid process, the anterior part of the condylar
354 process, as well as on the ramus, posteriorly to the second lower molar.
355
356 Internal pterygoid muscle
357 The internal pterygoid muscle is comparatively more developed than its external counterpart,
358 particularly in terms of width (Fig. 3G-H). It originates from the pterygoid muscle fossa, between the
359 external and internal processes of the pterygoid bone. The ventral side of the muscle is very concave
360 (Fig. 3H). It inserts on the medial side of the angular process of the mandible and extends anteriorly
361 almost to the *pars reflexa* of the superficial masseter muscle.
362
363 External pterygoid muscle
364 The external pterygoid muscle is longer and thinner than its internal counterpart. It extends from
365 the ventral border of the most posterior part of the condylar process to the back of the upper tooth row
366 (Fig 3G-H). Its origin is located just posteriorly and laterally to the upper third molar; it covers the
367 lateral and ventral (delimited by the external pterygoid process) sides of the basisphenoid bone and the
368 ventral part of the squamosal. Its muscular insertion is located on the medial side of the condylar
369 process of the mandible.
370
371 *Mus fragilicauda* (Fig. 4)
372 Superficial masseter muscle
373 The superficial masseter muscle represents an important part of the masseter muscles. It is long,
374 with a muscular anterior part, although it ends with a tendon (Fig. 4A). The origin is attached on a
375 small round process, oriented slightly anteriorly and located on the antero-ventral side of the zygomatic

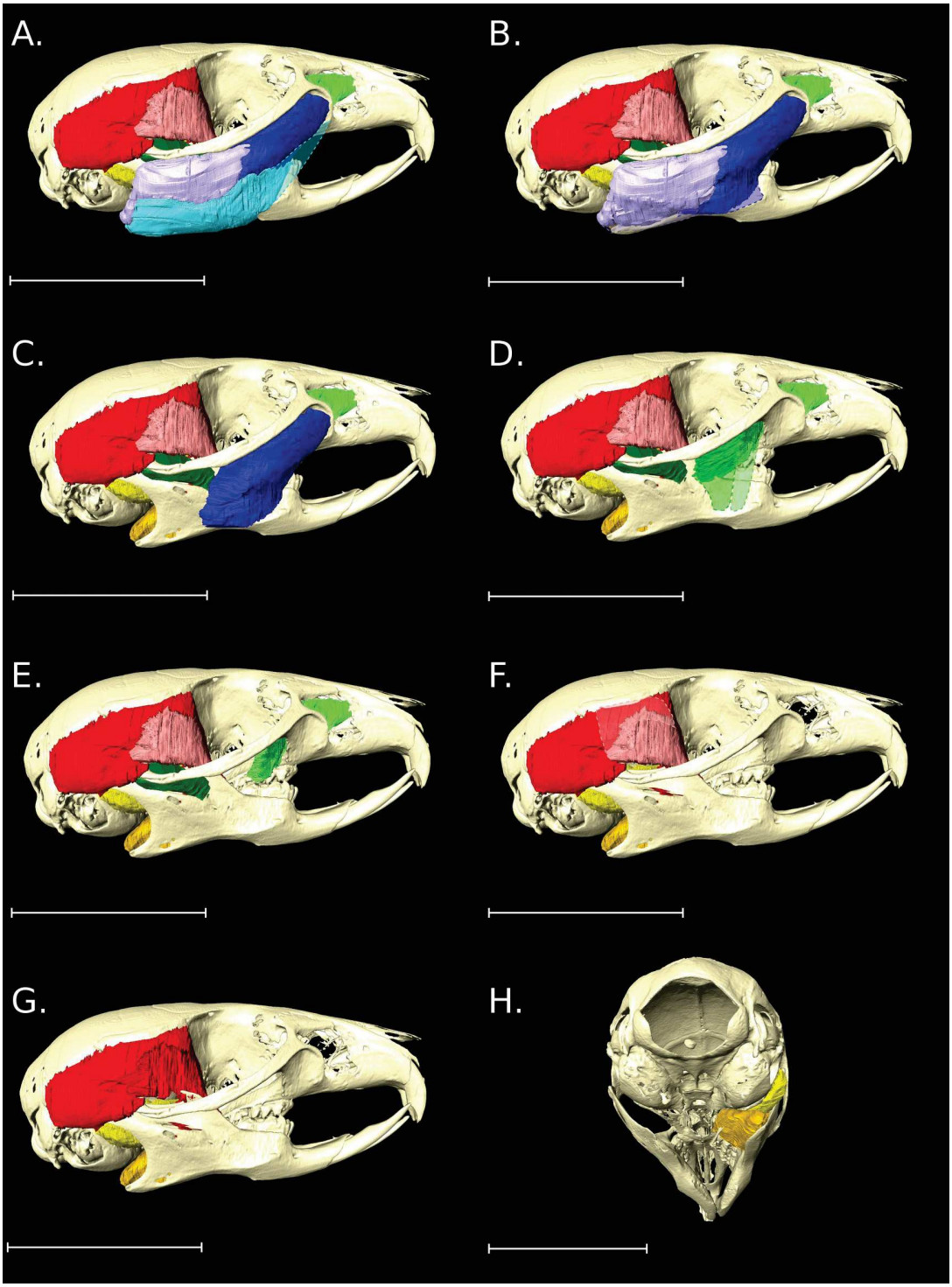

Figure 4. Three-dimensional reconstruction of the masticatory muscles of *Mus fragilicauda*. In this species, the skull could not be reconstructed, and is shown only in transparent surface rendering. Colors for the muscles are the same as in Fig. 1, with sky blue: superficial masseter; dark blue: anterior deep masseter; light purple: posterior deep masseter; pink: lateral temporalis; red: medial temporalis; sea green infraorbital zygomaticomandibularis; green: anterior zygomaticomandibularis; dark green: posterior zygomaticomandibularis; yellow: external pterygoid; golden yellow: internal pterygoid. The separation between the orbital and posterior parts of the medial temporalis was often unclear, therefore they were represented by the same color (red) in Fig. 2 to 6. Coloured areas outlined by dashes represent aponeuroses and tendons that were described in the dissections, but could not be segmented in 3D reconstructions. Scale bar = 1cm.

plate, just ventrally to the anterior border of the origin of the anterior deep masseter muscle. The anterior part of the superficial masseter muscle is oriented ventrally and overlies the anterior part of the deep masseter muscle. Posteriorly, the superficial masseter muscle is oriented almost horizontally where it overlies the ventral half of the posterior deep masseter muscle; it widens in its posterior half before reaching the insertion area. Its insertion is muscular and runs along the ventral border of the posterior half of the ramus to the ventral part of the angular process. It also inserts on the medial side of the mandible with a long and wide *pars reflexa*, oriented postero-dorsally and attached to the ridge formed by the incisor alveolus.

Anterior deep masseter muscle

The anterior part of the deep masseter muscle is also important, although it appears less developed than the two other parts of the masseter muscle (Fig. 4B-C). The dorsal part of the muscle is slender and projects anteriorly. It does not extend posteriorly (Fig. 4C). The origin of the muscle runs from the zygomatic plate to the middle of the zygomatic arch. The ventral part of the muscle is markedly thinner than the rest, which is due to the development of the superficial masseter muscle. The muscle insertion extends more posteriorly than its area of origin; it inserts on the mandible by a strong aponeurosis from the anterior limit of the masseteric ridge, just ventrally to the first lower molar, to more than half of the ridge. The muscular part of the muscle does not extend much ventrally.

Posterior deep masseter muscle

The posterior part of the deep masseter muscle roughly forms a large parallelogram, with its upper and lower side oriented almost parallel to the tooth row (Fig. 4B). The antero-dorsal and postero-ventral parts of the muscle are particularly extended, and the antero-ventral part is reduced. Its origin is muscular and runs along the posterior half of the zygomatic arch from a point ventral to the suture

between the maxillar and the jugal bones to a point just antero-ventral to the suture between the jugal and the squamosal bones. It inserts on the mandible by an aponeurosis that runs along the posterior half of the masseteric ridge, to the tip and dorsal edge of the angular process. The postero-ventral part of the muscle is thinner than its dorsal part, due to the superficial masseter muscle overlying it.

Infraorbital zygomaticomandibularis muscle

The infraorbital zygomaticomandibularis muscle is much larger than its anterior counterpart (Fig. 4D-E). It is long, but does not extend much ventrally, similarly to the anterior zygomaticomandibularis muscle. Its origin on the rostrum is long, and is continuous on the medial side of both the zygomatic plate and the zygomatic process of the maxillary. Like the anterior zygomaticomandibularis muscle, its muscular fibers are not very developed ventrally; it inserts on the mandible by a long aponeursis, anteriorly and ventrally to the insertion of the anterior zygomaticomandibularis muscle.

Anterior zygomaticomandibularis muscle

The anterior zygomaticomandibularis muscle is small and diamond-shaped (Fig. 4D-E). It does not easily separate from the infraorbital part of the zygomaticomandibularis; however, it is well separated from the posterior part (Fig. 4D). Its origin is located on the medial side of the zygomatic process of the maxillary and extends to the anterior part of the jugal bone. The muscular fibers do not extend much ventrally; they insert on the mandible via a long aponeurosis ventrally to the second lower molar.

Posterior zygomaticomandibularis muscle

The posterior zygomaticomandibularis muscle is long and oriented obliquely, with a more ventral position in its anterior half (Fig. 4D-E). Its posterior half is thicker than the anterior one. Its origin lies on the medial side of the posterior end of the zygomatic arch, on the zygomatic process of the

425 squamosal bone. It is oriented ventrally in its anterior half so that its insertion area is located on the
426 ventral border of the coronoid process.
427
428 Lateral temporalis muscle
429 The lateral temporalis muscle is reduced, and comparatively much smaller than the medial
430 temporalis muscle (Fig. 4F). In particular, its muscular fibers do not reach dorsally the temporal crest;
431 its antero-ventral part is thin and does not develop ventrally. Consequently, the origin of the muscle is
432 an aponeurosis that extends dorsally to the parietal, although some muscular fibers also seem to be
433 intertwined with the medial temporalis muscle. The insertion area is small and limited to the dorsal tip
434 of the lateral side of the coronoid process.
435
436 Medial temporalis muscle
437 The medial temporalis muscle is one of the most important muscles (Fig. 4F-G). Its area of origin
438 extends along most of the lateral side of the braincase, on the frontal, squamosal and parietal bones, and
439 reaches the suture between the parietal and supraoccipital bones posteriorly. The posterior part of the
440 medial temporalis muscle extends ventrally on the post-tympanic hook, but does not overlie the
441 tympanic bulla. More anteriorly it also attaches on the zygomatic process of the squamosal. The orbital
442 part of the temporalis muscle is not developed dorsally, but thickens ventrally and is tightly linked to
443 the posterior part. The muscle extends deep in the orbit and inserts of the medial side of the coronoid
444 process and part of the ramus, and reaches the incisor alveolus and the back of the tooth row.
445
446 Internal pterygoid muscle
447 The internal pterygoid muscle is short antero-posteriorly, although it is rather wide medio-laterally
448 (Fig. 4G-H). It originates from the fossa located posteriorly to the upper tooth row, between the

449 external and internal pterygoid processes. The ventral side of the muscle is slightly concave (Fig. 4H).
450 It inserts on the mandible on the medial side of the angular process but does not extend much
451 anteriorly. Furthermore, its posterior half does not appear to entirely cover the angular process and is
452 widely separated from the ventral border of the external pterygoid muscle (Fig. 4G).
453
454 External pterygoid muscle
455 The external pterygoid muscle is much longer, as well as thinner than its internal counterpart. It
456 extends from the most posterior part of the condylar process, reaching the anterior edge of the tympanic
457 bulla, to the back of the upper tooth row (Fig 4G-H). Its origin is located just posteriorly and laterally
458 to the upper third molar, and covers the lateral and ventral sides of the basisphenoid bone (delimited by
459 the external process of the pterygoid bone) and the ventral part of the squamosal. Its insertion is
460 muscular, and located in the middle of the medial side of the condylar process of the mandible.
461
462 *Mus minutoides* (Fig. 5)
463 Superficial masseter muscle
464 The superficial masseter muscle represents the most important part of the masseter muscles (Fig.
465 5A). The anterior part of the muscle is wide and attached via a strong tendon on a marked and antero-
466 posteriorly developed process, which is located anteriorly to the ventral edge of the zygomatic plate.
467 The superficial masseter muscle then runs obliquely and overlies the postero-ventral part of the anterior
468 deep masseter muscle and the most ventral third of the posterior deep masseter muscle. Its insertion is
469 muscular and runs along the ventral border of the posterior half of the ramus and covers the ventral part
470 and the whole angular process. It also inserts on the medial side of the mandible with a small *pars*
471 *reflexa*, which is attached posteriorly to the ventral part of the ridge formed by the incisor alveolus.
472

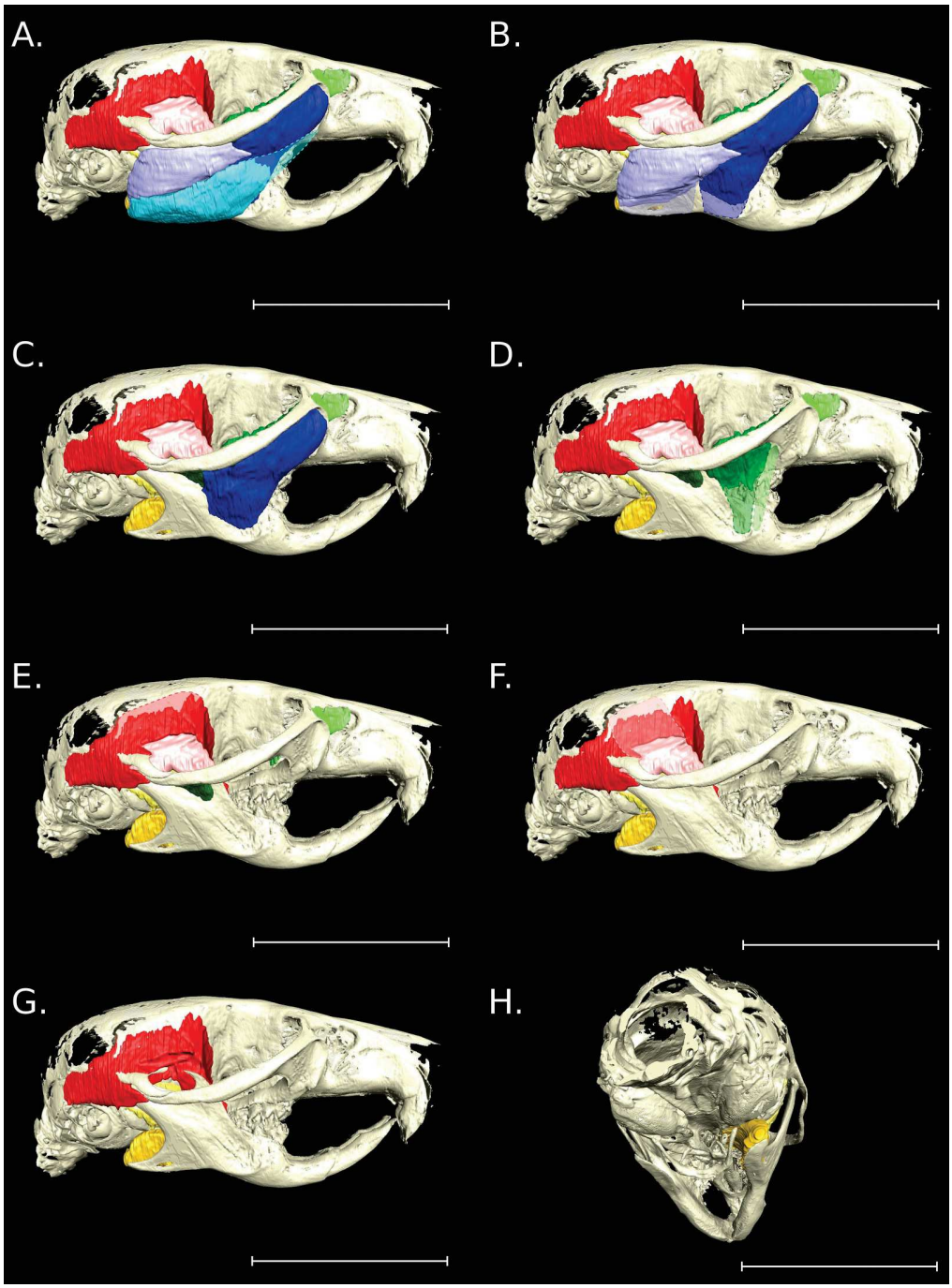

Figure 5. Three-dimensional reconstruction of the masticatory muscles of *Mus minutoides*. Colors for the muscles are the same as in Fig. 1, with sky blue: superficial masseter; dark blue: anterior deep masseter; light purple: posterior deep masseter; pink: lateral temporalis; red: medial temporalis; sea green infraorbital zygomaticomandibularis; green: anterior zygomaticomandibularis; dark green: posterior zygomaticomandibularis; yellow: external pterygoid; golden yellow: internal pterygoid. The separation between the orbital and posterior parts of the medial temporalis was often unclear, therefore they were represented by the same color (red) in Fig. 2 to 6. Coloured areas outlined by dashes represent aponeuroses and tendons that were described in the dissections, but could not be segmented in 3D reconstructions. Scale bar = 1cm.

Anterior deep masseter muscle

The anterior part of the deep masseter muscle is also important, especially in its anterior half (Fig. 5B-C). This part of the muscle is thick and developed anteriorly, in association with the anterior projection of the zygomatic plate. The origin of the muscle runs from the zygomatic plate to more than half of the zygomatic arch, reaching the jugal bone (Fig. 5C). The ventral part of the muscle is thinner than the rest, due to the presence of the superficial masseter muscle. The muscle does not extend much ventrally, and is therefore attached to the mandible by a strong aponeurosis. Its insertion area spreads from the anterior part of the masseteric ridge, ventrally to the second lower molar, to approximately half of the masseteric ridge, more anteriorly than the posterior limit of the origin area.

Posterior deep masseter muscle

The posterior part of the deep masseter muscle is roughly parallelogram shaped, oriented horizontally (Fig. 5B). However, the antero-dorsal part of the muscle is greatly extended anteriorly and overlies the postero-dorsal part of the anterior deep masseter muscle. Its origin area is long and extends from the anterior side of the suture between the maxillary and the jugal bones to the posterior side of the ventral suture between the jugal and the squamosal bones. On the other hand, its insertion area is shorter and runs along the masseteric ridge and starts posterior to the maximum ventral curvature of the mandible to extend just before to the tip of the angular process. The ventral part of the muscle underlies the superficial masseter muscle, and is thinner than its dorsal part.

Infraorbital zygomaticomandibularis muscle

The infraorbital zygomaticomandibularis muscle is reduced in length, comparatively to its anterior counterpart (Fig. 5E). It passes through the infraorbital foramen and occupies only a small portion of the rostrum. Its origin is limited to the rostrum and to the medial side of the zygomatic plate. The

498 infraorbital zygomaticomandibularis therefore inserts on the mandible by a lengthy tendon, which
499 attaches ventrally to the first lower molar; its fibers do not extend ventrally below the zygomatic plate.
500
501 Anterior zygomaticomandibularis muscle
502 The anterior zygomaticomandibularis muscle is the longest of the three parts of the
503 zygomaticomandibularis muscle (Fig. 5D-E). It is particularly developed anteriorly, but is not in
504 contact with the posterior zygomaticomandibularis muscle postero-ventrally. Its origin extends from the
505 dorsal part of the zygomatic plate, to the half of the zygomatic arch, at the level of the suture between
506 the maxillary and the jugal bones. Its muscular fibers extend ventrally to the level of the upper tooth
507 row; hence, the muscle inserts by an aponeurosis ventrally to the first and second lower molars.
508
509 Posterior zygomaticomandibularis muscle
510 The posterior zygomaticomandibularis muscle is the smallest of the three parts of the
511 zygomaticomandibularis muscle (Fig. 5E). It originates from the medial side of the zygomatic arch, at
512 the level of the dorsal suture between the jugal and squamosal bones. It then runs obliquely through the
513 fossa between the incisor alveolus and coronoid process, and inserts along the ventral part of the
514 coronoid process.
515
516 Lateral temporalis muscle
517 The lateral temporalis muscle is small and thin, especially in its posterior part (Fig. 5F). It is
518 generally difficult to separate from the medial temporalis muscle, due to some dorsal intertwining of
519 the fibers. The muscle does not reach the parietal bone dorsally, but is attached to it by a large
520 aponeurosis (not visible in 3D reconstructions). The muscle thickens slightly in its antero-ventral part,
521 and inserts along the anterior edge of the lateral side of the dorsal tip of the coronoid process.

522

523 Medial temporalis muscle

524 The medial temporalis muscle is extended posteriorly, and reaches the suture between the parietal
525 and occipital bones (Fig. 5G). It is not much developed dorso-ventrally, and does not cover the
526 zygomatic squamosal process or the tympanic bulla. It does extend over the posterior part of the
527 condylar process, but does not overlie its ventral edge.

528

529 Internal pterygoid muscle

530 The internal pterygoid muscle is an important muscle, larger than its external counterpart (Fig.
531 5H). It originates from the fossa located posteriorly to the upper tooth row between the external and
532 internal pterygoid processes, and reaches the anterior edge of the tympanic bulla. The medio-ventral
533 side of the muscle is very concave. The insertion area of the internal pterygoid muscle covers the whole
534 medial side of the angular process, which is rather small in this species, and extends anteriorly to reach
535 the insertion area of the superficial masseter muscle *pars reflexa*.

536

537 External pterygoid muscle

538 The external pterygoid muscle is smaller than its internal counterpart. It extends from the posterior
539 part of the condylar process to the back of the upper tooth row (Fig 5G-H). Its origin is located just
540 posteriorly and laterally to the upper third molar, over the lateral side of the basisphenoid and the
541 ventral part of the squamosal. Its insertion is muscular, and covers the middle of the medial side of the
542 condylar process of the mandible from its ventral to its dorsal edge (Fig. 5G).

543

544 *Mus pahari* (Fig. 6)

545 Superficial masseter muscle

546 The superficial masseter muscle is the most important of the three parts of the masseter muscle. It
547 is developed both antero-posterioly and dorso-ventrally (Fig. 6A). It overlies the ventral halves of both
548 the anterior and posterior deep masseter muscles. It is particularly wide in its anterior part, and to a
549 lesser extent in its posterior third. The muscle originates by a tendon attached to an undeveloped
550 process located anteriorly along the ventral edge of the zygomatic plate. It inserts strongly over the
551 border of the entire posterior half of the mandible, but also covers the angle and the ventral part of the
552 angular process. It inserts on the medial side of the mandible by a very long *pars reflexa*, which follows
553 the posterior half of the incisor alveolus.
554
555 Anterior deep masseter muscle
556 The anterior deep masseter muscle is smaller than its posterior counterpart (Fig. 6B-C) but its
557 anterior part is wide. It originates from the zygomatic plate, continuing posteriorly along the ventral
558 edge of the zygomatic arch to a point posterior to the suture between the maxillary and the jugal bones.
559 The muscle extends ventrally with an oblique orientation; its ventral half underlies the superficial
560 masseter muscle. It inserts along the anterior edge of the masseteric ridge from a point ventral to the
561 first lower molar to approximately half of the masseteric ridge (Fig. 6C).
562
563 Posterior deep masseter muscle
564 The posterior deep masseter muscle is the most important muscle of the masseter muscle group. It
565 forms a long parallelogram oriented horizontally, with its antero-dorsal angle slightly overlying the
566 anterior deep masseter muscle (Fig. 6 B). Both muscles can be easily separated. Its origin is located on
567 most of the posterior half of the zygomatic arch from the suture between the jugal and maxillary bones
568 to the posterior side of the ventral suture between the jugal and the squamosal bones. The muscle is
569 thick but thins down slightly ventrally where it underlies the superficial masseter muscle. The insertion

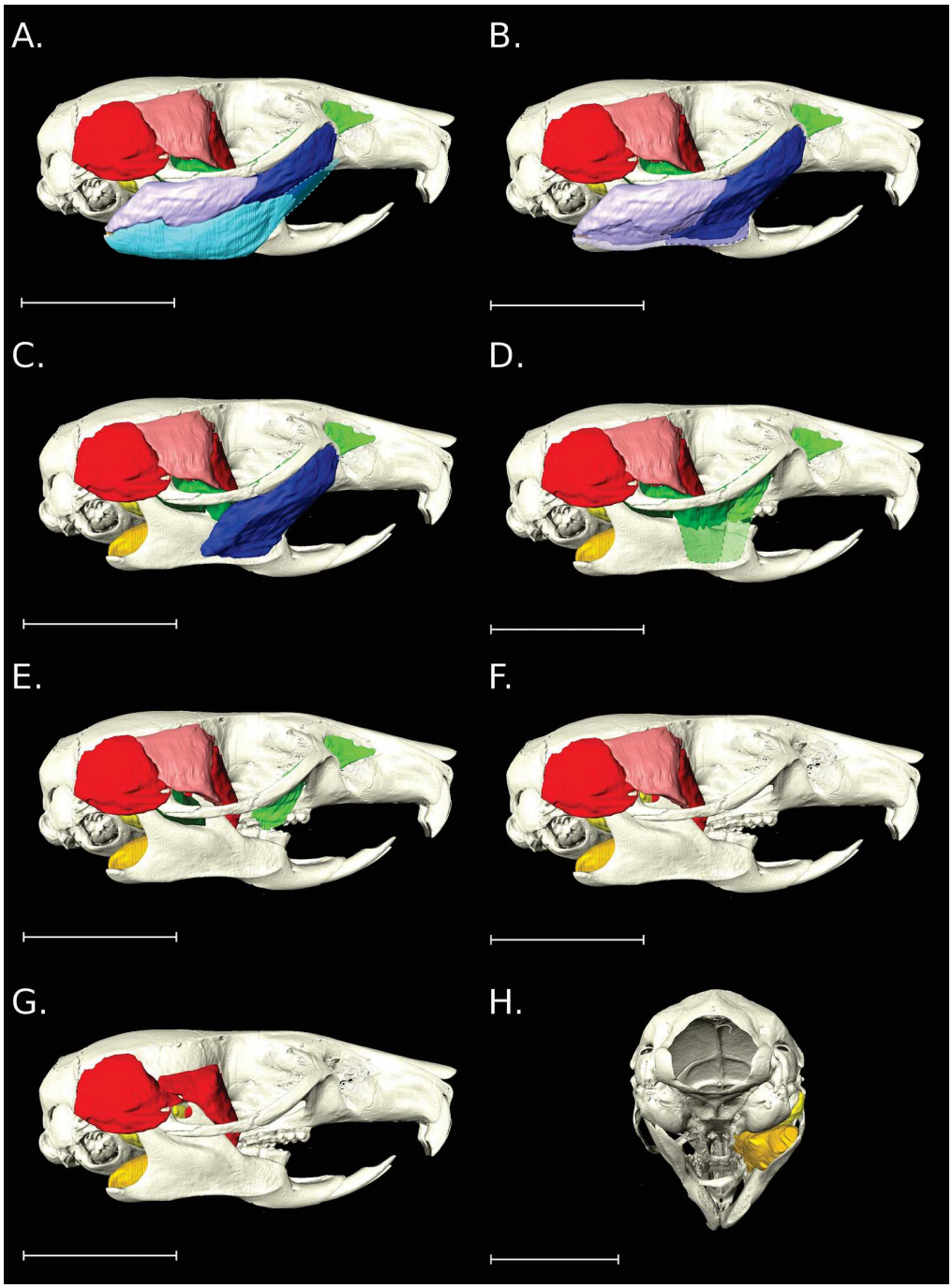

Figure 6. Three-dimensional reconstruction of the masticatory muscles of *Mus pahari*. Colors for the muscles are the same as in Fig. 1, with sky blue: superficial masseter; dark blue: anterior deep masseter; light purple: posterior deep masseter; pink: lateral temporalis; red: medial temporalis; sea green infraorbital zygomaticomandibularis; green: anterior zygomaticomandibularis; dark green: posterior zygomaticomandibularis; yellow: external pterygoid; golden yellow: internal pterygoid. The separation between the orbital and posterior parts of the medial temporalis was often unclear, therefore they were represented by the same color (red) in Fig. 2 to 6. Coloured areas outlined by dashes represent aponeuroses and tendons that were described in the dissections, but could not be segmented in 3D reconstructions. Scale bar = 1cm.

571 area runs along the posterior half of the masseteric ridge to the dorsal edge of the angular process.

572

573 Anterior zygomaticomandibularis muscle

574 The anterior zygomaticomandibularis muscle is developed antero-posteriorly along the zygomatic
575 arch (Fig. 6D). Its origin extends on the medial side of the arch, from a point anterior to the suture
576 between the maxillary and the jugal bones, posteriorly to the dorsal suture between the jugal and the
577 squamosal bones. The muscle extends ventrally only in its middle part to reach the ventral border of the
578 lower tooth row. It inserts by an aponeurosis ventrally to the second and third lower molars. The
579 anterior and infraorbital zygomaticomandibularis muscle could not be clearly separated using
580 traditional dissections, although they were separable in the 3D reconstructions.

581

582 Infraorbital zygomaticomandibularis muscle

583 The infraorbital zygomaticomandibularis muscle is also mainly developed antero-posteriorly (Fig.
584 6D-E). Its rostral part is thin but much extended anteriorly. The origin extends form the rostrum and the
585 medial side of the zygomatic plate, to the anterior side of the suture between the maxillary and the jugal
586 bones. In its posterior half, the fibers of the infraorbital extend postero-ventrally approximately to the
587 level of the second upper molar (Fig. 6E). It inserts on the mandible by an aponeurosis located just
588 anterior to that of the anterior zygomaticomandibularis muscle and ventrally to the first lower molar.

589

590 Posterior zygomaticomandibularis muscle

591 The posterior zygomaticomandibularis muscle is shorter than both other parts (Fig. 6E). Its anterior
592 part is reduced dorsally due to the presence of the posterior half of the anterior zygomaticomandibularis
593 muscle (Fig. 6D). The muscle thickens posteriorly, but is limited to the space between the condylar
594 process and the posterior end of the zygomatic arch. The origin of the muscle is therefore restricted to

595 the posterior half of the zygomatic process of the squamosal, while the insertion is mainly on the
596 postero-ventral part of the coronoid process.
597
598 Lateral temporalis muscle
599 The lateral temporalis muscle is rather developed in this species (Fig. 6F). In particular, it extends
600 anteriorly and dorsally to the back of the orbit, covering parts of the parietal and squamosal along the
601 temporal crest. Ventrally, the muscle remains wide, except along the anterior edge of the coronoid
602 process where it inserts.
603
604 Medial temporalis muscle
605 Because of the development of the lateral temporalis muscle, the medial temporalis muscle is
606 reduced in its antero-dorsal part (Fig. 6G). The posterior part is large and extends dorsally to the
607 temporal crest of the parietal, posteriorly to the occipital crest, and ventrally overlies the dorsal edge of
608 the tympanic bulla, the postero-ventral edge of the condylar process, and the posterior end of the
609 zygomatic arch. Although shortened dorsally, the orbital part is particularly thick and wide within the
610 orbit. It inserts on a wide area on the medial side of the orbit. It covers the coronoid process and
611 extends anteriorly to the second lower molar and posteriorly to the posterior end of the incisor alveolus.
612
613 Internal pterygoid muscle
614 The internal pterygoid muscle is much larger than its external counterpart (Fig. 6G-H). It originates
615 from the fossa located posteriorly to the upper tooth row, between the external and internal processes of
616 the pterygoid bone, and reaches the anterior edge of the tympanic bulla (Fig. 6H). The ventral side of
617 the muscle is not concave. The insertion area of the internal pterygoid muscle covers the medial side of
618 the angular process and extends anteriorly to reach the insertion area of the superficial masseter muscle

pars reflexa.

External pterygoid muscle

The external pterygoid muscle is small. It extends from the posterior part of the medial side of the condylar process but does not reach the back of the upper tooth row (Fig 6G-H). Its origin is located much posteriorly and laterally to the upper third molar, over the lateral side of the basisphenoid bone and the ventral part of the squamosal. Its insertion is muscular, and covers the middle of the medial side of the condylar process of the mandible from its ventral to its dorsal edge (Fig. 6G).

Intraspecific variation

Because several specimens were manually dissected in each species, intraspecific variation of muscular mass and proportions could be assessed (Fig. 7). Compared to interspecific differences, intraspecific variation appears to be fairly large, however this may be partly explained by the presence of mixed ontogenetic stages in our sample (subadult and adult specimens), which are difficult to characterize in wild specimens. Still, muscular differences do appear to discriminate between species, either in terms of mass (Fig. 7A, or in terms of proportions (Fig. 7B). In particular, the masseter muscles seem to show limited intraspecific variation (with the exception of *M. fragilicauda*, in which the two specimens had largely different size) compared to interspecific differences.

Discussion

Overall, the insertions and origins of the various masticatory muscles appear to be essentially similar among our sample of mice species. However, some differences can be observed in the muscular organization and proportions (Table 1, Table 3, Fig. 1 to 6). Most of these differences involved the deep masseter muscle, the lateral and medial temporalis muscle, as well as the anterior and infraorbital part

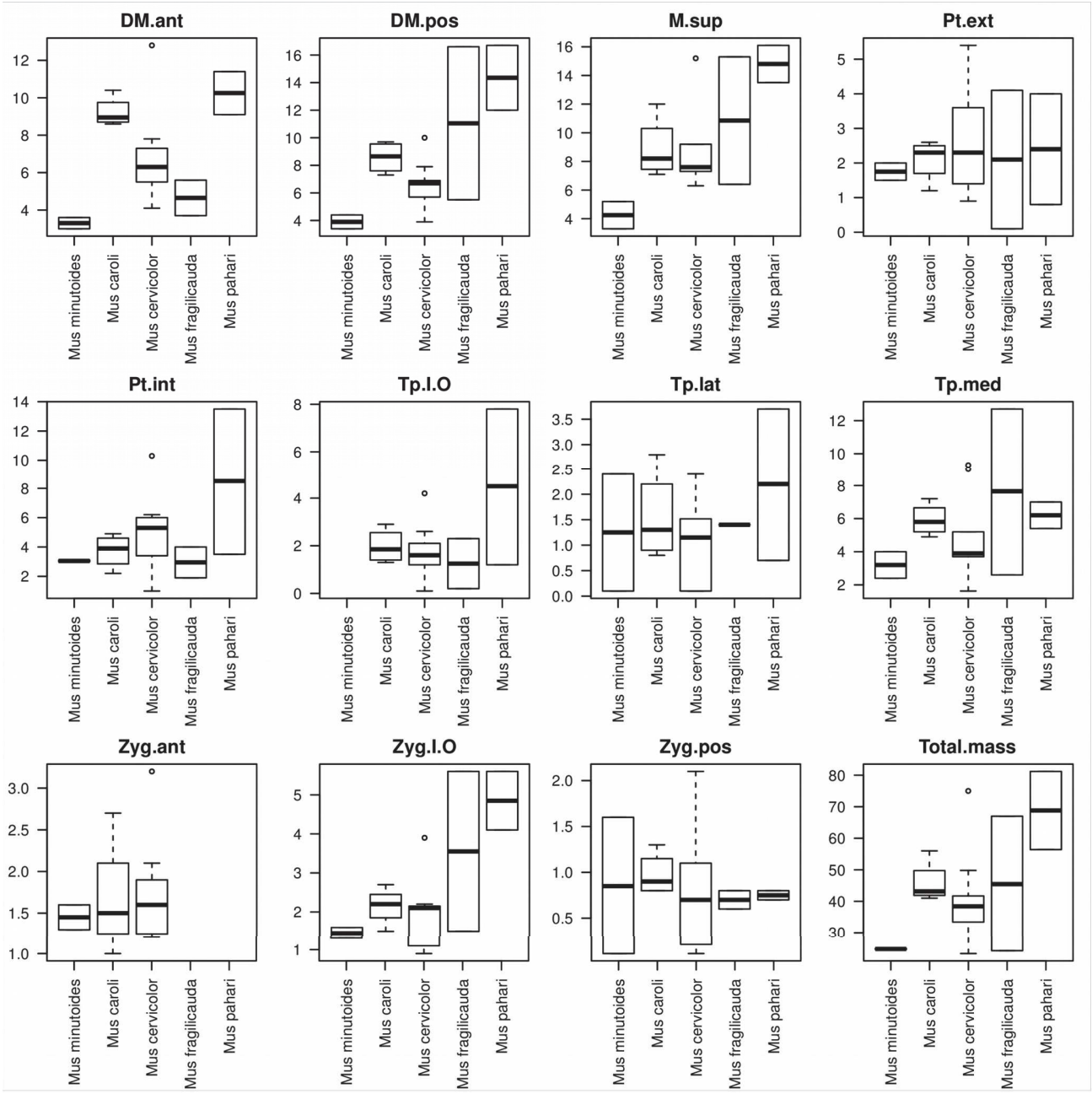

Figure 7. Boxplots showing intraspecific variation and interspecific differences in muscle mass (first set of panels), or in porportion of total muscle mass (second set of panels, see next page). Each panel represents one muscle. Abbreviations: DM.ant: anterior deep masseter; DM.pos: posterior deep masseter; M.sup: superficial masseter; Pt.ext: external pterygoid; Pt.int: internal pterygoid; Tp.I.O: orbital part of the medial temporal; Tp.lat: lateral temporal; Tp.med: posterior part of the medial temporal; Zyg.ant: anterior zygomaticomandibularis; Zyg.I.O: infra-orbital zygomaticomandibularis; Zyg.pos: posterior zygomaticomandibularis. Continued on next page.

643 of the zygomaticomandibularis muscle. Comparison of 3D volumes and dissection volumes (Table 1
644 and 2) suggests that shrinkage due to the iodine staining did not significantly impact our interpretations,

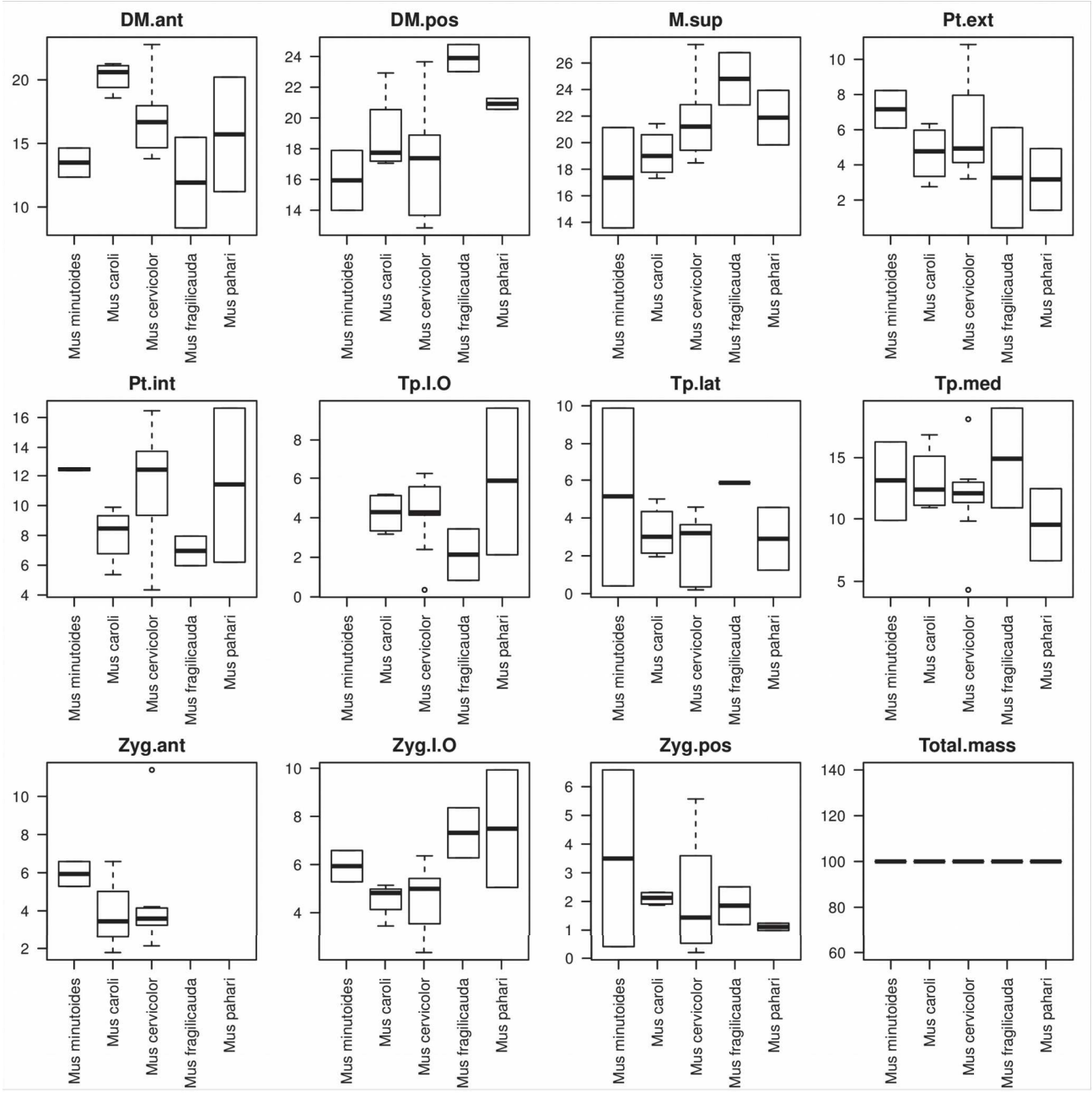

Figure 7 (continued from previous page). Boxplots showing intraspecific variation and interspecific differences in porportion of total muscle mass. Each panel represents one muscle. Abbreviations: DM.ant: anterior deep masseter; DM.pos: posterior deep masseter; M.sup: superficial masseter; Pt.ext: external pterygoid; Pt.int: internal pterygoid; Tp.I.O: orbital part of the medial temporal; Tp.lat: lateral temporal; Tp.med: posterior part of the medial temporal; Zyg.ant: anterior zygomaticomandibularis; Zyg.I.O: infra-orbital zygomaticomandibularis; Zyg.pos: posterior zygomaticomandibularis.

as 3D volumes were generally larger than volumes from dissections. This unexpected result may be explained by the fact that dissection volumes were obtained from the mass of the individual muscles,

647 which were kept in alcohol and then dried before weighting and therefore may have been dehydrated.

648

649 *Muscular differences in our sample of* Mus *species.*

650 Differences are summarized in Table 3. In the superficial masseter muscle, most of the variation is
651 found in the anterior extension of the muscle. In *M. caroli* (Fig. 2A), muscular fibers almost reach the
652 origin of the muscle ventral to the zygomatic plate. In *M. fragilicauda* (Fig. 4A) and *M. pahari* (Fig.
653 6A), the muscle extends to the anterior edge of the first upper molar, while it does not reach this point
654 in *M. cervicolor* (Fig. 3A) and *M. minutoides* (Fig. 5A). In all species, the superficial masseter muscle
655 represents around 20% of total muscle mass (Tab. 1, Fig. 1). In *M. fragilicauda* and *M. pahari*, this
656 proportion is slightly higher (23.5 and 21.5% respectively), correspondingly with their anterior
657 development. However, in *M. caroli* in which the muscle is the most anteriorly extended, the superficial
658 masseter muscle represents only 18.3% of the total muscular mass, showing that the muscle is mainly
659 extended in length, while its volume does not increase as much (although tendon weight could bias
660 these differences). In *M. minutoides*, the superficial masseter muscle represents only 17.4% of the total
661 mass. The superficial masseter muscle is rather short in *M. cervicolor*, but still represents 20.6% of the
662 total muscular mass. In *M. cervicolor*, *M. minutoides*, and *M. pahari*, the superficial masseter muscle is
663 the biggest of the three masseter muscle parts, while it is slightly smaller than the posterior deep
664 masseter muscle in *M. fragilicauda* and smaller than the anterior deep masseter muscle in *M. caroli*.

665 The anterior deep masseter muscle varies mostly in length, which is mainly due to variations in the
666 posterior extension of its insertion and origin. It is particularly long and wide in *M. cervicolor* (Fig.
667 3C), in which the insertion of the muscle reaches the posterior half of the ramus. The anterior deep
668 masseter muscle is also long, but less voluminous in *M. pahari* (Fig. 6C), whereas it is shorter in *M.*
669 *caroli* (Fig. 2C) and *M. fragilicauda* (Fig. 4C) mostly because the insertion area on the mandible is
670 shortened posteriorly. In *M. caroli*, this is combined with a more posteriorly placed area of origin

671 (zygomatic plate), so that the anterior deep masseter muscle is more vertically oriented, while it is
672 oblique in other species. In *M. minutoides* (Fig. 5C), the muscle is shortened posteriorly and ventrally,
673 and does not reach the masseteric ridge of the mandible. In terms of proportion of overall muscular
674 mass, the anterior deep masseter muscle represents 10 to 20% of total mass. It is rather developed in *M.*
675 *cervicolor* (16.1%) that displays a long and wide anterior deep masseter muscle, but it is surprisingly
676 the most voluminous of the three masseter muscles (19.7%) in *M. caroli*, in which it is short. This
677 suggests that in *M. caroli*, the anterior deep masseter muscle is shortened due to a change in its
678 orientation, but at the same time has gained in volume, compared to the rest of the masseter muscles. In
679 *M. pahari*, the muscle is long but less developed ventrally; it represents 14.9% of total muscular mass
680 and is the smallest of the three masseter parts. This is also the case in *M. fragilicauda* and *M.*
681 *minutoides*, in which the anterior deep masseter muscle is less developed and less voluminous
682 compared to other species (with only 10.1 and 13.5% of total mass respectively). *Mus fragilicauda* is
683 the most extreme case of anterior deep masseter muscle reduction, with the other masseter parts
684 representing more than twice its mass. The anterior deep masseter muscle is generally the least
685 important of the three masseter parts, except in *M. cervicolor*, in which it is equivalent to the posterior
686 deep masseter muscle, and *M. caroli* in which it is the largest of the three parts.

687 The shape of posterior deep masseter muscle varies greatly among our sample, especially its
688 antero-posterior length. It usually forms a rough parallelogram, horizontally oriented, with extended
689 antero-dorsal and postero-ventral corners. In *M. caroli* (Fig. 2B), the posterior deep masseter muscle is
690 short, almost rectangular in shape, but its width thickens dorsally. In *M. cervicolor* (Fig. 3B), the
691 muscle is more oval-shaped, due to a shortening of its origin on the zygomatic arch, and a more acute
692 angle of insertion on the mandible. In other species, *M. pahari* (Fig. 6B) in particular, the muscle forms
693 a long parallelogram which is linked to a lengthening of the mandible, and in *M. minutoides* (Fig. 5B)
694 in which the origin of the muscle extends much anteriorly. In terms of mass, the posterior deep

masseter muscle is generally larger than its anterior counterpart, but smaller than the superficial masseter muscle. In *M. caroli* it is the smallest of the three parts, in accordance with its shortened appearance (however still representing 18.3% of total muscular mass). In *M. cervicolor*, the ventral part of the muscle is reduced where it underlies the superficial masseter muscle. Accordingly, it is the smallest of the three masseter parts (16% of total muscle mass), especially compared to the superficial masseter muscle, suggesting a trade-off between the development of both muscles. In *M. fragilicauda* (Fig. 4B) it constitutes the largest part and represents almost 24% of total muscular mass. It is posteriorly extended, almost reaches the posterior limit of the zygomatic arch, and covers most of the angular process. In *M. minutoides* and *M. pahari*, the muscle is the second largest masseter muscle part, after the superficial masseter muscle (15.6 and 20.9% of total mass respectively); both species display an anterior development of this muscle, which overlies a reduced anterior deep masseter muscle.

In some cases, the anterior zygomaticomandibularis muscle was tightly associated with the infraorbital part of zygomaticomandibularis muscle. Although we were able to distinguish them in our 3D reconstructions, the limits between these muscles remain doubtful, and could partly explain variations in their respective proportions. From our 3D reconstructions, we found the anterior zygomaticomandibularis muscle to be proportionally largest in *M. caroli* (Fig. 2D) and *M. minutoides* (Fig. 5D). In other species, this muscle is generally equivalent in size or slightly smaller than the infraorbital zygomaticomandibularis muscle. Most of the shape variation in the anterior zygomaticomandibularis muscle relates to its posterior extension along the zygomatic arch and in the ventral extent of its muscular fibers. In *M. caroli* (Fig. 2D) and *M. cervicolor* (Fig. 3D), the muscular fiber insert on the mandible only by a short aponeurosis. In the other species, they are short ventrally and attach to the mandible by long aponeuroses. In *M. fragilicauda* (Fig. 4D) and to a lesser extent *M. minutoides* (Fig. 5D), the anterior zygomaticomandibularis muscle does not extend much posteriorly, thereby creating a space between itself and the posterior zygomaticomandibularis muscle. In other

719 species, these muscles are always in contact, even if they were easily separated during dissections.

720 The infraorbital zygomaticomandibularis muscle varies mostly in its posterior and ventral
721 extension. In this regard, *M. caroli* (Fig. 2E) and *M. minutoides* (Fig. 5E) display a short infraorbital
722 zygomaticomandibularis muscle that barely extends out of the infraorbital foramen posteriorly. In these
723 species this muscle inserts on the mandible by a long but thin tendon. In other species, especially *M.*
724 *cervicolor* (Fig. 3E) and *M. fragilicauda* (Fig. 4E), the muscle fibers extend ventrally, but do not reach
725 the mandible itself, therefore inserting by a shorter tendon. Overall, the infraorbital and anterior
726 zygomaticomandibularis muscle represent 7 to 12% of the total muscular mass.

727 The posterior zygomaticomandibularis muscle is the smallest of the masticatory muscles,
728 representing only from 1.1 to 3.5% of the total muscular mass. It is sometimes difficult to extract using
729 traditional dissections, but it is easily delimited in the 3D reconstructions. Although it can vary in
730 length and width, its morphology appears fairly stable in our sample. *Mus cervicolor* (Fig. 3E) and
731 especially *M. minutoides* (Fig. 5E) display a slightly longer posterior zygomaticomandibularis muscle
732 than other species although they vary in terms of proportion of the total muscular mass, respectively
733 1.5% and 3.5 %. The muscle is shorter and thinner in *M. pahari* (Fig. 6E), in which the anterior
734 zygomaticomandibularis muscle is extended posteriorly and fills up the space between the mandible
735 and the zygomatic arch. Accordingly, the posterior zygomaticomandibularis muscle only represents
736 1.1% of total muscular mass in this species.

737 Although the lateral temporalis muscle can be easily separated from the medial temporalis muscle
738 at their insertions, their origin on the cranium is often unclear since their muscle fibers are sometimes
739 intertwined in the dorsal part of the lateral temporalis muscle. This is the case in both traditional and
740 virtual dissections. Furthermore, because the lateral temporalis muscle can be very thin in its dorsal
741 part, or end in an aponeurosis, it is commonly torn off during dissections, leaving some fibers or part of
742 the aponeurosis embedded in the medial temporalis muscle. Despite this, the lateral temporalis muscle

743 varies mainly in its dorsal extension, but also in the size of its insertion area on the coronoid process. In
744 *M. caroli* (Fig. 2F), its dorsal part extends much posteriorly and inserts along the temporal crest of
745 parietal bone. The anatomy of the muscle is similar in *M. cervicolor* (Fig. 3F), although less extended
746 posteriorly; its insertion is longer than in all other species, wrapping around the tip of the coronoid
747 process. In *M. fragilicauda* (Fig. 4F) and *M. minutoides* (Fig. 5F), the muscle fibers do not seem to
748 reach the temporal crest. Instead, the muscle originates from a wide aponeurosis. In *M. pahari* (Fig.
749 6F), the lateral temporalis muscle is developed dorsally and reaches the temporal crest, but more
750 anteriorly than in *M. cervicolor* and *M. caroli*, as it also occupies part of the back of the orbit. Even
751 though the lateral temporalis muscle appears more or less developed in our sample, it should be noted
752 that the muscle is very thin, and therefore represents only 3 to 5% of the total muscular mass.

753 The medial temporalis muscle is a much more important muscle than its lateral counterpart in all
754 our species. It can generally be divided up into two parts based on the area of origin and fiber
755 orientation: a posterior and an orbital part. The posterior part constitutes the bulk of the muscle, while
756 the orbital part is generally smaller. Both parts are joined ventrally at the level of the insertion on the
757 medial side of the coronoid process. The posterior part is very large in *M. caroli* (Fig. 2G), *M.*
758 *cervicolor* (Fig. 3G), and *M. fragilicauda* (Fig. 4G), in which it extends posteriorly but also ventrally,
759 reaching the edge of the tympanic bulla. This is also the case in *M. pahari* (Fig. 6G), although the
760 medial temporalis muscle is reduced overall by the presence of a large lateral temporalis muscle.
761 Conversely, it is reduced in terms of width and thickness in *M. minutoides* (Fig. 5G), although it does
762 reach the posterior limit of the parietal. In all species but *M. minutoides*, the medial temporalis muscle
763 also attaches on the zygomatic process of the squamosal bone. In *M. cervicolor*, *M. fragilicauda*, and
764 *M. pahari*, the orbital part of the temporalis muscle medial is large, and the insertion area of the medial
765 temporalis muscle is particularly wide. In all species, the medial temporalis muscle represents over
766 15% of the total muscle mass, the only exception being *M. minutoides* for which the muscle only

767 reaches 13% of the total mass.

768 The pterygoid muscles display very similar insertions and origins in our sample, and their variation
769 is mostly limited to the volume and shape of the muscles. Generally, the internal pterygoid muscle is
770 twice as voluminous as the external pterygoid muscle, which is mainly explained by the fact that the
771 latter is located between the medial side of the mandible and lateral side of the cranium. In *M.*
772 *fragilicauda* (Fig. 4H), however, the internal pterygoid muscle is comparatively reduced, almost of the
773 same size as its external counterpart. In *M. pahari* (Fig. 6H) on the other hand, the internal pterygoid
774 muscle is almost four times as big as the external pterygoid muscle. In terms of proportions, the
775 pterygoid muscles are more important in *M. cervicolor* (Fig. 3H), *M. minutoides* (Fig. 5H), and *M.*
776 *pahari* (Fig. 6H), representing 16 to 20% of the total muscle mass. The internal pterygoid muscle
777 appears to show a more or less important concavity on its ventral side. This concavity is most visible in
778 *M. minutoides* and *M. cervicolor*, suggesting that these species may display a developed tongue and
779 hyoid musclulature.

780 When looking at the species sampled here, classified by increasing size (Fig. 1), no interspecific
781 allometric trend seems to appear, with the exception of the zygomaticomandibularis muscle group,
782 which appears to be proportionally reduced in larger species, or enlarged in smaller species..

783

784 *Comparison with* Mus musculus

785 Because we used similar approaches and methods as Baverstock et al. (2013), we can easily
786 compare our observations with the data and reconstructions they proposed for the house mouse. Our
787 results are very congruent with theirs, in terms of the 3D reconstruction, dissections and muscles
788 masses. Most muscular insertions and origins are similar, and the proportions of each muscular group
789 are very similar. It should be noted that Baverstock and colleagues (2013) used BALB/c albino mice in
790 their study. The overall resemblance between the musculature of this lab bred and lab reared mice and

791 the wild specimens studied here show that, despite many generations of controlled breeding, albino
792 mice still possess a similar organisation of the masticatory apparatus as their wild congenerics. This is
793 despite a large and general increase in terms of absolute muscular mass values in the BALB/c mice
794 used by Baverstock et al. (2013), compared to the wild mice studied here.

795 Its superficial masseter muscle amounts for 19.1%, versus a range of 17.4 to 23.5% in our sample.
796 The deep masseter muscle of the house mouse (Baverstock et al., 2013) represents 33.3% of the total
797 muscle mass, while our values range from 29.4 to 38%. The pterygoid muscle group represents 16.3%
798 of the total muscle mass in the house mouse, while it ranges from 10.1 to 19.6% in our species. Both
799 temporalis muscles represent 22.4% in *Mus musculus*, which is slightly higher than the upper limit for
800 our range of values (18.7 to 22.3%). Finally, the zygomaticomandibularis muscle group in the house
801 mouse (8.1%) reached the inferior limit in our species (ranging from 8.1 to 15.3%).

802 The main qualitative differences between their dissections and ours seem to be limited to the
803 insertions of the anterior and posterior zygomaticomandibularis muscle, which we found to be more
804 extended ventrally, partially reducing the area of insertion of the deep masseter muscle. Moreover, we
805 were able to separate the anterior deep masseter muscle from the posterior part in all our species,
806 although we acknowledge that their fibers may not actually be fully separated in some areas. The
807 anterior zygomaticomandibularis muscle appears much more developed in the house mouse than in any
808 of our species, which may be mainly explained by differences in our reconstructions methods. Indeed,
809 Baverstock et al. (2013) could reconstruct tendon and aponeuroses, while we were not able to do so. In
810 *M. cervicolor*, the insertion of the lateral temporalis muscle was also more extended than in *M.*
811 *musculus*, while it was more similar in all other species. Our data corroborate the finding that part of
812 the the medial temporalis muscle attaches at the back of the zygomatic arch (*i.e.* on the zygomatic
813 process of the squamosal bone), as noted by Baverstock et al. (2013). However, the extent of this
814 attachment might vary, as it is the case with *M. minutoides*, in which it is much smaller. Baverstock et

al. (2013, p. 55) proposed that this attachment could play a biomechanical role by "stabilizing the arch during downward loading". Our data partially support this hypothesis since the attachment is reduced in the pygmy mouse (*M. minutoides*), in which we may expect overall lower masticatory forces.

Comparison with Rattus norvegicus

Cox and Jeffery (2011) described in details the masticatory musculature of *Rattus norvegicus* using similar approaches. Despite some visible differences, such as in the temporal muscles, most muscle groups *R. norvegicus* resemble the ones described in *Mus* species. In terms of proportions, the superficial masseter muscle of the brown rat represents 20.4% of the total mass, which is within the range of observed values for the mice species. The same holds true for the deep masseter muscle, which represents 34.3% of the total muscle mass in *R. norvegicus*. The pterygoid muscle group proportion for the rat (11.6%) is at the lower part of the observed range of values for our sample (10.9 to 19.6%), but still falls within this range. The main differences involved the temporalis muscle group, which is much more developed in the rat (26.9%) than in any of our mice (18.2 to 22.3%) or in the house mouse (22.4%). Conversely, the zygomaticomandibularis muscle is proportionally smaller in the rat (6.8%) than in the mice (8.1 to 15.3%), which may relate to the apparent negative allometric trend observed in our mice sample (Fig. 1, and section above). Based on 3D reconstructions, Cox and Jeffery (2011) interpreted the greater importance of the temporalis muscle group in the rat as a consequence of a greater development of the lateral temporalis muscle, combined with a very posteriorly developed medial temporalis muscle, which covers most of the tympanic bulla. The marked temporal crests present on the skull of rats may be linked to the importance of this muscle group. On the other hand, the orbital part of the medial temporalis muscle appears slightly reduced in the rat, probably due to space constraints. The reduced proportion of the zygomaticomandibularis muscle group is probably explained by a smaller posterior zygomaticomandibularis muscle and the limited anterior development

839 of the anterior zygomaticomandibularis muscle. The infraorbital zygomaticomandibularis muscle,
840 however, is more ventrally extended than in any of the mice; it is completely separated from the
841 anterior zygomaticomandibularis muscle, which clearly contrasts from the configuration observed in
842 any of the mice. When compared to the rat dissection of Hiiemae and Houston (1971), it appears that
843 part of the the anterior zygomaticomandibularis muscle of Cox and Jeffery (2011) might be a
844 misidentified part of the lateral temporalis muscle. Cox and Jeffery (2011) described but did not
845 illustrate the pterygoid muscle group, their description and proportions suggest that it is similar to what
846 is observed in mice.
847
848 *Comparison with* Hydromys chrysogaster *and* Melomys obiensis
849 Fabre and colleagues (2017) recently described the masticatory musculature of *Hydromys*
850 *chrysogaster*, a carnivorous water-rat from the Australasian region, and showed muscular and osseous
851 changes linked to the specialized diet in this species. Compared to our sample, the water-rat also
852 appears to show important muscular differences. Most notable is the reduction of the posterior deep
853 masseter, which is clearly shorter than in any species studied here, accordingly representing only 7.2 %
854 of total muscular mass, while it ranges from 15.9 % to 23.9 % in mice. This reduction may be linked to
855 space constraints produced by an important increase in the superficial masseter, which extends much
856 more dorsally in the water-rat than in our sample. In terms of proportions, the superficial masseter
857 represents over 25 % of total muscular mass in the water-rat, while it ranges from 17.4 to 23.5 % in our
858 sample. Finally, the lateral temporal muscle appears hypertrophied in the water-rat compared to other
859 species, reaching 16.2 % of total muscular mass, while it amounts only from 3 to 5.1 % in the mice
860 studied here. This increase is once more linked to a trade-off in the development of the orbital part of
861 the medial temporal, which appears very reduced in the water-rat, while it occupies an important part of
862 the orbit in other species.

863 Although qualitative descriptions or figures representing *M. obiensis* are lacking, quantitative
864 comparisons are possible. Muscular proportions in this species show that the posterior deep masseter is
865 reduced (10.7% of total muscular mass) compared to other species (15.9 % to 23.9 % in mice), as is
866 seen in the water-rat, but to a lesser extent. Contrary to the water-rat, it seems that this reduction is not
867 linked with an increase in the superficial masseter. Similarly, we observed an increase in the lateral
868 temporal (14.5%), as in the water-rat, but again to a lesser extent. Since *Melomy*s and *Hydromy*s are
869 more closely related than with any of the other species, their important muscular differences may
870 reflect phylogenetic history. However, the differences observed between *Hydromys* and *Melomys*
871 notably in the masseter muscles may not appear in the same way (e.g. reduction of the posterior deep
872 masseter appears to be linked to the increase of the superficial masseter in *Hydromys* but not *Melomys*).
873 This, as well as functional data of Fabre et al. (2017), clearly suggests that differences in diet can
874 explain some variations of the masticatory musculature observed in these species.
875
876 *Functional interpretation of muscular variation*
877 The variation described within the genus *Mus*, when compared with the larger differences seen
878 with *R. norvegicus*, and to an even greater extent with *Hydromys chrysogaster*, suggests that size
879 explain most of the muscular variation in murine rodents, as suggested by Ginot et al. (2018).
880 Furthermore, our comparisons also suggest that muscular variation has a phylogenetic component, and
881 that specialized diets may also add to the differences. However, the finer scale intra-generic differences
882 between mice do not seem to follow any particular allometric or phylogenetic pattern. Considering the
883 diversity of muscular arrangements highlighted here, the idea that skull morpho-anatomy is stable in all
884 murines, making them "high-performance generalists" (Cox and Jeffery 2011) may be inaccurate when
885 encompassing the entire subfamily. Furthermore, intraspecific variation should also be taken into
886 account, as we showed that it may be fairly large in comparison to interspecific differences. Looking at

887 the ontogeny and senescence of muscles may be one of the main aspects requiring further investigation.

888 The interspecific variation shown in the mice described in this study might underlie some subtle
889 functional changes. *M. caroli* shows the largest deep masseter muscle group and second largest
890 temporalis muscle group, both these muscular groups being the main adductors of the mandible, and
891 most active during the mastication phase (Hiiemae 1971, Weijs and Dantuma 1975, Satoh 1997). These
892 proportions suggest that *M. caroli* might be able to produce large occlusal forces at the molar level. The
893 vertical orientation of the anterior deep masseter muscle and the development of the anterior
894 zygomaticomandibularis muscle in this species are congruent with this hypothesis. Furthermore, data
895 from Ginot et al. (2018) show that predicted bite force in *M. caroli* is higher than expected for its size,
896 which may also relate to the development of its adductor muscles. *M. cervicolor*, on the other hand,
897 generally has median values for the percentage of total muscular mass represented by each muscle
898 group (Tab. 1, Fig. 1). This may indicate that *M. cervicolor* is more generalist compared to other
899 species studied here. It should also be noted that the ventral extension of the fibers of its anterior and
900 infraorbital zygomaticomandibularis muscles suggest that they may stretch more than in other species,
901 giving *M. cervicolor* the possibility of a large gape angle (e.g. Satoh and Iwaku 2006). This would
902 allow this mouse to prey on food of a wider range of size. In *M. fragilicauda* the superficial masseter
903 muscle is proportionally larger than in all other species, and so is its medial temporalis muscle. Both
904 muscles have a large horizontal component in their lines of action, and are generally considered to be
905 the main muscles responsible for the antero-posterior movements of the mandible (Hiiemae 1971, note
906 that the medial temporalis muscle is therein referred to as the "posterior temporalis muscle"). The
907 development of this two antagonist muscles in *M. fragilicauda* therefore suggests important propalinal
908 movements of the jaw in this species.

909 Comparing *M. caroli*, *M. cervicolor*, and *M. fragilicauda* is interesting as they are often found in
910 sympatry, or syntopy, in Southeast Asia. Furthermore, *M. cervicolor* and *M. fragilicauda* display very

911 similar skull morphology despite of their phylogenetic distances (Auffray et al. 2003). The differences
912 in the masticatory apparatus of these three species revealed here can be considered as rather small, but
913 they might reflect functional differences linked to differences in diet. Following the above functional
914 interpretation, *M. caroli* would specialize in crushing with strong occlusion, while *M. fragilicauda*
915 would specialize in grinding food with propalinal movements, and *M. cervicolor* may be a more
916 generalist species. However, previous studies and fieldwork suggest that *M. cervicolor* and *M. caroli*
917 are both able to subsist around rice fields as well as in areas where insects are the main available food
918 (Marshall 1977). The diet of *M. fragilicauda* remains unknown.

919 The pygmy mice *M. minutoides* shows a reduction in the superficial and deep masseter muscles, as
920 well as in the medial temporalis muscle. In the case of dwarf squirrels, the reduction of the temporalis
921 muscle has been linked to allometric trends (e.g. Hautier et al. 2009), but our results do not show such
922 trend in the *Mus* genus. Instead, the reduction of the posterior part of the medial temporalis muscle may
923 be functionally explained by the reduction of the deep masseter muscle. Indeed, the attachment of the
924 temporalis muscle to the posterior part of the zygomatic arch was hypothesized to compensate strong
925 downward forces exerted on the arch during mastication (Baverstock et al. 2013, see also Hiiemae
926 1971). If the deep masseter muscle is reduced, these forces are reduced, therefore diminishing the need
927 to counteract them. On the other hand, *M. minutoides* displays a larger zygomaticomandibularis
928 muscle, in particular in its anterior and posterior parts. These muscles are sometimes considered as part
929 of the deep masseter muscle (e.g. Hiiemae 1971, Weijs and Dantuma 1975, Satoh 1997), and their lines
930 of action are generally similar. Therefore, the decrease in deep masseter muscle proportions may be
931 partly compensated by the increase in zygomaticomandibularis muscle proportions. In any case, the
932 reduction in the masseteric musculature is expected to cause a decrease in the bite and mastication
933 forces, which may be partly compensated by the increase in the zygomaticomandibularis muscle. In
934 accordance with this, data reported in Ginot et al. (2018) show that *in vivo* and predicted bite force at

935 the incisor of *M. minutoides* correspond to what is expected for its size. This reduction of the masseter
936 complex and bite force may be due to the size constraints of this dwarf species, or may be explained by
937 a reduced hardness of their food items. Indeed, food hardness was shown to be positively related with
938 food size in several different types of food (insects, fruits, seeds, see Aguirre et al. 2003). We might
939 expect that the reduction in size of *M. minutoides* was related to a reduction in the size of its preys.
940 Smaller sized prey being less hard, they should require less important masticatory forces. It should be
941 noted that *M. minutoides* was lab-reared, so these muscular differences are not purely
942 phenotypic/developmental plasticity, but may be conserved between species.

943 Finally, *M. pahari* is known to be insectivorous (Marshall 1977), and its bony morphology presents
944 some specialized characters, with a lengthened cranium and mandible. In terms of masticatory muscles,
945 *M. pahari* has large (although not the largest) masseter muscles compared to other species. These
946 muscles also have anteriorly displaced origin areas, which increase their inlever arm and therefore
947 mechanical advantage. These types of muscular arrangements were shown to be linked to the evolution
948 toward a more carnivorous diet in a cricetid rodent (*Onychomys leucogaster*, Satoh and Iwaku 2006).

949

950 **Conclusion**

951 In this paper we described and compared for the first time the masticatory apparatus of four
952 species of wild mice, and one wild-derived strain of pygmy mice. To do so, we combined thorough
953 dissections and newly developed method of iodine-enhanced CT-scanning. Both approaches were
954 congruent and complementary. Subtle but potentially functionally significant anatomical differences
955 were detected among these species. We also found very congruent results and confirmed some
956 observations made on the house mouse and brown rat (Cox and Jeffery 2011, Baverstock et al. 2013).
957 The brown rat showed more differences, which was to be expected due to its greater size and
958 phylogenetic distance. The specialized carnivorous water-rat was the most divergent species in terms of

musculature, probably combining effects linked to size, phylogeny, and diet. Among our sample, we could identify functional differences, which we interpreted in terms of diet and ecology. However, the hypotheses proposed will require to study the diet of these species in greater datails (for example using stomach content or feces analyses). Overall, this type of approaches may help us better understand how muscles and bones interact in the skull and may become a useful tool for functional and ecomorphological studies, especially with the increasing number of thoroughly described species. Finally, our results suggest that the anatomical diversity of the murine skull may have been underestimated, as only a small number have been studied so far; and as we show that disparity exists even within a genus. Accordingly, regarding the Murinae or Muridae overall as "high-performance generalist" (Cox and Jeffery 2011) may hold only true when comparing to distant rodent groups, but may hide the reality of fine scale adaptations in mice and rats. These fine scale adaptations may be one ignored but key aspect to explain the large specific diversity in murine rodents.

Acknowledgements

The authors are thankful to S. Morand and the BiodivhealthSEA program (**ANR** 07 BDIV 012) who allowed us to participate in their fieldwork. We are also grateful F. Veyrunes who lended us the *M. minutoides* specimens.

References

Aguirre, L. F., Herrel, A., Van Damme, R., and Matthysen, E. (2003). The implications of food hardness for diet in bats. *Functional Ecology*, *17*(2), 201-212.

Auffray, J. C., Orth, A., Catalan, J., Gonzalez, J. P., Desmarais, E., and Bonhomme, F. (2003). Phylogenetic position and description of a new species of subgenus *Mus* (Rodentia, Mammalia) from Thailand. *Zoologica Scripta*, *32*(2), 119-127.

983 Baverstock, H., Jeffery, N. S., and Cobb, S. N. (2013). The morphology of the mouse masticatory
984 musculature. *Journal of Anatomy*, *223*(1), 46-60.
985 Byron, C. D., Borke, J., Yu, J., Pashley, D., Wingard, C. J., and Hamrick, M. (2004). Effects of
986 increased muscle mass on mouse sagittal suture morphology and mechanics. *The Anatomical*
987 *Record*, *279*(1), 676-684.
988 Cox, P. G., and Jeffery, N. (2011). Reviewing the morphology of the jaw-closing musculature in
989 squirrels, rats, and guinea pigs with contrast-enhanced microCT. *The Anatomical*
990 *Record*, *294*(6), 915-928.
991 Cox, P. G., Rayfield, E. J., Fagan, M. J., Herrel, A., Pataky, T. C., and Jeffery, N. (2012). Functional
992 evolution of the feeding system in rodents. *PLoS One*, *7*(4), e36299.
993 Druzinsky, R. E., Doherty, A. H., and De Vree, F. L. (2011). Mammalian masticatory muscles:
994 homology, nomenclature, and diversification. *Integrative and comparative biology*, *51*(2), 224-
995 234.
996 Fabre, P. H., Herrel, A., Fitriana, Y., Meslin, L., and Hautier, L. (2017). Masticatory muscle architecture
997 in a water-rat from Australasia (Murinae, *Hydromys*) and its implication for the evolution of
998 carnivory in rodents. *Journal of Anatomy, 231*(3), 380-397.
999 Ginot, S., Herrel, A., Claude, J., and Hautier, L. (2018). Skull size and biomechanics are good
1000 estimators of *in vivo* bite force in murid rodents. *The Anatomical Record*, *301*(2), 256-266.
1001 Hallgrímsson, B., and Lieberman, D. E. (2008). Mouse models and the evolutionary developmental
1002 biology of the skull. *Integrative and Comparative Biology*, *48*(3), 373-384.
1003 Hautier, L., Fabre, P. H., and Michaux, J. (2009). Mandible shape and dwarfism in squirrels
1004 (Mammalia, Rodentia): interaction of allometry and adaptation. *Naturwissenschaften*, *96*(6), 725-
1005 730.
1006 Hiiemae, K. (1971). The structure and function of the jaw muscles in the rat (*Rattus norvegicus*

1007 L.). *Zoological Journal of the Linnean Society*, *50*(1), 111-132.
1008 Hiiemae, K., and Houston, W. J. B. (1971). The structure and function of the jaw muscles in the rat
1009 (*Rattus norvegicus* L.) I. Their anatomy and internal architecture. *Zoological Journal of the*
1010 *Linnean Society*, *50*(1), 75-99.
1011 Maestri, R., Patterson, B. D., Fornel, R., Monteiro, L. R., and Freitas, T. R. O. (2016). Diet, bite force
1012 and skull morphology in the generalist rodent morphotype. *Journal of evolutionary*
1013 *biology*, *29*(11), 2191-2204.
1014 Marshall, J. T. (1977). A synopsis of Asian species of Mus (Rodentia, Muridae). Bulletin of the AMNH;
1015 v. 158, article 3.
1016 Satoh, K. (1997). Comparative functional morphology of mandibular forward movement during
1017 mastication of two murid rodents, *Apodemus speciosus* (Murinae) and *Clethrionomys rufocanus*
1018 (Arvicolinae). *Journal of Morphology*, *231*(2), 131-142.
1019 Satoh, K. (1998). Balancing function of the masticatory muscles during incisal biting in two murid
1020 rodents, *Apodemus speciosus* and *Clethrionomys rufocanus*. *Journal of morphology*, *236*(1), 49-
1021 56.
1022 Satoh, K. (1999). Mechanical advantage of area of origin for the external pterygoid muscle in two
1023 murid rodents, *Apodemus speciosus* and *Clethrionomys rufocanus*. *Journal of*
1024 *morphology*, *240*(1), 1-14.
1025 Satoh, K., and Iwaku, F. (2006). Jaw muscle functional anatomy in northern grasshopper mouse,
1026 *Onychomys leucogaster*, a carnivorous murid. *Journal of Morphology*, *267*(8), 987-999.
1027 Satoh, K., and Iwaku, F. (2009). Structure and direction of jaw adductor muscles as herbivorous
1028 adaptations in *Neotoma mexicana* (Muridae, Rodentia). *Zoomorphology*, *128*(4), 339-348.
1029 Weijs, W. A., and Dantuma, R. (1975). Electromyography and mechanics of mastication in the albino
1030 rat. *Journal of Morphology*, *146*(1), 1-33.

1031 Willmore, K. E., Leamy, L., and Hallgrímsson, B. (2006). Effects of developmental and functional
1032 interactions on mouse cranial variability through late ontogeny. *Evolution and development*, *8*(6),
1033 550-567.

1.2 – Anatomie cranio-mandibulaire et force de morsure chez les Murinae.

Bien que le plan général de la morphologie crânienne reste assez stable chez les Murinae, des différences notables peuvent être révélées en anatomie comparée, comme dans la section précédente. Certaines de ces différences peuvent être corrélées à la diversité de tailles, d'écologies et de régimes alimentaires observés dans ce groupe. Bien que de nombreuses études interprètent des changements morphologiques en termes fonctionnels (Michaux et al. 2007, Samuels 2009, Satoh 1997, Satoh and Iwaku 2006, 2008), les tests directs de l'influence de la morphologie cranio-mandibulaire sur la force de morsure restent rares chez les rongeurs (e.g. Freeman & Lemen 2008, Cox et al. 2012, Van Daele et al. 2008).

Cette partie de la thèse concerne donc la caractérisation du lien entre différents traits morpho-anatomiques (musculature, forme et taille) et force de morsure. Elle a en même temps pour objectif de déterminer lesquels de ces traits morpho-anatomiques pourraient être utilisés comme proxys pour déduire la performance de rongeurs pour lesquels les données *in vivo* ne sont pas disponibles.

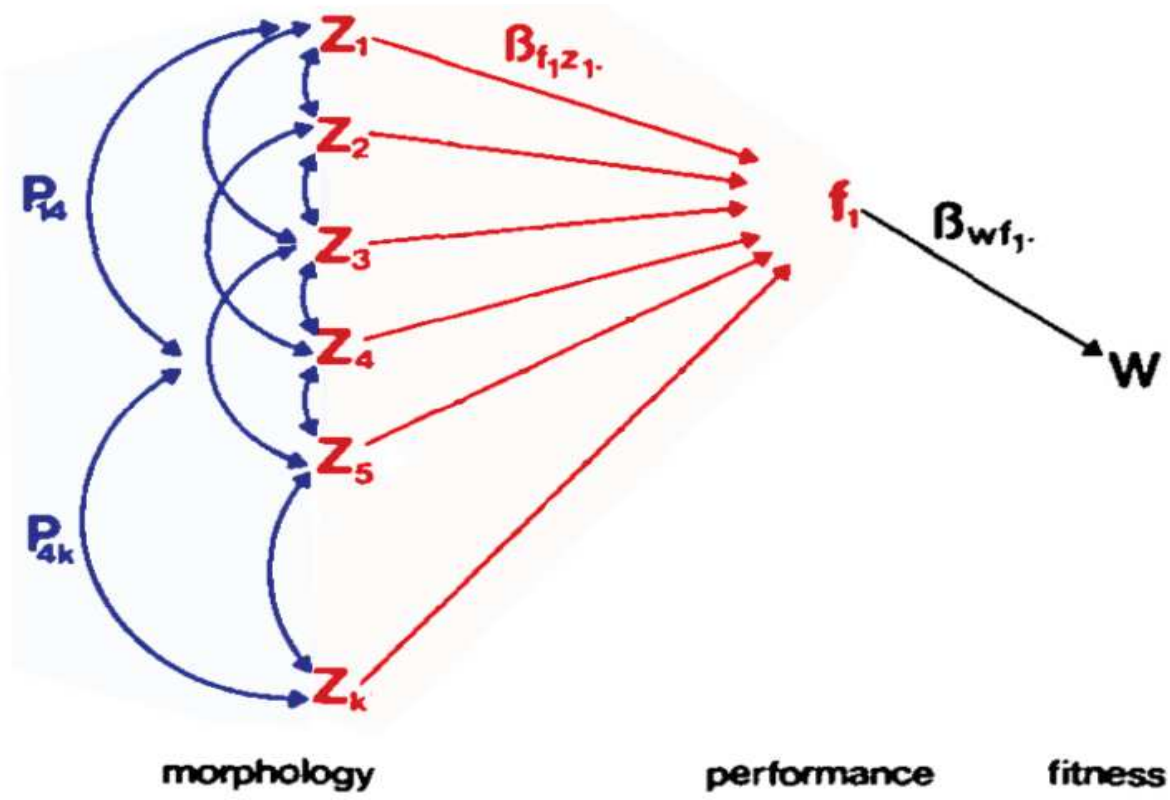

Figure 1.2.1: Diagramme des corrélations entre morphologie, performance et fitness, adapté de Arnold (1983), représentant en rouge les effets sur lesquels se concentre cette section de la thèse (c'est à dire le lien morphologie-performance) et en bleu les effets indirectement inclus. En noir sont les corrélations non étudiés.

La Fig. 1.2.1 résume visuellement les relations sur lesquelles se focalise cette section. En rouge sont les effets des traits morphologiques **Z** sur la performance **f**, ici la force de morsure, qui se traduisent par un "gradient de performance" $\boldsymbol{\beta_{fz}}$. En bleu sont surlignées les relations **P** entre les traits morphologiques liés à leur intégration, qui ne seront pas étudiées directement ici.

1.2.1 – Lien entre musculature et force de morsure au niveau interspécifique (article publié dans The Anatomical Record*).*

Au niveau interspécifique, les différences de taille, ainsi que dans l'anatomie cranio-mandibulaire (os et muscles liés à la mastication) fournissent généralement la principale explication pour les changements adaptatifs dans la performance. Bien que cela ait été démontré chez plusieurs groupes d'animaux, y compris de mammifères (e.g. Herrel et al. 2010, Santana et al. 2010), cela n'ajamais été vérifié chez les murinés qui incluent des espèces très nombreuses mais souvent similaires en termes anatomiques.

Plus spécifiquement, la force produite par chaque muscle peut être estimée par la section en coupe physiologique, associée à l'angle d'action du muscle (voir Introduction – Cadre méthodologique et la section *Material and Methods* de l'article suivant).

Considérant la variation dans la musculature décrite dans la partie précédente, on peut chercher à quantifier comment celle-ci influence la performance. C'est ce qui a été réalisé dans l'article suivant chez un éventail d'espèces de Murinae sauvages et de laboratoire. Les effets de la taille, de la phylogénie et de multiples variables musculaires sur la force de morsure mesurée et estimée y ont été testés.

THE ANATOMICAL RECORD 301:256–266 (2018)

Skull Size and Biomechanics are Good Estimators of *In Vivo* Bite Force in Murid Rodents

SAMUEL GINOT [1]*, ANTHONY HERREL,[2] JULIEN CLAUDE,[1] AND LIONEL HAUTIER[1]

[1]Institut des Sciences de l'Evolution de Montpellier, Université de Montpellier, Montpellier, France

[2]Museum National d'Histoire Naturelle, Paris, France

ABSTRACT

Rodentia is a species-rich group with diversified modes of life and diets. Although rodent skull morphology has been the focus of a voluminous literature, the functional significance of its variations has yet to be explored in live animals. Myomorphous rodents, including murids, have been suggested to represent "high-performance generalists." We measured *in vivo* bite force in 14 species of wild and lab-reared murid rodents of various sizes and diets to investigate potential morphofunctional differences between them. We dissected their skulls and computed a biomechanical model to estimate bite force. We first tested if our model allowed good estimation of *in vivo* data. Then, using morphological, *in vivo* and estimated bite force data in a phylogenetic context, we aimed to find the drivers of bite force differences among species. Estimated and *in vivo* bite forces were strongly correlated, which indicates that (a) biomechanical models allow a good estimation of real performance, and that (b) size and muscular changes (increased mass, fiber length, and PCSA) are the main drivers of bite performance differences. Myomorphous rodents, therefore, may have evolved high bite force through a combination of changes in size and musculature, which gave them a great versatility in their ability to process food. We found mixed results at the intraspecific level, with only some species displaying a good fit between estimated and *in vivo* measurements. We suggest that limited variation in size and muscular organization, and increased behavioral variation might decrease the precision of bite force estimates within species. Anat Rec, 301:256–266, 2018. © 2018 Wiley Periodicals, Inc.

Key words: Muscle; adaptation; vertebrates; Muridae; bite force

Rodents are by far the most speciose group of mammals, while murids represent almost half of this specific diversity. Historically, variation in skull morphology has been used as a classification tool for rodents (Waterhouse, 1839, Brandt, 1855, Tullberg, 1899, Simpson, 1945; Wood, 1965; Hautier et al., 2015). Based on the relative importance of the distinct parts of the masseter muscle, as well as the positions of their origins and insertions on the cranium and the mandible, four combinations of skull morphologies are distinguished: sciuromorphy, hystricomorphy, myomorphy, and protrogomorphy (Supporting

Additional Supporting Information may be found in the online version of this article.

*Correspondence to: Samuel Ginot, Institut des Sciences de l'Evolution de Montpellier, Université de Montpellier, Batiment 22, Place Eugène Bataillon, Montpellier 34095, France. E-mail: samuel.ginot@umontpellier.fr

Received 16 March 2017; Revised 31 July 2017; Accepted 24 August 2017.

DOI 10.1002/ar.23711

Published online in Wiley Online Library (wileyonlinelibrary.com).

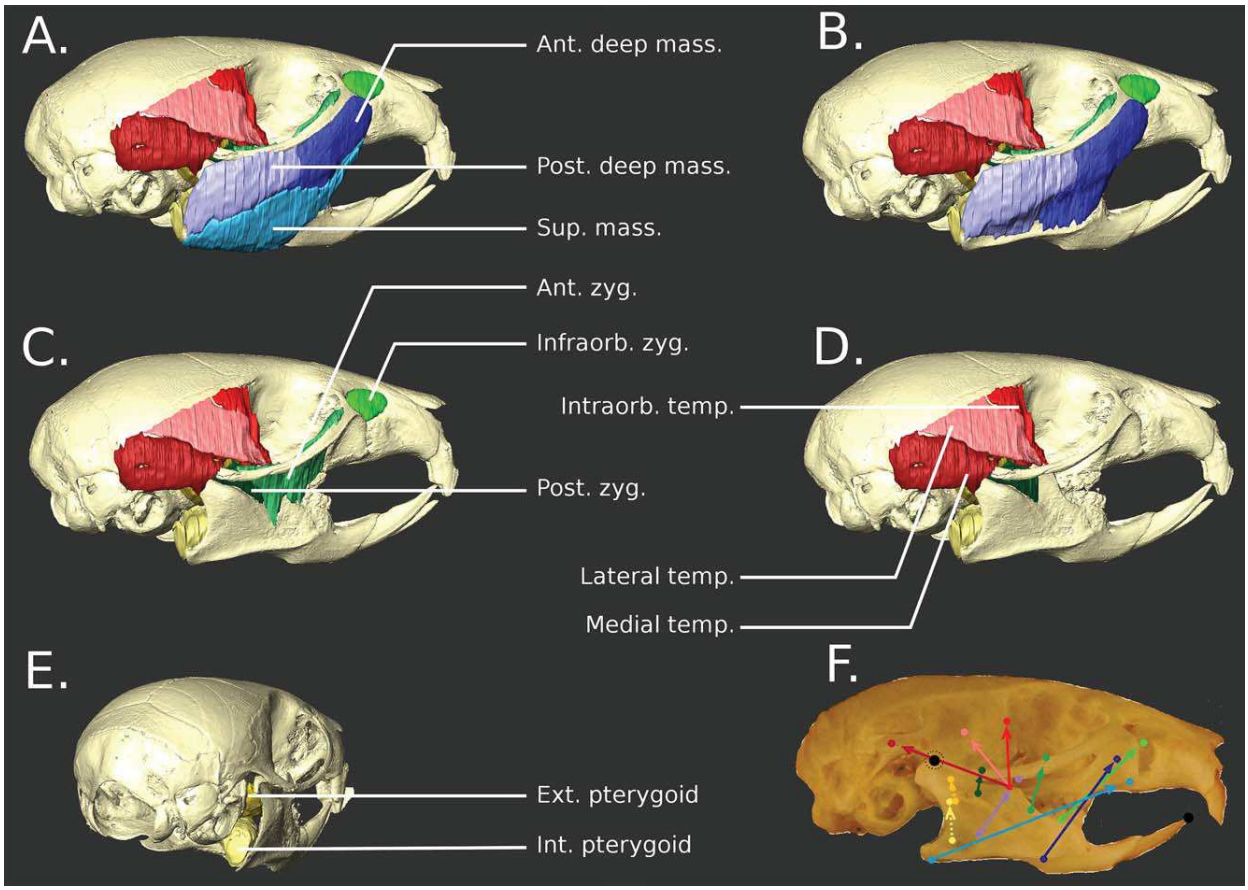

Fig. 1. (**A–E**) 3D rendering of the skull and muscles of *M. caroli*, obtained by iodine-enhanced CT scanning, as an example to illustrate Muridae skull morphology and musculature. (**F**) lateral view of the same skull, with arrows representing the lines of action of the muscles, and full circles representing theirs origins and insertions. The bigger black circles represent the point of application of the resistance force, and the point of rotation (dotted circle). Colors for all figures correspond to the different muscles. Sky blue: superficial masseter; dark blue: anterior deep masseter; pale blue: posterior deep masseter. Green: anterior zygomaticomandibularis; fluo green: Infraorbital zygomaticomandibularis; dark green: posterior zygomaticomandibularis. Red: intraorbital part of the medial temporalis; pale pink: lateral temporalis; dark red: medial temporalis. Yellow: internal pterygoid; golden: external pterygoid.

Information, Fig. 1). Among these morphotypes, the sciuromorphous and hystricomorphous rodents have been shown to specialize in gnawing and chewing, respectively. Myomorphous rodents, on the other hand, seem to encompass both gnawing and chewing, making them "high-performance generalists" (Cox et al. 2012; Maestri et al. 2016), overperforming both the sciuromorphous and hystricomorphous rodents in their respective specialties.

Myomorphs, murids especially, are the most diverse and widespread group among rodents. Their great adaptability, exemplified by several species that are spread across a wide latitudinal gradient and whose ecologies may range from feral to commensal within the same species (e.g. *Rattus tanezumi*, Aplin et al. 2011; *Mus musculus*, Berry and Jakobson 1975, Le Roux et al. 2002), might partly explain this diversity. This extraordinary lability is certainly related with their ability to exploit a wide array of food items (Navarrette and Castilla 1993, Le Roux et al. 2002, Corbalàn 2006, Samuels 2009, Maestri et al. 2016). Despite showing several dietary specializations (e.g. to carnivory, herbivory or insectivory; Samuels 2009), the murid skull morphology (Fig. 1) is often considered to be fairly stable (e.g., Rowe et al. 2011) in most species. This stable, but efficient, morphology was proposed to be related to an important functional versatility of their masticatory apparatus that enables most mice and rats to use various dietary resources (Cox et al. 2012). Still, the general morphological homogeneity should not be interpreted as a lack of adaptation or evolution. In fact, subtle but significant changes in skull morphology have been detected using geometric morphometrics (e.g. Siahsarvie et al. 2012, Michaux et al. 2007, Samuels 2009), dissections (e.g. Satoh and Iwaku 2006, 2008, Baverstock et al. 2013), iodine-enhanced CT scanning (e.g. Cox et al. 2011, 2012, Baverstock et al. 2013), and Finite Elements Analyses (FEA) methods (e.g. Cox et al. 2011, 2012). In most cases, these methods were used to better understand the relationship between phylogeny, phylogeography, function, and ecology. However, the functional consequences of the observed anatomical variation have remained poorly studied in live animals.

More specifically, how variation in the anatomy impacts ecologically relevant performance traits (bite force, speed, endurance, etc.) *in vivo* remains unknown. As making functional, ecological, and evolutionary inferences based on skull morphology and myology has been widely used in many fields from paleontology to ecology and development (e.g. Michaux et al. 2007, Samuels 2009, Satoh 1997, Satoh and Iwaku 2006, 2008), testing how these factors actually influence *in vivo* performance is necessary. Some studies have presented data on estimated bite force through muscular biomechanical models in rodents (e.g. Satoh 1997, Druzinsky 2010, Becerra et al. 2011). Yet, to our knowledge, only a handful of studies have so far validated morpho-functional estimations with *in vivo* measurements of bite force (Freeman and Lemen 2008a,b, Cox et al. 2012, Van Daele et al. 2009) Among them, only Van Daele et al. (2009) used a model based on the masticatory muscles for estimated bite force at an interspecific level (but see Nies and Ro 2004, Becerra et al. 2011 for intraspecific studies). In other vertebrate groups (*e.g.*, bats: Herrel et al. 2008a; shrews: Cornette et al. 2013, Young et al. 2007; lizards: Herrel et al. 1998a, 1998b), *in vivo* bite force was shown to be predictable by biomechanical estimates of the forces of the jaw adductor muscles (e.g. Herrel et al. 1998a, 1998b, 2008a). Bite force, whether *in vivo* or estimated, has been correlated with anatomy (size, shape, and myology) in various groups of animals (e.g. Verwaijen et al. 2002, Herrel et al. 2005, Santana et al. 2010). Ecologically, it also has been shown to play an important role in sexual competition (*e.g.*, Herrel et al. 2010), and feeding behavior and diet (e.g., Aguirre et al. 2003, Young et al. 2007, Herrel et al. 2008b, Santana and Dumont 2009). In light of these results, investigating bite force in myomorphous rodents is a great opportunity to better understand what functional advantage or structural constraints their unique skull morphology may hold.

Here, we aimed to test the predictive power of biomechanical models based on adductor musculature for bite force, and to explain any discrepancies between *in vivo* and estimated bite force, both at the intra- and interspecific levels. Doing so, we also tried to disentangle the effects of size, phylogeny, and muscular variation on bite force differences in our sample of species. Finally, we used our data to identify the modes of evolution of the muscular, bite force and size traits along the diversification of the rats and mice studied here which represent a small sample of the murid radiation.

MATERIALS AND METHODS

Specimens

In total, 75 rodents representing 14 different species were used in this study. Out of these, 68 were captured in the wild as part of the Ceropath and BiodivhealthSEA program fieldwork in Thailand in 2015 and 2016. Bite forces were measured directly after capture. Specimens were then euthanized and their heads were fixed in 70% ethanol before further treatment. Wild rodent specimens included in the study are neither on the CITES list, nor the Red List (IUCN). Animals were treated in accordance with the guidelines of the American Society of Mammalogists, and within the European Union legislation guidelines (Directive 86/609/EEC). Approval notices for trapping and investigation of rodents were provided by the Ethical Committee of Mahidol University, Bangkok, Thailand, number 0517.1116/661. The seven remaining specimens were acquired dead from animal facilities at the University of Montpellier (one *Mus mattheyi*, two *Mus minutoides*, two *Mus caroli* from the "KTK" strain and two *Mus pahari f*rom the "PAH" strain).

Bite Force Measurements

All *in vivo* bite force data were recorded at the incisors using a Kistler force transducer linked to a charge amplifier, similar to the set-up presented in Herrel et al. (1999) and Aguirre et al. (2002). After capture, we performed three consecutive trials for each animal. The maximal bite force recorded across the three trials was retained and used in subsequent analyses. We obtained *in vivo* bite force data for all wild individuals, and used the average species' values in our interspecific analyses. To broaden our interspecific data set, we added the lab specimens for which we used the averaged *in vivo* bite force obtained in their respective lab colonies.

Morphology

To test if biomechanical models could correctly estimate the *in vivo* data, we dissected the jaw musculature (Fig. 1) on one side for all specimens, and kept each muscle individually in 70% ethanol. We then blotted the muscle dry and weighted them with a 0.01 mg precision balance (Sartorius A 120 S). Next, muscles were transferred into a 30% nitric acid solution during 20 to 24 hours to separate their fibers. To stop the digestion the nitric acid solution was removed and replaced by a 50% glycerol solution. Finally, fibers were observed under a Wild Heerbrugg M3Z binocular microscope (ocular x10 Wild 445111, objective x1 Wild 411589) and 10–15 of them were selected randomly for each muscle and drawn using a camera lucida (Wild Heerbrugg TYP 308700). The drawings were scanned and the fiber lengths were then determined in ImageJ software. The muscular nomenclature used here follows that used in Baverstock et al. (2013), with the addition of a separate anterior and posterior deep masseter, and an orbital part of the medial temporal

Bite Model

The biomechanical model used to estimate bite force was similar to that described by Herrel et al. (1998a, 1998b), and relies on the computation of the static force equilibrium. As input for the model, the three-dimensional coordinates of the origins and the insertions and the physiological cross sectional areas of the jaw muscles are needed. Additionally, the three-dimensional coordinates of the point of application of the bite force and the center of rotation are needed (Fig.1F). These coordinates were determined by the mean of lateral and dorsal pictures of the skull with a 10-mm scale taken after the dissection (using a Pentax K200D reflex camera). For muscle with relatively broad areas of origin and insertion, the approximate centroid of the insertion area was used, based on knowledge from the dissections and literature data (e.g. Baverstock et al. 2013). All insertion and origin landmarks (Fig. 1F) were digitized using tpsDig2 software. Skull length was computed using the same pictures, in dorsal view by placing one

TABLE 1. Individual muscular data acquired for this study

		Muscle mass (mg)			Muscle mass (mg) cont'd			Muscle mass (mg) cont'd			Muscle mass (mg) cont'd			Fiber length (mm)			Fiber length (mm) cont'd			Fiber length (mm) cont'd			Fiber length (mm) cont'd				
Species	Specimen	Digas	DM.ant	DM.pos	M.sup	Pt.ext	Pt.int	Tp.I-O	Tp.lat	Tp.med	Zyg.ant	Zyg.I-O	Zyg.pos	Digas	DM.ant	DM.post	M.sup	Pt.ext	Pt.int	Tp.I-O	Tp.lat	Tp.med	Zyg.ant	Zyg.I-O	Zyg.post	In vivo bite force	Skull length (cm)
Berylmys berdmorei	7184	NA	179.6	101.4	118.6	124	62.5	28.5	24.4	81.7	16.5	63.2	8.8	5.84	5.84	5.21	5.56	2.43	3.6	3.56	4.73	4.57	4.25	4.59	2.3	21.26	5.41
B. berdmorei	7214	20.7	45.7	54.1	55	13.6	20	8.6	10.8	28.8	NA	21.8	3.9	3.37	4.01	3.45	4.37	2.31	3.12	3.63	3.59	3.5	NA	3.59	2.24	11.52	3.97
B. berdmorei	7215	24.6	70.9	52	63.1	20	20.8	18.2	NA	43.7	NA	36.8	15.9	3.11	3.26	3.29	3.61	3.34	2.92	2.95	NA	3.67	NA	3.46	2.45	15.4	4.58
Berylmys bowersi	7219	41.4	118	153.9	126.5	28.7	40.2	35.7	7.4	126.1	26.3	59.7	10.4	3.56	5.01	4.57	5	3.06	2.49	3.59	4.06	4.11	4.49	3.6	3.03	27.42	5.13
B. bowersi	7220	156.6	145.4	144.3	159.6	66	106.3	59.5	51.1	120.4	14.1	78.7	17.4	4.09	5.18	4.37	4.1	3.97	3.52	2.93	3.5	5.06	4.36	4.72	2.99	18.9	5.15
B. bowersi	7221	35.4	169.4	158.3	154	61	70.9	27.6	21.6	94.7	32.9	42.3	22.9	3.08	5.36	4.65	3.57	4.73	3.78	3.98	3.59	3.64	5.24	6.21	2.05	23.07	5.67
B. bowersi	7234	51.3	430.7	NA	191.3	NA	89.4	NA	19.8	217	19.2	80	10.5	5.93	5.93	NA	4.75	NA	3.59	NA	3.48	4.57	3.91	5.17	1.85	17.21	5.74
Berylmys sp.	7202	29.7	56.4	52.6	49	4.4	23.2	11.1	6.2	27.5	NA	24.9	8.8	3.82	3.52	3.33	3.71	2.05	3.07	2.96	2.95	4.41	NA	3.84	2.16	12.13	3.84
Maxomys surifer	7185	45.6	201.5	162.1	144.2	40.5	91.8	26.8	18.6	86.7	NA	87.8	21.1	3.83	4.04	3.78	3.6	3.53	3.01	3.56	3.33	3.38	NA	3.8	2.78	23.33	4.9
M. surifer	7186	24.4	97.5	97.5	91.7	29.2	41.2	18	11	49.9	14.3	25.7	7.1	3.55	NA	3.57	4.27	4.09	2.36	2.78	2.63	3.57	2.66	3.24	2.66	13.42	4.28
M. surifer	7187	22	94.9	94.9	85.9	20.1	24.5	NA	24.9	25.5	59.7	NA	10.8	3.87	5.77	4.91	4.82	3.36	3.33	NA	4.44	3.47	4.51	NA	2.83	18.08	4.51
M. surifer	7191	23.8	108.3	93.3	127.9	8.4	48.6	30.6	8.1	61.2	36.5	34	11.7	3.91	4.52	4.68	4.86	3.4	3.73	3.53	3.2	3.88	4.3	4.16	2.82	23.45	4.8
M. surifer	7192	29.5	117.4	103	108.7	29.8	25	17.9	12.4	51.9	16.4	52.9	3.9	4.43	6.13	6.05	5.25	3.65	4.99	3.28	3.8	3.83	3.08	5.24	2.34	26.05	4.86
M. surifer	7193	22.5	62.2	122.5	98	24.9	57.9	19.1	14.3	38.8	25.1	17.3	6.8	4.06	4.8	4.2	4.25	3	2.85	2.7	3.41	3.87	3.12	2.77	1.89	17.21	4.84
M. surifer	7194	36.1	122.6	111.7	103	50	769	34.3	12	60.5	16.4	42.2	17.1	3.96	5.74	5.05	4.67	4.19	3.83	3.58	4.02	3.98	4.36	3.78	2.58	22.69	4.93
Mus caroli	7195	2.2	8.8	7.9	8.6	1.2	4.3	2.2	1.6	4.9	1.5	1.5	1	2.28	3.45	3.35	3.57	2.81	2.89	2.77	3.07	3.13	3.13	3.38	1.86	1.87	2.05
M. caroli	7225	3.3	10.4	9.7	12	2.2	4.9	2.9	2.8	6.1	1	2.7	1.3	2.31	3.14	3.29	2.71	2.87	2.42	2.21	2.37	2.39	1.94	2.65	1.7	4.84	2.04
M. caroli	7236	4.5	9.1	7.3	7.8	2.4	3.5	1.5	1	7.2	NA	2.2	0.8	2.18	3.18	3.19	3.18	1.7	1.97	2.29	2.26	2.78	NA	2.45	1.94	2.77	1.86
M. caroli	7264	2	8.6	9.4	7.1	2.6	2.2	1.3	0.8	5.5	2.7	NA	0.8	2.57	3.66	3.05	2.99	2.85	3.02	2.46	2.62	3.1	3.21	NA	2.36	3.97	1.85
M. caroli	KTK24-13	5.2	31.7	NA	7.6	5	4.4	4.1	2.5	4	1.1	0.5	NA	4.13	4.05	NA	4.59	2.7	2.72	3.21	3.84	3.82	3.09	3.37	NA	9.69	2.28
M. caroli	KTK24-7	4.8	19.7	10.2	12.4	3	3	NA	4.2	4.9	1.9	1.8	0.9	3.85	4.7	4.41	4.61	3.84	3.15	NA	4.42	3.99	3.95	4.37	2.22	9.69	2.43
Mus cervicolor	7255	2.3	5.2	6.9	7.3	3	6.2	1.63	1.63	1.63	NA	2.1	2.1	2.67	3.38	3.59	3.48	3	2.72	2.33	2.46	2.85	NA	3.48	2.1	3.47	2.12
M. cervicolor	7258	2.2	4.1	4.6	6.3	1	1	1.2	NA	2.6	NA	1.1	1.1	2.57	3.55	2.92	2.49	2.53	2.35	3.04	NA	3.32	NA	3.77	1.73	3.09	2.07
M. cervicolor	7259	NA	5.5	6.7	7.6	3.6	5	1.6	1.4	4.4	1.3	1.1	0.2	2.69	2.69	3.49	2.82	3.69	2.03	2.73	2.91	2.75	2.49	2.72	1.93	3.88	2.13
M. cervicolor	7262	1.8	7.8	5.7	8.1	2.3	5.3	2.6	0.1	5.2	1.7	2.2	0.7	2.93	3.41	3.82	3.26	2.31	2.45	2.95	2.95	3.15	3.17	3.72	1.87	4.05	2.06
M. cervicolor	7263	1.6	6.4	3.9	6.3	0.9	3.4	0.1	0.1	3.7	3.2	NA	0.1	1.93	2.73	3.29	2.63	2.39	2.44	2.42	2.33	2.46	2.83	NA	1.88	3.88	1.94
M. cervicolor	7286	1.5	6	7.9	7.4	1.4	2.4	0.8	1.2	3.9	1.2	NA	1.2	2.9	3.22	3.43	2.84	3.08	2.78	3.04	3.55	3.59	2.96	NA	2.5	3.3	2.13
M. cervicolor	7304	3.2	7.3	6.4	9.2	5.4	6	2.1	0.1	9	2.1	2.1	0.1	2.39	3.26	3.55	3.08	3.55	3.07	2.47	2.79	2.59	2.67	2.87	1.52	2.89	2.1
M. cervicolor	7313	2.1	6.3	6.7	9.2	1.6	5.6	1.6	1.1	3.8	1.2	0.9	0.7	2.37	2.82	3.23	3.11	2.37	2.4	3.08	2.06	2.79	2.46	3.23	1.77	3.59	1.95
M. cervicolor	7314	6.6	12.8	10	15.2	4.4	10.3	4.2	2.4	9.3	1.6	3.9	0.9	3.1	2.9	3	2.98	2.84	3.02	2.45	3.14	2.9	2.59	3.14	2.02	4.81	2.06
M. cervicolor	7315	3.9	7.4	9.5	11.5	1.8	4.7	2.8	2.3	6.5	NA	3.2	0.6	2.6	2.98	3.04	2.87	2.33	2.35	2.84	3.18	3.38	NA	2.44	1.87	5.4	2.02
Mus cookii	7210	4.8	8.3	13.1	16	6.6	9.3	3.2	2.2	6.9	NA	5.4	1.8	2.52	2.68	2.99	2.76	2.77	2.47	2.45	3.34	3.13	NA	2.6	2.15	6.1	2.12
M. cookii	7238	2.8	9.2	12.5	13.6	3.6	3.9	3.4	1.2	7.2	3.2	1.7	1.5	3.33	3.58	3.87	3.53	2.23	2.96	2.78	3.11	3.25	2.97	3.54	1.85	4.46	2.17
M. cookii	7239	3.3	9.6	7.3	9.3	2.7	7.4	1.5	1	5	NA	2.2	2.2	2.75	3.18	3.3	3.33	2.58	2.83	3.09	2.71	3.31	NA	3.26	1.67	4.84	2.4
M. cookii	7243	NA	8.1	14.3	19.6	5.8	11.5	5.4	1.5	9.6	1.9	2.9	1.1	3.83	3.83	3.56	3.17	3.07	2.68	2.68	2.99	3.14	2.97	2.96	2.41	4.7	2.42
Mus fragilicauda	7254	3.9	5.6	16.6	15.3	4.1	4	2.3	NA	12.7	NA	5.6	0.8	3.4	3.03	3.32	3.22	2.15	2.52	3.22	NA	3.19	NA	3.14	2.58	4.52	2.29
M. fragilicauda	7261	1.2	3.7	5.5	6.4	0.1	1.9	0.2	1.4	2.6	NA	1.5	0.6	2.67	2.57	3.43	3.34	2.76	2.52	2.02	2.32	2.74	NA	2.83	1.58	4.26	2.1
Mus mattheyi	mattheyi1	NA	1.6	3.6	2.4	0.6	1.5	NA	0.7	1.9	0.8	0.8	0.8	2.74	2.74	3.52	3.45	2.6	2.26	NA	2.84	2.77	2.51	2.88	1.81	2.48	1.88
Mus minutoides	minut1	1.1	3	3.4	3.3	2	3	NA	2.4	2.4	1.6	1.6	1.6	3.07	3.24	3.64	3.58	1.91	1.65	NA	1.64	1.9	2.83	3.7	1.25	3.52	2.12
M. minutoides	minut2	1.4	3.6	4.4	5.2	1.5	3.1	NA	0.1	4	1.3	1.3	0.1	2.7	2.72	2.97	2.79	2.81	2.23	NA	2.8	2.63	2.39	2.68	1.87	3.52	2
Mus pahari	7226	5.2	9.1	16.7	16.1	4	13.5	7.8	3.7	5.4	NA	4.1	0.8	2.77	3.18	3.39	4.03	3.01	3.37	2.67	2.7	2.89	NA	2.77	1.7	7.58	2.47
M. pahari	7235	4	11.4	12	13.5	0.8	3.5	1.2	0.7	7	NA	5.6	0.7	2.93	3.2	3.23	3.37	2.07	2.86	2.37	2.69	3.29	NA	2.59	1.93	5.54	2.55
M. pahari	PAH54-7	NA	17.9	17.9	27.3	5.6	1.5	4.6	7.1	6.1	2.7	7.8	2.3	4.87	4.87	3.72	4.5	3.29	3.74	3.6	3.79	3.74	3.84	3.58	3.07	10.22	3.09
M. pahari	PAH54-9	4	18.1	17	27.2	3.7	11.3	5.5	5.2	8	2.3	6.9	1.7	3.83	4.22	3.56	4.29	3.81	3.37	3.98	4.04	3.64	3.51	4.03	3.3	10.22	2.96
Niviventer fulvescens	7198	25.9	92	89.1	98.4	22	33	21.6	4.3	37.2	10	30	7.5	3.53	4.18	3.88	3.73	2.54	2.24	3.02	3.68	3.07	3.75	3.86	2.39	20.94	4.11
N. fulvescens	7200	22.2	49.8	76.4	59	9.6	12.7	9.8	12	19.7	7	19.5	5.6	3.57	3.18	3.61	4.26	3.13	3.07	2.66	2.56	3.1	3.1	3.44	2.24	16.63	3.84
N. fulvescens	7227	2.7	20.7	14.6	17.4	0.5	12.1	6.2	0.7	4.1	1.6	0.8	0.2	2.76	3.24	2.92	3.13	2.63	1.98	2.4	3.16	2.84	3.41	2.35	2.17	7.23	2.98
N. fulvescens	7240	31	62	83.3	82.1	34.4	53.4	25.1	9.6	37.3	5.8	28.7	8.8	4.47	3.21	2.99	3.62	2.33	2.24	3.19	3.53	3.88	2.55	3.58	3.01	14.61	4.25
N. fulvescens	7244	15.9	96.4	67.5	67.1	26.3	10.8	8.7	9.9	38	NA	34.8	4.9	3.05	4.33	3.97	3.95	3.06	2.84	2.92	3.56	3.8	NA	4.77	2.57	17.38	4.09
N. fulvescens	7245	25.5	71	63.5	84.5	18.7	45.7	20.2	12.6	46.6	9.9	37.4	3.3	2.9	3.33	3.01	3.71	1.99	2.65	2.86	3.22	3.13	2.81	3.34	2.27	17.06	4.44
N. fulvescens	7246	22.5	84.2	62.4	91	17	34.9	27.9	16.1	39.5	29.15	29.15	9.8	2.82	4.14	3.85	3.86	3.43	2.64	2.41	3.14	2.97	2.74	3.41	2.61	12.8	3.83
N. fulvescens	7248	NA	59.4	73.9	69.7	7.5	38.1	10.2	14.7	38.4	17	18.5	8.2	3.59	3.59	3.46	3.1	2.17	2.75	2.57	2.56	3.49	3.21	3.03	1.95	16.6	3.96
Rattus andamanensis	7216	62.6	245	132.7	190.5	73.6	117.5	72.1	14.2	183.6	40.2	61.1	15.2	4.24	4.41	5.86	4.54	3.55	2.93	3.43	6.03	4.27	3.73	4.51	2.95	26.98	5.44
Rattus exulans	7267	NA	17	24.5	19.4	11.7	5.3	5.6	3.1	13.5	6.8	5.7	2.4	3.56	3.56	2.74	3.79	2.89	2.36	2.43	3.24	2.99	3.74	3.61	1.71	7.38	2.9
R. exulans	7288	6.5	23.3	23.7	17.3	4.6	8.4	5.2	4.1	13.6	4.2	5.5	0.8	3.13	2.79	3.07	2.79	2.22	1.9	2.43	2.77	2.8	2.8	3.07	1.71	4.61	2.99
R. exulans	7291	7.7	27.8	27.6	30.2	NA	66.5	NA	2	26	1	10.7	1.3	3.89	3.94	3.8	4.47	NA	2.56	NA	3.5	3.76	2.95	5.01	1.55	6.68	3
R. exulans	7292	13.2	27.3	10.3	33.4	4.5	4.6	NA	6.1	23.1	NA	13.5	NA	2.24	2.66	2.8	2.87	2.15	1.83	NA	3.05	3.54	NA	2.7	NA	8.05	2.98
R. exulans	7296	6.7	21.7	19.7	22.6	4.5	7.3	7.6	3.2	12.9	13.3	NA	1.4	2.82	3.87	4.01	4.54	2.1	2.54	3.48	4	3.59	3.4	NA	1.94	7.82	3.09
R. exulans	7298	4.8	25.9	25.9	23.4	7.7	12.4	7.1	5.8	15.5	4.1	7.3	2.6	2.68	3.99	3.4	3.9	2.62	2.51	2.92	3.29	3.95	3.41	3.39	2.44	8.9	3.06
R. exulans	7306	6.5	20.2	18.4	19.3	5	7.8	6.8	3.3	12.9	3.5	5.3	2.3	3.61	3.62	3.3	3.53	2.8	2.19	2.82	3.43	3.63	3.31	4.23	2.4	6.27	2.88
R. exulans	7311	11.5	29.5	28.4	38.4	5.6	14.2	5	8.6	24.7	NA	14.5	1.1	2.77	4.18	3.71	4.2	1.96	2.07	2.76	4.08	3.55	NA	3.57	1.83	8.78	3.13
Rattus tanezumi	7201	14.8	37.4	47.6	39.3	16.1	25.4	13.6	8.5	26.1	8.8	11.3	NA	3.26	3.33	3.29	3.82	2.13	2.32	2.2	3.03	3.37	3.24	3.17	NA	15.6	3.27
R. tanezumi	7206	19.9	62.7	59.2	75.4	11.9	26.8	5.6	8.6	39.8	7.1	21.5	3	3.11	3.51	3.09	3.92	2.96	2.32	2.46	3.45	3.4	3.27	3.84	2.47	23.63	3.67
R. tanezumi	7208	16.1	49.7	47.3	52.2	16	27.9	15.3	9.5	27.6	9.6	15.6	3.8	3.77	4.69	4.84	5.45	4.06	3.77	3.54	3.86	4.55	3.91	5.46	2.01	22.02	4.06
R. tanezumi	7209	10.8	55.5	39.4	63	7.2	22	17	4.7	34.8	NA	12.2	2.5	3.36	3.44	3.35	3.49	2.73	2.12	2.97	3.16	3.87	NA	3.44	1.72	17.06	3.43
R. tanezumi	7217	23.8	75.3	58.5	89.6	14.1	37.1	13.1	9.6	45.1	15.3	13.5	4.6	3.87	4.5	5	5	4.3	3.4	3.25	3.99	4.21	4.61	5.67	2.13	20.56	3.62
R. tanezumi	7257	21	76.2	82.9	93	14.6	27.6	30.9	15.6	39.2	46.1	18.8	4.4	3.25	4.36	3.5	4.47	2.71	2.36	3.08	3.44	2.82	4.3	4.08	2.55	28.38	3.98
R. tanezumi	7270	26.3	123.5	90.8	98.2	10.4	18	19.9	13.5	80.4	17.5	19.7	4.4	3.38	4.72	4.76	4.97	3.21	2.65	2.71	4.11	4.06	3.53	5.13	2.32	22.2	4.27
R. tanezumi	7273	55.9	166	130.2	156.7	26.9	25.8	66.6	40.1	68.2	32.2	30.1	12.4	4.07	5.25	3.05	5.92	2.16	3.85	3.75	4.34	3.01	4.1	4.97	2.49	28	4.74
R. tanezumi	7284	25.6	82.3	126.5	96.1	23.1	68	26.1	14.3	73.5	26	20.2	12	4.18	4.73	4.59	4.63	3.14	3.04	3.82	3.2	4.39	4.16	3.56	2.47	26.19	4.06
R. tanezumi	7302	35.4	77.3	139.6	126.7	22.7	72.4	29.1	22	106.9	17.3	31.6	13.9	4.47	5.64	4.9	5.42	2.96	3.1	4.03	4.86	5.91	4.36	4.27	3.03	15.9	4.26
R. tanezumi	7317	45.8	125.4	207.5	133	8.5	22.8	30.6	16.9	90.5	NA	70.5	11.4	4.19	4.19	4.23	4.36	2.53	2.16	3.2	4.04	4.6	NA	4.51	2.84	23.45	4.88
R. tanezumi	7319	8.9	29.1	18.5	22.3	4.1	17	3.3	4.2	16.8	NA	23.4	7	3.12	2.84	2.94	2.92	2.7	2.27	2.31	3.15	3.21	NA	2.74	1.26	11.93	3.44
R. tanezumi	7320	49.2	98	140.5	145.5	9.1	47	28	37.6	130.5	NA	67.8	22.1	4.71	5.38	7.12	6.37	2.96	2.84	3.17	4.88	4.46	NA	5	3.66	22.55	4.61

Abbreviations for muscle names are as follows: Digas = digastric; DM.ant = anterior deep masseter; DM.pos = posterior deep masseter; M.sup = superficial masseter; Pt.ext = external pterygoid; Pt.int = internal pterygoid; Tp.I-O = intraorbital part of the temporalis; Tp.lat = lateral temporalis; Tp.med = medial temporalis; Zyg.ant = anterior zygomaticomandibularis; Zyg.I-O = infraorbital zygomaticomandibularis; Zyg.pos = posterior zygomaticomandibularis.

landmark at the most anterior tip of the nasal bones and a second at the most posterior point of the occiput, and calculating the distance between them. Skull length was used as the size estimator throughout the analyses.

Physiological cross sectional areas (PCSA) were calculated based on the mass of the muscles, a density of 1.06 g cm^{-3} (Mendez and Keys, 1960), and the average fiber length for each muscle.

$$\text{PCSA} = \frac{\text{Muscle mass}}{1.06 \times \text{fiber length}}$$

As complex pennate muscles were separated into their component parts, no additional correction for pennation was considered. To calculate muscle forces, cross sectional areas were multiplied by a conservative muscle stress estimate of 30 $N.cm^{-1}$ (Herzog 1994), and by the cosine of the angle (Φ) of the muscle vector relative to the reaction force on the teeth (set vertical).

$$\text{Muscle force} = \text{PCSA} \times 30 \times \cos(\Phi)$$

Muscular data used are presented in Table 1.

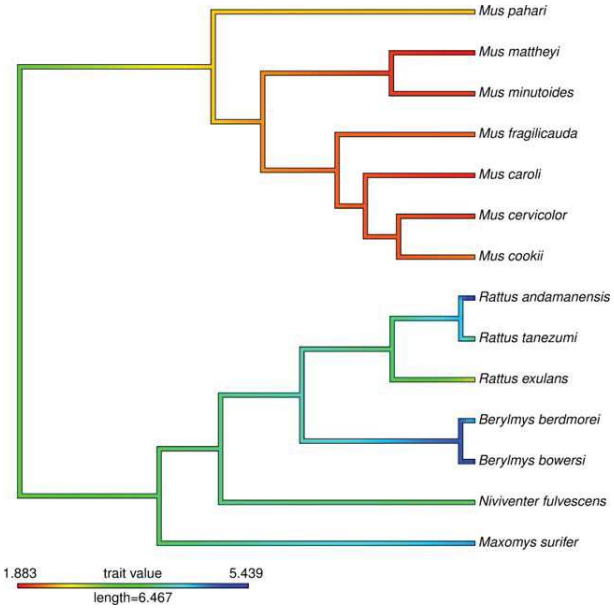

Fig. 2. Phylogenetic tree used in this study (extracted and modified from Fabre et al., 2013), with skull size mapped onto it (blue = larger; red = smaller) using the contMap function of package "phytools" in R.

Statistical Analyses

All analyses were run in R software (R Core Team 2016) and all data were natural log-transformed before analyses. For interspecific level analyses, we computed the species means for bite force and muscular variables. When looking at the influence of muscular variables on bite force, we grouped muscle of the same muscular group together rather than using separate values (to reduce the number of explanatory variables and allow the use of specimens with missing values). Thus, we ran the analyses with five muscle groups: superficial masseter, deep masseter, temporalis, pterygoid, and zygomaticomandibularis. We used the same muscular variables, and calculated and *in vivo* bite force, to test their scaling with size. Finally we ran the same scaling analyses using independent contrasts of size, muscular variable, and estimated and in vivo bite force.

To test the validity of our bite force estimates we correlated individual values to their corresponding *in vivo* observations, both at the interspecific and intraspecific levels (in species for which eight or more specimens had both values available). A redundancy analysis (RDA) was used to visualize which muscular variables were the main drivers of bite force variation. For this analysis only, we used raw (rather than log transformed) values centered on their means and scaled to unity variance, since our variables had different units. Muscular attributes (including fiber length, muscle mass, and muscle PCSA) were our response variables, while size, *in vivo* and estimated bite force were the explanatory variables. This RDA also allowed us to test which muscular traits were at the root of the discrepancies between *in vivo* and estimated bite force.

To test the potential effect of phylogeny and size on bite force, we pruned a tree from the one published by Fabre et al. (2013) with divergence time estimates. *Mus mattheyi* and *Mus fragilicauda* were missing from the

TABLE 2. Scaling of muscular traits (mass and fiber length) and bite forces against skull size at the interspecific level

	Slope	Estimate	SE	*t* value	*P* value
Mass DM	**3.373**	0.373	0.101	3.697	<0.001
Mass M.sup	3.191	0.191	0.1099	1.737	0.0866
Mass Ptery	3.148	0.148	0.1953	0.76	0.45
Mass Temp	**3.301**	0.3009	0.1304	2.308	<0.05
Mass Zyg	**3.602**	0.6016	0.1216	4.949	<0.001
Fiber DM	**0.365**	−0.635	0.0635	−9.995	<0.001
Fiber M.sup	**0.4247**	−0.5753	0.0523	−10.99	<0.001
Fiber Ptery	**0.1989**	−0.8011	0.0671	−11.94	<0.001
Fiber Temp	**0.3936**	−0.6064	0.0622	−9.742	<0.001
Fiber Zyg	**0.5266**	−0.4734	0.0943	−5.021	<0.001
In vivo bite force	2.013	0.0126	0.0959	0.132	0.895
Estimated bite force	**2.843**	0.843	0.0967	8.713	<0.001

Values in bold differ significantly from their expected slopes (1 for fiber length, 3 for muscle mass, and 2 for bite force). Abbreviations for the groups of muscles are as follows: DM = deep masseter; M.sup = superficial masseter; Ptery = pterygoids; Temp = temporalis; Zyg = zygomaticomandibularis.

TABLE 3. Scaling of the independent contrasts of muscular traits and bite forces against the independent contrasts of size

	Slope	Estimate	SE	*t* value	*p* value
Mass DM (IC)	3.197	0.197	0.276	0.715	0.49
Mass M.sup (IC)	3.126	0.126	0.291	0.435	0.672
Mass Ptery (IC)	3.607	0.607	0.326	1.86	0.09
Mass Temp (IC)	**3.743**	0.743	0.319	2.332	0.04
Mass Zyg (IC)	3.309	0.309	0.162	1.906	0.083
Fiber DM (IC)	**0.521**	−0.479	0.052	−9.196	<0.0001
Fiber M.sup (IC)	**0.063**	−0.937	0.087	−10.72	<0.0001
Fiber Ptery (IC)	**0.442**	−0.558	0.079	−7.084	<0.0001
Fiber Temp (IC)	**0.628**	−0.372	0.138	−2.686	0.021
Fiber Zyg (IC)	0.872	−0.128	0.253	−0.505	0.623
In vivo bite force (IC)	1.505	−0.495	0.24	−2.06	0.064
Estimated bite force (IC)	**2.766**	0.766	0.247	3.101	0.01

Expected slopes and abbreviations are the same as in Table 2.

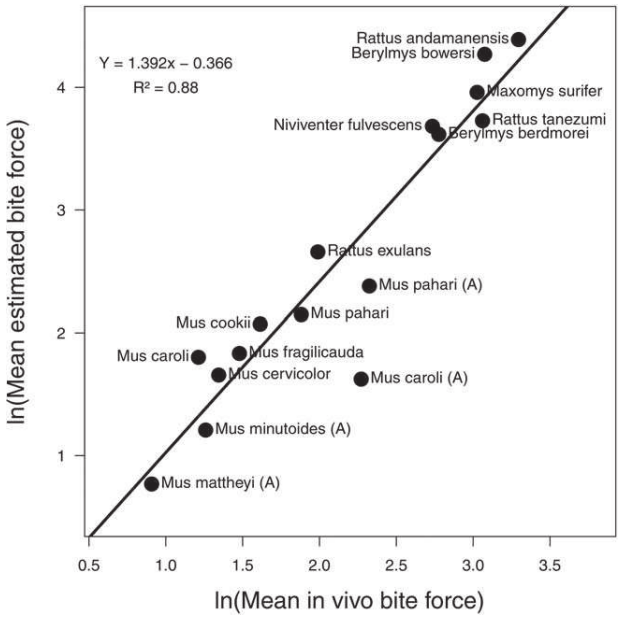

Fig. 3. Plot showing the linear relationship between log transformed *in vivo* and estimated bite force at the interspecific level. Each point represents the average value for one species. (A) denotes lab-reared populations.

tree, and were added using divergence times from Veyrunes et al. (2005) and Suzuki et al. (2004) (Fig. 2).

As size is usually the main variable driving differences in bite force and morphology, most studies have used residuals from linear regression of the trait of interest against size to filter out the effect of size. Because they are not orthogonal from the regression line, ordinary residuals from linear regressions can still covary with size as a technical artefact. Therefore, instead of linear regressions, we computed orthogonal regression of estimated bite force against size, and of *in vivo* bite force against size and used the minor axis as a size corrected variable. We were then able to calculate independent contrasts (IC) for our size independent variables (i.e., the aforementioned minor axis), to assess their correlations when accounting for phylogenetic nonindependence (Felsenstein 1985).

Using orthogonal regression, we computed the major and minor axis of covariation of muscular data (fiber length, mass and PCSA) with size. We also calculated the IC for the size-independent axes of covariation for PCSA, muscle mass and fiber lengths, and tested their correlation with *in vivo* bite force and estimated bite force. We used the fitContinuous function from the R package Geiger (Harmon et al. 2008), to check for phylogenetically driven variation in our sample, and to compare between different models of the evolution of bite force, size, and muscular variables. We fit Brownian Motion (BM), Ornstein-Ulhenbeck (OU), lambda, Early Burst (EB) and White Noise (WN) models, and used AIC to assess which of them best described the evolution of bite force. We used the same function to test for models of size and muscle evolution along the diversification of mice and rats.

As bite force estimations are sometimes imprecise at the intraspecific level, we also tested this in our sample. We performed some analyses at the intraspecific level in four species for which we had eight or more representatives. Again, we correlated *in vivo* bite force and estimated bite force as well as their correlation to skull size. As with interspecific analysis, we computed orthogonal regressions to check if size-independent *in vivo* bite force and estimated bite force would still be significantly linked.

RESULTS

Scaling of Variables to Size

Most muscle groups had significant positive allometries for their mass (with the exception of the superficial masseter and pterygoid), with slopes much higher than the expected value of 3 predicted by geometric similarity models. On the other hand, fiber lengths showed negative allometries for all muscle groups with slopes significantly smaller than the expected value of 1. For bite force, allometries differed, with *in vivo* bite force being isometric, while estimated bite force showed significant positive allometry (Table 2). Different results were found using independent contrasts (Table 3), with muscle mass scaling with the expected slope of 3, excepted for the temporalis which shows significantly positive allometry. As with the nonphylogenetic analyses, fiber lengths scaled with size with significantly smaller than expected slopes, except for the zygomaticomandibularis. Finally, *in vivo* bite force did not have a slope significantly different from isometry, but estimated bite force had significantly positive allometry, as was found with the nonphylogenetic analyses.

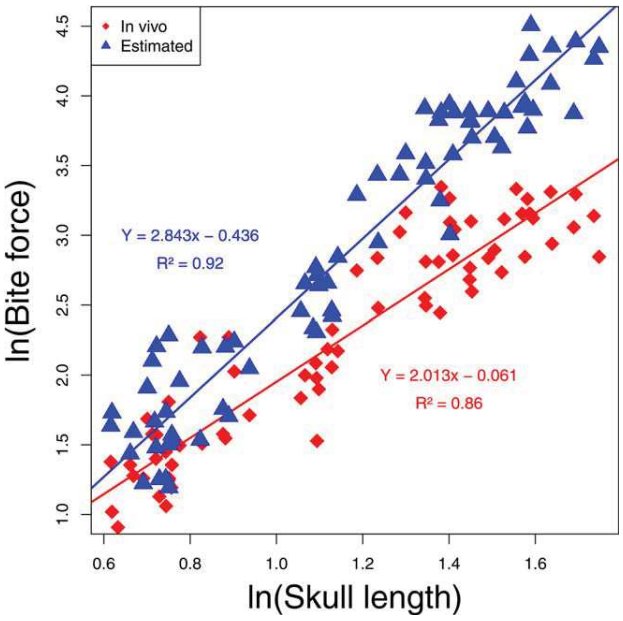

Fig. 4. Plot showing the difference in the scaling of log transformed *in vivo* bite force and estimated bite force against size. Both slopes are significantly different with slope∼2 for *in vivo* bite force (red diamonds) versus slope∼2.8 for estimated bite force (blue triangles).

Correlation Between Bite Force Values

We computed biomechanical estimates of bite force and compared them to our *in vivo* data. At the interspecific level, the log transformed values showed a very significant correlation ($r^2 = 0.88$, $P < 0.001$) (Fig. 3). Lab-reared populations of *M. pahari* (PAH) and *M. caroli* (KTK) deviated from this relationship, with much higher *in vivo* than estimated bite force. The slope of the linear regression between *in vivo* and estimated bite force was >1 (slope = 1.4, $t = 3.08$, $P < 0.01$), meaning that estimates diverge slightly but significantly from measured bite force (Fig. 4). Orthogonal regressions revealed that size explained most of the variance of *in vivo* bite force and estimated bite force (89% and 88%, respectively). Residuals (i.e., minor axis) from these regressions were still strongly related ($r^2 = 0.67$, $P < 0.001$), which shows that the good fit of estimated bite force is not only explained by size.

Redundancy analysis (RDA) (Fig. 5)

The RDA was performed on muscular variables constrained by size, estimated, and *in vivo* bite forces. This analysis allowed us to pinpoint the muscular attributes that correlate with each of these three constraining variables (size, *in vivo* bite force, and estimated bite force). It showed that 87% of the variance in muscular attributes was "redundant" with (i.e., explained by) the constraining variables, while 13% remained, independent of the constrained axes. As expected, we found that the first constrained axis is mainly linked to size, and that all muscular variables, and bite forces, are correlated to it (Fig. 5A). We also showed that *in vivo* bite force and estimated bite force are divergent along the second constrained axis. Therefore, the variables that explain this

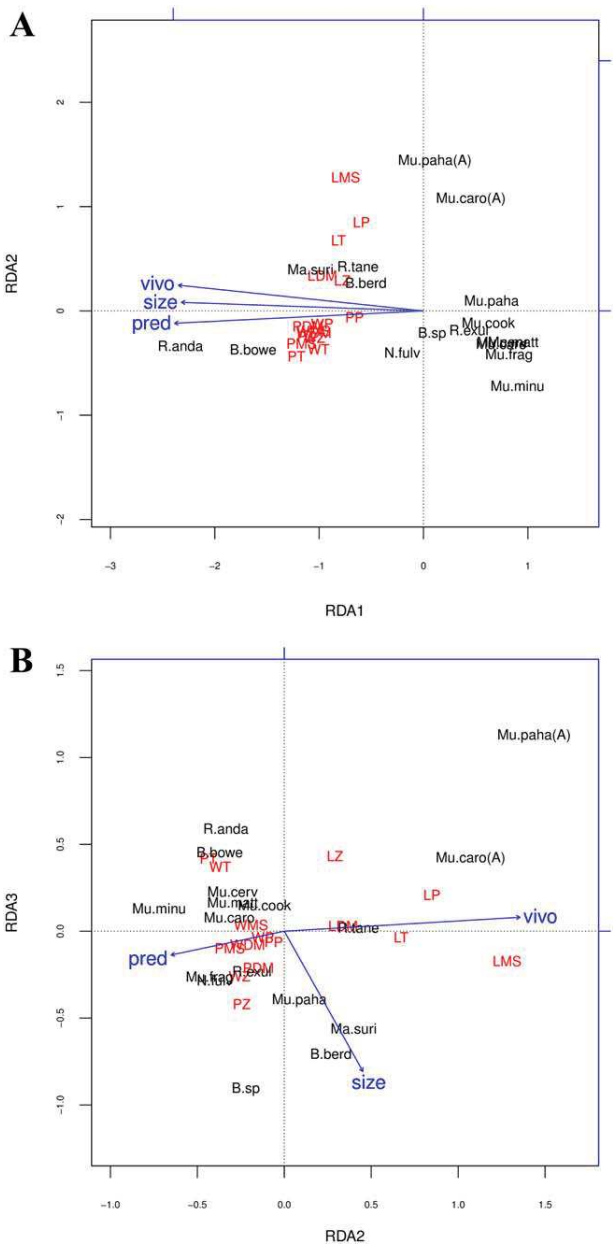

Fig. 5. Plot of the RDA run on muscular variables, constrained by bite forces and size. (**A**) Constrained axes 1 and 2. (**B**) Constrained axes 2 and 3. Species names are abbreviated. B.berd: *Berylmys berdmorei*; B.bowe: *Berylmys bowersi*; M.suri: *Maxomys surifer*; M.caro: *Mus caroli*; M.cerv: *Mus cervicolor;* M.cook: *Mus cookii;* M.frag: *Mus fragilicauda*; M.matt: *Mus mattheyi*; M.minu: *Mus minutoides*; M.paha: *Mus pahari*; N.fulv: *Niviventer fulvescens*; R.anda: *Rattus andamanensis*; R.exul: *Rattus exulans*; R.tane: *Rattus tanezumi*; M.caro(A): lab-reared *Mus caroli;* M.paha(A): lab-reared *Mus pahari*. Variables abbreviations as follow, pred: estimated bite force; vivo: in vivo bite force; size: skull length; LDM, LMS, LP, LT, LZ: mean muscular fiber lengths for the deep masseter, superficial masseter, pterygoid, temporal and zygomaticomandibularis muscular groups, respectively; WDM, WMS, WP, WT, WZ: mean muscle mass for the same muscular groups; PDM, PMS, PP, PT, PZ: mean PCSA for the same muscular groups.

divergence should scale along this axis. Interestingly, it appeared that the ordination of muscular attributes along axis RDA2 mainly separates fiber lengths, correlated with *in vivo* bite force, from muscular masses and PCSAs, which correlated with estimated bite force (Fig. 5B).

Effect of the Phylogeny on Bite Force, Size, and Muscular Variation

Independent contrasts of both *in vivo* and estimated bite forces were very tightly correlated to the independent contrasts of size ($r^2 = 0.68$ and $r^2 = 0.89$, respectively, with $P < 0.001$) at the interspecific level. Moreover, the IC of size-independent *in vivo* bite force and estimated bite force (obtained by orthogonal regression) were strongly correlated ($r^2 = 0.87$, $P < 0.0001$). As expected, the IC of PCSA, muscular mass and fiber length also showed robust correlations (length vs mass $r^2 = 0.74$, mass vs PCSA $r^2 = 0.96$, PCSA vs length $r^2 = 0.78$ with all $P < 0.0001$). However, we found no correlation between the IC of either *in vivo* bite force or estimated bite force and PCSA, muscle mass, or fiber length (all $P > 0.3$).

To complement these analyses and better understand how phylogeny influenced musculature and bite force, we tested models of evolution for size-independent *in vivo* bite force, estimated bite force, and size. For both *in vivo* bite force and estimated bite force, white noise model showed the best results (i.e., lowest AIC), while for size lambda model was selected, showing significant phylogenetic signal (lambda = 0.71, $P < 0.01$). Similar to bite force, size independent variation in PCSA, fiber length, and muscle mass were best described by the white noise model.

Variation in Muscular Attributes and Bite Force

Using size-independent muscle masses, PCSA, and fiber lengths, we found that the size independent axes of muscular covariation was not significantly correlated with the size independent bite force axes, suggesting that muscular changes did not relate significantly to bite force changes (both *in vivo* and estimated). Similar results were obtained with the IC of PCSA, fiber lengths, and muscle mass, compared to the IC of *in vivo* bite force and estimated bite force. In any case, we found that only a rather small part of muscular variation was independent of size, with about 13% for PCSA and 12% for muscle mass. Fiber length, however, showed 20% of size-independent variation.

Intraspecific Level Analyses

Four species in our dataset had eight or more specimens with associated *in vivo* bite force, dissections and therefore estimated bite force data: *Rattus tanezumi* (N = 13), *Mus cervicolor* (N = 10), *Rattus exulans* (N = 8), and *Niviventer fulvescens* (N = 8). For *R. tanezumi* and *M. cervicolor*, a significant correlation between *in vivo* and estimated bite force was found (respectively $r^2 = 0.61$, 0.66 and $P < 0.05$). *N. fulvescens* showed marginally significant correlation ($r^2 = 0.7$, $P = 0.052$); however, this was mainly driven by one juvenile outlier, whose removal from the analysis produced a nonsignificant correlation ($P > 0.8$). No correlation was found in *R. exulans*.

In *R. tanezumi*, both *in vivo* bite force and estimated bite force were correlated with skull size ($r^2 = 0.57$ and 0.83, with $P < 0.05$ and $P < 0.001$, respectively). When looking at size-independent (i.e., after orthogonal regressions against size) *in vivo* bite force and estimated bite force, the correlation remained significant ($r^2 = 0.59$, $P < 0.05$), suggesting that musculature differences at the individual level drive bite force differences.

In *M. cervicolor*, *in vivo* bite force and estimated bite force were not significantly correlated with skull size, and the correlation between them actually improved when using their size-independent values (from $r^2 = 0.66$, $P < 0.05$ to $r^2 = 0.95$, $P < 0.0001$). It is worth noting that skull size variance was very small in our sample of *M. cervicolor*.

In *R. exulans*, neither estimated bite force nor *in vivo* bite force were significantly linked to size. However, size-independent estimated bite force and *in vivo* bite force were correlated ($r^2 = 0.79$, $P < 0.02$). Similarly to *M. cervicolor*, *R. exulans* had a very small variance in skull size.

DISCUSSION

The predictive power of our biomechanical model is good (Fig. 3) with size being, as expected, the main explanatory variable for the variation in both estimated and *in vivo* bite force. Divergence between estimates and *in vivo* measurements are clearly shown by the differences in their scaling with size (estimated bite force has positive allometry, while *in vivo* bite force is isometric Fig. 4 and Table 2). RDA showed that this divergence is mainly due to differences in which muscular attributes are correlated with bite force (Fig. 5). *In vivo* bite force is more dependent on fiber length variation while estimated bite force is more dependent on muscle mass variation. This result is coherent with their differences in allometry, as muscle mass (linked to estimated bite force) shows positive allometry while fiber lengths (linked to *in vivo* bite force) show negative allometry. It therefore appears that higher values of estimated bite force are probably linked to the higher estimated muscular mass (Fig. 5). The RDA also showed that all muscular groups were indifferently involved in the variation of bite forces. The differences between estimated and *in vivo* bite force may be explained by imperfections in the biomechanical model, due to errors in dissections or fiber measurements for example, or by the fact that in vivo bite force is influenced by many biological factors, as well as by the settings of the force transducer. In any case, the very good correspondence between *in vivo* and estimated bite force shows that using dissections to estimate bite force can yield results very close to reality. Therefore, using biomechanical models for rodents when *in vivo* bite force data are unavailable is entirely justified.

At the intraspecific level, it appears that the biomechanical model has good results only in some cases. The lack of accuracy may be due to small sample size with animals being of similar size in contrast to those included in our interspecific analyses. When variation in size is reduced, behavioral variation and plastic changes in muscles among individuals within a species may become more powerful factors, causing discrepancies between *in vivo* bite force and estimated bite force. In

two species out of four studied here, we were able to get a good fit between modelled and real values. For *R. tanezumi*, this correlation is mostly due to size, but musculature still plays a significant role. For *M. cervicolor* the good fit of estimated values despite a limited variation in size probably reveals a very significant effect of muscle differences on bite force. In *R. exulans*, no correlation was found between *in vivo* bite force and estimated bite force, but when removing the effect of size, both values did correlate. It implies that size-independent muscle differences induce bite force differences in this species. This counterintuitive result might be due to the commensal niche occupied by this rat. Indeed, *R. exulans* has been frequently caught in basements, or around human infrastructures feeding on waste, rice stocks, or even farm animal food. These types of food may provide a very rich, yet rather soft diet, compared to that of wild animals. Such a diet may therefore allow normal or increased growth (due to the nutritional value of the food) while being functionally less demanding (due to its softness), furthermore very fine scale diet adaptation may be permitted by a great plasticity. Our results also show that one should exercise more caution when using biomechanical models for bite force at the intraspecific levels than at the interspecific level.

Populations of *M. pahari* and *M. caroli* from the lab are clearly differentiated from other species (including their wild conspecifics), with a much higher *in vivo* than estimated bite force. This could be due to an effect from laboratory rearing, as these lab mice show disproportionate muscle weights compared to their wild counterparts (Table 1), which may bias the bite force estimations. These mice may also be in generally better condition due to lowered threats (predation, parasites, and stress). Another explanation may be that the *in vivo* bite force used for these lab-reared specimens was not measured on the same specimens as the ones we dissected, but correspond to a mean value of the colony.

As expected, independent contrasts analyses showed strongly correlated evolution between size and bite force, independent of phylogeny. Furthermore, estimated bite force and *in vivo* bite force were still correlated independently of phylogeny and size, suggesting that skull morphology and muscular attributes also play a significant role in shaping performance. Based on Pagel's lambda values, it appears that size is not independent of phylogeny in our case. This nonindependence is probably due to the split between mice (smaller) and rats (bigger), which structures the size variation along the tree (Fig. 2). Furthermore, the scalings of musclular mass with size appeared to be different from the scalings of their independent contrasts, suggesting that phylogeny is also related to changes in the allometry of the muscles. Due to the strong correlation between size and bite force, the phylogenetic signal on size, and on the allometry of the muscles is likely the main factor explaining a potential effect of phylogeny on *in vivo* or estimated bite force when not correcting for the effect of size. As previously mentioned, the sole effect of size is not sufficient to fully explain the correlation between *in vivo* bite force and estimated bite force. Indeed, variation in the musculature was found to be correlated with bite force. However, most of this variation was also explained by the positive allometric relationships between muscles and size (Table 2). The remaining differences in muscles (i.e., nonallometric structural differences) between species did not correlate to size-independent differences in bite force, and followed a white noise (i.e. random) model of evolution. This may indicate that rodents can rapidly evolve their muscular organisation, or that it can be subject to important phenotypic plasticity. In any case, these changes do not appear directly linked to performance, which could suggest a case of many-to-one mapping, as found in other mammals (Young et al. 2007). Overall, size has a twofold effect on bite force: firstly via the phylogenetically driven size changes among species, whereby bigger animals have stronger bites; and secondly via the positively allometric differences in musculature, meaning that muscular mass (and PCSA) increases more than expected with size among species (Table 2). At a wider scale, when we compare the scaling of muscles in rodents with those of bats (Herrel et al. 2008a), it appears that muscle masses scale much more positively in the former. This may bring support to the hypothesis that bats have important muscle mass limitations due to flight. Interestingly, the slope of bite force against size is much smaller in bats (1.71) than in rodents (2.01 for *in vivo* bite force and 2.84 for estimated bite force; Fig. 4), which illustrates the twofold effect of size on bite force in our group of interest.

When accounting for the influence of size, the remaining phylogenetic effect on bite force was limited and the evolution of the bite force appeared to be random. Similarly, size-independent muscular variation was small and apparently random among our species. These elements are coherent with the hypothesis that skull structure and mechanics are quite stable in myomorphous rodents, or at least in murids. Indeed the randomness of size-independent variation and its limited scale suggest very subtle adaptive changes, and/or a more important role of plasticity. In other terms, the overall skull structure and function was conserved during the evolutionary history of our sample of the Muridae and skull evolution was mainly related to that of size, but morphological changes still appear to have happened, although they may not have produced large differences in performance. This could indicate that most murid rodents have a functional output that enables them to use a wide range of resources without requiring major morphological changes, and/or that architectural constraints of the skull limit major muscular changes. Other myomorphous rodent groups may show similar high performance through their convergence in skull morphotype, although we did not include any in this study. We also showed that skull size alone drives most of the functional changes observed in our species. Since size- and allometry-independent variation in musculature does not appear to be related to size-independent bite force differences, our results might also be explained by the fact that different anatomies may produce similar functional outputs (Bock 1959, Schmidt-Kittler 1997, Alfaro et al. 2005, Young et al. 2007).

Even if our results hold true for bite force, other functionally significant elements of performance may also vary with musculature, such as bite force at different gape angles or angular speed of jaw closure (e.g., Satoh and Iwaku 2006, Santana and Portugal 2016). Other available models for bite force estimation, such as those including the 3D skull morphology may also improve the precision of estimations (e.g., Davis et al. 2010). Indeed,

the 2D representations of the muscular attachments and line of actions used here may be a source of error in the modeled bite force. Another caveat is that we only tested muscular variation in terms of mass, fiber length, and PCSA against bite force. We did not test for an effect of bone morphology modifications on muscle organization. Indeed, size- and phylogeny-independent variation in mass, fiber length, and PCSA is reduced, but functional adaptation may for example be brought via changes in lever arms rather than in muscle themselves.

Our conclusions may not apply to all myomorphous rodents since our dataset was strictly restricted to a limited number of murine species. Furthermore, our dataset lacked extreme specialists. While mice and rats are often regarded as best representatives of the myomorphous morphotype, it is clear that other myomorphous rodents (e.g., Cricetidae and Gliridae) depart from the skull variation seen in murines. Owing to the predictive power of our biomechanical models, it would be now particularly interesting to ascertain the biomechanical implications of the zygomasseteric arrangement in glirids that convergently evolved a pseudomyomorphous type of skull (*sensu* Vianey-Liaud 1989, but see also Hautier et al. 2008).

ACKNOWLEDGEMENTS

The authors would like to thank Serge Morand and other members of the Ceropath and Biodiv-healthSEA projects who helped organize and participated in the field work. They are also very grateful to Frederic Veyrunes and Jean-Jacques Duqesne who gave some specimens and allowed us to measure bite forces in their lab colonies. Pierre-Henri Fabre's help with the phylogeny was invaluable. Finally, they would like to Adam Hartstone-Rose for the invitation to participate in this issue, and S. Santana and two anonymous reviewers for their helpful and constructive comments. Parts of the experiments were performed using the μ-CT facilities of the MRI platform and of the LabEx CeMEB. This publication is a contribution of the Institut des Sciences de l'Evolution de Montpellier (UMR 5554 – UM2 + CNRS + IRD) No. ISEM 2017-280

LITERATURE CITED

Aguirre LF, Herrel A, van Damme R, Matthysen E. 2002. Ecomorphological analysis of trophic niche partitioning in a tropical savannah bat community. Proc R Soc Lond B 269:1271–1278.

Aguirre LF, Herrel A, van Damme R, Matthysen E. 2003. The implications of food hardness for diet in bats. Funct Ecol 17:201–212.

Alfaro ME, Bolnick DI, Wainwright PC. 2005. Evolutionary consequences of many-to-one mapping of jaw morphology to mechanics in labrid fishes. Am Nat 165:E140–E154.

Aplin KP, Suzuki H, Chinen AA, Chesser RT, Ten Have J, Donnellan SC, Austin J, Frost A, Gonzalez JP, Herbreteau V, et al. 2011. Multiple geographic origins of commensalism and complex dispersal history of black rats. PLoS ONE 6:e26357.

Baverstock H, Jeffery NS, Cobb SN. 2013. The morphology of the mouse masticatory musculature. J Anat 223:46–60.

Becerra F, Echeverria A, Vassallo AI, Casinos A. 2011. Bite force and jaw biomechanics in the subterranean rodent Talas tuco-tuco (*Ctenomys talarum*) (Caviomorpha: Octodontoidea). Can J Zool 89:334–342.

Berry RJ, Jakobson ME. 1975. Adaptation and adaptability in wild-living House mice (*Mus musculus*). J Zool 176:391–402.

Bock WJ. 1959. Preadaptation and multiple evolutionary pathways. Evolution 13:194–211.

Brandt JF. 1855. Untersuchungen über die craniologischen Entwicklungsstufen und Classification der Nage der Jetzwelt. Mémoires de l'Academie Imperiale des Sciences de St Pétersbourg Série 6 9:1–365.

Corbalàn V. 2006. Microhabitat selection by murid rodents in the Monte desert of Argentina. J Arid Environ 65:102–110.

Cornette R, Baylac M, Souter T, Herrel A. 2013. Does shape covariation between the skull and the mandible have functional consequences? A 3D approach for a 3D problem. J Anat 223:329–336.

Cox PG, Fagan MJ, Rayfield EJ, Jeffery NS. 2011. Finite element modelling of squirrel, guinea pig and rat skulls: Using geometric morphometrics to assess sensitivity. J Anat 219:696–709.

Cox PG, Rayfield EJ, Fagan MJ, Herrel A, Pataky TC, Jeffery NS. 2012. Functional evolution of the feeding system in rodents. PLoS ONE 7:e36299.

Davis JL, Santana SE, Dumont ER, Grosse IR. 2010. Predicting bite force in mammals: Two dimensional versus three dimensional lever models. J Exp Biol 213:1844–1851.

Druzinsky RE. 2010. Functional anatomy of incisal biting in *Aplodontia rufa* and sciuromorph rodents – part 2: Sciuromorphy is efficacious for production of force at the incisors. Cells Tissues Organs 192:50–63.

Fabre P-H, Pagès M, Musser GG, Fitriana YS, Fjeldså J, Jennings A, Jønsson KA, Kennedy J, Michaux J, Semiadi G, et al. 2013. A new genus of rodent from Wallacea (Rodentia: Muridae: Murinae: Rattini), and its implication for biogeography and Indo-Pacific Rattini systematics. Zool J Linn Soc 169:408–447.

Felsenstein J. 1985. Phylogenies and the comparative method. Am Nat 125:1–15.

Freeman PW, Lemen CA. 2008a. A simple morphological predictor of bite force in rodents. J Zool 275:418–422.

Freeman PW, Lemen CA. 2008b. Measuring bite force in small mammals with a piezo-resistive sensor. J Mammal 89:513–517.

Harmon LJ, Weir JT, Brock CD, Glor RE, Challenger W. 2008. GEIGER: Investigating evolutionary radiations. Bioinformatics 24:129–131.

Hautier L, Cox P, Lebrun R. 2015. Grades and clades among rodents: The promise of geometric morphometrics. In: Cox P & Hautier L, editors. Evolution of the rodents: Advances in phylogeny, functional morphology and development. Cambridge: Cambridge University Press. p 277–299.

Hautier L, Michaux J, Marivaux L, Vianey-Liaud M. 2008. The evolution of the zygomasseteric construction in Rodentia, as revealed by a geometric morphometric analysis of the mandible of *Graphiurus* (Rodentia, Gliridae). Zool J Linn Soc 154:807–821.

Herrel A, Aerts P, De Vree F. 1998a. Ecomorphology of the lizard feeding apparatus: A modelling approach. Neth J Zool 48:1–25.

Herrel A, Aerts P, De Vree F. 1998b. Static biting in lizards: Functional morphology of the temporalis ligaments. J Zool 244:135–143.

Herrel A, Spithoven L, Van Damme R, De Vree F. 1999. Sexual dimorphism of head size in *Gallotia galloti*: Testing the niche divergence hypothesis by functional analyses. Funct Ecol 13:289–297.

Herrel A, De Smet A, Aguirre LF, Aerts P. 2008a. Morphological and mechanical determinants of bite force in bats: Do muscles matter?. J Exp Biol 211:86–91.

Herrel A, Huyghe K, Vanhooydonck B, Backeljau T, Breugelmans K, Grbac I, van Damme R, Irschick DJ. 2008b. Rapid large-scale evolutionary divergence in morphology and performance associated with exploitation of a different dietary resource. PNAS 105:4792–4795.

Herrel A, Moore JA, Bredeweg EM, Nelson NJ. 2010. Sexual dimorphism, body size, bite force and male mating success in tuatara. Biol J Linn Soc 100:287–292.

Herrel A, Podos J, Huber SK, Hendry AP. 2005. Bite performance and morphology in a population of Darwin's finches: Implications for the evolution of beak shape. Funct Ecol 19:43–48.

Herzog W. (1994). Muscle. In Biomechanics of the Musculoskeletal System (ed. B. M. Nigg and W. Herzog), pp. 154–187. Chichester: John Wiley.

Le Roux V, J-L C, Y F, P V. 2002. Diet of the house mouse (*Mus musculus*) on Guillou Island, Kerguelen archipelago, Subantarctic. Polar Biol 25:49–57.

Maestri R, Patterson BD, Fornel R, Monteiro LR, De Freitas TRO. 2016. Diet, bite force and skull morphology in the generalist rodent morphotype. J Evol Biol 29:2191–2204.
Michaux J, Chevret P, Renaud S. 2007. Morphological diversity of Old World rats and mice (Rodentia, Muridae) mandible in relation with phylogeny and adaptation. J Zool Syst Evol Res 45:263–279.
Navarrete SA, Castilla JC. 1993. Predation by Norway rats in the intertidal zone of central Chile. Mar Ecol Prog Ser 92:187–199.
Nies M, Ro JY. (2004). Bite force measurement in awake rats. Brain research protocols, 12:180–185.
R Core Team. 2016. R: A language and environment for statistical computing. Vienna, Austria: R Foundation for Statistical Computing. Url https://www.R-project.org/.
Rowe KC, Aplin KP, Baverstock PR, Moritz C. 2011. Recent and rapid speciation with limited morphological disparity in the genus *Rattus*. Syst Biol 60:188–203.
Samuels JX. 2009. Cranial morphology and dietary habits of rodents. Zool J Linn Soc 156:864–888.
Santana SE, Dumont ER. 2009. Connecting behaviour and performance: The evolution of biting behaviour and bite performance in bats. J Evol Biol 22:2131–2145.
Santana SE, Dumont ER, Davis JL. 2010. Mechanics of bite force production and its relationship to diet in bats. Funct Ecol 24:776–784.
Santana SE, Portugal S. 2016. Quantifying the effect of gape and morphology on bite force: Biomechanical modelling and *in vivo* measurements in bats. Funct Ecol 30:557–565.
Satoh K. 1997. Comparative functional morphology of mandibular forward movement during mastication of two Murid rodents, *Apodemus speciosus* (Murinae) and *Clethrionomys rufocanus* (Arvicolinae). J Morphol 231:131–142.
Satoh K, Iwaku F. 2006. Jaw muscle functional anatomy in northern grasshopper mouse, *Onychomys leucogaster*, a carnivorous murid. J Morphol 267:987–999.
Satoh K, Iwaku F. 2008. Masticatory muscle architecture in a murine murid, *Rattus rattus*, and its functional significance. Mammal Study 33:35–42.
Schmidt-Kittler N. 1997. Non-selective emergence of patterns and gradual change in macroevolution. Courier Forschungsinstitut Senckenberg 201:393–408.
Siahsarvie R, Auffray J-C, Darvish J, Rajabi-Maham A, Yu H-T, Agret S, Bonhomme F, Claude J. 2012. Patterns of morphological evolution in the mandible of the house mouse *Mus musculus* (Rodentia: Muridae). Biol J Linn Soc 105:635–647.
Suzuki H, Shimada T, Terashima M, Tsuchiya K, Aplin K. 2004. Temporal, spatial, and ecological modes of evolution of Eurasian *Mus* based on mitochondrial and nuclear gene sequences. Mol Phylogenet Evol 33:626–646.
Tullberg T. 1899. Über das System der Nagetiere. Eine phylogenetische studie. Nova Acta Regiae Societatis Scientiarium Upsaliensis 18:1–514.
Van Daele PAAG, Herrel A, Adriaens D. 2009. Biting performance in teeth-digging African mole-rats (*Fukomys*, Bathyergidae, Rodentia). Physiol Biochem Zool 82:40–50.
Verwaijen D, van Damme R, Herrel A. 2002. Relationships between head size, bite force, prey handling efficiency and diet in two sympatric lacertid lizards. Funct Ecol 16:842–850.
Veyrunes F, Britton-Davidian J, Robinson TJ, Calvet E, Denys C, Chevret P. 2005. Molecular phylogeny of the African pygmy mice, subgenus *Nannomys* (Rodentia, Murinae, *Mus*): Implications for chromosomal evolution. Mol Phylogenet Evol 36:358–369.
Vianey-Liaud M. 1989. Parallelism among Gliridae (Rodentia): The genus *Gliravus* Stehlin and Schaub. Hist Biol 2:213–226.
Waterhouse GR. 1839. Observations on the Rodentia with a view to point out groups as indicated by the structure of the crania in this order of mammals. Magaz Nat Hist 3:90–96. 184–188, 274–279, 593–600.
Young RL, Haselkorm TS, Badyaev AV. 2007. Functional equivalence of morphologies.

1.2.2 – Modélisation morphométrique de la force de morsure au niveau intraspécifique

(travail présenté oralement lors du congrès ICVM2016, article en préparation)

La mandibule étant la partie en mouvement de l'ensemble masticateur, sa taille, sa forme et son articulation avec le crâne sont soumises à des contraintes importantes liées à sa fonction. En effet, toute la musculature masticatrice s'y insère, permettant d'adducter la mandibule vers le crâne pour mordre ou mâcher. La variation morphologique de la mandibule est donc très fréquemment reliée à des différences de régime alimentaire et de mode de vie. Cependant, bien que le lien entre mandibule et fonction semble intuitif, il est rarement testé avec des données *in vivo*.

Il est apparu dans la section précédente que les estimations de performance réalisées à partir de la taille et de la musculature pouvaient manquer de précision au niveau intra-spécifique. De plus, elles ne s'appliquent généralement qu'à des spécimens dont la musculature est conservée, et demande la mise en place d'un protocole complexe et long. D'autres proxys de la force de morsure peuvent donc être recherchés, notamment par la morphométrie, comme la forme ou les bras de leviers de la mandibule, dont la variation peut entraîner des modifications fonctionnelles

Grâce aux données de force de morsure collectées sur le terrain, il est possible de comparer des estimations, modélisées à partir de la morphologie, à la force réellement déployée. Au niveau intra-spécifique, cette vérification est particulièrement nécessaire, car la force de morsure est certainement un caractère plastique et très dépendant de facteurs tels que la température, le stress ou la motivation (Anderson et al. 2008).

Morphometric models for estimating bite force in murid rodents : Empirical versus analytical models.

Samuel Ginot[1,2], Anthony Herrel[3], Julien Claude[1], Lionel Hautier[1]

[1] Institut des Sciences de l'Évolution de Montpellier (UMR5554), Montpellier, France.

[2] Institut de Génomique Fonctionnelle de Lyon (UMR5242), Lyon, France.

[3] Muséum National d'Histoire Naturelle (UMR7179), Paris, France.

Introduction

For decades, deductions of functional outputs from morphology have been routinely used in an adaptationist framework, to infer potential selective advantages linked to one phenotype or the other (Gould and Lewontin 1979, Mayr 1983). Although this has sometimes been done without actually measuring functional performance, the inclusion of functional morphology within the evolutionist paradigm has partly remedied to this (Arnold 1983). Today, ecomorphology and functional morphology have shown some of the best examples of adaptation and adaptive radiation (*e.g.* Grant and Grant 2002, Herrel et al. 2005, 2009). Yet, relationships between morphology and function varies between groups and at different scales (*e.g.* inter-specific, intra-specific or intra-population), and it remains necessary to prove and quantify the links between morphological and functional variation, to avoid the pitfalls of an extreme adaptationist point of view (Mayr 1983).

In the very diversified clade of rodents, links between skull or mandible morphology and diet and/or ecology have been shown in several groups and at different scales (Michaux et al. 2007, Samuels 2009, Hautier et al. 2009, Cox et al. 2012). Influence of skull and mandible morphology on *in vivo* bite force performance also has been directly tested, using various morpho-anatomical variables

(*e.g.* Freeman and Lemen 2008, Ginot et al. 2018). The biomechanical model or mechanical descriptors used in the these articles allows very good estimations of bite force (compared to *in vivo* data) at the interspecific level. However, Ginot et al. (2018) showed that their estimates of bite force were less precise at the intraspecific level. Furthermore, their approach requires a rather heavy protocole, and is inapplicable to specimens in which muscles have not been conserved. Therefore, other proxies may be used to estimate bite force, notably at the intra-specific level, and morphometric data may be used in this way.

In the following work, we will estimate bite force intraspecifically in five species of murine rodents (*Mus musculus*, *M. cervicolor*, *M. caroli*, *Rattus exulans*, *R. tanezumi*), for which we also have sufficient numbers of *in vivo* measurements. Several osteological proxies will be tested : mandible shape, temporal mechanical advantage, superficial masseter mechanical advantage and deep masseter mechanical advantage. Although mechanical advantages make mechanical sense and have been previously used as proxies for functional changes, their relationship with bite force has never been formally tested (*e.g.* Hautier et al. 2009, Renaud et al. 2015). We expect that higher mechanical advantage should be linked to higher bite force. Shape data may more fully include morphological variability, and therefore be a more precise proxy for bite force.

Materials and methods

Specimens

Most specimens were wild caught, with no control for age other than biological cues (development of testicles, presence of nippples): *M. cervicolor* (n=65), *M. caroli* (n=13), *R. exulans* (n=42) and *R. tanezumi* (n=29). All were caught with live traps (either locally bought rat cage traps, or Sherman traps) over the course of two weeks around the town of Sahatsakhan, Kalasin Province,

Thailand, during the dry season (February-March). *M. musculus* specimens (n=51), on the other hand, were raised in the lab but are descendants from wild ancestors captured on the Orkney islands (Scotland). Males and females were pooled to improve the sample size on which the predicitve bite force models were built (see below).

Bite force measurements

Shortly after capture we measured the animals' voluntary bite force at the incisors using a piezoelectric force transducer (Kistler, type 9203, range 0-500 N, accuracy 0.01–0.1 N; Amherst, NY, USA ; calibrated by the constructor at 25 °C and 36% humidity) attached to a handheld charge amplifier (Kistler, type 5995, Amherst, NY, USA ; Herrel et al. 1999). The force transducer was mounted between two steel bite plates as described in Herrel et al. (1999). We adjusted the distance between the bite plates by measuring it with a caliper, and by increasing or decreasing it via the micrometer head, so that each individual bit at a consistent gap angle. All animals bit directly onto steel at the same spot on the plates (*i.e.* at the tip), to ensure a consistent out-lever length. We recorded three trials in a row for each individual, and the maximal score was used in the analyses. All measurements were taken by one user (SG) to avoid inter-user variation.

Animals were treated in accordance with the guidelines of the American Society of Mammalogists, and within the European Union legislation guidelines (Directive 86/609/EEC). Approval notices for trapping and investigation of rodents were provided by the Ethical Committee of Mahidol University, Bangkok, Thailand, number 0517.1116/661. All lab procedures were under the Approval No. A34-172-042 (Hérault Prefecture).

Morphometric analyses

All mandibles were cleaned manually, after which they were photographed in a standardized

way (camera at a fixed distance, mandible positioned flat with the lingual side down) using a Pentax K200D reflex camera, with a 45mm focal distance. In total, 17 landmarks were placed on each mandible (Fig. 1) using tpsDig2.x software to represent shape, and to calculate the length of lever arms. The coordinates data were imported in R (R Core Team 2017) and scaled, centered and superimposed using Procrustes analyses routines from Claude (2008). Shape data were submitted to principal component analyses for variable reduction, and the principal components representing a total of 90 % of variation were kept. Mechanical advantages for the temporal, superficial masseter and deep masseter were obtained by computing their respective inlever / outlever ratios (Fig. 1).

Bite force estimations

Using mechanical advantage or shape data, we fitted linear models of *in vivo* bite force at the intraspecific level. To test the precision of the estimations of these models, we used a leave-one-out validation approach. To do so, we took out one individual from the dataset, fitted the model, then used

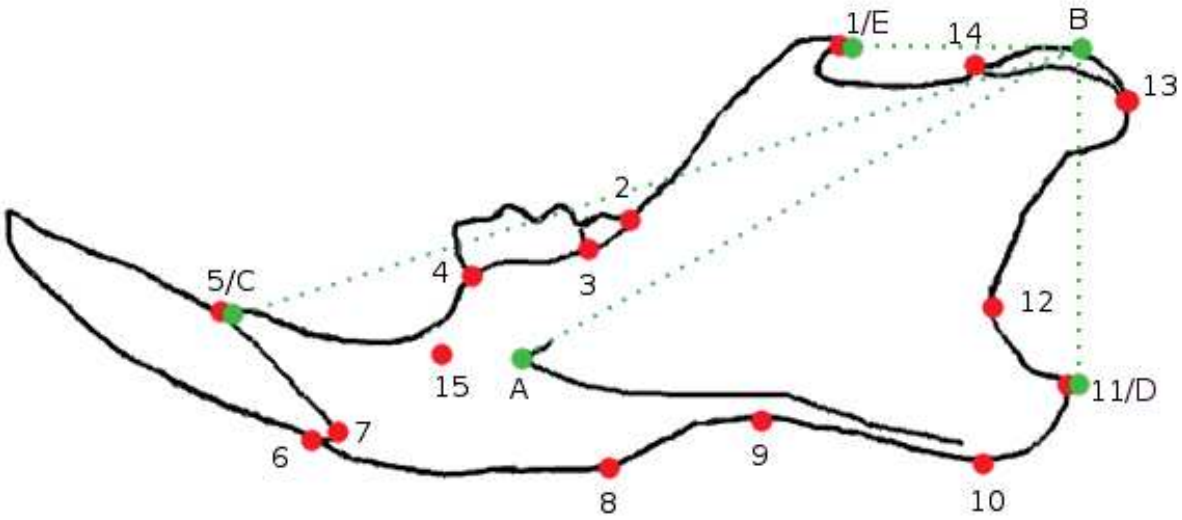

Figure 1. Mice mandible outline drawing, with the landmarks used in this study represented. Red landmarks are those used for shape analysis, and green landmarks to calculate lever arms. Shape and lever-arms were used in separate analyses. AB : Deep masseter inlever; BD : superficial masseter inlever ; BE : temporal inlever ; BC : outlever.

the 'predict' function in R to compute a bite force estimate for this individual. After iterating this process for all individuals, we compared estimated and *in vivo* bite force using one-tailed Pearson's correlation coefficient in which the alternative hypothesis was that the correlation was greater than 0, because estimations should be positively correlated with *in vivo* measures.

Results

Among the three mechanical advantages measured, only the deep masseter mechanical advantage allowed estimations that were correlated with the *in vivo* bite force. For the temporal and superficial masseter, estimated values of bite force were never significantly correlated with *in vivo* bite force (all $P > 0.1$). Therefore only the results for the deep masseter mechanical advantage will be detailed. Mandible shape also allowed us to estimate bite force with some success.

Mus musculus

In our lab-reared mice (Fig. 2A and D), age was controlled, and all specimens in this study were 68 days old. We found a significant relationship between shape-estimated bite force and *in vivo* bite force ($cor = 0.33$, $t = 2.48$, $df = 49$, $P = 0.0084$). On the other hand, the estimations based on masseter mechanical advantage were not significantly correlated to in vivo data ($cor = 0.11$, $t = 0.781$, $df = 49$, $P = 0.22$).

Mus caroli

In this wild species (Fig. 2B and E), for which we had less specimens than others, we found a very strong correlation between shape estimates of bite force and *in vivo* bite force ($cor = 0.71$, $t = 3.38$, $df = 11$, $P = 0.0031$). Again, the mechanical advantage based estimations were not significantly related to in vivo data ($cor = -0.42$, $t=-1.51$, $df = 11$, $P = 0.92$).

Mus cervicolor

In this wild mice, our sample was larger than *M. caroli*, and shape-estimated bite force values were significantly correlated to *in vivo* data (cor = 0.25, t = 2.06, df = 63, P = 0.0218, Fig. 2C). However, the mechanical advantage estimates were not correlated to *in vivo* values (cor = 0.16, t = 1.30, df = 63, P = 0.0985, Fig. 2F).

Rattus exulans

For *R. exulans* both estimations were correlated to *in vivo* bite forces (Fig. 2G and I), with a stronger correlation for the shape estimates (cor = 0.42, t = 2.89, df = 40, P = 0.0031) than for the mechanical advantage ones (cor = 0.35, t = 2.35, df = 40, P = 0.0118).

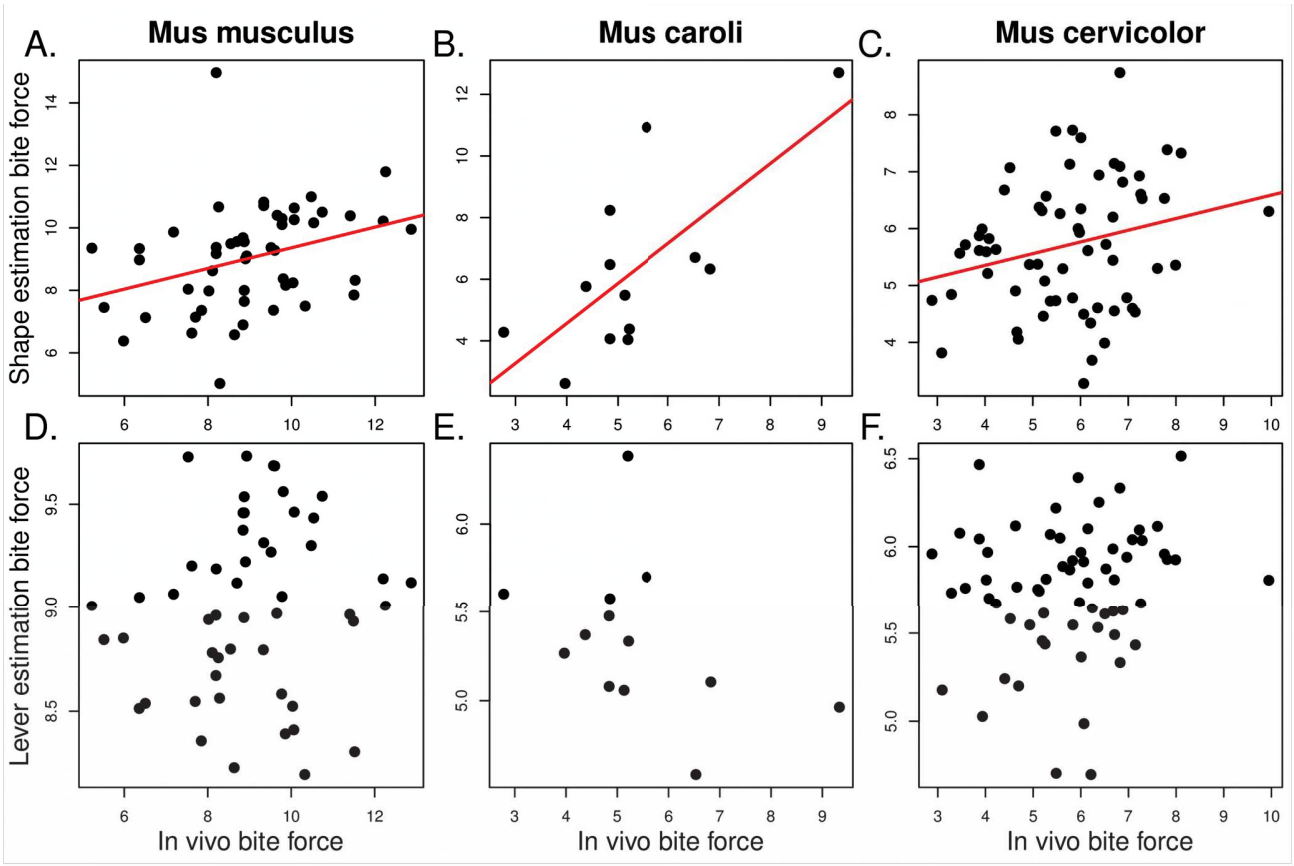

Figure 2. Bite force estimations plotted against *in vivo* bite force in the three species of mice studied here. A to C are mandible shape estimates, D to F are mechanical advantage estimations. Red lines represent significant regression lines.

Rattus tanezumi

Contrary to all other species, the shape estimated bite force did not correlate significantly with *in vivo* data (cor = 0.15, t = 0.77, df = 27, P = 0.2232, Fig. 2H). However there was a significant correlation between mechanical advantage estimates and in vivo bite force (cor = 0.47, t = 2.78, df = 27, P = 0.0049, Fig. 2J).

Discussion

Our results show that despite being used as functional proxies, mechanical advantages and mandible shapes (*e.g.* Hautier et al. 2009, Renaud et al. 2015) generally do not appear to be very reliable estimators of *in vivo* bite force in our sample of species. In particular, the temporal and

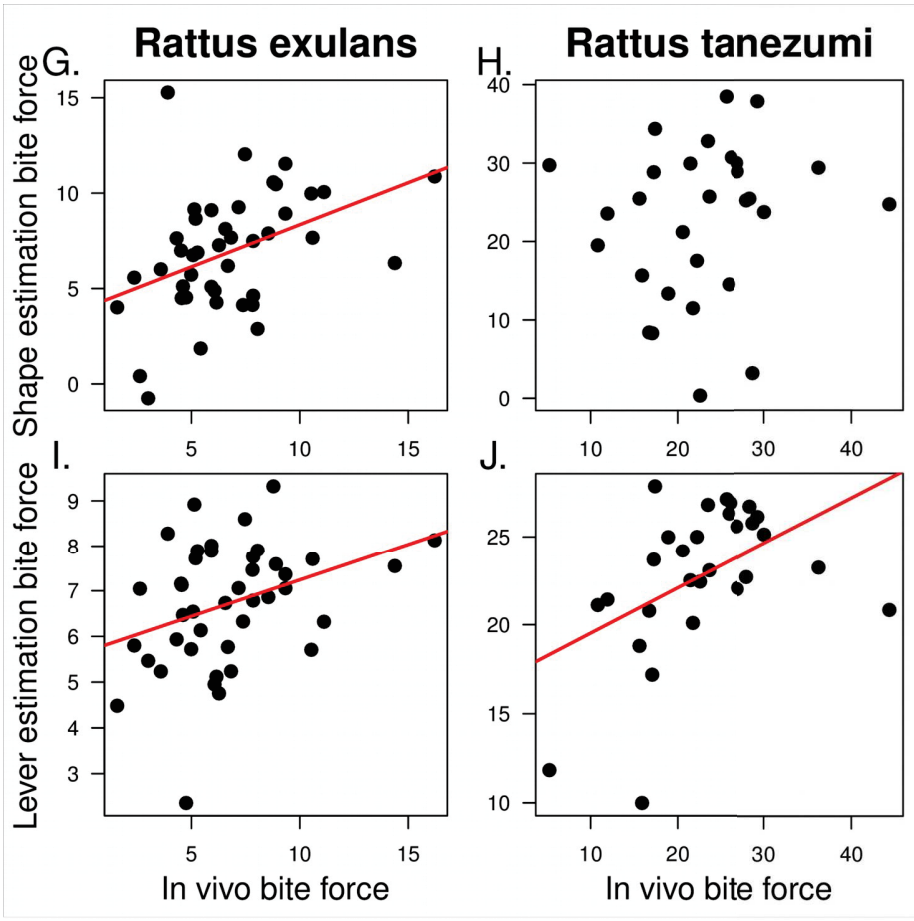

Figure 2 (cont'd). Bite force estimations plotted against *in vivo* bite force for two species of rats. Red lines represent significant regression lines.

superficial masseter mechanical advantages bite force estimates were never significantly related to *in vivo* bite force. On the other hand, deep masseter mechanical advantage and mandible shape had some significant predictive power in some of the species studied here.

Overall, it appears that mandible shape is a better bite force estimator than the masseter mechanical advantage, with stronger correlations between estimated and *in vivo* bite force, in more species. However, our results also suggest that this depends on the group studied, since mechanical advantage estimates were related to *in vivo* data in both rats, but in none of the mice. Although our results partly corroborate the use of mandible morphology as a proxy for performance, they also reveal important imprecisions in the estimated values, as was found for estimates based on muscular data at the intra-specific level (Ginot et 2018). It appears clear that bite force at the intra-specific level is under the influence of more numerous factors, and that morphological variation is not sufficient to explain performance variation. Such factors may include sex (Ginot et al. 2017), age (which was mostly unontrolled in our wild species sample ; Ginot et al. in prep.), behaviour, hormones, social status, health status, inbreeding or genetics, as well as a general plasticity of *in vivo* bite force depending on abiotic environmental conditions (*e.g.* temperature, food availability).

Our study also suggests that, at least at the intra-specific level, testing the quality morphological proxy estimates of performance should be a prerequisite before making functional and adaptive inferences based on morphology, to avoid the pitfalls of an fully adaptationist point of view (Arnold 1983, Gould and Lewontin 1979).

References

Arnold, S. J. (1983). Morphology, performance and fitness. American Zoologist, 23(2), 347-361.

Claude, J. (2008). Morphometrics with R. Springer Science & Business Media.

Cox, P. G., Rayfield, E. J., Fagan, M. J., Herrel, A., Pataky, T. C., & Jeffery, N. (2012). Functional

evolution of the feeding system in rodents. PLoS One, 7(4), e36299.

Freeman, P. W., & Lemen, C. A. (2008). A simple morphological predictor of bite force in rodents. Journal of Zoology, 275(4), 418-422.

Ginot, S., Claude, J., Perez, J., & Veyrunes, F. (2017). Sex reversal induces size and performance differences among females of the African pygmy mouse, *Mus minutoides*. Journal of Experimental Biology, 220(11), 1947-1951.

Ginot, S., Herrel, A., Claude, J., Hautier, L. (2018). Skull size and biomechanics are good estimators of *in vivo* bite force in murid rodents. *The Anatomical Record*, *301*(2), 256-266.

Gould, S. J., & Lewontin, R. C. (1979). The spandrels of San Marco and the Panglossian paradigm: a critique of the adaptationist programme. Proceedings of the Royal Society of London B: Biological Sciences, 205(1161), 581-598.

Grant, P. R., & Grant, B. R. (2002). Unpredictable evolution in a 30-year study of Darwin's finches. science, 296(5568), 707-711.

Hautier, L., Bover, P., Alcover, J. A., & Michaux, J. (2009). Mandible morphometrics, dental microwear pattern, and paleobiology of the extinct Balearic Dormouse *Hypnomys morpheus*. Acta Palaeontologica Polonica, 54(2), 181-194.

Herrel, A., Spithoven, L., Van Damme, R., & De Vree, F. (1999). Sexual dimorphism of head size in *Gallotia galloti*: testing the niche divergence hypothesis by functional analyses. Functional Ecology, 13(3), 289-297.

Herrel, A., Podos, J., Huber, S. K., & Hendry, A. P. (2005). Bite performance and morphology in a population of Darwin's finches: implications for the evolution of beak shape. Functional Ecology, 19(1), 43-48.

Herrel, A., Podos, J., Vanhooydonck, B., & Hendry, A. P. (2009). Force–velocity trade-off in Darwin's finch jaw function: a biomechanical basis for ecological speciation?. Functional Ecology, 23(1),

119-125.

Mayr, E. (1983). How to carry out the adaptationist program?. The American Naturalist, 121(3), 324-334.

Michaux, J., Chevret, P., & Renaud, S. (2007). Morphological diversity of Old World rats and mice (Rodentia, Muridae) mandible in relation with phylogeny and adaptation. Journal of Zoological Systematics and Evolutionary Research, 45(3), 263-279.

Team, R. C. (2017). R: A language and environment for statistical computing. Vienna, Austria; 2014.

Renaud, S., Gomes Rodrigues, H., Ledevin, R., Pisanu, B., Chapuis, J. L., & Hardouin, E. A. (2015). Fast evolutionary response of house mice to anthropogenic disturbance on a Sub-Antarctic island. Biological journal of the Linnean Society, 114(3), 513-526.

1.2.3 – Ontogénie et fonction (article en préparation pour être soumis dans Journal of Experimental Biology*).*

La morphologie crânienne des rongeurs est liée à leur alimentation. La plupart des rongeurs incorporent dans leur régime des aliments durs ou résistants. Cependant, antérieurement au sevrage (<20 jours chez la souris), les petits se nourrissent de lait (Falconer 1947). Il est donc probable que d'importants changements, à la fois musculaires et osseux se produisent au cours de la croissance des jeunes, en particulier après le sevrage. Ces modifications doivent avoir un effet fonctionnel permettant aux jeunes de changer d'alimentation et d'ingérer des aliments devant être mâchés.

La morphologie crânienne des jeunes de la population de souris des Orcades élevée en animalerie nous renseigne sur le type de changements caractéristiques de leur croissance. Chez ces souris, le sevrage est réalisé à un âge de 21 jours. Les petits sont séparés de leur mère et doivent donc se nourrir exclusivement de "croquettes" relativement dures. Il faut cependant noter que les jeunes ont également accès aux croquettes avant le sevrage, ce qui pourrait leur permettre de les incorporer de manière plus progressives à leur régime.

Dans cette section on s'intéressera aux changements de morphologie de la mandibule et de force de morsure au cours de la croissance de ces souris, d'âges variant de 7 à 100 jours, afin de mieux comprendre à quel tempo ces changements se produisent, et s'ils sont synchrones ou non.

Ontogeny of bite force and mandible morphology in wild-derived lab mice (*Mus musculus domesticus*).

Running title: Bite force and mandible ontogeny in mice.

Authors: Samuel Ginot* [1,2], Sylvie Agret[1], Julien Claude[1].

[1] Institut des Sciences de L'Evolution de Montpellier, Université de Montpellier, Montpellier, France.

[2] Institut de Génomique Fonctionnelle de Lyon, École Normale Supérieure de Lyon, Lyon, France.

* Corresponding author: samuel.ginot@umontpellier.fr, current address: samuel.ginot@ens-lyon.fr

Key words: *In vivo* performance, development, growth, weaning, geometric morphometrics.

Summary statement: This study shows that, in mice, mandible morphology and bite force ontogenies are synchronous in their first stages. Morphology stabilizes around 30 days, while bite force also increases later, during sexual maturation.

Abstract:

Linking performance and morphology has been one of the main aims of recent evolutionary biology. Yet, intraspecifically, most studies have proven that these correlations can be imperfect. In vertebrates, many studies have linked *in vivo* bite force to cranio-mandibular morphology, yet, the ontogeny of bite force is still poorly known, despite being an important source of intraspecific variation. Here, ontogenetic trajectories of *in vivo* bite force and mandible size and shape are reported for the first time

in mice. Mice were sampled among a wild-derived lab-reared population, with controlled ages. Bite forces were measured *in vivo* and mandible morphology was assessed through geometric morphometrics. It appeared that the major part of changes in morphology and bite force are synchronous and restricted to the first stages of growth, prior to weaning. Mandible shape and size appear to be stabilized by 30 days of age. On the other hand, despite slowing down following weaning, bite force has a second phase of increase around the start of sexual maturation (30-40 days). This second phase may be explained by hormonal changes, and may explain some discrepencies in the correlation between morphology and performance at the intraspecific level. Properly deciphering the connection between performance and morphology still requires more detailed studies of their ontogeny.

Introduction

Study of the link between morphology and performance is one of the major axes of evolutionary biology (Arnold 1983). This is particularly true in wild populations, in which performance can be linked to fitness and ultimately to adaptation. Yet, good and precise morphological proxies of *in vivo* performance have proven difficult to access at the population scale (e.g. in rodents Becerra et al. 2011, Ginot et al. 2018). At the intraspecific level, ontogeny is usually a major source of variation, for morphology as well as for performance (Erickson et al. 2003, Huber et al. 2006, Herrel and Gibb 2005, Habegger et al. 2012). Furthermore, in wild populations, age is generally quite diffcult to determine precisely (e.g. Morris 1972). Consequently, differences in ontogenetic stages may be one of the major reasons explaining variations in performance in the aforementioned wild populations. Because age was not exactly determined in these studies, estimates of performance (i.e. bite force) based on morphology (i.e. size and biomechanial variables) can be biased by mixing ontogenetic changes. This could be particularly true if morphology and bite force do not covary linearly throughout ontogeny. More importantly, in ecological terms, the ontogeny of performance and morphology is a major component of fitness, since young individuals generally occupy the same environment as adults (Herrel and Gibb 2005). Yet, to this date, not much is known about the changes in performance that occur throughout development, and this is especially true of feeding performance, more so in mammals (but see Binder and Van Valkenburg 2000, Thompson et al. 2003, La Croix et al. 2011, Chazeau et al. 2013, Santana and Miller 2016). To our knowledge, this study is the first exploring ontogenetic variation of morphology linked to *in vivo* bite force in rodents.

Studies of laboratory animals allows to circumvent the difficulty of age determination in wild animals, to assess the age-induced variation of morphology and performance. Here, we use lab-reared

mice, which allows us to have a very good control of age. We look at the evolution of bite force and morphology in many lab specimens, including some which were euthanized at younger stages and in which we measured bite force. Most previous studies (including both endotherms and ectotherms ; see Herrel and Gibb 2005) have found positive allometries of bite force against size and body mass, showing that young individuals do not compensate in terms of absolute performance. This may be accentuated in mammals, in which young individuals feed essentially on milk prior to weaning. We therefore expect very rapid increase of bite force prior to weaning so young individuals may be able to cope with hard food items. Because weaning (i.e. rapid transition from milk to hard food) in these mice happens at 21 days of age, we may also expect that bite force and morphological changes will accelerate in synchrony at that stage due to mechanical demands (i.e. individuals eating only hard food) then slow down as the individuals approach adulthood. Despite the potentially enormous effects of weaning on feeding performance, this has only be documented once, in bats, in which bite force maintains a rapid increase after weaning (Santana and Miller, 2016).

If the synchronicity of bite force and morphological development is maintained until adulthood, age discrepencies in wild populations should not be a factor of noise in the morpho-functional correlations. On the other hand, partial lack of synchrony in performance and morphology may imply that errors will happen in morphological proxies of performance in wild populations in which age is not precisely estimated.

Material and Methods

Specimens

Mice used in this study are all part of a colony kept at the University of Montpellier, and

founded from wild individuals from the Orkney Islands (Scotland). In the colony, dates of birth are systematically recorded by checking every two days, which allows exact determination of age. When individuals must be euthanized, their bite force and body mass are also systematically recorded. The colony is split into three lineages, originating from different islands, with different pedigree management and inbreeding levels, all of which were combined in this study. Ages at euthanasia in our sample ranged from 7 days to 100 days old, and bite force measurements could be obtained from 12 days old, when incisors erupt. A total of 2318 individuals had their bite force measured *in vivo*, and a subset of 751 individuals were used for the morphological analyses.

Geometric morphometrics analyses

In the aforementioned subset, we cleaned the mandibles manually and photographed them in a standardized way (camera at a fixed distance, mandible positioned flat with the lingual side down) using a Pentax K200D reflex camera, with a 45mm focal distance. We then placed 13 landmarks, represented on Fig. 1, on the mandible using the software tpsDig2.0 (Rohlf 2010). Landmark data were imported and analyzed in R (R Foundation for Statistical Computing, Vienna, Austria), using the Procrustes superimposition method, with functions from Claude (2008) to obtain comparable mandible shapes, as well as centroid sizes.

Bite force measurements

All *in vivo* bite force data were recorded at the incisors using a Kistler force transducer (Kistler, type 9203, range 0-500 N, accuracy 0.01–0.1 N; Amherst, NY, USA) mounted between two bite plates and linked to a charge amplifier (Kistler, type 5995, Amherst, NY, USA), similar to the set-up presented in Herrel et al. (1999) and Aguirre et al. (2002). The same user (SG) did all the

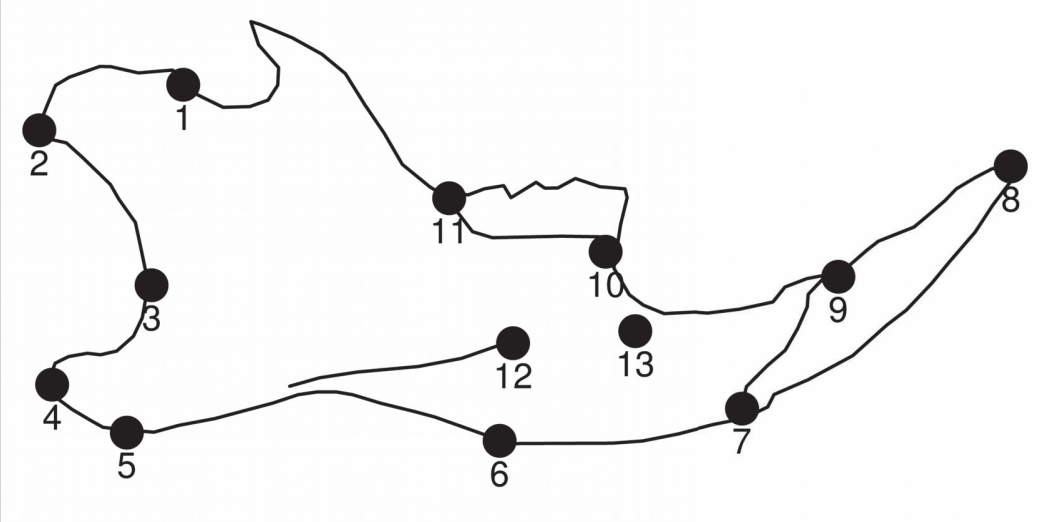

Figure 1. A mouse mandible outline drawing, displaying the landmarks used in the geometric morphometric analyses of this study.

measurements to avoid inter-user variability. All animals bit directly onto the steel plates at the same spot (*i.e.* at the tip), to ensure a consistent out-lever length. The space between bite plates was adjusted depending on the age and size of the individuals, to avoid large inter-individual variation in the gape angle, which can impact bite force (Dumont and Herrel 2003). Each mouse bit three times in a row and only its highest bite force was selected to be used in the following analyses.

Ontogeny of bite force and mandible morphology

To represent the changes in morphology and performance through the developmental time represented in this study, slinding averages were computed. This method aims at reducing noisy variation due to litter effects (usually all individuals from one litter were euthanized at the same age), and / or to small sample sizes at one given age. To produce this sliding average, we considered individuals of age x ± 15% (*e.g.* to calculate the average at 30 days of age, we included individuals 26 to 34 days old). This was applied directly to bite force, centroid size, and to the first principal

component (PC) of mandible shape variation (Fig. 2). To visualize shape change, mean mandible shapes were produced for 16-18 days old individuals ("young"), 30 days old individuals ("subadults"), 68 days old individuals ("adults"), and 97-100 days old individuals ("old"), which were considered to be important and representative stages of development (Fig. 3).

Bite force allometry

In the subset of specimens for which we had centroid size, body mass and bite force data, we tested the allometry of bite force through least square linear regression. To do so, we compared the slopes obtained for log bite force against log size and log bite force against log body mass to their expected slopes of 2 and 2/3 respectively.

Results

Ontogeny of bite force and mandible morphology

The ontogeny of bite force does not appear to follow a linear trajectory, but rather a logarithmic curve (Fig. 2A). The fastest increase in bite force is clearly in the first days, prior to weaning (21 days). In the days following weaning, the increase continues, despite slowing down, and a second phase of rapid increase happens slightly before 40 days of age. After 40 days, the average bite force is essentially stabilized.

Mandible morphology also varies greatly with age (Fig. 2B-C and Fig. 3). Mandible shape matures rapidly, and by the time of weaning, changes become more reduced. Mandible size also shows rapid increase prior to weaning, however, it keeps on increasing – although more slowly – even after adulthood is reached (around 68 days). The main shape changes are the lengthening and heightening of the angular process, the heightening of the molar alveolar region and the lengthening of the incisor

(Fig. 3). Clearly, the major part of these changes seem to happen from the most juvenile state studied here (16-18 days) to the "subadult" stage (here 30 days). This is visible on Fig. 3 in which the 30 days old group is clearly closer to the 68 days old group than to the 16-18 days old group, despite a greater age difference.

When comparing rates of change between morphology and bite force (Fig. 2D), it appears that in the first stages of development, bite force and morphological changes are synchronous. After 30 days

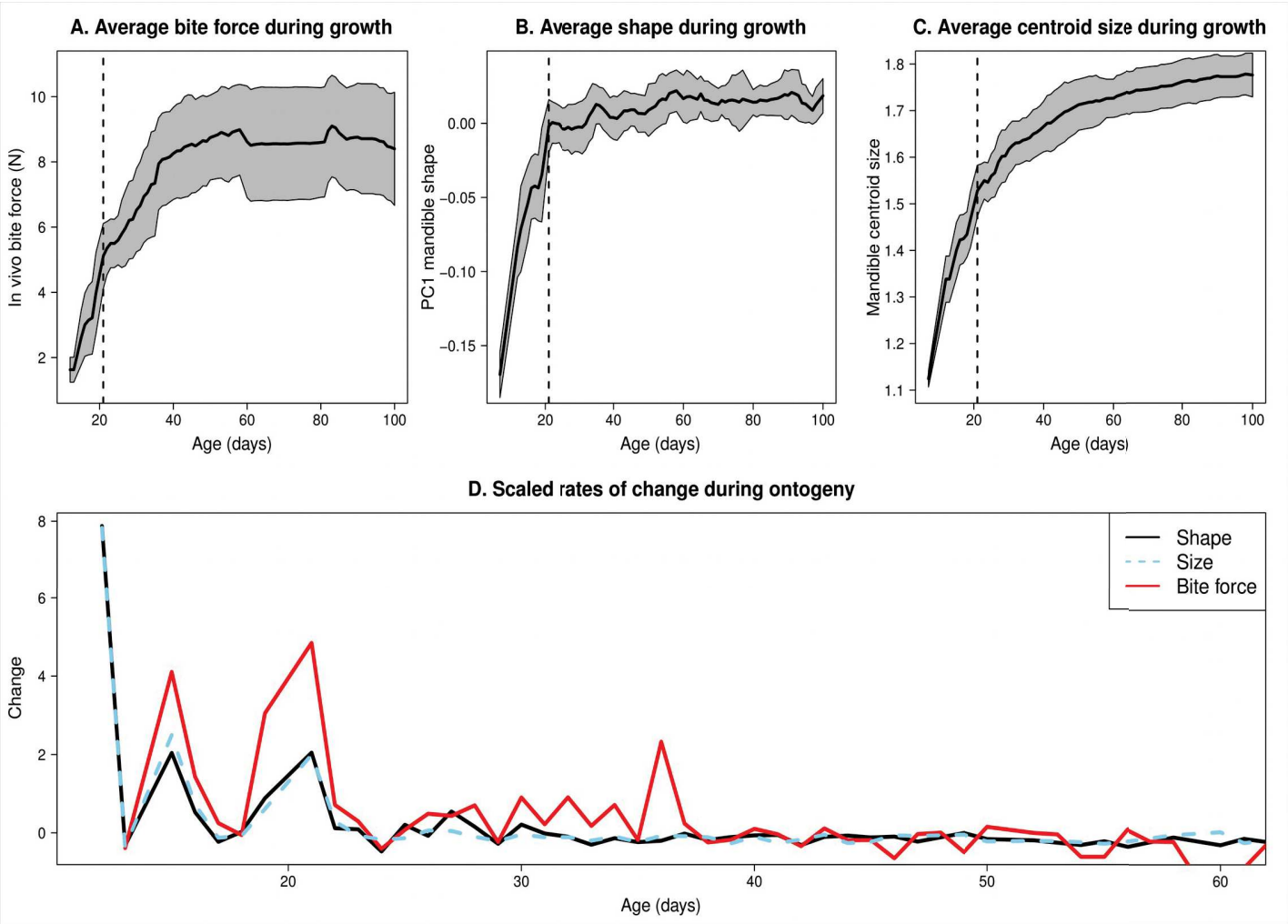

Figure 2. Ontogenetic changes in (A) bite force, (B) mandible shape and (C) mandible size, represented by their respective sliding averages to smooth out noisy variations due to litter effects. Panel (D) shows the rates of change obtained from (A), (B) and (C) betweeen the earliest stages of growth and 60 days old. All rates of changes had their respective variance scaled to make them visually comparable.

of age, morphology appears to stabilize, while changes in bite force continue, peaking around 35 days. Thus, bite force ontogeny is clearly linked to morphological development, however with a partial disconnection in subadult individuals.

Bite force allometry

The correlation between log mandible size and log bite force is very significant ($R^2 = 0.568$, $P < 0.0001$). A similar result is obtained for body mass ($R^2 = 0.546$, $P < 0.0001$). The slopes of these regression lines are significantly higher than their expected slopes under isometry. For centroid size, we found a slope of 4.85, while the expected slope is 2. This difference is very significant ($t = 28.60$, $df = 691$, $p < 0.0001$). The expected slope for bite force against weight is 2/3, while the observed slope is 0.97. The difference is also significant ($t = 28.835$, $df = 689$, $p < 0.0001$). In both cases we observe a positive allometry of bite force. In other terms, bite force increases proportionally faster than size

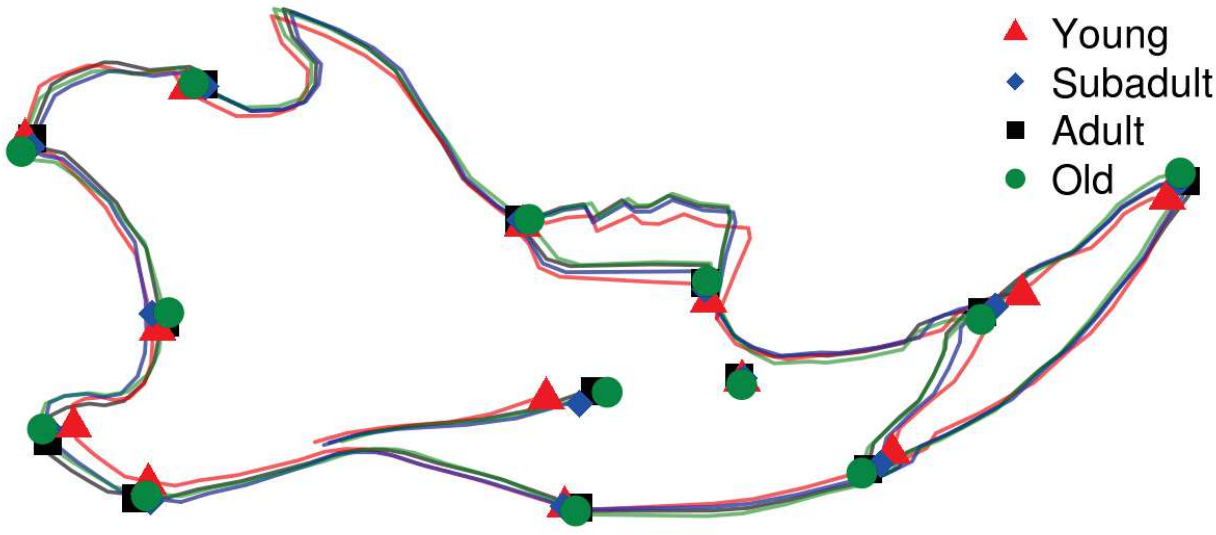

Figure 3. Mean mandible shape outlines at different ages during growth, representing different life-history stages: "Young" = 16-18 days old ; "Subadult" = 30 days old ; "Adult" = 68 days old ; "Old" = 97-100 days old.

overall (whether for mandible size or body mass).

Discussion

In this study, we described for the first time the ontogeny of bite force performance in relation with the morphogenesis of the mandible. The above results suggest that bite force ontogeny is more spread out than morphological ontogeny. Indeed, bite force increases in two phases, the first being very rapid, happening before weaning, in conjunction with major morphological changes ; and the second later, after weaning, potentially relating to sexual maturity, between 35 and 40 days (Fig. 2A,D). This second phase of increase might be related to hormonal changes which are known to happen at that time (e.g. O'Shaughnessy et al. 2002), or muscular development, both potentially being interlinked.

Overall, bite force reaches an adult level well after 40 days, while the shape of the mandible at 30 days is already close to that of an adult (Fig. 2B-D, Fig. 3). The positive allometry of bite force shows the increase is proportionally more rapid than that of size, showing that young mice do not compensate for their reduced performance. This is in accordance with previous studies to date, in mammals and in other groups (e.g. Herrel and Gibb 2006, Chazeau et al. 2013, Santana and Miller 2016). However, we expected that mechanical demands would produce an acceleration of bite force increase following weaning, which we found not to be the case. In fact, we found a short but conspicuous slowing down of bite force increase right after weaning (Fig. 2A). This may be explained by the physiological stress induced by the stopping of milk consumption, and the energetic requirements of breaking down exclusively hard foods. Not much work has been dedicated to the effects of weaning on performance (but see Santana and Miller 2016), and our results suggest they may be of importance, although in nature, the transition between pre- and post-weaning diets may extend over longer times.

Furthermore, it appears that the ontogeny of bite force and morphology (size and shape) are partially asynchronous (or at least do not have the same tempo throughout development). In a wider context, the partial disconnection between performance and morphology during ontogeny may participate in the weak correlations found at the intra-specific level in wild populations (e.g. Ginot et al. 2018). Indeed, an individual of unknown age may have a morphology close to that of an adult while still being in a phase of increase of bite force. This way, mixing adult and subadult individuals may introduce a bias due to a non-morphologically correlated variation in bite force.

It appears clearly from our work and others (e.g. Herrel and Gibb 2006, Santana and Miller 2016) that our knowledge of performance ontogeny is still incomplete. In particular in mammals, the weaning stage may be a pivotal stage for the youngs' fitness and survival. Mechanisms allowing young individuals to survive and grow despite competing with older individuals seem to represent an understudied yet crucial field of evolutionary biology.

References

Aguirre, L. F., Herrel, A., Van Damme, R., & Matthysen, E. (2002). Ecomorphological analysis of trophic niche partitioning in a tropical savannah bat community. Proceedings of the Royal Society of London B: Biological Sciences, 269(1497), 1271-1278.

Arnold, S. J. (1983). Morphology, performance and fitness. American Zoologist, 23(2), 347-361.

Becerra, F., Echeverría, A., Vassallo, A. I., & Casinos, A. (2011). Bite force and jaw biomechanics in the subterranean rodent Talas tuco-tuco (*Ctenomys talarum*)(Caviomorpha: Octodontoidea). Canadian Journal of Zoology, 89(4), 334-342.

Binder, W. J., & Valkenburgh, B. (2000). Development of bite strength and feeding behaviour in

juvenile spotted hyenas (Crocuta crocuta). *Journal of Zoology*, *252*(3), 273-283.

Chazeau, C., Marchal, J., Hackert, R., Perret, M., & Herrel, A. (2013). Proximate determinants of bite force capacity in the mouse lemur. *Journal of Zoology*, *290*(1), 42-48.

Claude, J. (2008). Morphometrics with R. Springer Science & Business Media.

Dumont, E. R., & Herrel, A. (2003). The effects of gape angle and bite point on bite force in bats. *Journal of Experimental Biology*, *206*(13), 2117-2123.

Erickson, G. M., Lappin, A. K., & Vliet, K. A. (2003). The ontogeny of bite-force performance in American alligator (*Alligator mississippiensis*). *Journal of Zoology*, *260*(3), 317-327.

Ginot, S., Herrel, A., Claude, J., Hautier, L. (2018). Skull size and biomechanics are good estimators of *in vivo* bite force in murid rodents. *The Anatomical Record*, *301*(2), 256-266.

Habegger, M. L., Motta, P. J., Huber, D. R., & Dean, M. N. (2012). Feeding biomechanics and theoretical calculations of bite force in bull sharks (*Carcharhinus leucas*) during ontogeny. *Zoology*, *115*(6), 354-364.

Herrel, A., & Gibb, A. C. (2005). Ontogeny of performance in vertebrates. *Physiological and biochemical Zoology*, *79*(1), 1-6.

Herrel, A., Spithoven, L., Van Damme, R., & De Vree, F. (1999). Sexual dimorphism of head size in *Gallotia galloti*: testing the niche divergence hypothesis by functional analyses. *Functional Ecology*, *13*(3), 289-297.

Huber, D. R., Weggelaar, C. L., & Motta, P. J. (2006). Scaling of bite force in the blacktip shark *Carcharhinus limbatus*. *Zoology*, *109*(2), 109-119.

La Croix, S., Zelditch, M. L., Shivik, J. A., Lundrigan, B. L., & Holekamp, K. E. (2011). Ontogeny of feeding performance and biomechanics in coyotes. *Journal of Zoology*, *285*(4), 301-315.

Morris, P. (1972). A review of mammalian age determination methods. *Mammal review*, *2*(3), 69-104.

Rohlf, F. J. (2010). TpsDig, ver. 2. 16. Department of Ecology and Evolution, State University New York at Stony Brook, New York.

Santana, S. E., & Miller, K. E. (2016). Extreme postnatal scaling in bat feeding performance: a view of ecomorphology from ontogenetic and macroevolutionary perspectives. *Integrative and comparative biology*, *56*(3), 459-468.

Team, R. C. (2017). R: A language and environment for statistical computing. Vienna, Austria; 2014.

Thompson, E. N., Biknevicius, A. R., & German, R. Z. (2003). Ontogeny of feeding function in the gray short-tailed opossum *Monodelphis domestica*: empirical support for the constrained model of jaw biomechanics. *Journal of Experimental Biology*, *206*(5), 923-932.

Partie 1 – Conclusion

La variation morpho-anatomique crânienne des murinés semble relativement faible au niveau intra-générique (ici au sein du genre *Mus*). Mais il apparaît tout de même des différences pouvant avoir des conséquences fonctionnelles et donc liées à l'écologie des espèces, qui demandent d'être confirmées par des tests plus directs. Lorsque l'on modélise biomécaniquement la force musculaire au niveau interspécifique (et en s'intéressant à plusieurs genres), les résultats obtenus sont très proches des valeurs *in vivo*. Il s'avère cependant que le facteur principal expliquant cette bonne estimation soit la taille. Comme la taille présente un bon signal phylogénétique parmi les murinés étudiés, la force de morsure est également similaire entre espèces apparentées. Lorsque l'on utilise la même approche au niveau intraspécifique, les résultats révèlent une moins bonne corrélation, bien que cette dernière soit différente d'espèce à espèce. De même, lorsque l'on utilise des proxys osseux (bras de levier ou forme de la mandibule) de la force de morsure au niveau intraspécifique, il sont moins bien corrélés à la force de morsure réelle qu'au niveau interspécifique. L'un des facteurs pouvant expliquer le décalage entre valeurs *in vivo* et estimées est l'âge des individus. En effet, bien que l'on modélise la relation entre force de morsure et morpho-anatomie de manière linéaire, il apparaît que celles-ci ne varient pas de manière synchrone durant l'ontogénie. Ainsi, la force de morsure continue de se développer après que l'évolution de la morphologie se soit stabilisée, ce qui peut provoquer un biais, surtout dans les espèces sauvages où l'âge n'est pas contrôlé.

Cette première partie a montré la diversité interspécifique pouvant exister dans l'appareil masticateur des murinés, et les conséquences fonctionnelles fines qu'elle peut avoir. Le lien fort entre la force de morsure *in vivo* et celle estimée grâce à la musculature a été démontré, au niveau interspécifique. Dans le même temps, cette approche a montré les limites de sa précision au niveau intraspécifique. Il en va de même pour la force de morsure estimée à partir de proxys osseux. Il semble qu'au niveau intraspécifique, l'âge puisse jouer un rôle important dans la différence entre estimation et réalité. Cependant, en dehors de la variation importante liée à l'âge, d'autres facteurs influencent la performance au niveau intraspécifique. En effet, même dans ce cas, le lien entre force de morsure *in vivo* et estimée n'est jamais une corrélation parfaite. La seconde partie cherchera donc à montrer si des différences génotypiques et génétiques jouent également un rôle dans le déterminisme de la force de morsure et de la morphologie.

Partie 2 – Effets de la variation génétique et héritabilité de la morphologie et de la force de morsure.

La première partie a permis décrire la variation morphologique du crâne et de la mandibule chez les Murinae et ses effets sur la performance. De manière générale, les études d'écologie fonctionnelle chez différents groupes d'animaux cherchent ensuite à comprendre l'évolution de la morphologie et de la performance à travers leurs conséquences sur leur valeur sélective (e.g. Irschick et al. 2008). Cependant, les effets génétiques et génotypiques sous-jacents à la variation de performance sont souvent ignorés, puisqu'ils ne sont pas nécessaires pour l'étude de la sélection et de l'évolution du

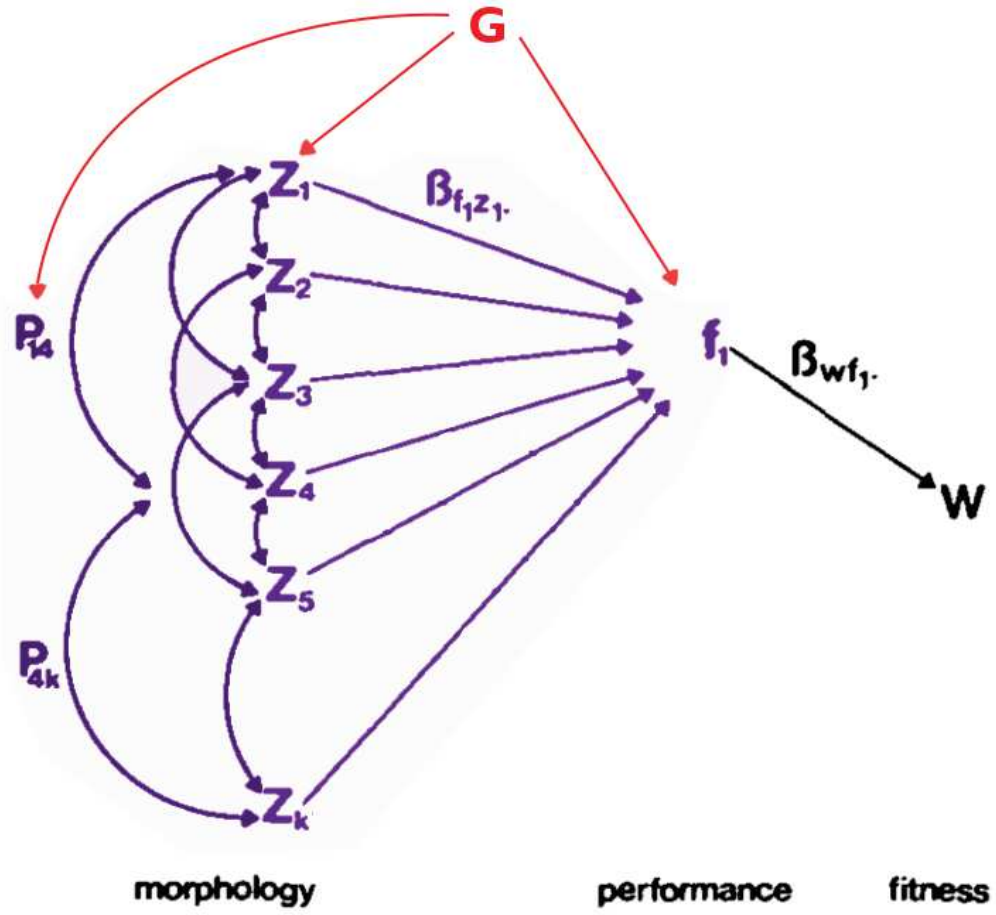

Figure 2.1 : Diagramme des chemins adapté et étendu à partir de Arnold (1983). Les différents effets potentiels de la génétique sur le phénotype, étudiés dans cette partie, sont surlignés en rouges. En bleu sont les différents traits et corrélations morphologiques et fonctionnels qui seront étudiés dans le même temps.

phénotype (Arnold 1983). Différents facteurs génétiques et génotypiques seront donc étudiés dans cette partie afin de tester leur influence sur la morphologie et sur la performance : les chromosomes sexuels, la consanguinité et la variance génétique additive. Ceci est schématisé sur la Fig. 2.1, qui représente en rouge les effets génétiques (**G**) sur lesquels ce concentre cette partie, et en bleu ceux qui sont étudiés de manière indirecte.

2.1 – Effets des chromosomes sexuels sur la performance et la morphologie crânienne chez *Mus minutoides* (article publié dans *Journal of Experimental Biology*).

Dans la première partie, les aspects intra-spécifiques de la variation morpho-fonctionnelle on été étudiés sans prendre en compte les potentielles différences inter-sexes. Or, les chromosomes sexuels sont connus pour avoir des effets hormonaux, comportementaux et morphologiques pouvant influencer la performance (voir par exemple Fénichel et al. 2013). Chez les Murinae, le dimorphisme sexuel est généralement considéré comme faible voire absent (e.g. Valenzuela-Lamas et al. 2011). Cependant, certaines études parviennent à le détecter (e.g. Renaud et al. 2010). Dans d'autres groupes, notamment chez les lézards, il a été montré que le dimorphisme sexuel pouvait avoir un effet important sur la morphologie et sur la force de morsure (Herrel et al. 1995, 1999). Il est donc possible que les chromosomes sexuels influencent la morphologie et la performance aussi chez certains rongeurs.

Parmi les souris (genre *Mus*), le sous-genre africain *Nannomys* est connu pour avoir des systèmes de déterminisme sexuel inhabituels pour des mammifères. Dans ce genre, l'espèce *M. (Nannomys) minutoides* présente trois types de chromosomes sexuels différents: X, Y et X*, ce qui produit donc des mâles XY, des femelles XX, ainsi que des femelles X*Y, c'est à dire des mâles "féminisés" par le chromosome X* (Veyrunes et al. 2010). Saunders et al. (2016) ont montré qu'il existait des différences d'agressivité entre ces trois types de souris, les femelles X*Y se rapprochant du comportement des mâles XY. Cependant, les femelles X*Y ne divergent pas des femelles XX en termes de morphologie gonadale et externe (Rahmoun et al. 2014).

Grâce à ce modèle, il est donc possible de tester l'influence des chromosomes sexuels sur la force de morsure de manière fine. Par ailleurs, ce modèle permet également d’évaluer les effets respectifs des changements de comportements et de morphologie crânienne sur la force de morsure.

Erratum :

Comme mentionné dans la partie Introduction de cette thèse, l’article qui suit a été publié avec des données de forces de morsure surestimées. Bien que la significativité et l’interprétation des résultats ne soient pas modifiés suite à la correction de ces données, la figure 2 et le tableau 2 de l’article sont ici présentés avec les données correctes.

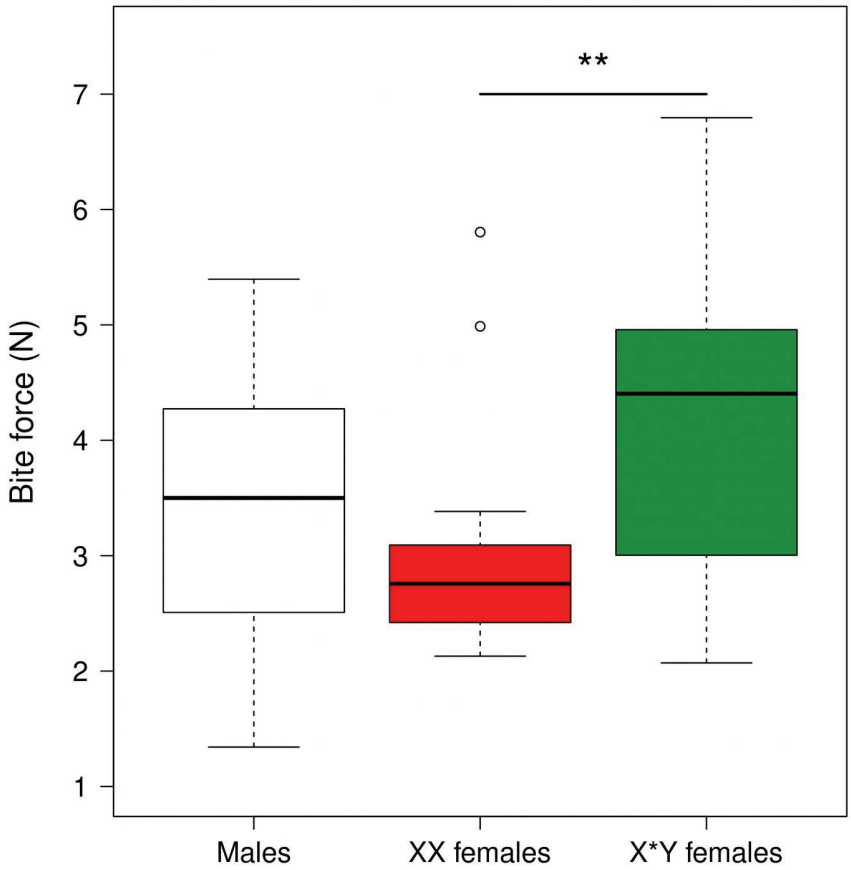

Erratum figure 1. Cette figure est la même que la Fig. 2 de l'article qui suit, avec des données de force de morsure corrigées (divisées par un facteur de 2.4).

	Difference	Lower	Upper	P value
Bite force				
♂ vs ♀	-0.36	-1.27	0.56	0.62
X*Y ♀ vs ♂	0.80	-0.13	1.73	0.10
X*Y ♀ vs ♀	1.16	0.22	2.10	0.01
Mandible centroid size				
♂ vs ♀	3.15	-20.86	27.16	0.95
X*Y ♀ vs ♂	31.7	7.33	56.07	0.01
X*Y ♀ vs ♀	28.55	3.86	53.24	0.02
Skull centroid size				
♂ vs ♀	-4.53	-41.21	32.14	0.95
X*Y ♀ vs ♂	67.56	30.33	104.78	<0.01
X*Y ♀ vs ♀	72.09	34.38	109.80	<0.01

Erratum tableau 1. Ce tableau est le même que le Tab. 2 de l'article qui suit, avec des données de force de morsure corrigées (divisées par un facteur de 2.4). Noter que les valeurs-p ne sont pas modifiées, bien que les différences inter-groupes aient changé.

© 2017. Published by The Company of Biologists Ltd | Journal of Experimental Biology (2017) 220, 1947-1951 doi:10.1242/jeb.157552

SHORT COMMUNICATION

Sex reversal induces size and performance differences among females of the African pygmy mouse, *Mus minutoides*

Samuel Ginot*, Julien Claude, Julie Perez and Frederic Veyrunes

ABSTRACT

Differences in biological performance, at both intra- and inter-specific levels, have often been linked to morphology but seldom to behavioural or genotypic effects. We tested performance at the intraspecific level by measuring bite force in the African pygmy mouse, *Mus minutoides*. This species displays an unusual sex determination system, with sex-reversed, X*Y females carrying a feminizing X* chromosome. X*Y females cannot be differentiated from XX females based on external or gonadal morphology; however, they are known to be more aggressive. We found that bite force was higher in X*Y females than in other females and males. We then performed geometric morphometric analyses on their skulls and mandibles and found that the higher performance of X*Y females was mainly explained by a greater overall skull size. The effects of the X* chromosome thus go beyond feminization, and extend to whole-organism performance and morphology. Our results also suggest limited effects of behaviour on bite force.

KEY WORDS: Behaviour, Bite force, Geometric morphometrics, Intra-sex competition, Sex reversal

INTRODUCTION

Bite force is a frequently used performance trait in functional morphological studies. Most of these studies have clearly demonstrated the link between osteology, muscular activity and biting performance at the intraspecific as well as interspecific levels (e.g. Herrel et al., 1999; Aguirre et al., 2002; Davis et al., 2010; Santana et al., 2010). Morphology has also been shown to be a driver of performance and fitness via intra-sexual competition (Herrel et al., 2010; Lailvaux et al., 2004). However, to our knowledge, the interactions between genetics, behaviour, morphology and performance at the intraspecific and even intra-sex levels have not yet been studied in mammals.

Here, we investigated bite force and skull morphology in the African pygmy mouse, *Mus* (*Nannomys*) *minutoides* Smith 1834. This species is known to have a unusual sex determination system, with three types of sex chromosomes: X, Y and a feminizing X*, producing XY males and XX, XX* females and a high proportion of sex-reversed, X*Y females (Veyrunes et al., 2010). The three types of females present no differences in external morphology or gonad anatomy (Rahmoun et al., 2014), but are known to vary in other traits: X*Y females have a higher reproductive success (Saunders et al., 2014), and have a much more aggressive behaviour (latency to attack, number of attacks; Saunders et al., 2016) than the XX and XX* females. Because biting is one of the characteristics of attacks that relates to aggressiveness, we compared the bite force of the X*Y females with that of other females and males to assess the effect of their genotypic changes on performance. In parallel, we performed measurements of morphological attributes of the skull and mandible in all genotypes. By doing so, we tried to link chromosomal differences to performance, through potential morphological and/or behavioural (aggressiveness) variations. Examining these interactions in *M. minutoide*s could also help improve our understanding of the ecological and evolutionary implications of the emergence of this unusual sex determination system.

MATERIALS AND METHODS

Specimens

All mice were raised in the facilities of Montpellier University (France). The colony was established from wild-caught animals from South Africa (see details in Saunders et al., 2014). Overall, 54 mice were used in the experiments with 19 males and 35 females, all adults. Seventeen females were found to carry a Y chromosome using PCR amplification of the *Sry* gene (following Veyrunes et al., 2010). The 18 others did not have the *Sry* gene, and thus were either XX or XX*. XX and XX* females do not differ in terms of behaviour and reproductive success (Saunders et al., 2014, 2016) and were pooled in this study after checking that they did not represent distinct phenotypic groups. Recognizing all XX* females requires karyotyping, which is technically demanding; instead, we were able to identify eight of them in our dataset thanks to their genealogy. These eight individuals were compared with the other non-X*Y females, and their morphology and bite force were roughly equivalent in mean and variance (results not shown). These XX and XX* females are hereby referred to as 'XX females'. The experimental protocol was performed in accordance with European guidelines and with the approval of the Ethical Committee on Animal Care and Use of France (no. CEEA-LR-12170).

Bite force measurements

Bite force was measured using a piezoelectric force transducer (Herrel et al., 1999; Aguirre et al., 2002). Measurements were performed prior to PCR amplification, avoiding user-behaviour bias, and by a single user, to avoid inter-user error. Each mouse bit three times in a row and the highest bite force was selected for analysis. Group means were compared using Tukey's HSD test. The mice were then euthanized by CO_2 inhalation, and kept at −20°C until further treatment.

Morphometric geometrics and statistical analyses

All skulls were cleaned manually and kept in the collections of Montpellier University. Eleven landmarks were digitized on the

Institut des Sciences de l'Evolution de Montpellier, Universite de Montpellier, CNRS, IRD, Cc 064; Place Eugene Bataillon, Montpellier Cedex 5 34095, France.

*Author for correspondence (samuel.ginot@umontpellier.fr)

S.G., 0000-0003-0060-9660

Received 1 February 2017; Accepted 16 March 2017

Journal of Experimental Biology (2017) 220, 1947-1951 doi:10.1242/jeb.157552

dorsal side of the skull, and 16 on the mandible using the software tpsDig2.0 (Fig. 1A,B). Landmark data were imported and analyzed in R (R Foundation for Statistical Computing, Vienna, Austria), using the procrustes superimposition method, with functions from Claude (2008). Missing landmarks (owing to the fragility of the mandible), if any, were estimated using a tps interpolation. Centroid sizes of the skulls and mandibles were computed and used as the size variables (Bookstein, 1991). Principal component analyses (PCAs) were run on superimposed coordinates to check for shape differences between males, XX females and X*Y females. In all analyses, the PC axes retained represented 90% of shape variation. A type II ANOVA was run

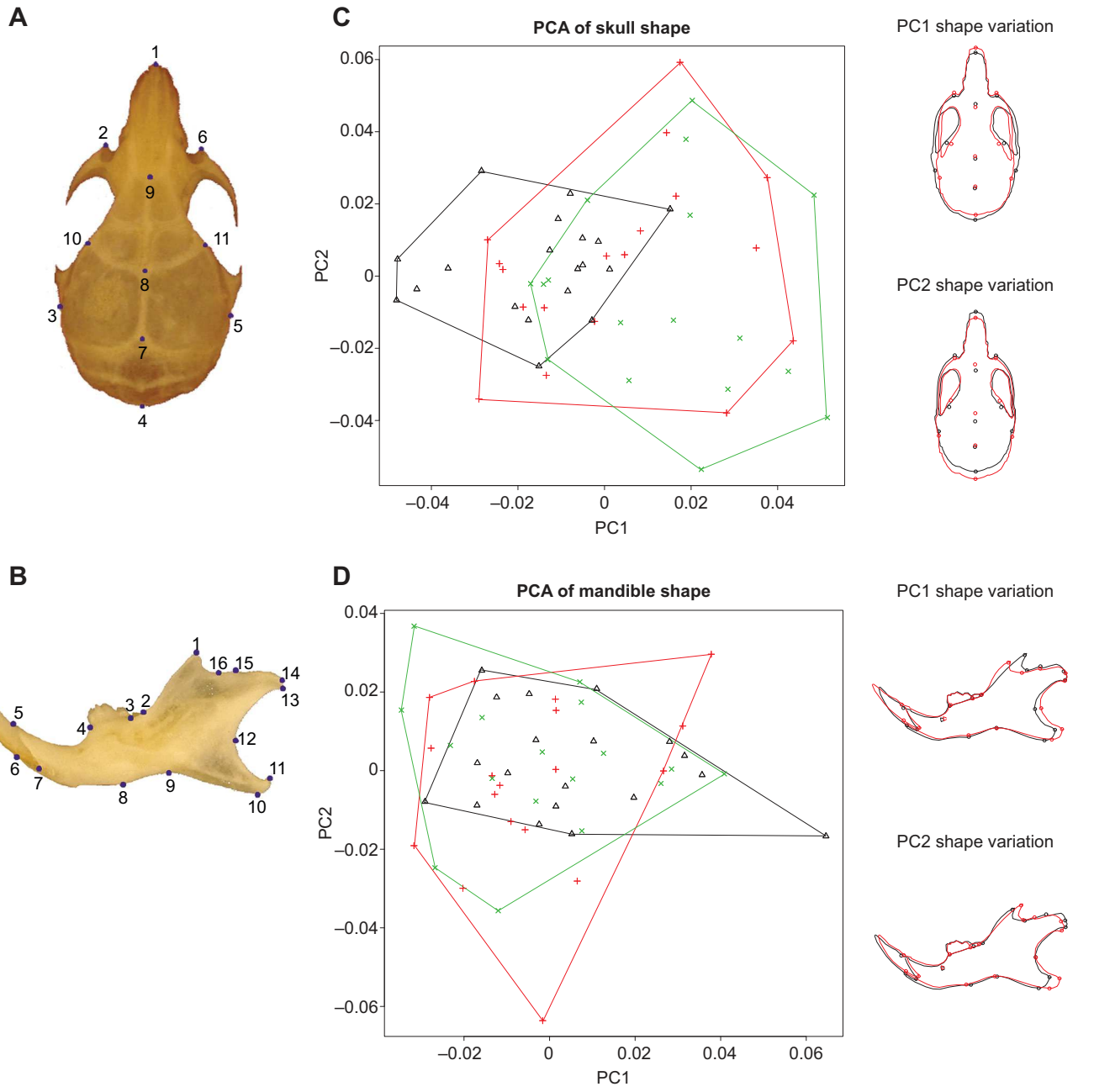

Fig. 1. Geometric morphometric analyses of the skull and mandible of the males, XX females and X*Y females of *Mus minutoides*. Landmarks for (A) the skull and (B) the mandible of *Mus minutoides*. (C) PCA based on the landmark data for the skull, with PC1 representing 16.4% and PC2, 15.3% of the variation. (D) PCA for the mandible, with 10.8% and 9% of the variation displayed by PC1 and PC2, respectively. Black triangles are males (n=19), green crosses are X*Y females (n=17) and red plus signs are XX females (n=18). Skull and mandible shapes on the right of the graph represent minimal (black) and maximal (red) shapes along the PC axes. No significant shape differences were found between these groups. For the skull, positive values on PC1 represent a narrower skull with a longer snout but a shorter braincase, while negative values represent a broader skull with a shorter snout and a longer braincase. On PC2, positive values have a shorter snout and a wider inter-orbital region in comparison to negative values. For the mandible, positive values on PC1 correspond to overall flatter mandibles, with the angular process more posteriorly developed, while the coronoid process is shorter and in a more anterior position than for negative values. On PC2, positive values correspond to mandibles with a shorter molar row, more posterior coronoid process, shorter condylar process and longer angular process than negative values.

Journal of Experimental Biology

Journal of Experimental Biology (2017) 220, 1947-1951 doi:10.1242/jeb.157552

Table 1. Results of the ANOVA and MANOVAs run on bite force and morphology of *Mus minutoides*

ANOVA	Factor	SS	d.f.	*F*	*P*		
Bite force~Age+Size+Genotype+ Age:Genotype+Size:Genotype	Age	1.15	1	0.0915	0.76		
	Size	133.46	1	10.6033	<0.01		
	Genotype	32.26	2	1.2817	0.29		
	Age:Genotype	35.01	2	1.3907	0.26		
	Size:Genotype	46.17	2	1.8343	0.17		
	Residuals	528.63	42				
Skull MANOVAs		d.f.	Pillai	Approx. *F*	d.f.	den. d.f.	*P*
Shape~Size+Genotype×Bite force	Size	1	0.75292	4.6512	19	29	<0.001
	Genotype	2	0.88973	1.2653	38	60	0.20
	Bite force	1	0.40731	1.0489	19	29	0.44
	Genotype:Bite force	2	0.69426	0.8395	38	60	0.71
Shape~Size×Genotype	Size	1	0.73743	4.4344	19	30	<0.001
	Genotype	2	0.85127	1.2091	38	62	0.25
	Size:Genotype	2	0.79094	1.0673	38	62	0.40
Shape~Genotype+Size	Genotype	2	0.83306	1.2399	38	66	0.22
	Size	1	0.70173	3.9624	19	32	<0.001
Mandible MANOVAS		d.f.	Pillai	Approx. *F*	d.f.	den. d.f.	*P*
Shape~Size+Genotype×Bite force	Size	1	0.77051	5.1247	19	29	<0.001
	Genotype	2	0.84372	1.1521	38	60	0.31
	Bite force	1	0.48403	1.4318	19	29	0.19
	Genotype:Bite force	2	0.81584	1.0878	38	60	0.38
Shape~Size×Genotype	Size	1	0.75837	4.9555	19	30	<0.001
	Genotype	2	0.80526	1.0997	38	62	0.36
	Size:Genotype	2	0.77411	1.0303	38	62	0.45
Shape~Genotype+Size	Genotype	2	0.82901	1.2296	38	66	0.23
	Size	1	0.74118	4.823	19	32	<0.001

The Genotype factor refers to the chromosomal group: XY males, XX females or X*Y females.

to test the effects of sex chromosomal group, age, size and their interactions on bite force. For shape, several models were fitted with a different sum of squares partitioning (Table 1), and MANOVAs were used to assess the influence of sex chromosomal groups on the principal components of shape variation.

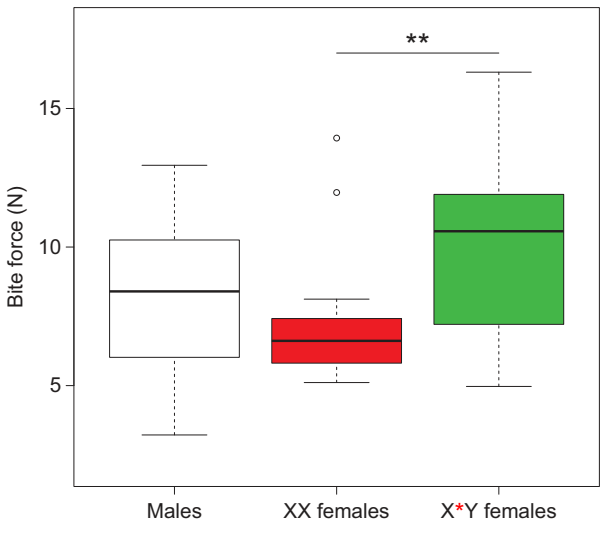

Fig. 2. Boxplot of bite forces of the three *M. minutoides* groups. Data are shown for males (n=19), XX females (n=18) and X*Y females (n=17). Limits of the boxes represent the upper and lower quartiles, the bar is the median, the whiskers represent the maximum and minimum value, or 1.5 times the interquartile distance in cases where outliers are present, and the circles are outliers. Asterisks indicate significant differences between means. Tukey's HSD test revealed a significant increase in bite force in X*Y females compared with XX females (P<0.01).

RESULTS AND DISCUSSION

X*Y females bit significantly harder than other females (Fig. 2; data are available on request from the corresponding author). They also bit harder than males, but not significantly so; bite force was similar between males and XX females. Table 2 shows the results of the Tukey's HSD test.

No major morphological differences appeared between the three groups,which overlapped in morphospace (Fig. 1C,D, Table 1).

X*Y females displayed a significantly greater centroid size than males and XX females (Table 2), even independently of age (Table 1). MANOVAs did not reveal any effect of the group on shape; however, they showed significant allometry shared by all groups (Table 1).

Table 2. Results of Tukey's HSD test for differences in bite force, mandible centroid size and skull centroid size

	Difference	Lower	Upper	*P*
Bite force				
♂ vs XX ♀	–0.86	–3.05	1.34	0.62
X*Y ♀ vs ♂	1.92	–0.308	4.15	0.1
X*Y♀ vs XX ♀	2.78	0.52	5.03	0.01
Mandible centroid size				
♂ vs XX ♀	3.15	–20.86	27.16	0.95
X*Y ♀ vs ♂	31.7	7.33	56.07	0.01
X*Y♀ vs XX ♀	28.55	3.86	53.24	0.02
Skull centroid size				
♂ vs XX ♀	–4.53	–41.21	32.14	0.95
X*Y ♀ vs ♂	67.56	30.33	104.78	<0.01
X*Y♀ vs XX ♀	72.09	34.38	109.8	<0.01

Journal of Experimental Biology

There was a significant size–bite force correlation ($r\approx0.6$, d.f.=52, $P<0.01$ for both bones) when considering the data as a whole (i.e. not taking the groups into account). A relationship was also found between age and bite force ($r=0.3$, d.f.=49, $P<0.05$). In the linear model created, the type II ANOVA revealed that, once age and size were taken into account, bite force differences were no longer significant between the groups ($F=1.28$, d.f.=2, den. d.f.=42, $P>0.2$), although the tendency for X*Y females to have higher bite force than XX remained. In this model, age had no significant effect, and size remained the main explanatory variable.

We showed that in the African pygmy mouse, X*Y females bite harder than the XX females and, more surprisingly, also bite harder than males (although not significantly so). Limited shape variation between the sex chromosomal groups (Fig. 1C,D) shows that skull and mandible shape are not at the root of the higher bite force of X*Y females. It also suggests that the presence of the Y and/or X* chromosomes does not significantly influence shape. However, without considering the groups, we found a positive relationship between size and bite force, as shown in previous studies (Herrel et al., 2001; Lailvaux et al., 2004; Freeman and Lemen, 2008). Furthermore, X*Y females displayed a greater skull size, which appears to explain part of their increased bite force (Tables 1, 2). Performance changes independent of size but owing to behavioural differences between the groups are subtle and not significant, suggesting that aggressiveness has a much lower impact on performance variation than morphological determininants (here size).

Hormones are also known to influence performance, as demonstrated by hormonal and molecular screening of elite female athletes, which detected sex development disorders with hyperandrogenism (e.g. XY females) in an occurrence 200 times greater than in the general population (e.g. Fénichel et al., 2013). In our model, however, the *M. minutoides* X*Y females harbour typical ovarian anatomy (no ovotestes) and a normal anogenital distance, suggesting a low level of circulating androgen (Rahmoun et al., 2014), observations that have been recently confirmed by preliminary hormonal assays on testosterone (F.V., unpublished data). Therefore, the increased skull size of X*Y females appears to be the main cause of their higher bite force.

Although not much is known about the ecology of *M. minutoides* (Britton-Davidian et al., 2012), the advantages of having higher performance may be twofold. Higher bite force may increase the range of available food resources (Aguirre et al., 2003) by allowing the X*Y individuals to feed on harder food. Second, higher aggressiveness coupled with stronger bites may have a role in intra-sex competition: X*Y females may increase their reproductive success by taking dominance over other females via attacks (Lailvaux and Irschick, 2006). This has been shown for lizards, in which dominance, territorial defense and the outcome of fights are all linked to performance (Herrel et al., 2010; Lailvaux et al., 2004).

Chromosomal changes in the X*Y females may thus give them a dominant position, consistent with the hypothesis that an increase in fitness explains the maintenance of these females, despite the costly loss of the unviable YY embryos (Saunders et al., 2014). Considering our results and those of Saunders et al. (2014, 2016), it appears that the X*Y females obtain selective advantages through many aspects of their fitness: reproductive success, behaviour and whole-organism performance. The effect of the X* chromosome thus goes well beyond feminization, and is at the origin of a complex and multi-factorial X* syndrome that extends to life history traits, behaviour (Saunders et al., 2014, 2016), size variation and performance (present study). Interestingly, these X*Y females were characterized as ‘super females’ because they were shown to have a better reproductive output than the XX females (Saunders et al., 2014), but in addition, they present hyper-masculinized traits with an enhanced aggressiveness, larger skulls and stronger bite forces than males. It is notoriously hard to assign performance modifications to naturally occurring genetic changes, but this model offers a fantastic framework with which to further connect performance, morphology, behaviour and sex chromosomes.

Acknowledgements
The authors thank the CECEMA animal facility. We also thank Paul A. Saunders for his comments on the manuscript. We are grateful to A. Herrel and one anonymous reviewer for their insightful comments. This publication is a contribution of the Institut des Sciences de l’Evolution de Montpellier (UMR 5554 – UM2+CNRS+IRD+EPHE) No. ISEM 2017-055.

Competing interests
The authors declare no competing or financial interests.

Author contributions
Conceptualization: S.G., J.C., F.V.; Methodology: S.G., J.C., J.P., F.V.; Formal analysis: S.G., J.C.; Investigation: S.G., J.P., F.V.; Resources: S.G., J.C., F.V.; Writing - original draft: S.G.; Writing - review & editing: S.G., J.C., F.V.; Supervision: J.C., F.V.

Funding
This research received no specific grant from any funding agency in the public, commercial or not-for-profit sectors.

References

Aguirre, L. F., Herrel, A., van Damme, R. and Matthysen, E. (2002). Ecomorphological analysis of trophic niche partitioning in a tropical savannah bat community. *Proc. R. Soc. Lond. B Biol. Sci.* **269**, 1271-1278.
Aguirre, L. F., Herrel, A., Van Damme, R. and Matthysen, E. (2003). The implications of food hardness for diet in bats. *Funct. Ecol.* **17**, 201-212.
Bookstein, F. L. (1991). *Morphometric Tools for Landmark Data*. Cambridge: Cambridge University Press.
Britton-Davidian, J., Robinson, T. J. and Veyrunes, F. (2012). Systematics and evolution of the African pygmy mice, subgenus *Nannomys*: a review. *Acta Oecolog.* **42**, 41-49.
Claude, J. (2008). *Morphometrics with R*. New York: Springer Science & Business Media.
Davis, J. L., Santana, S. E., Dumont, E. R. and Grosse, I. R. (2010). Predicting bite force in mammals: two-dimensional versus three-dimensional lever models. *J. Exp. Biol.* **213**, 1844-1851.
Fénichel, P., Paris, F., Philibert, P., Hiéronimus, S., Gaspari, L., Kurzenne, J. Y., Chevallier, P., Bermon, S., Chevalier, N. and Sultan, C. (2013). Molecular diagnosis of 5alpha-reductase deficiency in 4 elite young female athletes through hormonal screening for hyperandrogenism. *J. Clin. Endocrinol. Metabol.* **98**, E1055-E1059.
Freeman, P. W. and Lemen, C. A. (2008). A simple morphological predictor of bite force in rodents. *J. Zool.* **275**, 418-422.
Herrel, A., Spithoven, L., Van Damme, R. and De Vree, F. (1999). Sexual dimorphism of head size in *Gallotia galloti*: testing the niche divergence hypothesis by functional analyses. *Funct. Ecol.* **13**, 289-297.
Herrel, A., Van Damme, R., Vanhooydonck, B. and De Vree, F. (2001). The implications of bite performance for diet in two species of lacertid lizards. *Can. J. Zool.* **79**, 662-670.
Herrel, A., Moore, J. A., Bredeweg, E. M. and Nelson, N. J. (2010). Sexual dimorphism, body size, bite force and male mating success in tuatara. *Biol. J. Linn Soc.* **100**, 287-292.
Lailvaux, S. P. and Irschick, D. J. (2006). A functional perspective on sexual selection: insights and future prospects. *Anim. Behav.* **72**, 263-273.
Lailvaux, S. P., Herrel, A., VanHooydonck, B., Meyers, J. J. and Irschick, D. J. (2004). Performance capacity, fighting tactics and the evolution of life–stage male morphs in the green anole lizard (*Anolis carolinensis*). *Proc. R. Soc. B Biol. Sci.* **271**, 2501-2508.
Rahmoun, M., Perez, J., Saunders, P. A., Boizet-Bonhoure, B., Wilhelm, D., Poulat, F. and Veyrunes, F. (2014). Anatomical and molecular analyses of XY ovaries from the African pygmy mouse *Mus minutoides*. *Sex. Dev.* **8**, 356-363.
Santana, S. E., Dumont, E. R. and Davis, J. L. (2010). Mechanics of bite force production and its relationship to diet in bats. *Funct. Ecol.* **24**, 776-784.
Saunders, P. A., Perez, J., Rahmoun, M., Ronce, O., Crochet, P.-A. and Veyrunes, F. (2014). XY females do better than the XX in the African pygmy mouse, *Mus minutoides*. *Evolution* **68**, 2119-2127.

Journal of Experimental Biology (2017) 220, 1947-1951 doi:10.1242/jeb.157552

Saunders, P. A., Franco, T., Sottas, C., Maurice, T., Ganem, G. and Veyrunes, F. (2016). Masculinised behaviour of XY females in a mammal with naturally occuring sex reversal. *Sci. Rep.* **6**, 22881.

Veyrunes, F., Chevret, P., Catalan, J., Castiglia, R., Watson, J., Dobigny, G., Robinson, T. J. and Britton-Davidian, J. (2010). A novel sex determination system in a close relative of the house mouse. *Proc. R. Soc. B Biol. Sci.* **277**, 1049-1056.

Journal of Experimental Biology

2.2 – Influence de la consanguinité sur l'asymétrie et la performance (article accepté dans *Evolutionary Biology*).

On a montré dans la précédente section que les chromosomes sexuels pouvaient avoir une influence sur les composantes de la morphologie (notamment la taille dans notre cas), qui induit des changements dans la performance. D'autres facteurs peuvent produire des changements morphologiques plus ou moins importants, qui peuvent se répercuter sur la performance. Notamment, le développement peut subir les effets de stress environnementaux ou génétiques (en particulier la consanguinité). Cette instabilité peut être la source de changements morphologiques importants comme l'augmentation de l'asymétrie entre les côtés gauches et droits chez les animaux bilatériens (e.g. Roldan et al. 1998, Carter et al. 2009). Cependant, l'importance fonctionnelle d'un caractère pourrait être associée à des processus de stabilisation développmentale tamponnant l'effet des stress (Badyaev et al. 2000, Debat et David 2001). Ici on s'intéressera aux effets de ces stress sur l'asymétrie des mandibules et sur la force de morsure des rongeurs. Il a été démontré qu'une plus grande asymétrie fluctuante pouvait causer une baisse des performances sur des caractères locomoteurs (Martin & Lopez 2001, Vervust et al. 2008, Rivera & Claude 2008). En revanche, l'influence de l'asymétrie du crâne ou des mandibules sur la morsure n'a jamais été étudiée.

L'article suivant s'intéresse à trois lignées de souris d'animalerie, descendantes de souris sauvages des Orcades, ayant été soumises à différents régimes de croisements (consanguins ou non). La force de morsure au sein des trois lignées a été mesurée, à différents niveaux de consanguinité, ainsi que l'asymétrie au niveau des mandibules, afin de vérifier si la perte de diversité génétique et/ou l'augmentation de l'asymétrie pouvaient entraîner une baisse de la performance.

Bite force performance, fluctuating asymmetry and antisymmetry in the mandible of inbred and outbred wild-derived strains of mice (*Mus musculus domesticus*).

Samuel Ginot* (1), Sylvie Agret (1) & Julien Claude (1)

(1) Institut des Sciences de l'Evolution de Montpellier, Universite de Montpellier, CNRS, IRD, Cc 065; place Eugène Bataillon, 34095 Montpellier Cedex 5, France

*Corresponding author : samuel.ginot@umontpellier.fr, +33 464144782

Abstract

Developmental instability, as measured by fluctuating asymmetry is generally considered to increase with genetic and environmental stresses. Few studies have, however, addressed the role of asymmetry in altering organism performance. Here, we measured bite force performance in three strains of inbred and outbred mice derived from wild ancestors. We quantified size and shape directional, and fluctuating asymmetry, as well as inter-individual variation of their mandibles using geometric morphometrics. We also developed a way to estimate shape antisymmetry, to filter it out of the fluctuating asymmetry component. Contrary to our expectations, we found no significant link between bite force and asymmetry levels. Inbreeding did not produce any clear and significant increase or decrease in neither inter-individual variance, nor fluctuating asymmetry. Furthermore, fluctuating asymmetry levels were unrelated to inter-individual variance levels, although these two types of variation affected the same areas of the mandible. We did not highlight any impact of inbreeding depression on bite force. Fluctuating asymmetry was reduced in the mandible, which we argue may be

28 linked to its functional relevance. We found some significant but very reduced antisymmetry possibly
29 linked to lateralization. This lateralization did not relate to any bite force difference. Our results show
30 that neither inbreeding, nor asymmetry (combining fluctuating, directional asymmetry and
31 antisymmetry) significantly affect bite force performance in mice, and that despite affecting the same
32 morphological regions, developmental stability and canalization are independent.
33 **Keywords :** asymmetry ; performance ; inbreeding ; rodents ; lateralization

Introduction

Asymmetry of the cranio-mandibular and tooth structures has been a pervasive topic of research for a long time (*e.g.* Woo 1931, Ballard 1944, Van Valen 1962). This is particularly true in humans, for which excessive asymmetry in these structures may produces pathological conditions (see for example the many different kinds of malocclusion; Angle 1900). Asymmetry of the skull also has been widely studied during the past decades in animals (*e.g.* Sumner and Huestis 1921, Badyaev et al. 2000, Vervust et al. 2008, Fahlke et al. 2011). Today, three separate kinds of asymmetries are usually defined: directional asymmetry (DA), fluctuating asymmetry (FA) and antisymmetry (AS) (see for example Palmer 1994 for definitions and a detailed mathematical description). Directional asymmetry can be defined as a directionally consistent difference between sides, for example when in a population the left structure is generally larger than the right. Fluctuating asymmetry consists of non-directional random deviations from symmetry. Finally, antisymmetry is a case in which deviations from symmetry are favored, but without preferential direction, which means that the distribution of left-right differences will be bimodal, with symmetric individuals being less frequent. Despite fairly constant research, the interplay between these types of asymmetry is still a matter of discussion (see for instance Van Dongen et al. 1999, Kart 2001). Furthermore, the influences of genetic and environmental factors (as well as their interactions) on the different asymmetries as well as their heritabilities do not necessarily show strong consistency (see Palmer 1999 for discussion of this point).

Directional asymmetry is generally considered to have a genetic basis due to observations of cases such as the mammalian heart (Van Valen 1962), the rostrum of odontocetes (*e.g.* Macleod et al. 2007, Fahlke et al. 2011), or testes size in swallows (in this case linked to sexual selection, Moller 1994). As such, it is usually not considered to be driven by environmental or developmental stress.

Fluctuating asymmetry has been linked to developmental instability and individual condition (Clarke et al. 1986, Moller & Pomiankowski 1993). It has been shown to increase in organisms

developing in stressful environments (Clarke et al. 1986), and is considered, in a sexual selection context, to be an honest cue of the ability of an individual to cope with deleterious factors (*e.g.* pathogens, deleterious genetic factors, abiotic factors), although there is still some discussion about this role for FA (Grammer et al. 2003). Yet, the relationship between environmental and genetic stress and FA may not be as straightforward as sometimes thought. In particular, they depend on the species and on the character(s) studied (Clarke et al. 1986, Kruuk et al. 2003). Furthermore, publication biases may be fairly important in this field (Palmer 1999). Authors also suggest that fluctuating asymmetry may be partially under the control of epistatic interactions rather (Leamy et al., 2015) than the direct effect of genes, suggesting that a modification of genetic relationships between loci can affect it. Hybridization, for instance, may disturb developmental stability and canalization because networks of coadapted genes may have evolved in isolated populations and these networks could be disrupted in hybrids (Hallgrimsson 1998, Debat et al. 2001). Phenotypic extremeness has also been linked to developmental instability through various potential effects (heterozygosity or canalizing selection), though this relationship has been rarely studied (Hallgrimsson 1998, Gonzalez et al. 2016). Finally FA has been shown to change across developmental time and with aging, due to the accumulation or compensation of developmental noise (Kobyliansky and Livshits 1989, Hallgrimsson 1998, Gonzalez et al. 2014).

Although there is still some debate around the genetic and epigenetic effects that may cause fluctuating asymmetry, one might expect FA level to be modified and to increase in inbred animals due to genetic and developmental stresses, which may also be inter-linked (Hallgrimsson 1988). However, it should also depend on the functional significance of the trait studied (Siegel & Doyle 1975, Badyaev et al. 2000). Indeed, functionally relevant characters (such as limb morphology) appear less prone to being asymmetric than others (Siegel & Doyle 1975), which could be linked to a direct performance disadvantage of asymmetry in these characters (Martin & Lopez 2001). Inbreeding may also influence performance directly (inbreeding depression), or through non-morphological factors such as behaviour. For instance, differences are found between inbred and F1 mice in terms of activity patterns and

84 performance in tests (*e.g.* Logue et al. 1997, Tang et al. 2002). However, hybrids do not always display
85 better scores, suggesting that homozygosity is not necessarily deleterious to performance.

86 So far, few studies have considered the relationship between the different components of
87 asymmetry and performance *in vivo*. According to previous works, fluctuating asymmetry could lead to
88 a decrease in performance and individual fitness. In vertebrates, most studies of performance and FA
89 have focused on locomotory performance, in which symmetry is of utmost mechanical importance
90 (Martin & Lopez 2001, Vervust et al. 2008, Rivera & Claude 2008). Here we look at bite force which is
91 also a functionally relevant and fitness-related trait (*e.g.* Herrel et al. 2005, Husak et al. 2006). To our
92 knowledge, the study by Vervust and colleagues (2008) is the only attempt to test bite force against
93 asymmetry. Although they found no relationship, it should be kept in mind that this study only used FA
94 of meristic characters, functionally unrelated to biting, due to high error rate in skull linear
95 measurements.

96 Mastication in murine rodents is generally accepted to be symmetrical, with chewing happening
97 on both sides simultaneously (Weijs 1975, Weijs & Dantuma 1975). Furthermore, the mandible
98 morphology of rodents is known to be related to bite force (*e.g.* Freeman & Lemen 2008, Ginot et al. *in*
99 *press*). In this context, one might expect to find some negative effect of mandible asymmetry on bite
100 force. It may however be more complicated, because little is known about mastication in murines. For
101 instance, lateralization (*e.g.* side preference) may influence mandible morphology and asymmetry
102 (Pirttiniemi & Kantomaa 1992, Pirttiniemi 1998). Research on mastication in humans has shown that
103 there is often a side preference linked to handedness (Nissan et al. 2004, Zamanlu et al. 2012), that
104 muscular activity is asymmetrical (Naeije et al. 1989, McCarroll et al. 1989) and that side preference is
105 linked to side performance (Rovira-Lastra et al. 2014). Despite having mainly symmetrical masticatory
106 muscle activity, murines may also show some small degree of side preference, related to their
107 handedness (Collins 1991, Collins et al. 1993), and this may slightly influence some aspects of
108 asymmetry (*i.e.* directional asymmetry or antisymmetry). In other terms, there may be opposite effects

of function on asymmetry in the mandible: although functional traits may be more developmentally stable causing their fluctuating asymmetry to be lower (Siegel & Doyle 1975, Badyaev et al. 2000), the function itself (here, mastication and biting) may be lateralized (as is the case in humans), which would increase directional asymmetry or antisymmetry (and consequently measures of FA since antisymmetry is rarely quantified and often part of that component, see Levinton et al. 1995).

In the present study, we investigate the links between inbreeding, asymmetry and *in vivo* bite force by testing several hypotheses in lab-reared mice. Considering the elements above we expect (Fig. 1) that the bilateral bite force at the incisors will be negatively affected by 1) the fluctuating asymmetry of the mandibles, and 2) by an increase in inbreeding. Furthermore, 3) inbreeding may increase intra-

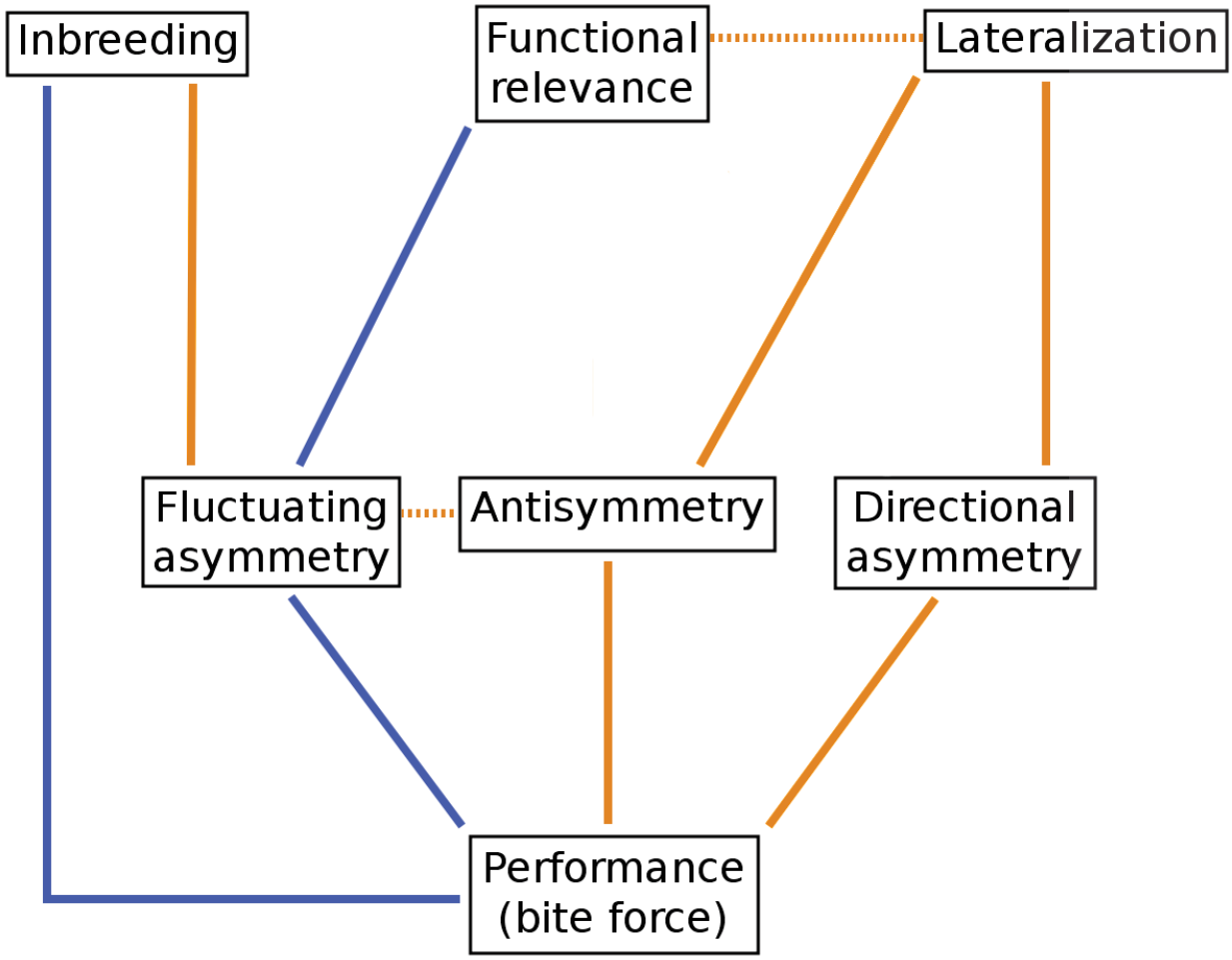

Figure 1. Schematic representation of the relationships tested in the present study. Blue lines correspond to relationships expected to be negative, and orange lines to relationships expected to be positive. Dotted lines show related factors that may have opposite effects.

individual (FA) and decrease inter-individual morphological variance; and therefore generate a negative correlation between these two components of phenotypic variation. Because mandible morphology is functionally significant, 4) mandible FA is expected to be reduced, but 5) DA and AS may be present if there is some degree of lateralization in mastication. If this is the case, we expect that 6) DA and AS should be positively related to bite force.

Material and methods

Wild-derived mouse strains

Three strains were considered, all descending from wild ancestors from the Orkney archipelago (Scotland). The founders of the strains were captured on three islands: Papa Westray (PW; 4 founders), South Ronaldsay (SR; 6 founders), and Mainland (ML; 88 founders). Mainland is the largest island in the Orkney archipelago (about 10 times larger than South Ronaldsay, and 50 times larger than Papa Westray). Descendants of these founders were raised in the CECEMA facilities in the University of Montpellier (France), while controlling for crosses and pedigrees. One strain was kept outbred (ML), and the two others were progressively inbred. Among the latter two, one (PW) was actively selected for the fixation of a dental character (an elongation of the first upper molar), while the other (SR) was actively selected for the absence of this trait.

Specimens

When the mice were 68 +/-5 days old, we measured their bite force, then immediately euthanized them using carbon dioxyde gas. Their skulls and mandibles were then prepared manually. Their inbreeding coefficient (IC) was calculated from the pedigree, using the 'pedigree' package (Coster 2013) in R (R Development Core Team, 2017).

When running asymmetry analyses, individuals were pooled in groups, as FA, DA and AS are population-level estimates. Here, the groups were based on the inbreeding coefficient (IC). SR and PW mice were separated in three groups each: "LPW" and "LSR" with 0 < IC =< 0.33, "MPW" and "MSR" with 0.33 < IC =< 0.66, and "HPW" and "HSR" with IC > 0.66. The ML mice all had an IC of 0, and were pooled as one "ML" group. Each group contained 29 to 38 individuals, with the exception of the ML group, which contained 50 individuals. Finally, we also included PW and SR mice from first and second lab generations, even though these mice had variable ages, with no bite force data available, and were in smaller numbers than the other groups (n=8 and 19 respectively). These two groups had an IC of 0, based on the pedigree, and were coined "NPW" and "NSR". Overall we used 271 mice, from various litters, with both males and females included.

Bite force measurements

Bite force was measured using a Kistler piezo-electric force transducer, similar to that described in Herrel et al. (1999). The same user (SG) did all the measurements to avoid inter-user variability. Each mouse bit three times in a row and only its highest bite force was selected to be used in the following analyses.

Geometric morphometric analyses

All left and right mandibles were cleaned manually and photographed in a standardized way (camera at a fixed distance, mandible positioned flat with the lingual side down) using a Pentax K200D reflex camera, with a 45mm focal distance. Twelve landmarks (Fig. 2) were selected on each side. Landmarks were digitized using the tpsDig2 software (Rohlf 2010). After mirroring the images for all left mandibles, both right and left mandibles were digitized at the same time. The whole procedure (taking photographs and digitizing landmarks) was repeated a second time to allow quantification of measurement error. All mandibles were centered and superimposed using Procrustes analyses functions

169 from Claude (2008) in R (R Core Team 2017). Centroid size of the mandible constituted the size
170 variable throughout the study. Distributions of size and shape were inspected graphically and no
171 extreme outliers were detected.
172
173 *Asymmetry analyses*
174 Procrustes coordinates and centroid size were used in separate mixed-effect model ANOVAs
175 with individual and side as factors (Palmer 1994, Swaddle et al. 1994, Klingenberg & McIntyre 1998)
176 separately for each group of mice. This procedure allowed us to compute estimates of directional
177 asymmetry (DA), fluctuating asymmetry (FA), inter-individual variance (VAR), and measurement error
178 for both size and shape, and for each group. Practically, FA was estimated by the multivariate FA10
179 (Mean Squares (MS) of interaction effect - MS of residuals divided by number of replicates), VAR by
180 the sum of variances inferred for the symmetric part of individual variation (MS of individual effect -
181 MS of interaction effect divided by number of sides and number of replicates), and DA was inferred by
182 the part of variation related to side (MS of side effect - MS of interaction effect divided by number of
183 individuals and number of replicates). For centroid size, we applied a conventional ANOVA, but

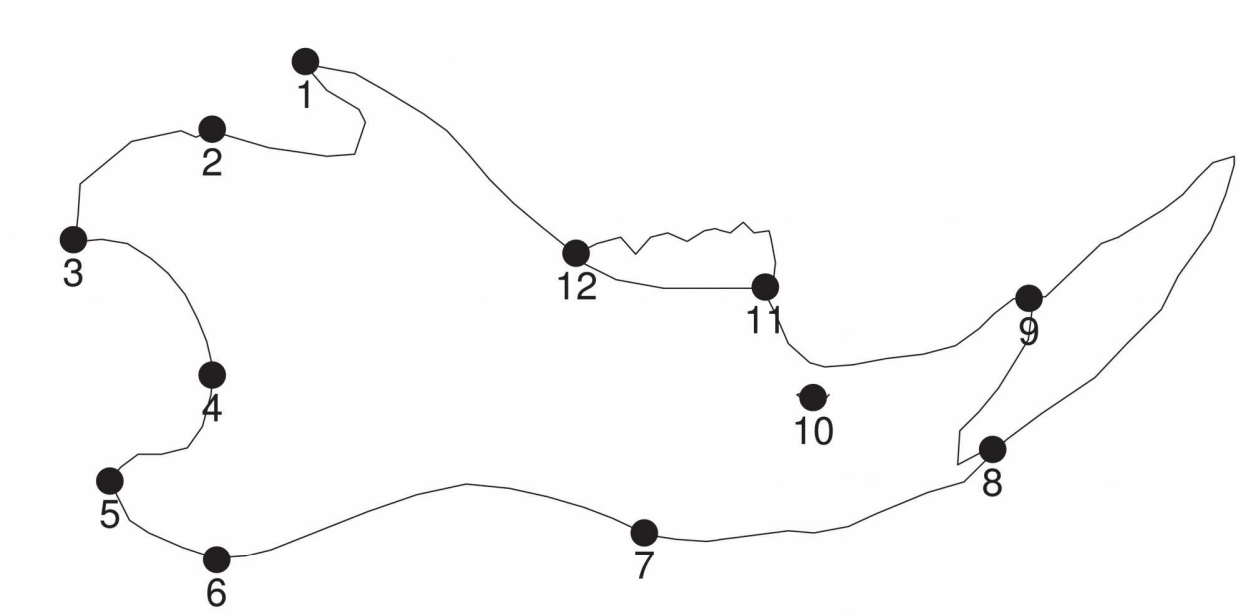

Figure 2. A mouse mandible drawing with the twelve landmarks used in this study.

applied a Procrustes ANOVA for shape (where we considered the trace of the mean squares and mean cross products for each effects, and where degrees of freedom were multiplied by the number of shape dimensions, as described in Klingenberg and McIntyre 1998 and Klingenberg et al. 2002). All significance values for these estimates were then computed comparing our F ratios to the F distribution. Between-groups and between sex differences in our asymmetry and inter-individual variance estimates were also tested using F ratios, with corrected degrees of freedom (or adapted, for shape data) following the formulas given by Palmer (1994 ; formulas 1, 2 and 3). Because of multiple testing, the significance levels for differences in FA, DA, VAR, as well as AFFA and AS (see after) were adjusted by a Bonferonni correction. We also computed bootstrap confidence intervals to assess the significance of asymmetry differences between groups. Because this produced similar results as the previously described approach, we did not show these analyses here.

Estimation of size antisymmetry

Antisymmetry in the centroid sizes of the mandibles was assessed using the distributions of the left-right differences (Palmer 1994). Divergence from normality of the distributions was tested using Shapiro-Wilk tests.

Estimation of shape antisymmetry

Although antisymmetry (AS) can be readily identified in univariate traits by the bimodal distribution of the differences between sides (Palmer 1994), to our knowledge no method is available to discriminate AS from FA for multivariate shape data or to measure AS precisely. Our approach considers that directional asymmetry is a by-product of antisymmetry when the frequency for the more developed side shifts from 50 percent. In that theoretical context, and in the way that the ANOVA model for FA/DA is computed, the effect of antisymmetry will spread in both the directional and fluctuating asymmetry components; possibly altering interpretations. If one side is systematically more

developed than the other, then DA will be correctly estimated, but if the more developed side varies, AS will become part of the FA component of variance. Therefore, we generated an antisymmetry index in the following way. If antisymmetry exists, a given mandibular shape should correspond to one side, while another mandibular shape should correspond to the opposite side. An individual should harbor these two typical shapes on either of its sides. The larger the antisymmetry, the more different these shapes will be. In order to measure this quantity, we ran analogous Procrustes ANOVA but allowing the side to be left or right to maximize variation due to side. This effect occupies the same position of directional asymmetry in the traditional Procrustes ANOVA protocol, and becomes a measure of antisymmetry. To achieve this, our procedure computes the mixed-model ANOVA recursively, while switching sides of each individual one by one in no particular order. If the switching increases the resulting AS, the sides are kept switched, if not, they are switched back the original way. After applying this to all individuals, the procedure is reiterated until maximal AS is reached (*i.e.* when the difference between the previous DA and new DA is 0). This new value represents antisymmetry, while the remaining interaction value (former FA10) value represents the fluctuating asymmetry that cannot be assigned to AS. We will refer to it later as the antisymmetry filtered fluctuating asymmetry (AFFA). Even though AFFA and AS are new estimates, formulas from Palmer (1994) can be used to estimate the associated degrees of freedom, by replacing the original mean squares by the corresponding mean squares computed for the mixed-model recursive ANOVA. As for VAR, DA and FA, F ratios were used to assess the significance of differences in AFFA and AS, with Bonferonni-adjusted significance levels. Again, we computed bootstrap confidence intervals to confirm these results.

Comparison between patterns of intra-individual and inter-individual shape variation

Shape variation patterns at the intra-individual (*i.e.* FA) and inter-individual (*i.e.* VAR) levels were obtained and compared visually, and the similarity between both was tested. To do so, we extracted the individual and the interaction variance-covariance matrices in the shape Procrustes

ANOVA. Then, we calculated the correlation coefficient between the two matrices, and obtained the associated P-values using a Mantel test, with 5000 permutations of the landmarks (*i.e.* x and y coordinates of one landmark are permuted together ; cf. Klingenberg & McIntyre, 1998).

Results

Sexual dimorphism

We first pooled all groups to test for sexual dimorphism. Two-tailed Welch t tests revealed that the inbreeding coefficient was not significantly different between males and females ($t = 1.517$, $df = 219.38$, $P > 0.1$), *i.e.* the sex ratio in the inbreeding level groups was not unbalanced. Overall, males had larger mean centroid size ($t = -8.136$, $df = 218.12$, $P < 0.001$, Fig. 3A), as well as greater bite force ($t = -3.753$, $df = 234$, $P < 0.001$, Fig. 3B). Type II ANOVA showed that the effect of sex on bite force was significant ($F = 5.28$, $df = 1, 237$, $P < 0.05$), while the effect of size was not ($F = 2.87$, $df = 1, 237$, $P>0.05$), and that the effect of the interaction between sex and size was also not significant ($F = 0.89$, $df = 1, 236$, $P>0.3$). MANOVA on the shape data revealed significant effects of size, sex, strain, and

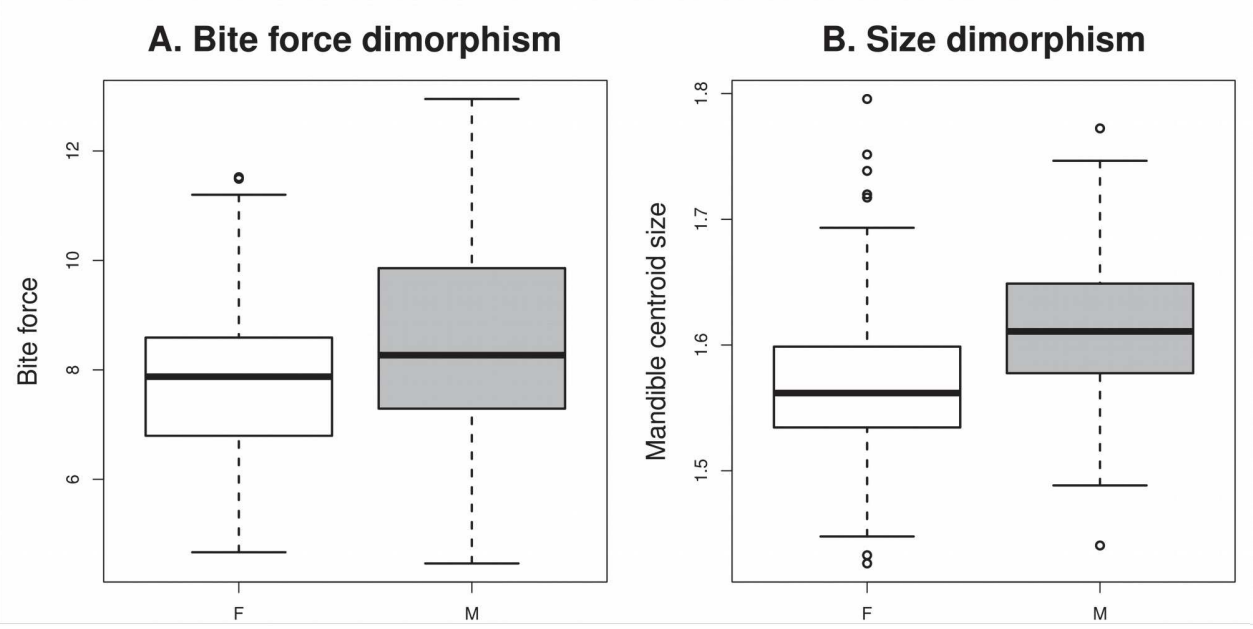

Figure 3. Sexual dimorphism in mandible bite force (A) and centroid size (B). In both cases males display significantly higher mean values (both $P<0.0001$ on 218 and 232 df respectively). Whiskers represent 1.5 times the interquartile distance, when outliers (circles) are present. If there are no outliers, whiskers represent the maximal and minimal values.

inbreeding level (Fig. 4A and B), as well as interactions between size and the inbreeding level, and between sex and the inbreeding level (*i.e.* the influence of size and sex on shape vary depending on the inbreeding level). When looking at individual strains (ML, SR and PW), it appeared that the sexual dimorphism of size was still present and significant in each one (all $P < 0.001$). However, sex had no significant effect of on shape in ML mice ($F = 1.30$, $df = 20, 27$, $P > 0.2$), while it did in PW and SR strains ($F = 5.10$ and 2.63, $df = 20, 73$ and $20, 69$, both $P < 0.001$, Fig. 4A and B).

Because size and shape varied between sexes, we also had to test for sexual dimorphism in their asymmetries. We did so within each group and found some asymmetry variation between males and females (Supp. Material Fig. 1), however the differences were not consistent (*i.e.* sometimes males had higher asymmetry, sometimes females did). Furthermore, they were never significant (with alpha = 0.007 due to Bonferonni correction), except in two cases for the fluctuating asymmetry, in the LPW and HPW groups where males had higher FA (respectively $F = 0.5914051$ and 0.5546741 $df = 87.28948$, 191.0259 and 131.38152, 122.5361, $P = 0.006$ and 0.001). Therefore, we grouped males and females within groups in the following asymmetry analyses to reduce the probability of type II error.

Inbreeding, size and bite force

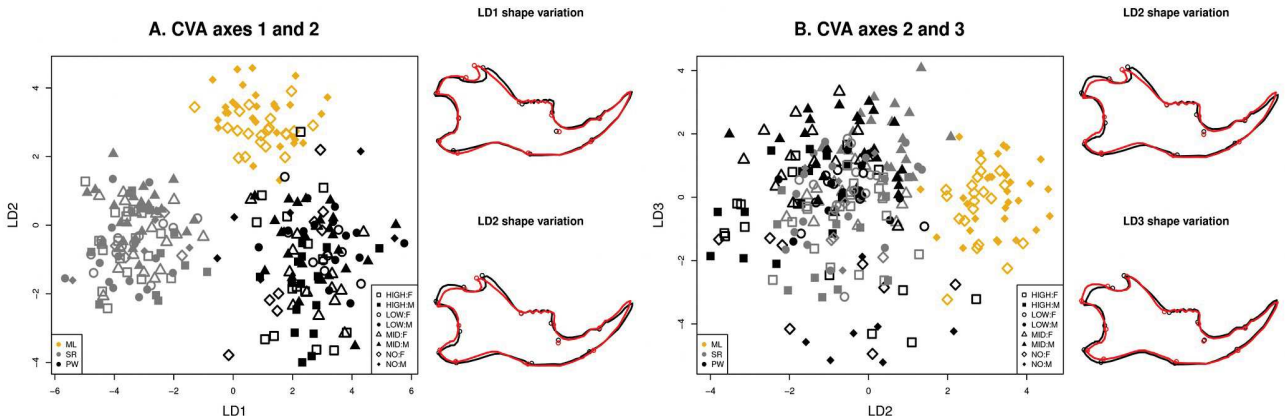

Figure 4. CVA of mandible shape variation with strain, sexes and inbreeding level as grouping factors. (A) Represents the first two axes of the analysis, with morphological changes associated with positive (black) and negative (red) values of the axes. (B) Shows axes 2 and 3 of the same analysis, also with morphological changes associated with the axes. Abbreviations : HIGH, highly inbred ; LOW, slightly inbred ; MID, intermediately inbred ; NO, outbred ; F, female ; M, male ; ML, mainland ; PW, Papa Westray ; SR, South Ronaldsay.

The correlation between bite force and mandible size when using all individual data was low but significant (Spearman's r = 0.165, P = 0.011, Fig. 5A). When separating the PW, SR (excluding the NPW and NSR groups, which had no bite force data available) and ML strains, the correlation was significant in the SR strain (r = 0.298, P = 0.004), while it was not significant in both other groups (r = 0.112, P = 0.284 for PW, and r = 0.094, P = 0.523 for ML). Finally, when separating both sexes (Fig. 5) the correlation between bite force and size only remained significant in the SR males (r = 0.323, P = 0.024).

In the strains where crosses were designed to produce inbred offspring (*i.e.* PW and SR), bite force was positively correlated with the inbreeding coefficient (Fig. 5B). Once again, the correlation was more significant for the SR (r = 0.289, P = 0.006) than for the PW strain (r = 0.278, P = 0.007). When separating sexes, the correlation remained for males and females of the SR strain (respectively, r = 0.294 and 0.364, P = 0.040 and 0.025), but only for females in the PW strain (r = 0.499, P = 0.0004).

In the same strains, still excluding the NSR and NPW groups, for which age was not controlled, mandible size decreased with the increased inbreeding (r = -0.42, P < 0.0001 for SR, and r = -0.386, P < 0.0001 for PW). When separating sexes, the relationship remained significant for PW males (r =

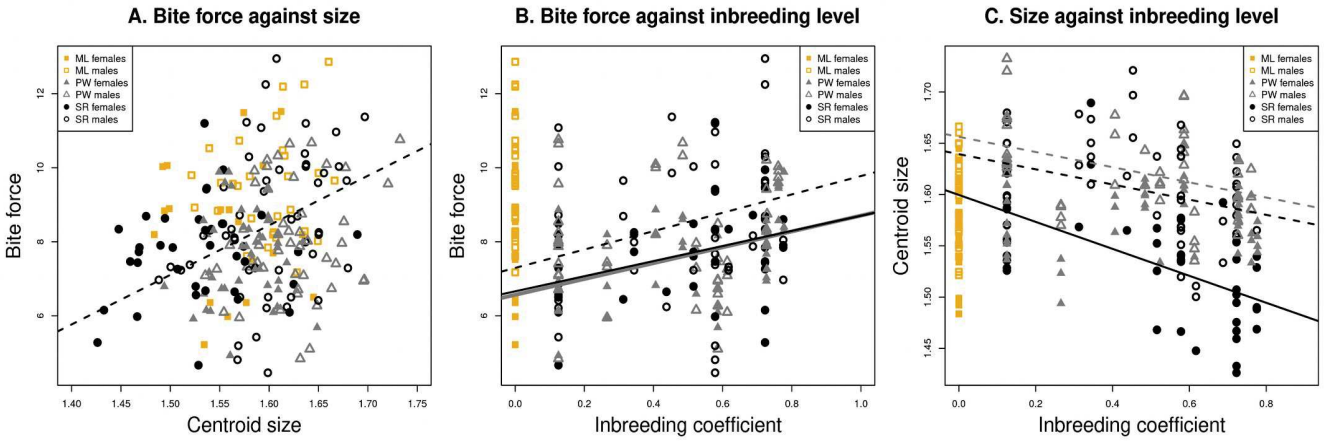

Figure 5. (A) Bite force (Newton) plotted against centroid size. Yellow squares represent the ML mice, the gray triangles are the PW mice, and the black circles are the SR mice. Full symbols represent females, empty symbols represent males. Only the male SR mice showed a significant positive correlation (P < 0.05), materialized by the black dashed regression line. (B) Bite force plotted against the inbreeding coefficient. There was a significant positive correlation for the SR males (black dashed line), SR females (black solid line) and PW females (gray solid line) (all P < 0.05). (C) Centroid size plotted against the inbreeding coefficient. There was a significant negative correlation for SR females (black solid line), SR males (black dashed line) and PW males (gray dashed line) (all P < 0.05).

281 -0.487, P = 0.0002), SR males (r = -0.390, P = 0.0014), and SR females (r = -0.535, P < 0.0001) (Fig.
282 5C).
283
284 *Mandible size asymmetry analyses*
285 Since asymmetry can only be estimated at the population/group level, in the following analyses
286 specimens were split into groups corresponding to the strain and the level of inbreeding (NPW, NSR,
287 LPW, LSR, MPW, MSR, HPW, HSR, and ML; see Materials and methods).
288 Our analyses revealed significant size FA10 in all groups (all P < 0.02, Tab. 1) except the MSR
289 group (P = 0.058). Size DA was significant only in the PW strain (P < 0.05), with the exception of the
290 NPW group (P > 0.1). Overall, size FA10 was generally two to forty times greater than DA. The
291 distributions of right-left differences (Fig. 6) showed a shift to the right for the PW groups with
292 significant DA, meaning that the right mandible was consistently larger than the left in these groups
293 (LPW, MPW and HPW, Fig. 6C-E). Although not significant, the NPW group (Fig. 6B) also showed a
294 right shift in its distribution. Other distributions of right-left differences (Fig. 6) were also inspected
295 visually and tested for deviation from normality to check for potential size antisymmetry using the

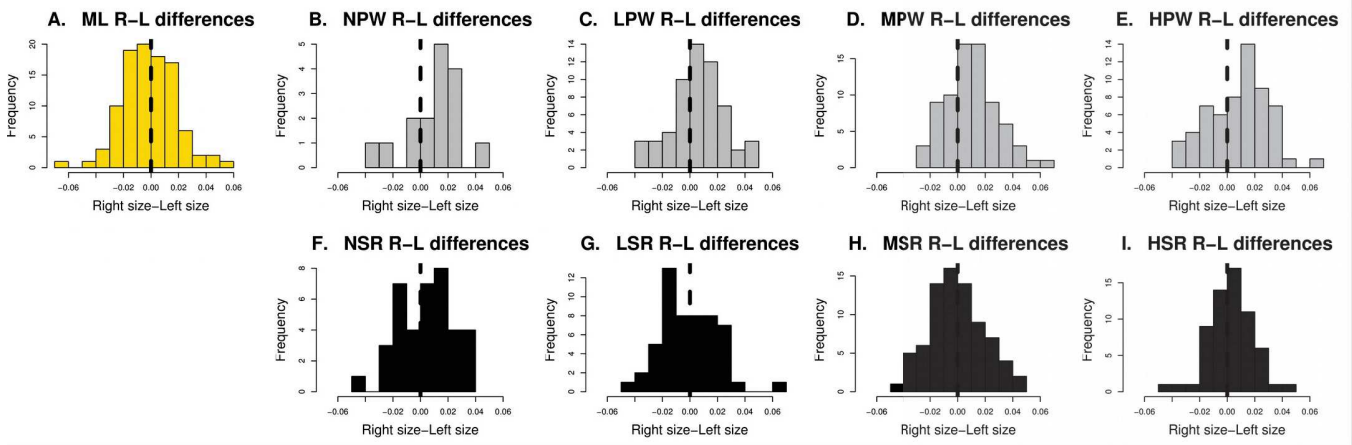

Figure 6. Distributions of Right-Left (R-L) differences in mandible centroid size. Yellow bars are for the ML mice (A), gray bars (upper row) are for the PW mice (B-E) and dark gray bars (bottom row) are for SR mice (F-I). No distribution differed from normality, which supported the absence of antisymmetry. However, the LPW, MPW and HPW groups (C-E) had significant directional asymmetry, visible by a shift of their distributions to the right. Abbreviations are the same as in text: ML, Mainland (outbred); NPW, non-inbred PW; LPW, low-inbreeding PW; MPW, intermediate-inbreeding PW; HPW, high-inbreeding PW; NSR, non-inbred SR; LSR, low-inbreeding SR; MSR, intermediate-inbreeding SR; HSR, high-inbreeding SR.

296 Shapiro-Wilk test. No distribution differed significantly from normality (all P > 0.09 and W > 0.9),
297 suggesting that no size antisymmetry was present (or that it was to subtle to be detected).

298 Finally size inter-individual variance was significant in all groups (all P<0.001), and was five to
299 one hundred times greater than size FA10. Between-group differences of inter-individual variance were
300 not significant (all P > 0.1). Between groups size FA10 was uncorrelated with size VAR (r = -0.6, P =
301 0.0968), *i.e.* the most variable groups intra-individually were not more variable inter-individually.

302

303 *Shape asymmetry analyses*

304 Shape FA10 was significant in all groups (all P < 0.0001, Tab. 2), while DA was one hundred
305 times lower and only significant in the MPW, MSR, ML and NSR groups. Inter-individual shape
306 variation was also very significant in all groups (all P < 0.0001), and consistently higher than FA10
307 (one to three times). Differences in inter-individual variance between groups were not significant (all P
308 > 0.2). There was no link between the levels of shape FA10 and shape VAR in the different groups (r =
309 0.45, P = 0.230). On the other hand, patterns of shape variation for FA10 and VAR were similar (Fig.
310 7), and their respective variance-covariance matrices were always significantly correlated, with all
311 Mantel correlation coefficients between 0.54 and 0.89 (all tests P < 0.01). Variable areas of the
312 mandible were generally the coronoid and condylar processes, and less frequently the angular process
313 and anterior part of the incisor alveolus (Fig. 7).

Group	Mean squares (MS)			Variance decomposition				P-values		
	Individuals MS	Side MS	Interaction MS	FA10	DA	VAR	Error	P-val FA	P-val DA	P-val VAR
ML	0.00746	0.00011	0.00029	0.0001049	-0.0000018	0.00179	0.0000835	< 0.00001	0.5419	< 0.00001
NPW	0.01056	0.00076	0.00028	0.000104	0.0000295	0.00257	0.000077	0.0143	0.1472	0.0001
NSR	0.04663	0.00029	0.00029	0.0001032	-0.0000001	0.01158	0.0000881	0.0009	0.3339	< 0.00001
LPW	0.01156	0.00126	0.00023	0.0000563	0.0000176	0.00283	0.0001213	0.0176	0.0281	< 0.00001
LSR	0.00775	0	0.00027	0.0000667	-0.0000049	0.00187	0.0001333	0.016	0.9367	< 0.00001
MPW	0.00612	0.00364	0.00024	0.0000694	0.0000448	0.00147	0.0001031	0.0009	0.0004	< 0.00001
MSR	0.01433	0.00002	0.00028	0.0000484	-0.0000034	0.00351	0.0001837	0.058	0.818	< 0.00001
HPW	0.00278	0.00201	0.00035	0.0001163	0.0000278	0.00061	0.0001128	0.0001	0.0224	< 0.00001

Table 1. Results from the size asymmetry mixed-effect model ANOVA, in the different groups (strains x inbreeding categories), showing mean squares of the various terms and interactions, variance decomposition and associated P-values. FA10: Fluctuating asymmetry, DA: directional asymmetry, VAR: inter-individual variance.

Shape AS was significant in all groups (all $P < 0.001$), and antisymmetry-filtered FA (AFFA) was still very significant (all $P < 0.0001$). AS was 2.5 to 7.5 times less than AFFA, which showed that AS did not inflate the original FA10 very much.

Effects of centroid size on size and shape asymmetries

Because asymmetry estimates can be biased by size (Palmer 1994), we tested if centroid size differences between our groups affected their asymmetry values. The mean centroid size of the groups did not correlate with either size or shape FA10 (R^2=0.17 and -0.11 respectively, with df=1 and 7, and both $P>0.1$). We also found no link between centroid size and size or shape DA (R^2=0.03 and -0.11 respectively, with df=1 and 7, and both $P>0.3$). Finally, there was no correlation between centroid size and shape AS or AFFA (R^2=0.1 and -0.14 respectively, with df=1 and 7, and both $P>0.2$).

Inbreeding and size asymmetry

Size FA10 was high in the NPW, NSR and ML groups (Fig. 8A), and diminished in the LPW and LSR groups. In the inbred groups of the SR and PW strains, we found opposite trends : the size FA10 kept on decreasing from the LSR to the HSR group, while it increased from the LPW to the HPW group. However, none of these between group differences were significant (all $P > 0.1$).

Group	Mean squares (MS)			Variance decomposition						P-values				
	Individuals MS	Side MS	Interaction MS	FA10	DA	VAR	Error	AS	AFFA	P-val FA	P-val DA	P-val VAR	P-val AS	P-val AFFA
ML	0.000187	0.000131	0.000067	0.000027	0.000001	0.00003	0.000013	0.000006	0.000022	<0.00001	0.007	<0.00001	<0.00001	<0.00001
NPW	0.00015	0.000041	0.000055	0.00002	-0.000001	0.000024	0.000015	0.000005	0.000014	<0.00001	0.779	<0.00001	0.000114	<0.00001
NSR	0.000381	0.000151	0.00007	0.000027	0.000002	0.000078	0.000016	0.000006	0.000023	<0.00001	0.003	<0.00001	<0.00001	<0.00001
LPW	0.000148	0.000065	0.000049	0.000018	0	0.000025	0.000013	0.000003	0.000016	<0.00001	0.158	<0.00001	<0.00001	<0.00001
LSR	0.000125	0.000054	0.000041	0.000014	0	0.000021	0.000012	0.000004	0.000011	<0.00001	0.161	<0.00001	<0.00001	<0.00001
MPW	0.000142	0.000127	0.000039	0.000014	0.000001	0.000026	0.000011	0.000004	0.000012	<0.00001	<0.00001	<0.00001	<0.00001	<0.00001
MSR	0.000144	0.000079	0.000042	0.000014	0	0.000026	0.000013	0.000003	0.000012	<0.00001	0.01	<0.00001	<0.00001	<0.00001
HPW	0.000127	0.000032	0.000051	0.000018	0	0.000019	0.000015	0.000002	0.000016	<0.00001	0.896	<0.00001	<0.00001	<0.00001
HSR	0.00014	0.000077	0.000052	0.00002	0	0.000022	0.000011	0.000004	0.000017	<0.00001	0.084	<0.00001	<0.00001	<0.00001

Table 2. Results from the shape asymmetry mixed-effect model ANOVA, in the different groups (strains x inbreeding categories), showing mean squares of the various terms and interactions, variance decomposition and associated P-values. The results correspond to a nested ANOVA on the Procrustes variables. FA10: Fluctuating asymmetry, DA: directional asymmetry, VAR: inter-individual variance, AS: antisymmetry, AFFA: antisymmetry-filtered fluctuating asymmetry.

Inbreeding and shape asymmetry

Shape FA10 was highest in the NPW, NSR and ML groups (Fig. 8C). Differences between pairs of groups were tested while adjusting for multiple tests ($\alpha = 0.00625$). Differences between inbreeding levels were not significant in the PW strain (all $P > 0.03$). In the SR strain, however, the NSR group had significantly higher FA than the other inbreeding levels (all $P < 0.003$). Furthermore, the MSR group had significantly smaller asymmetry than the HSR group ($P = 0.0011$)

Since most values of shape DA (Fig. 8D) were not significant, we could not compare between them. However, we were able to test for differences between groups in terms of AS and AFFA (Fig. 8E-F). Differences in AFFA were, as with FA10, not significant in the PW strain (all $P>0.1$). In the SR strain, the NSR group had higher AFFA than the LSR and MSR groups (both $P < 0.0001$). AFFA increased in the HSR group compared to the MSR and LSR groups (both $P < 0.002$). Finally, differences in AS were not significant between any of the groups (all $P >0.09$).

Bite force and asymmetry

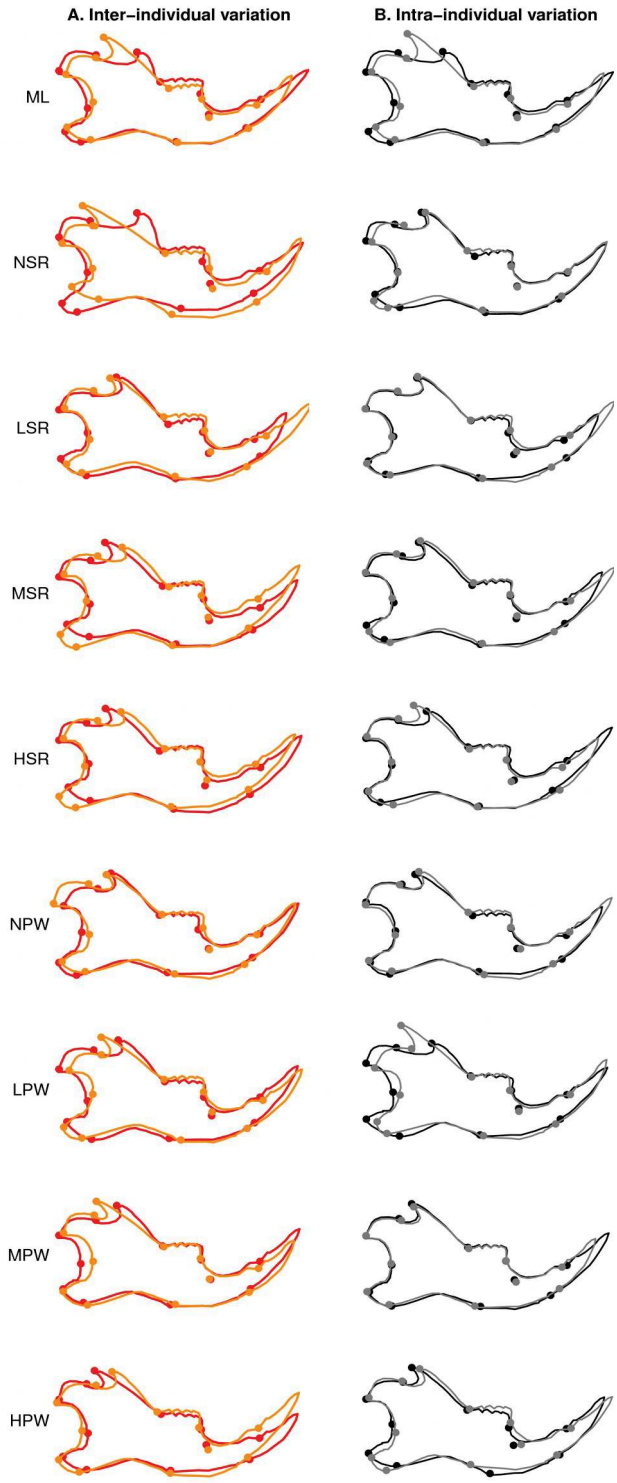

Figure 7. Mandible shape variation in each lineage for each inbreeding level. Abbreviations are the same as in Fig. 6. Inter-individual variation (VAR) is represented by red and orange outlines, while intra-individual variation (FA) is represented by grey and black outlines. Grey outlines and full circles represent shapes associated with the negative values of the first principal component of intra-individual variation, while black outlines and full circles represent shape associated with the maximal values. Orange outlines and full circles represent shapes associated with the negative values of the first principal component of inter-individual variation, while red outlines and full circles represent shape associated with the maximal values. Differences were magnified two times.

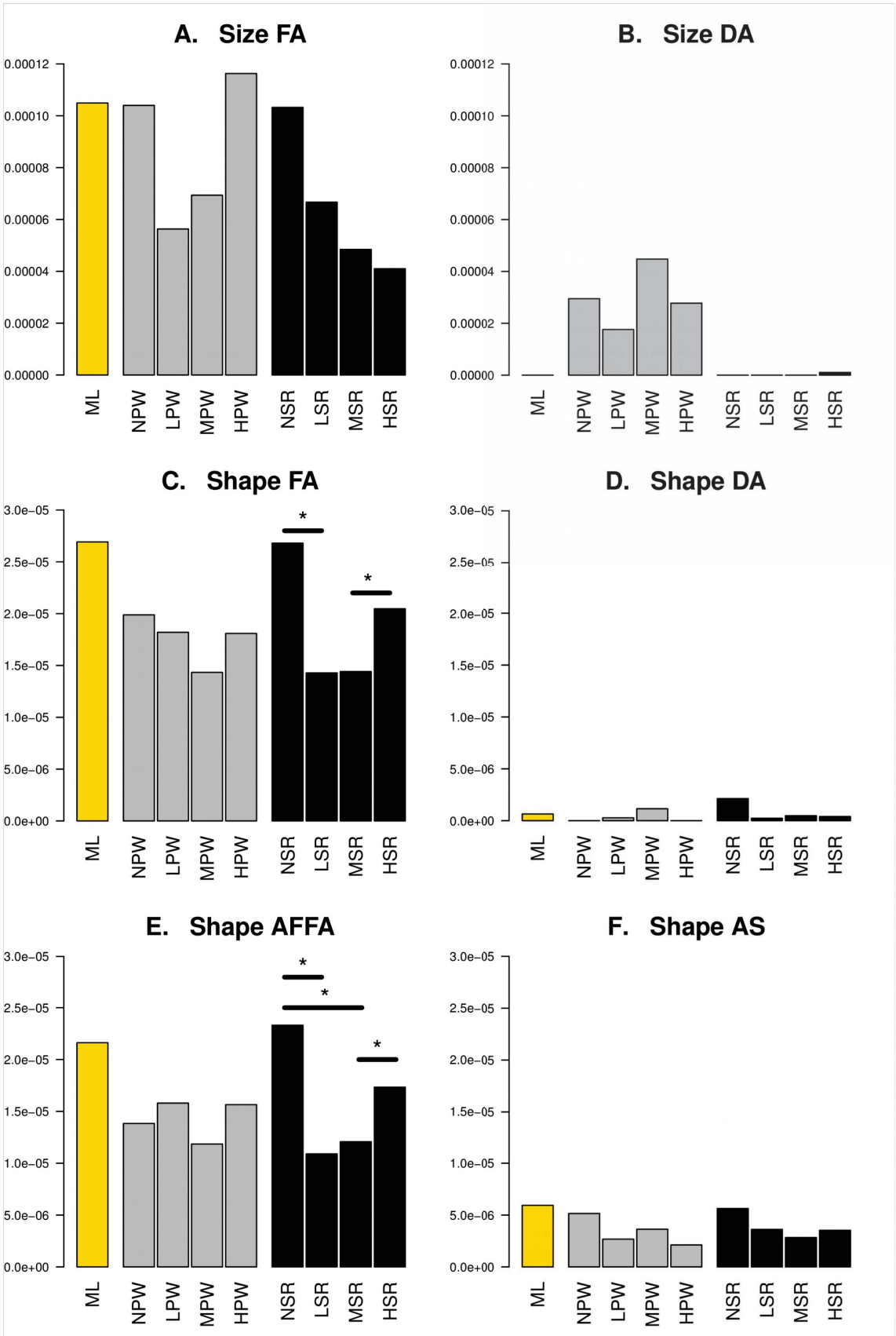

Figure 8. (A-B) Size asymmetry in the inbreeding categories and strains, abbreviations are as in text or in Fig. 6. (A) FA: fluctuating asymmetry (FA10); (B) DA: directional asymmetry. No between-group differences were significant. C-F Shape asymmetry in the different inbreeding categories and strains. (C) FA: fluctuating asymmetry (FA10); (D) DA: directional asymmetry; (E) AFFA: antisymmetry-filtered fluctuating asymmetry; (F) AS: antisymmetry. Each bar represents one of the groups defined in this study. Asterisks denote significant differences after correcting for multiple tests ($P < 0.00625$).

Mean group bite force was uncorrelated with size FA10 (r = 0.179, P = 0.713). Similarly the mean group bite force was not correlated with shape FA10 (r = 0.64, P = 0.139). The high Spearman's rho value was only due to the ML group which had the highest bite force and highest shape FA10. No significant relationship was found with bite force when using AFFA instead of shape FA10 (r = 0.643, P = 0.139). Similarly, we found no link between bite force and AS (r = 0.286, P = 0.556).

Size asymmetry and shape asymmetry

Finally, we found no relationship between size FA10 and shape FA10 (r = 0.25, P = 0.52), nor between size DA and shape DA (r = -0.167, P = 0.678). Because size and shape AS were not assessed in the same way, and because size AS did not appear to be significant, we could not test the correlation between the two.

Size and shape inter-individual variation and inbreeding

Size VAR and shape VAR were significant in all groups (Tables 1 and 2, Fig. 9). Size VAR and shape VAR were uncorrelated (r = 0.367, P = 0.336). Furthermore, between-group differences in VAR were not significant (all P>0.2). The correlations of inbreeding with both size VAR and shape VAR were also not significant (r = -0.593 and -0.339, P = 0.092 and 0.372).

Discussion

Contrary to most previous studies (*e.g.* Herrel et al. 2008, 2010, Ginot et al. 2018), we have shown that bite force was only slightly influenced by size (Fig. 5), which may be explained by the small size variation of our sample due to controlled age and environmental condition. Sexual dimorphism was significant for size, shape and bite force (Fig. 3-4). There was also an influence of the strain and the inbreeding level on morphology (Fig. 4), but generally not on asymmetry (Fig. 8). Bite

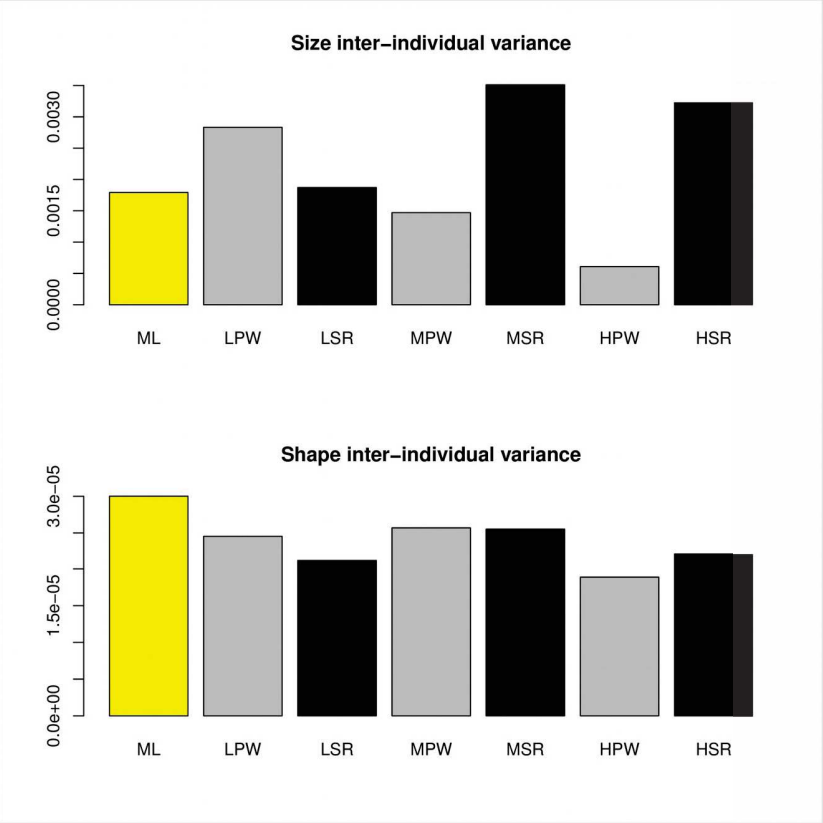

Figure 9. Inter-individual variance values for size and shape depending on the groups. No significant between-group differences were found. Abbreviations are the same as in the text or in Fig. 6.

384 force also increased with inbreeding, in spite of the concomitant size decrease, probably because the
385 relationship between size and bite force is weak in this study. Finally, bite force was neither positively
386 nor negatively correlated with any of the asymmetry measures that we calculated.
387
388 *Sexual dimorphism*
389 We found significant differences in terms of bite force, shape and size between males and
390 females. The latter was rather surprising, since sexual dimorphism in the morphology of the mandible
391 is often not found in the house mouse and wood mouse (*e.g.* Davis 1983, Renaud 2005, Valenzuela-
392 Lamas et al. 2011), or is directly corrected without being explicitly reported (*e.g.* Klingenberg et al.
393 2003, 2004). Yet, significant sexual dimorphism was found in the mandible shape of some laboratory
394 strains (*e.g.* strain C57BL/10 in Renaud et al. 2010, strain C57BL/6J-Chr#$^{PWD/Ph}$/ForeJ in Boell et al.
395 2011). These results and ours suggest either that this is specific to the *M. m. domesticus* subspecies, or

alternatively that in laboratory conditions, where other sources of variation are controlled for, underlying and small sexual dimorphism of the mice may be revealed (both effects being non-mutually exclusive). In our case, the insular origin of the mice population may also be linked to a larger than usual sexual dimorphism. Furthermore, the difference in bite force between males and females was not explained by the mandible size dimorphism, showing that bite force may be under sexual selection in rodents (Herrel et al. 2010, Ginot et al. 2017), although other behavioral causes might also explain this bite force dimorphism (*e.g.* mandible shape differences related to different levels of aggressiveness, Corti & Rohlf 2001). Despite this strong effect on size and shape, we found no significant sex differences within groups for asymmetry, except in one group for DA, and no differences in inter-individual variance.

Inbreeding and asymmetry

Overall, our results do not match with most hypotheses suggested or supported in the literature (Grammer et al. 2003, Siegel & Doyle 1975, Weijs 1975). Inbred mice did not necessarily show higher fluctuating asymmetry (FA), contrary to several previous studies (*e.g.* Hutchison & Cheverud 1995, Lacy & Horner 1996). The more outbred NPW, NSR and ML mice had higher size and shape FA10 than all inbred groups, although not always significantly. This is true not only within strain but also between strains, since we may expect that mice from Mainland (ML), a large island where several localities were sampled, may be originally more outbred than the ones from the small islands South Ronaldsay (SR) and Papa Westray (PW). In any case, FA10 (size or shape) did not show any strong and consistent increase with inbreeding (Fig. 8), since only the HSR group were significantly more asymmetric in shape than the LSR and MSR groups. Even so, the HSR group still had lower asymmetry than the NSR group (more outbred).

Both shape antisymmetry (AS) and antisymmetry-filtered FA (AFFA) were significant in all groups (Tab. 2). Still, the between-group differences in either AS or AFFA were generally not

421 significant (except for AFFA in the SR strain, similar to FA10), and neither AS nor AFFA correlated
422 with inbreeding. Finally, we did not find significant AS for size.

423 The fact that FA10 (or AS / AFFA) in the PW and SR strains is not significantly related to their
424 inbreeding level might be explained in several ways. First, inbreeding may not actually be an important
425 cause of developmental noise in the controlled conditions of the lab, or in natural populations
426 (Hallgrimsson 1998, Badyaev et al. 2000, Armbruster & Reed 2005). Second, one of the mechanisms
427 proposed to explain the correlation between FA and inbreeding is the reduction of the buffering of
428 development against environmental perturbations (Lerner 1954, Hallgrimsson 1998). In that context
429 and since environmental conditions are stable in captivity, the buffering of developmental noise is not
430 decreased by inbreeding. Finally, another explanation may be that the small effects of inbreeding on
431 FA are compensated due to the functional role of the mandible, which is expected to increase
432 phenotypic stability (Siegel & Doyle 1975, Badyaev et al. 2000).

433 Inbreeding also did not affect inter-individual variance significantly, contrary to our
434 expectations (Fowler and Whitlock 1999, Debat et al. 2000). Furthermore, it appeared that there was no
435 link between shape inter-individual variation and shape FA10, nor between size VAR and size FA10.
436 FA10 has been used as a proxy for developmental stability, and VAR as a proxy for canalization (*e.g.*
437 Klingenberg & McIntyre 1998, Debat et al. 2000, Réale and Roff 2003, Breuker et al. 2006). Whether
438 canalization and developmental stability are due to independent biological remains an open debate. In
439 line with the original proposition of Waddington (1942, 1957), several studies have shown at least
440 partial independence of both phenomena (*e.g.* Debat et al. 2000, 2009, Réale and Roff 2003, Milton et
441 al. 2003, Gonzalez et al. 2016), but other authors suggest no distinction between both (*e.g.* Clarke
442 1998, Klingenberg and McIntyre 1998, Breuker et al. 2006); in any case, there is no general agreement
443 and results depend on the studied species and traits. Our results show an absence of relationship
444 between the levels of VAR and FA10, therefore suggesting that patterns of variation at the individual
445 and interindiviudal levels are caused and buffered by independent mechanisms. Yet, the similar patterns

446 of shape variation at the intra- and inter-individual levels (Fig. 7) show that FA and VAR produce
447 morphological variance in the same areas of the mandible. Taken together, these results suggest that,
448 although developmental stability and canalization may act independently (therefore not producing
449 synchronized decreases in FA or VAR), they also may act on the same morphological structures,
450 thereby causing similar morphological results. Indeed, if the least canalized traits (*e.g.* least
451 functionally important traits) are also the least developmentally stable, different levels of FA and VAR
452 may be attained through distinct pathways of canalization and developmental stability, but in both
453 cases, morphology will be affected in the same manner.
454
455 *Inbreeding and bite force*
456 Excluding the NSR and NPW groups for which we had no bite force measurements, increased
457 inbreeding was correlated with increased bite force in the PW and SR strains (Fig. 5). The heritability
458 of performance traits related to fitness is generally expected to be low (Mousseau & Roff 1987), which
459 would not allow important effects of selection on bite force. However, there may be an habituation
460 phenomenon and/or a bias towards mice that adapted better to the lab conditions (which reproduced
461 more) in the later generations and/or physiological changes due to the laboratory diet. Therefore, the
462 observed increase in bite force may reflect better individual condition (despite higher inbreeding and
463 lower centroid size) in later generations (Herrel et al. 2010). Whatever the explanation, this result was
464 to our knowledge the first evidence that an increase in inbreeding does not necessarily entail negative
465 effects in terms of bite force performance.
466
467 *Asymmetry and performance*
468 Our results showed that overall asymmetry is not necessarily linked to lower bite force. This
469 may seem surprising, since previous studies (Swaddle and Witter 1998, Martin and Lopez 2001, Rivera
470 & Claude 2008) generally found diminished performance in more asymmetric animals. However, those

471 studies looked at locomotory characters (turtle shell shape, limb size, wing size), and this type of
472 character directly influences mobility and therefore fitness.

473 The *a priori* relationship between mandible asymmetry and bite force performance appears less
474 straightforward. Studies of the masticatory apparatus, notably in humans, showed that asymmetry is
475 generally the norm (Pirttiniemi & Kantomaa 1992, Pirttiniemi 1998), in response to the lateralization of
476 mastication (Nissan et al. 2004, Zamanlu et al. 2012). In mice, lateralization is known, at least for
477 pawedness (Collins 1991, Collins et al. 1993), but their mastication is generally considered to be
478 symmetrical (Weijs 1975, Weijs & Dantuma 1975). Here, we found significant antisymmetry and
479 directional asymmetry in our mice, however both were much smaller than fluctuating asymmetry,
480 which was also much smaller than inter-individual variance. One notable finding was that the PW
481 strain displayed consistent directional asymmetry in mandible size. These results are coherent with the
482 facts that functional characters should show low asymmetry, and that murine rodents have an overall
483 symmetrical masticatory muscle activity. However, the significant DA and AS found in some cases
484 suggest that, in our mice, there may still be some side preferences or developmental constraints linked
485 to laterality. However, these are apparently very minor and not related to any functional effect.

486 Our results are consistent with those of Vervust et al. (2008), who found no link between
487 asymmetry and bite force. In our case, however, the character studied was directly related to bite force.
488 This brings evidence that, contrary to locomotory characters, mandible asymmetry is not directly linked
489 with bite force performance.

490

491 *Conclusion*

492 The working hypotheses that were listed in the introduction (see also Fig. 1) are generally not
493 supported by our data. 1) We found no significant link between bite force and overall mandible
494 asymmetry. 2) Inbreeding did not decrease inter-individual variance, and did not increase fluctuating
495 asymmetry. 3) Furthermore inbreeding depression did not have a direct negative impact on bite force.

However, some hypotheses were corroborated: 4) Fluctuating asymmetry was rather small in the mandible (*i.e.* twenty times less than inter-individual variance, when averaging shape and size), potentially due to its functional relevance. 5) We found some significant but reduced lateralization, which may indicate some laterality, counterbalanced by the symmetrical masticatory activity of murines. 6) Furthermore, these limited amounts of antisymmetry and directional asymmetry in the mandible did not relate to any functional changes in terms of bite force. Our study constitutes some of the first evidence that bite force performance may not be directly affected by mandible asymmetry (contrary to locomotor characters), or by inbreeding depression.

Acknowledgements

The authors thank Jean-Christophe Auffray, Annie Orth, Josette Catalan, Pascale Chevret, Lionel Hautier, who constituted the fieldwork team to the Orkney Archipelago, where the mice originally came from and Roohollah Siahsarvie who took care of the lab colony until 2014. We are also grateful to Sabrina Renaud for leading the project which allowed to start the colony, and for her important comments on the early versions of the manuscript. Finally, we thank one anonymous reviewer for suggesting several interesting ways to improve the manuscript. This publication is a contribution of the Institut des Sciences de l'Evolution de Montpellier (UMR 5554 – UM2 + CNRS + IRD) No. ISEM XXXX. This study was supported by the ANR project Bigtooth (ANR-11-BSV7-008).

514 **References**

515 Adams, D.C., and E. Otarola-Castillo. 2013. Geomorph: an R package for the collection and
516 analysis of geometric morphometric shape data. Methods in Ecology and Evolution. 4:393-
517 399.

518 Angel, E. H. (1900). Treatment of malocclusion of the teeth and fractures of the maxillae: Angle's
519 system. *SS White Dental Manufacturing Company*.

520 Armbruster, P., & Reed, D. H. (2005). Inbreeding depression in benign and stressful
521 environments. *Heredity*, *95*(3), 235-242.

522 Badyaev, A. V., Foresman, K. R., Fernandez M. V. (2000). Stress and developmental stability :
523 vegetation removal causes increased fluctuating asymmetry in shrews. *Ecology*, 81(2), 336-
524 345.

525 Ballard, M. L. (1944). Asymmetry in tooth size: a factor in the etiology, diagnosis and treatment of
526 malocclusion. *The Angle Orthodontist*, *14*(3), 67-70.

527 Boell, L., Gregorova, S., Forejt, J., & Tautz, D. (2011). A comparative assessment of mandible
528 shape in a consomic strain panel of the house mouse (*Mus musculus*)-implications for
529 epistasis and evolvability of quantitative traits. *BMC evolutionary biology*, *11*(1), 309.

530 Bresin, A., Kiliaridis, S., & Strid, K. G. (1999). Effect of masticatory function on the internal bone
531 structure in the mandible of the growing rat. *European journal of oral sciences*, *107*(1), 35- 44.

532 Breuker, C. J., Patterson, J. S., & Klingenberg, C. P. (2006). A single basis for developmental
533 buffering of Drosophila wing shape. *PLoS one*, *1*(1), e7.

534 Clarke, G. M., Brand, G. W., & Whitten, M. J. (1986). Fluctuating asymmetry: a technique for
535 measuring developmental stress caused by inbreeding. *Australian Journal of Biological*
536 *Sciences*, *39*(2), 145-154.

537 Clarke, G. M. (1998). The genetic basis of developmental stability. V. Inter-and intra-individual
538 character variation. *Heredity*, *80*(5), 562-567.

539 Claude, J. (2008). *Morphometrics with R*. Springer Science & Business Media, New York.
540 Collins, R. L. (1991). Reimpressed selective breeding for lateralization of handedness in
541 mice. *Brain research*, *564*(2), 194-202.
542 Collins, R. L., Sargent, E. E., & Neumann, P. E. (1993). Genetic and behavioral tests of the McManus
543 hypothesis relating response to selection for lateralization of handedness in mice to degree of
544 heterozygosity. *Behavior genetics*, *23*(4), 413-421.
545 Coster, A. (2013). pedigree: Pedigree functions. R package version 1.4. https://CRAN.R-
546 project.org/package=pedigree
547 Davis, S. J. (1983). Morphometric variation of populations of house mice *Mus domesticus* in
548 Britain and Faroe. *Journal of Zoology*, *199*(4), 521-534.
549 Debat, V., Alibert, P., David, P., Paradis, E., & Auffray, J. C. (2000). Independence between
550 developmental stability and canalization in the skull of the house mouse. *Proceedings of the*
551 *Royal Society of London B: Biological Sciences*, *267*(1442), 423-430.
552 Debat, V., Debelle, A., & Dworkin, I. (2009). Plasticity, canalization, and developmental stability of
553 the *Drosophila* wing: joint effects of mutations and developmental
554 temperature. *Evolution*, *63*(11), 2864-2876.
555 Fahlke, J. M., Gingerich, P. D., Welsh, R. C., & Wood, A. R. (2011). Cranial asymmetry in Eocene
556 archaeocete whales and the evolution of directional hearing in water. *Proceedings of the*
557 *National Academy of Sciences*, *108*(35), 14545-14548.
558 Fowler, K. & Whitlock, M. C. (1999). The distribution of phenotypic variance with inbreeding.
559 *Evolution*, 1143-1156.
560 Freeman, P. W., & Lemen, C. A. (2008). A simple morphological predictor of bite force in
561 rodents. *Journal of Zoology*, *275*(4), 418-422.

562 Ginot, S., Claude, J., Perez, J. & Veyrunes, F. (2017). Sex-reversal induces size and performance
563 differences among females of the African pygmy mouse *Mus minutoides*. *Journal of*
564 *Experimental Biology (in press).*
565 Gonzalez, P. N., Lotto, F. P., & Hallgrímsson, B. (2014). Canalization and developmental instability
566 of the fetal skull in a mouse model of maternal nutritional stress. *American journal of*
567 *physical anthropology*, *154*(4), 544-553.
568 Gonzalez, P. N., Pavlicev, M., Mitteroecker, P., Pardo-Manuel de Villena, F., Spritz, R. A., Marcucio,
569 R. S., & Hallgrímsson, B. (2016). Genetic structure of phenotypic robustness in the
570 collaborative cross mouse diallel panel. *Journal of evolutionary biology*, *29*(9), 1737-1751.
571 Grammer, K., Fink, B., Moller, A.P. and Thornhill, R. (2003). Darwinian aesthetics: sexual selection
572 and the biology of beauty. *Biological Reviews*, 78, 385-407.
573 Hallgrímsson, B. (1998). Fluctuating asymmetry in the mammalian skeleton. In *Evolutionary*
574 *biology* (pp. 187-251). Springer US.
575 Herrel, A., Spithoven, L., Van Damme, R., & De Vree, F. (1999). Sexual dimorphism of head size in
576 *Gallotia galloti*: testing the niche divergence hypothesis by functional analyses. *Functional*
577 *Ecology*, 13(3), 289-297.
578 Herrel, A., De Smet, A., Aguirre, L. F., & Aerts, P. (2008). Morphological and mechanical
579 determinants of bite force in bats: do muscles matter? *Journal of Experimental*
580 *Biology*, *211*(1), 86-91.
581 Herrel, A., Moore, J. A., Bredeweg, E. M., & Nelson, N. J. (2010). Sexual dimorphism, body size, bite
582 force and male mating success in tuatara. *Biological Journal of the Linnean Society*, *100*(2),
583 287-292.
584 Herrel, A., Podos, J., Huber, S. K., & Hendry, A. P. (2005). Bite performance and morphology in a
585 population of Darwin's finches: implications for the evolution of beak shape. *Functional*
586 *Ecology*, *19*(1), 43-48.

587 Husak, J. F., Kristopher Lappin, A., Fox, S. F., & Lemos-Espinal, J. A. (2006). Bite-force
588 performance predicts dominance in male venerable collared lizards (*Crotaphytus*
589 *antiquus*). *Copeia*, *2006*(2), 301-306.
590 Hutchison, D. W., & Cheverud, J. M. (1995). Fluctuating asymmetry in tamarin (*Saguinus*) cranial
591 morphology: intra-and interspecific comparisons between taxa with varying levels of genetic
592 heterozygosity. *Journal of Heredity*, *86*(4), 280-288.
593 Kark, S. (2001). Shifts in bilateral asymmetry within a distribution range: the case of the chukar
594 partridge. *Evolution, 55(10)*, 2088-2096.
595 Kiliaridis, S., Bresin, A., Holm, J., & Strid, K. G. (1996). Effects of masticatory muscle function on
596 bone mass in the mandible of the growing rat. *Cells Tissues Organs*, *155*(3), 200-205.
597 Klingenberg, C. P., & McIntyre, G. S. (1998). Geometric morphometrics of developmental instability:
598 analyzing patterns of fluctuating asymmetry with Procrustes methods. *Evolution*, 1363-1375.
599 Klingenberg, C. P., Mebus, K., & Auffray, J. C. (2003). Developmental integration in a complex
600 morphological structure: how distinct are the modules in the mouse mandible?. *Evolution &*
601 *development*, *5*(5), 522-531.
602 Klingenberg, C. P., Leamy, L. J., & Cheverud, J. M. (2004). Integration and modularity of
603 quantitative trait locus effects on geometric shape in the mouse mandible. *Genetics*, *166*(4),
604 1909-1921.
605 Kobyliansky, E., & Livshits, G. (1989). Age-dependent changes in morphometric and biochemical
606 traits. *Annals of Human Biology*, *16*(3), 237-247.
607 Kruuk, L. E. B., Slate, J., Pemberton, J. M., & Clutton-Brock, T. H. (2003). Fluctuating asymmetry
608 in a secondary sexual trait: no associations with individual fitness, environmental stress or
609 inbreeding, and no heritability. *Journal of Evolutionary Biology*, *16*(1), 101-113.
610 Lacy, R. C., & Honer, B. E. (1996). Effects of inbreeding on skeletal development of R*attus*
611 *villosissimus*. *Journal of Heredity*, *87*(4), 277-287.

612 Lerner, I. M. (1954). Genetic homeostasis. *Genetic homeostasis.*

613 Levinton, J. S., Judge, M. L., & Kurdziel, J. P. (1995). Functional differences between the major and
614 minor claws of fiddler crabs (*Uca*, family Ocypodidae, Order Decapoda, Subphylum
615 Crustacea): A result of selection or developmental constraint?. *Journal of Experimental Marine*
616 *Biology and Ecology*, *193*(1-2), 147-160.

617 Logue, S. F., Owen, E. H., Rasmussen, D. L., & Wehner, J. M. (1997). Assessment of locomotor
618 activity, acoustic and tactile startle, and prepulse inhibition of startle in inbred mouse strains
619 and F1 hybrids: implications of genetic background for single gene and quantitative trait loci
620 analyses. *Neuroscience*, *80*(4), 1075-1086.

621 MacLeod, C. D., Reidenberg, J. S., Weller, M., Santos, M. B., Herman, J., Goold, J., & Pierce, G. J.
622 (2007). Breaking symmetry: The marine environment, prey size, and the evolution of
623 asymmetry in cetacean skulls. *The Anatomical Record*, *290*(6), 539-545.

624 Martín, J., & López, P. (2001). Hindlimb asymmetry reduces escape performance in the lizard
625 *Psammodromus algirus*. *Physiological and Biochemical Zoology*, *74*(5), 619-624.

626 McCarroll, R. S., Naeije, M., & Hansson, T. L. (1989). Balance in masticatory muscle activity
627 during natural chewing and submaximal clenching. *Journal of oral rehabilitation*, *16*(5),
628 441-446.

629 Milton, C. C., Huynh, B., Batterham, P., Rutherford, S. L., & Hoffmann, A. A. (2003). Quantitative
630 trait symmetry independent of Hsp90 buffering: distinct modes of genetic canalization and
631 developmental stability. *Proceedings of the National Academy of Sciences*, *100*(23), 13396-
632 13401.

633 Møller, A. P. (1994). Directional selection on directional asymmetry: testes size and secondary
634 sexual characters in birds. *Proceedings of the Royal Society of London B: Biological*
635 *Sciences*, *258*(1352), 147-151.

636 Møller, A. P., & Pomiankowski, A. (1993). Fluctuating asymmetry and sexual
637 selection. *Genetica*, *89*(1-3), 267.
638 Morgan, K. N., & Tromborg, C. T. (2007). Sources of stress in captivity. *Applied animal behaviour*
639 *science*, *102*(3), 262-302.
640 Mousseau, T. A., & Roff, D. A. (1987). Natural selection and the heritability of fitness
641 components. *Heredity*, *59*(Pt 2), 181-197.
642 Naeije, M., McCarroll, R. S., & Weijs, W. A. (1989). Electromyographic activity of the human
643 masticatory muscles during submaximal clenching in the inter-cuspal position. *Journal of*
644 *oral rehabilitation*, *16*(1), 63-70.
645 Nissan, J., Gross, M. D., Shifman, A., Tzadok, L., & Assif, D. (2004). Chewing side preference as a
646 type of hemispheric laterality. *Journal of oral rehabilitation*, *31*(5), 412-416.
647 Palmer, A. R. (1994). Fluctuating asymmetry analyses: a primer. In *Developmental instability: its*
648 *origins and evolutionary implications* (pp. 335-364). Springer Netherlands.
649 Palmer, A. R. (1999). Detecting publication bias in meta-analyses: a case study of fluctuating
650 asymmetry and sexual selection. *The American Naturalist*, *154*(2), 220-233.
651 Pirttiniemi, P., & Kantomaa, T. (1992). Relation of glenoid fossa morphology to mandibulofacial
652 asymmetry, studied in dry human Lapp skulls. *Acta Odontologica Scandinavica*, *50*(4), 235-
653 243.
654 Pirttiniemi, P. (1998). Normal and increased functional asymmetries in the craniofacial area. *Acta*
655 *Odontologica Scandinavica*, *56*(6), 342-345.
656 R Core Team (2017). R: A language and environment for statistical computing. R Foundation for
657 Statistical Computing, Vienna, Austria. URL https://www.R-project.org/.
658 Réale, D., & Roff, D. A. (2003). Inbreeding, developmental stability, and canalization in the sand
659 cricket *Gryllus firmus*. *Evolution*, *57*(3), 597-605.

660 Renaud, S. (2005). First upper molar and mandible shape of wood mice (*Apodemus sylvaticus)*
661 from northern Germany: ageing, habitat and insularity. *Mammalian Biology-Zeitschrift für*
662 *Säugetierkunde*, *70*(3), 157-170.
663 Renaud, S., Auffray, J.-C., de La Porte, S., 2010. Epigenetic effects on the mouse mandible: common
664 features and discrepancies in remodeling due to muscular dystrophy and response to food
665 consistency. BMC Evolutionary Biology 10, 28.
666 Rivera, G., & Claude, J. (2008). Environmental media and shape asymmetry: a case study on turtle
667 shells. *Biological Journal of the Linnean Society*, *94*(3), 483-489.
668 Rohlf, F. J. (2010). tpsDig v2. 16. *Department of Ecology and Evolution, State University of New*
669 *York, Stony Brook, New York*.
670 Rovira-Lastra, B., Flores-Orozco, E. I., Salsench, J., Peraire, M., & Martinez-Gomis, J. (2014). Is the
671 side with the best masticatory performance selected for chewing? *Archives of oral*
672 *biology*, *59*(12), 1316-1320.
673 Siegel, M. I., & Doyle, W. J. (1975). Stress and fluctuating limb asymmetry in various species of
674 rodents. *Growth*, *39*(3), 363-369.
675 Sumner, F. B., & Huestis, R. R. (1921). Bilateral asymmetry and its relation to certain problems of
676 genetics. *Genetics*, *6*(5), 445.
677 Swaddle, J. P., Witter, M. S., & Cuthill, I. C. (1994). The analysis of fluctuating asymmetry. *Animal*
678 *Behaviour*, *48*(4), 986-989.
679 Swaddle, J. P., & Witter, M. S. (1998). Cluttered habitats reduce wing asymmetry and increase
680 flight performance in European starlings. *Behavioral Ecology and Sociobiology*, *42*(4), 281-
681 287.
682 Tang, X., Orchard, S. M., & Sanford, L. D. (2002). Home cage activity and behavioral performance
683 in inbred and hybrid mice. *Behavioural brain research,136*(2), 555-569.

Valenzuela-Lamas, S., Baylac, M., Cucchi, T., Vigne, J.-D., 2011. House mouse dispersal in Iron Age Spain: a geometric morphometrics appraisal. Biological Journal of the Linnean Society 102, 483-497.

Van der Bilt, A., Tekamp, A., van der Glas, H., Abbink, J. (2008). Bite force and electromyography during maximum unilateral and bilateral clenching. *European Journal of Oral Sciences, 116,* 217:222

Van Dongen, S., Lens, L., Molenberghs, G. (1999). Mixture analysis of asymmetry: modelling directional asymmetry, antisymmetry and heterogeneity in fluctuating asymmetry. *Ecology Letters*, *2*, 387-396.

Van Valen, L. (1962). A study of fluctuating asymmetry. *Evolution*, 125-142.

Vervust, B., Van Dongen, S., Grbac, I., & Van Damme, R. (2008). Fluctuating asymmetry, physiological performance, and stress in island populations of the Italian Wall Lizard (*Podarcis sicula*). *Journal of Herpetology*, *42*(2), 369-377.

Verwaijen, D., Van Damme, R., & Herrel, A. (2002). Relationships between head size, bite force, prey handling efficiency and diet in two sympatric lacertid lizards. *Functional Ecology*, *16*(6), 842-850.

Waddington, C. H. (1942). Canalization of development and the inheritance of acquired characters. *Nature*, *150*(3811), 563-565

Waddington, C. H. (1957). The strategy of the genes. A discussion of some aspects of theoretical biology. With an appendix by H. Kacser. *The strategy of the genes. A discussion of some aspects of theoretical biology. With an appendix by H. Kacser.*.

Weijs, W. A. (1975). Mandibular movements of the albino rat during feeding. *Journal of morphology*, *145*(1), 107-124.

Weijs, W. A., & Dantuma, R. (1975). Electromyography and mechanics of mastication in the albino rat. *Journal of Morphology*, *146*(1), 1-33.

709 Woo, T. L. (1931). On the asymmetry of the human skull. *Biometrika*, 324-352.
710 Zamanlu, M., Khamnei, S., SalariLak, S., Oskoee, S. S., Shakouri, S. K., Houshyar, Y., Salekzamani, Y.
711 (2012). Chewing side preference in first and all mastication cycles for hard and soft
712 morsels. *International journal of clinical and experimental medicine*, *5*(4), 326.
713
714 **Figure legends**
715 **Figure 1.** Schematic representation of the relationships tested in the present study. Blue lines
716 correspond to relationships expected to be negative, and orange lines to relationships expected to be
717 positive. Dotted lines show related factors that may have opposite effects.
718 **Figure 2.** A mouse mandible drawing with the twelve landmarks used in this study.
719 **Figure 3.** Sexual dimorphism in mandible bite force (A) and centroid size (B). In both cases males
720 display significantly higher mean values (both $P<0.0001$ on 218 and 232 df respectively). Whiskers
721 represent 1.5 times the interquartile distance, when outliers (circles) are present. If there are no outliers,
722 whiskers represent the maximal and minimal values.
723 **Figure 4.** CVA of mandible shape variation with strain, sexes and inbreeding level as grouping factors.
724 (A) Represents the first two axes of the analysis, with morphological changes associated with positive
725 (black) and negative (red) values of the axes. (B) Shows axes 2 and 3 of the same analysis, also with
726 morphological changes associated with the axes. Abbreviations : HIGH, highly inbred ; LOW, slightly
727 inbred ; MID, intermediately inbred ; NO, outbred ; F, female ; M, male ; ML, mainland ; PW, Papa
728 Westray ; SR, South Ronaldsay.
729 **Figure 5.** (A) Bite force (Newton) plotted against centroid size. Yellow squares represent the ML mice,
730 the gray triangles are the PW mice, and the black circles are the SR mice. Full symbols represent
731 females, empty symbols represent males. Only the male SR mice showed a significant positive
732 correlation ($P < 0.05$), materialized by the black dashed regression line. (B) Bite force plotted against
733 the inbreeding coefficient. There was a significant positive correlation for the SR males (black dashed

734 line), SR females (black solid line) and PW females (gray solid line) (all $P < 0.05$). (C) Centroid size
735 plotted against the inbreeding coefficient. There was a significant negative correlation for SR females
736 (black solid line), SR males (black dashed line) and PW males (gray dashed line) (all $P < 0.05$).
737 **Figure 6.** Distributions of Right-Left (R-L) differences in mandible centroid size. Yellow bars are for
738 the ML mice (A), gray bars (upper row) are for the PW mice (B-E) and dark gray bars (bottom row) are
739 for SR mice (F-I). No distribution differed from normality, which supported the absence of
740 antisymmetry. However, the LPW, MPW and HPW groups (C-E) had significant directional
741 asymmetry, visible by a shift of their distributions to the right. Abbreviations are the same as in text:
742 ML, Mainland (outbred); NPW, non-inbred PW; LPW, low-inbreeding PW; MPW, intermediate-
743 inbreeding PW; HPW, high-inbreeding PW; NSR, non-inbred SR; LSR, low-inbreeding SR; MSR,
744 intermediate-inbreeding SR; HSR, high-inbreeding SR.
745 **Figure 7.** Mandible shape variation in each lineage for each inbreeding level. Abbreviations are the
746 same as in Fig. 6. Inter-individual variation (VAR) is represented by red and orange outlines, while
747 intra-individual variation (FA) is represented by grey and black outlines. Grey outlines and full circles
748 represent shapes associated with the negative values of the first principal component of intra-individual
749 variation, while black outlines and full circles represent shape associated with the maximal values.
750 Orange outlines and full circles represent shapes associated with the negative values of the first
751 principal component of inter-individual variation, while red outlines and full circles represent shape
752 associated with the maximal values. Differences were magnified two times.
753 **Figure 8.** (A-B) Size asymmetry in the inbreeding categories and strains, abbreviations are as in text or
754 in Fig. 6. (A) FA: fluctuating asymmetry (FA10); (B) DA: directional asymmetry. No between-group
755 differences were significant. C-F Shape asymmetry in the different inbreeding categories and strains.
756 (C) FA: fluctuating asymmetry (FA10); (D) DA: directional asymmetry; (E) AFFA: antisymmetry-
757 filtered fluctuating asymmetry; (F) AS: antisymmetry. Each bar represents one of the groups defined in
758 this study. Asterisks denote significant differences after correcting for multiple tests ($P < 0.00625$).

Figure 9. Inter-individual variance values for size and shape depending on the groups. No significant between-group differences were found. Abbreviations are the same as in the text or in Fig. 6.

Supp. Mat. Fig. 1. Shape asymmetry differences between sexes in the different groups of this study.

Table legends

Table 1. Results from the size asymmetry mixed-effect model ANOVA, in the different groups (strains x inbreeding categories), showing mean squares of the various terms and interactions, variance decomposition and associated P-values. FA10: Fluctuating asymmetry, DA: directional asymmetry, VAR: inter-individual variance.

768 **Table 2.** Results from the shape asymmetry mixed-effect model ANOVA, in the different groups
769 (strains x inbreeding categories), showing mean squares of the various terms and interactions, variance
770 decomposition and associated P-values . The results correspond to a nested ANOVA on the Procrustes
771 variables. FA10: Fluctuating asymmetry, DA: directional asymmetry, VAR: inter-individual variance,
772 AS: antisymmetry, AFFA: antisymmetry-filtered fluctuating asymmetry.

773

774

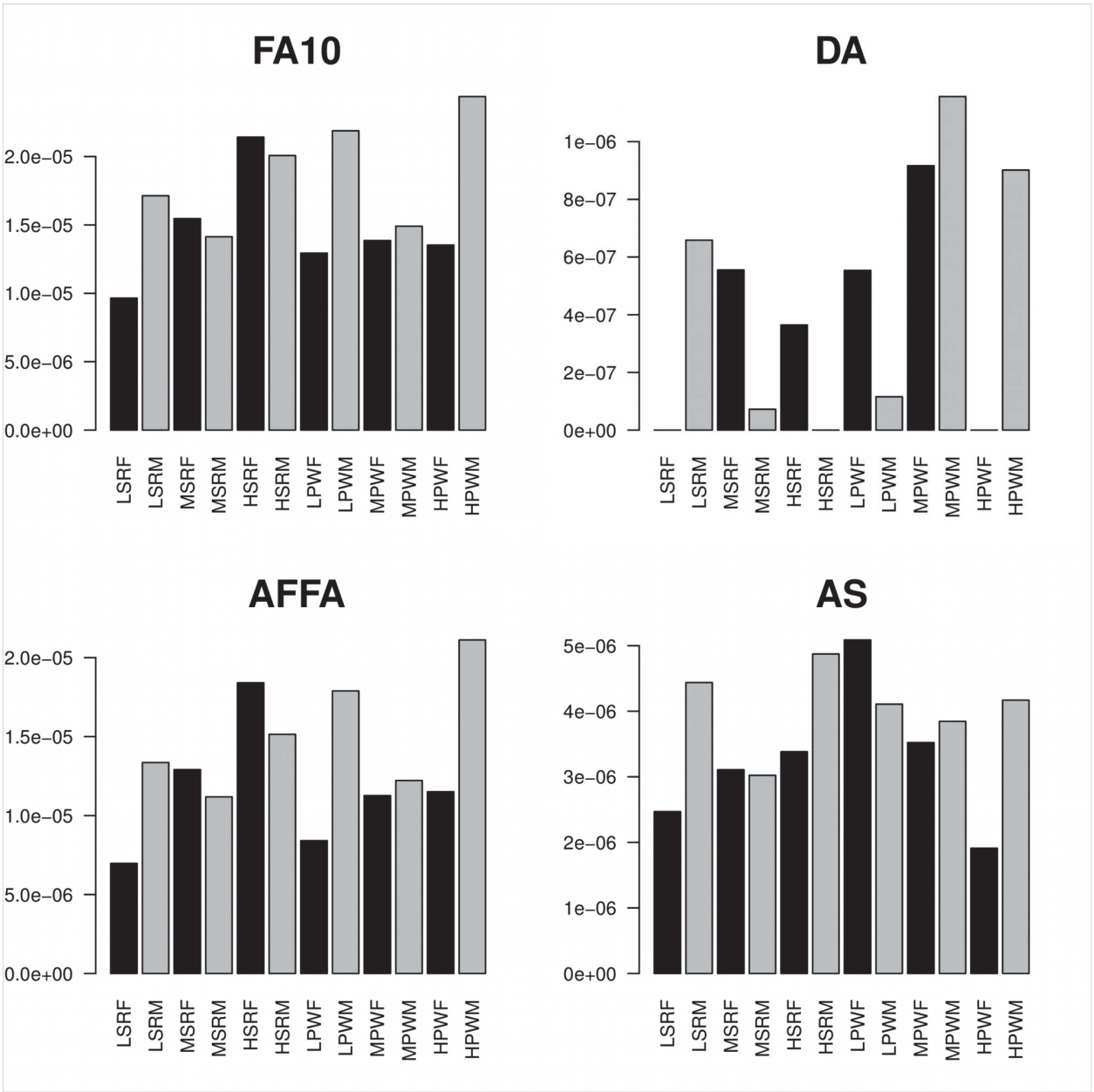

Supplementary figure 1. Shape asymmetry differences between sexes in the different groups of this study. Group names abbreviations are the same as in text and Fig. 6, ending with M (male) or F (female) depending on the sex.

2.3 – Génétique quantitative de la morphologie cranio-mandibulaire et de la force de morsure chez la souris domestique (article en préparation pour être soumis dans *Evolution*).

Les précédentes sections de la partie 1 et 2 ont confirmé le lien entre variation morphologique et performance. En revanche, ces résultats suggèrent également une influence indirecte de la génétique sur la performance, via les changements morphologiques qu'elle produit. Pour tester cette hypothèse de manière plus directe, la génétique quantitative peut être utilisée. En se basant sur la ressemblance phénotypique entre des individus apparentés au sein d'un pedigree connu, elle permet d'estimer la part de variation phénotypique observée expliquée par des effets génétiques additifs, c'est à dire l'héritabilité des caractères. Celle-ci permet à la fois de mieux délimiter l'influence du génome sur la variation d'un trait, mais elle permet en plus de déduire dans quelle mesure la sélection peut influencer l'évolution du trait sur plusieurs générations. Plus un trait sera variable et héritable, plus la sélection modifiera la trajectoire évolutive de la population.

Dans cette partie, en se basant sur un élevage en croisements "frères-demi-frères", les héritabilités de caractères morphologiques du crâne et de la mandibule, ainsi que celle de la force de morsure ont été calculées. De plus, les corrélations génétiques entre ces caractères ont également pu être calculées dans le but initial de déterminer le rôle de la morphologie dans la variation génétique de la performance.

Morphology and bite force heritabilies in a wild, outbred strain of *Mus musculus*.

Samuel Ginot[1,2], Sylvie Agret[1], Julien Claude[1]

[1] Institut des Sciences de l'Evolution, Université de Montpellier, Montpellier, France.

[2] Institut de Génomique Fonctionnelle de Lyon, ENS Lyon, Lyon, France.

Abstract

Skull morphology, in particular size, and *in vivo* bite force performance are correlated in several groups, including rodents. However, at the intraspecific level, some discrepencies in this relationship remain, suggesting that non-morphological factors influence performance. Quantitative genetic studies have shown that morphology and size are heritable characters. Conversely, fitness-related traits have been shown to have low heritabilities. Here, we aimed at verifying the link between morphology and bite force, and assessing if some variation of these traits was due to additive genetic (heritable) effects. To do so, we used a half-sib design in a colony of outbred lab mice derived from wild ancestors. Using parent-offspring regressions and mixed effect models, we found that bite force was not heritable. Morphology and size presented various levels of heritable variation. The most heritable traits were the out-levers of the mandible. Since bite force was not heritable, but correlated with morphology, our results suggest that morphological evolution drives the evolution of bite force. At the interspecific level, it appears that the lever arms of the mandible are often linked to adaptive changes, suggesting that they may represent evolutionary paths of least resistance, allowing functional changes despite the low performance heritability.

Key words : Quantitative genetics ; performance ; Rodentia ; geometric morphometrics ; half-sib design.

Introduction

Several studies (Aguirre et al. 2002, Herrel et al. 2008, Freeman & Lemen 2008, Van Daele et al. 2008, Becerra et al. 2011) showed that bite force and morphology are linked at both inter- and intraspecific levels. Size (or body mass) and head dimensions are generally the main explanatory variable of bite force. Yet, the relationship between morphology and performance can be less clear at the intra-specific level (e.g. Herrel et al. 2005, Van Daele et al. 2008, Becerra et al. 2011, Ginot et al. 2017), as it shows lower predictive power (in particular residual variation in bite force remains high in these cases). This is especially true when looking only at one age cohort in a population (Van Daele et al. 2008, Becerra et al. 2011, Ginot et al. 2017). These results suggest that bite force is a multi-factorial trait, and that intraspecific variation in bite force is not only due to changes in morphology.

Furthermore, quantitative genetic studies in the wild or in controlled conditions tend to show that morphological traits are more heritable than fitness-related traits (e.g. life-history, behavioural, performance traits ; Mousseau & Roff 1987, Houle 1992, Hoffman et al. 2016). As a performance trait, bite force can bridge morphology and fitness, as proposed by Arnold (1983). The low heritability of fitness-related traits is often explained through a common interpretation of Fisher's (1958) theorem of natural selection, which states that fitness-related traits will have lower additive genetic variance due to increased selection (Mousseau & Roff 1987). However, Houle (1992) also proposed that low heritabilities in fitness-related traits might be due to larger amounts of non additive genetic and environmental variation compared to morphological traits. These two views have different evolutionary implication because a trait with low additive genetic variance will be less easily evolvable than one with high additive genetic variance (Houle 1992, Hoffman et al. 2016). Therefore, Houle (1992) proposed that quantitative genetics studies should always report the partitioning of variance of a trait between the additive genetic and other effects rather than to report only the heritability.

On the other side of the spectrum, morpho-functional studies generally aim to link

morphological variation with performance (endurance, speed, bite force) and therefore tend to try to partly resolve the equation between the phenotype and fitness (e.g. Herrel et al. 2005, Van Daele et al. 2008, Becerra et al. 2011, Ginot et al. 2017, Aerts et al. 2000, Vanhooydonck & Van Damme 2001). However, these studies are rarely associated to quantitative genetic analyses. Since morphology, function and performance are related, using quantitative genetic approaches may help reconcile their aforementioned differential heritabilities, and at the same time better understand their co-evolution. This study therefore has several objectives: i) identifying the morphological characters that relate to bite force in our population of lab mice; ii) quantifying the importance of the additive genetic variation in *in vivo* bite force and skull morphology (size and shape); iii) proposing hypotheses regarding the co-evolution of characters having different heritabilities by comparing intra and interspecific patterns of morphological variation.

Materials and Methods

Specimens

All mice (*Mus musculus*) used in this study are from a colony of mice bred in the lab from wild ancestors captured on Mainland, the biggest of the Orkney Islands (Scotland). A half-sib design in which each father was bred with three different and unrelated females was realized. In total, we used 18 fathers that reproduced with 54 mothers, and gave birth to 336 offspring. Litter sizes varied among families from 3 to 10 pups, with a mean of 6.2 pups.

Bite force measurements

Bite force measurements were performed when the offspring were 68 days old. All *in vivo* bite force data were recorded at the incisors using a Kistler force transducer linked to a charge amplifier,

similar to the set-up presented in Herrel et al. (1999) and Aguirre et al. (2002). We performed three consecutive trials for each animal. The maximal bite force recorded across the three trials was retained and used in subsequent analyses. The mice were then euthanized by CO2 inhalation. We also measured the parents' bite force in the same fashion, although their age varied.

Morphometric data

Using the software TPSDig2.0 (Rohlf 2010), 24 landmarks were digitized on the crania of the parents and offsprings in palatal view, and 16 landmarks on the mandibles in lateral view (Fig. 1). All coordinates data were imported in R (R Core Team 2017) and the shapes were centered and superimposed using functions from Claude (2008). We also computed centroid sizes for the mandibles and crania.

In addition to these geometric morphometric data, we also used our landmarks to calculate univariate functional distances on the mandible (Fig. 1B). These traits represent in-levers lengths for three of the adductor muscles (temporal, deep masseter, and superficial masseter), and out-lever lengths at the molar and incisor. Using these lengths, we calculated the mechanical advantage (MA) for the various levers for each individual as MA = In-lever length / Out-lever length (Radinsky 1981).

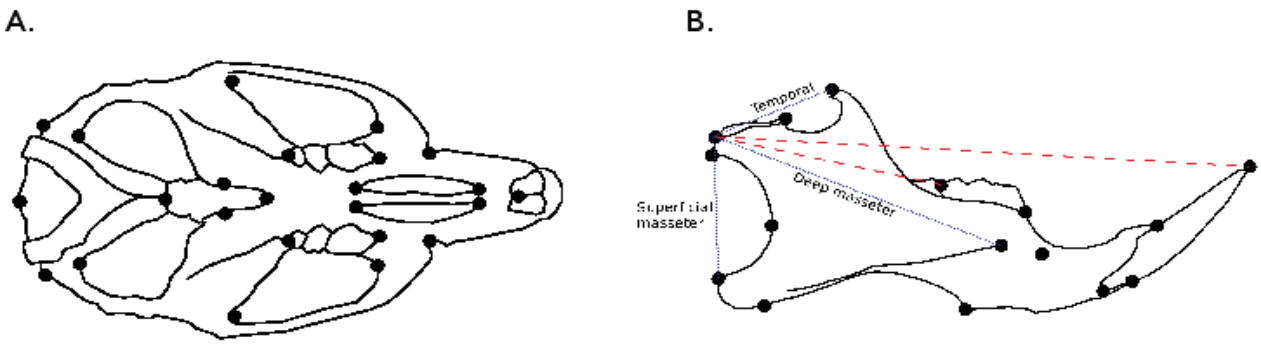

Figure 1. Landmarks used in this study on the A) cranium and B) mandible, also showing in levers (blue lines) and out levers (red lines) measured.

A PCA was applied on the shape data of offsprings only, and null PCs due to the Procrustes fit were dropped prior to performing a MANOVA between shape data and bite force. We predicted shape change due to bite force via that multivariate linear model.

Quantitative genetic analyses

Using *in vivo* bite force and selected univariate morphometric measurements (centroid sizes, inlever and outlever lengths, mechanical advantages), we calculated parent-offspring regressions for the mother and father separately. This allowed us to get a first estimate of heritability (h^2 = 2*slope). Parent-offspring regressions suffer from several biases, notably because the parents are of variable ages, and do not allow to easily partition the variance between additive genetic vs. other effects. To do this, we used a mixed effect model, with the 'lmer' function from package lme4 in R (Bates et al. 2015). This allowed us to partition the phenotypic variance of our traits into the additive genetic effects (Va), and mother, dominance, epistatic, common environment effects, and error (Vd+Ve) . We then calculated heritability as follows: $h^2 = \frac{4 * Va}{Va + Vd + Ve}$ (Falconer and Mackay 1996)

We also calculated the evolvability of the same traits as: $I_A = \frac{Va}{\bar{X}^2}$ (Houle 1992), where X bar is the mean of the trait studied.

Using nested MANOVAs corrected for litter unbalance, we computed the additive genetic variance-covariance matrices (G-matrices) of shape (cranium and mandible), sizes, and bite force data. From these matrices, we were able to compute the genetic correlation between sizes, shapes and bite force using the RV-coefficient (Robert & Escouffier 1976, Claude 2008) to estimate the genetic links between them.

Results

Correlations between bite force and morphology

Bite force is correlated with centroid size as well as shape of both the mandible and the cranium (Fig. 2A and 2B). Some lever-arms and mechanical advantages of the mandible are also correlated with bite force. These are the in-lever of the superficial masseter, the mechanical advantages for the superficial masseter/incisor, the temporal/incisor, and the temporal/molar levers, and the incisor and molar out-levers (Fig. 2B). As for the PC axes, the most functionally determined ones are the PC1, linked with the development of the coronoid process, the PC4 correlated with all lever measurements and the PC5 and PC6, both linked to the superficial masseter and deep masseter levers. Shape variation significantly associated with bite force is shown on Fig. 3A and 3B.

From these results, we selected traits for which we wanted to partition variance and compute heritability and genetic correlation: bite force, centroid size (cranium and mandible), superficial masseter in-lever length, superficial masseter/incisor mechanical advantage, temporal/incisor mechanical advantage, and out-lever lengths (molar and incisor).

Parent-offspring regressions

Parent-offspring regressions for the selected characters (Fig. 4) revealed differences between father and mother regressions. Father-offspring regressions suggested significant ($p < 0.05$) heritable variation for cranium and mandible centroid size ($h^2 = 0.25$ and $h^2 = 0.43$ respectively), temporal/incisor mechanical advantage ($h^2 = 0.4$), and incisor ($h^2 = 0.67$), and molar ($h^2 = 0.51$) out-lever lengths. However, the slopes were not significant for the superficial masseter in-lever and mechanical advantage. Mother-offspring regressions were significant for all characters expect for the superficial masseter in-lever lengths. When slopes were significant, the differences between the slopes

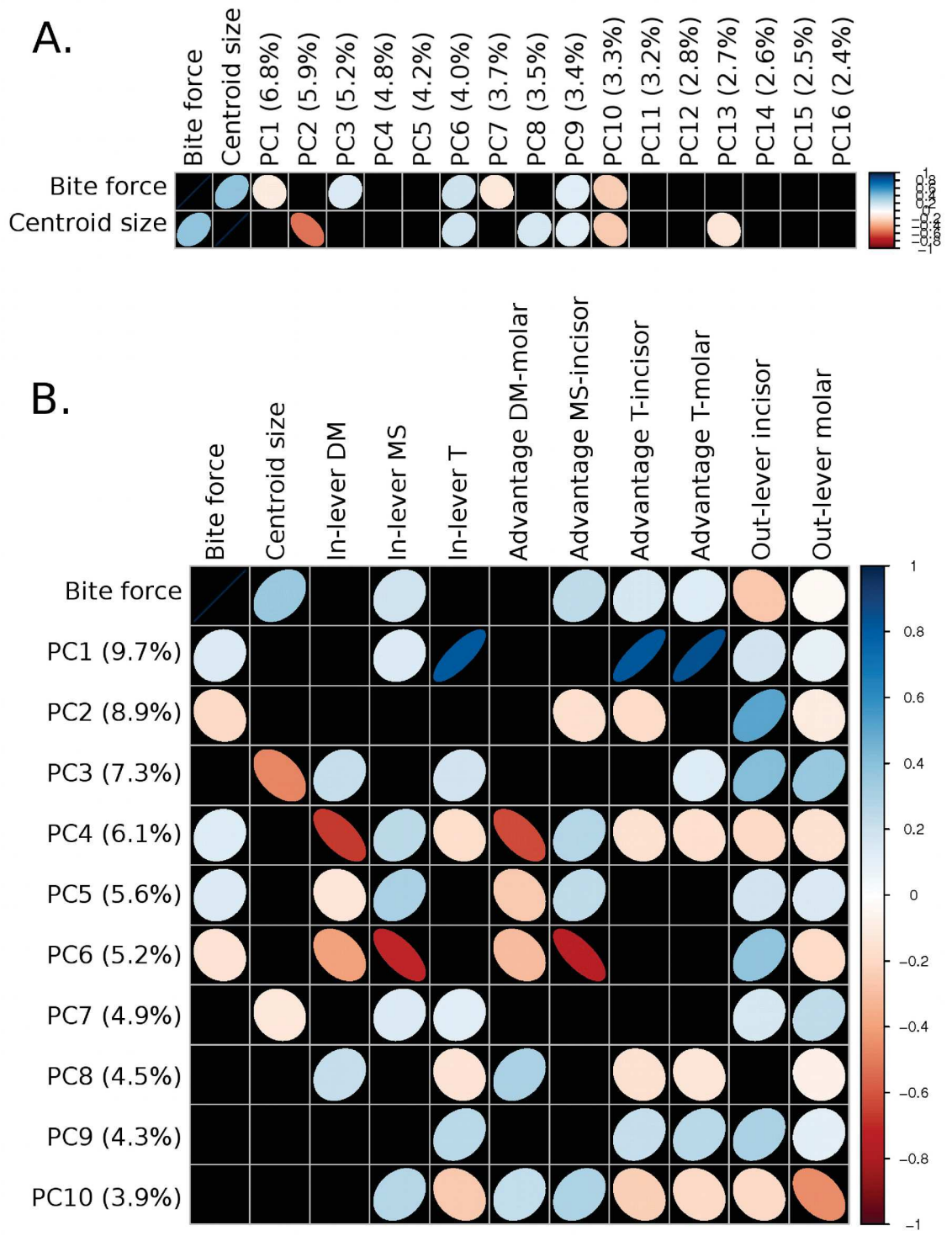

Figure 2. Correlation plots of the principal component axes (PC) of shape variation for A) the cranium and B) the mandible. Between parentheses are the percentage of variation represented by each PC. PCs were tested against bite force and centroid size in the cranium. In the mandible PCs were tested against bite force, centroid size, as well as other univariate morphometric traits. Abbreviations : DM : Deep masseter muscle ; MS : Superficial masseter muscle ; T : Temporal muscle ; Advantage : Mechanical advantage.

for males and females were not significant (all p > 0.1, Table 1) despite the intercept being always significantly different (p < 0.01). The incisor out-lever length appeared to show different slopes for males and females, but even in this case, it was not significant (Estimate = -0.225, S.E. = 0.139, t = -1.625, df = 330, p > 0.1). This showed that, although characters were sexually dimorphic (i.e. regressions had different intercepts for males and females), the patterns of transmission of variability were not different between sexes (i.e. the slopes were not different). Therefore, we pooled males and females in the following animal model analyses.

Half Sib and Mixed effect model analyses

The mixed effect l model analyses run on the selected traits allowed us to partition the

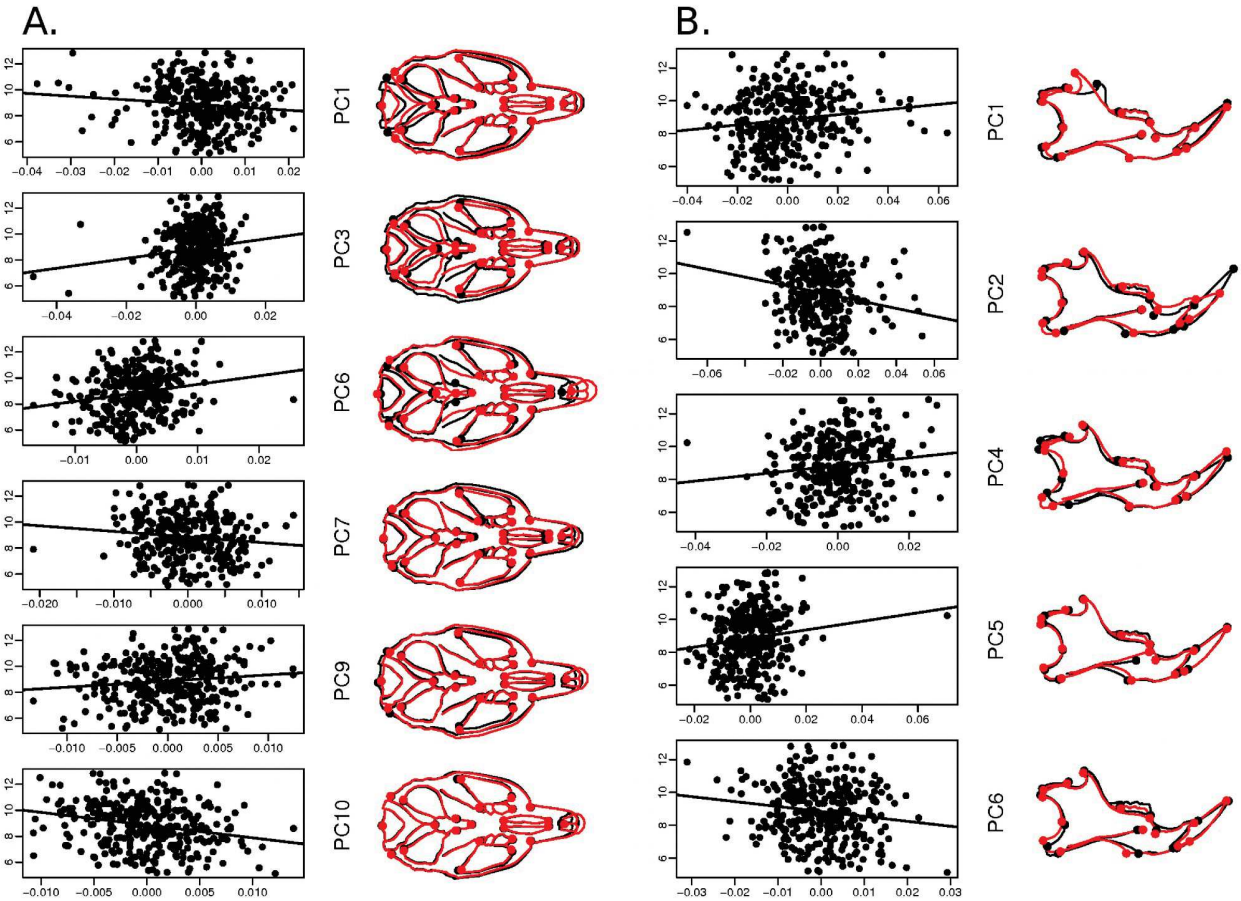

Figure 3. Plot of bite force against all shape principal components which were significantly correlated to it. Outlines on the right show the morphological variation associated with the corresponding PC. A) For the cranium, B) for the mandible.

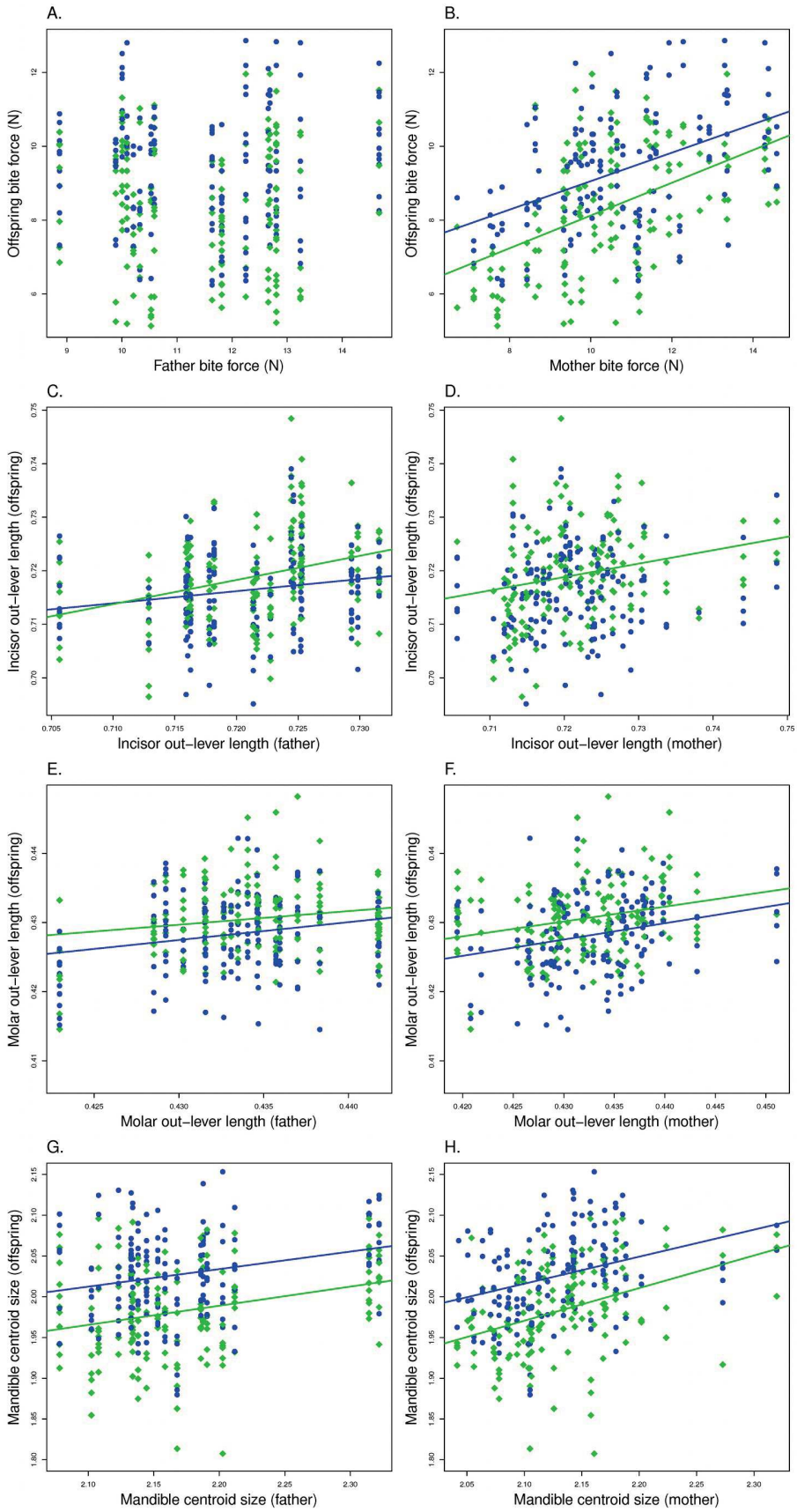

Figure 4. Parent-offspring regressions for the univariate morphometric traits significantly associated with bite force. Blue circles are male offspring, green diamonds are female offspring. Significant regression lines were plotted separately in green and blue when a significant sex effect was detected, or in black when no significant difference between males and females was found.

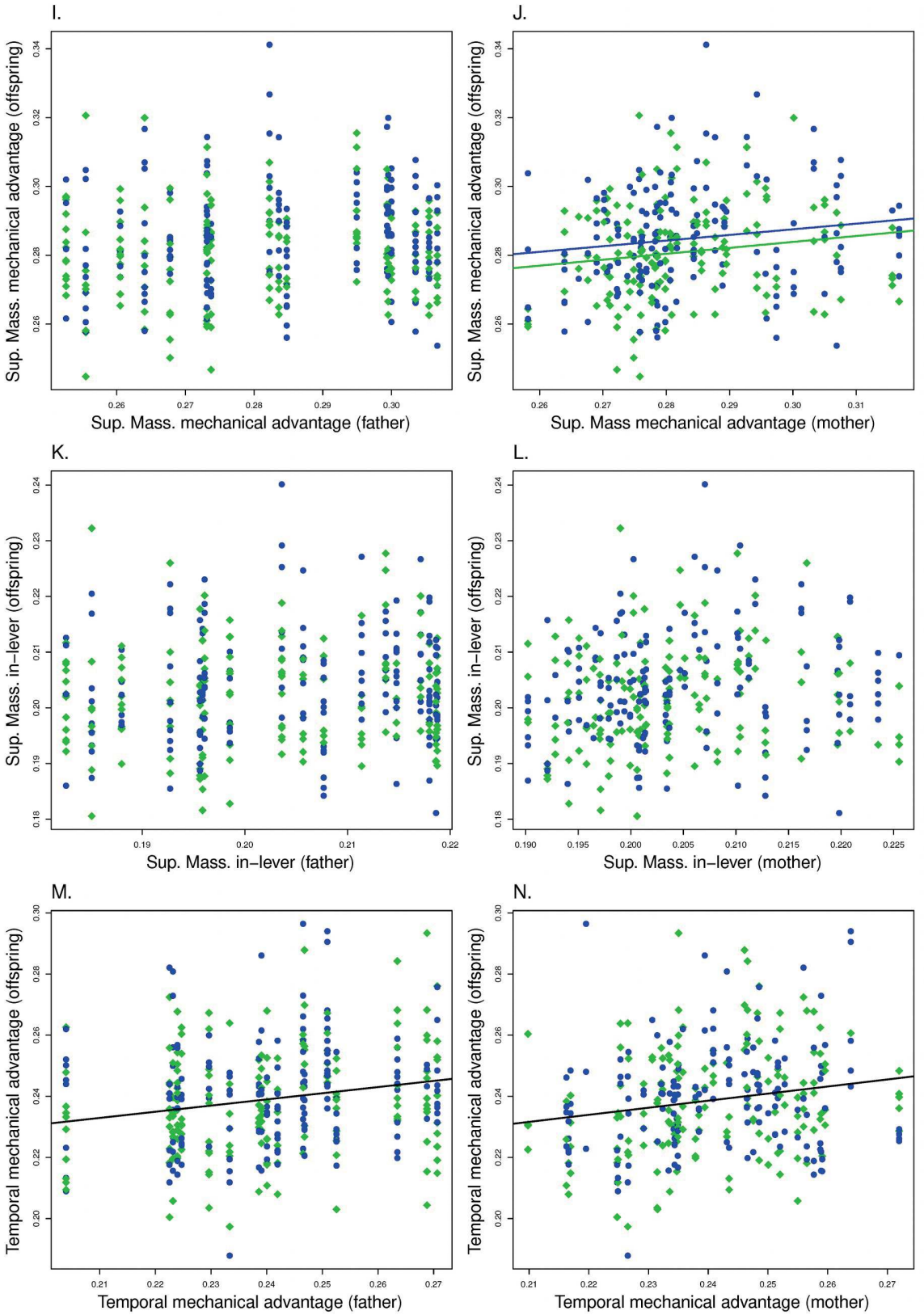

Figure 4 (continued). Parent-offspring regressions for the univariate morphometric traits significantly associated with bite force. Blue circles are male offspring, green diamonds are female offspring. Significant regression lines were plotted separately in green and blue when a significant sex effect was detected, or in black when no significant difference between males and females was found.

phenotypic variation between additive genetic, and dominance, environmental and error variance (Table 2, Fig. 5). Looking at the Va and Vd+Ve components of variance (Table 2), it appears that bite force has the lowest absolute Va, while having the highest absolute Vd+Ve. In comparison, all other variables have much lower total variance (therefore much lower Vd+Ve components). Among these traits, centroid sizes had both high Va and high Vd+Ve, followed by mechanical advantages (except for the superficial masseter, which had much lower Va than the temporal mechanical advantages). Although the in-levers and out-levers had rather low Va, they also had much lower Vd+Ve components than mechanical advantages or centroid sizes. In particular, the incisor and molar out-levers had much lower Vd+Ve components than all other variables.

Accordingly with the levels of additive genetic variance versus dominance and environmental variance, heritability for bite force is null, but it is high for the out-lever lengths especially the incisor out-lever length (molar out-lever $h^2 = 0.53$, incisor out-lever $h^2 = 0.77$). Centroid sizes and the temporal/incisor mechanical advantage have intermediate heritabilities (cranium centroid size $h^2 = 0.18$, mandible centroid size $h^2 = 0.25$, mechanical advantage $h^2 = 0.27$), while the superficial masseter in-lever and mechanical advantage have low heritability ($h^2 = 0.08$ and 0.07 respectively). These results are similar to the estimates obtained from the father-offspring regressions (Fig. 6).

Evolvability of the traits show divergent results (Table 2). However, since bite force Va is the lowest, bite force evolvability is also the lowest. Contrary to heritability, the out-levers have fairly low evolvability (especially the molar out-lever), as do centroid sizes and in-lever for the superficial masseter. Only the temporal mechanical advantage has a notably larger evolvability.

Using the G-matrices, we computed the RV-coefficients of genetic correlation between bite force, sizes and shape. As expected from the null additive genetic variance of bite force, its genetic correlation with cranium and mandible morphology (size, shape or both) was not significant ($RV < 0.001$, $p > 0.2$). However, the genetic links between size and shape of the cranium and mandible could

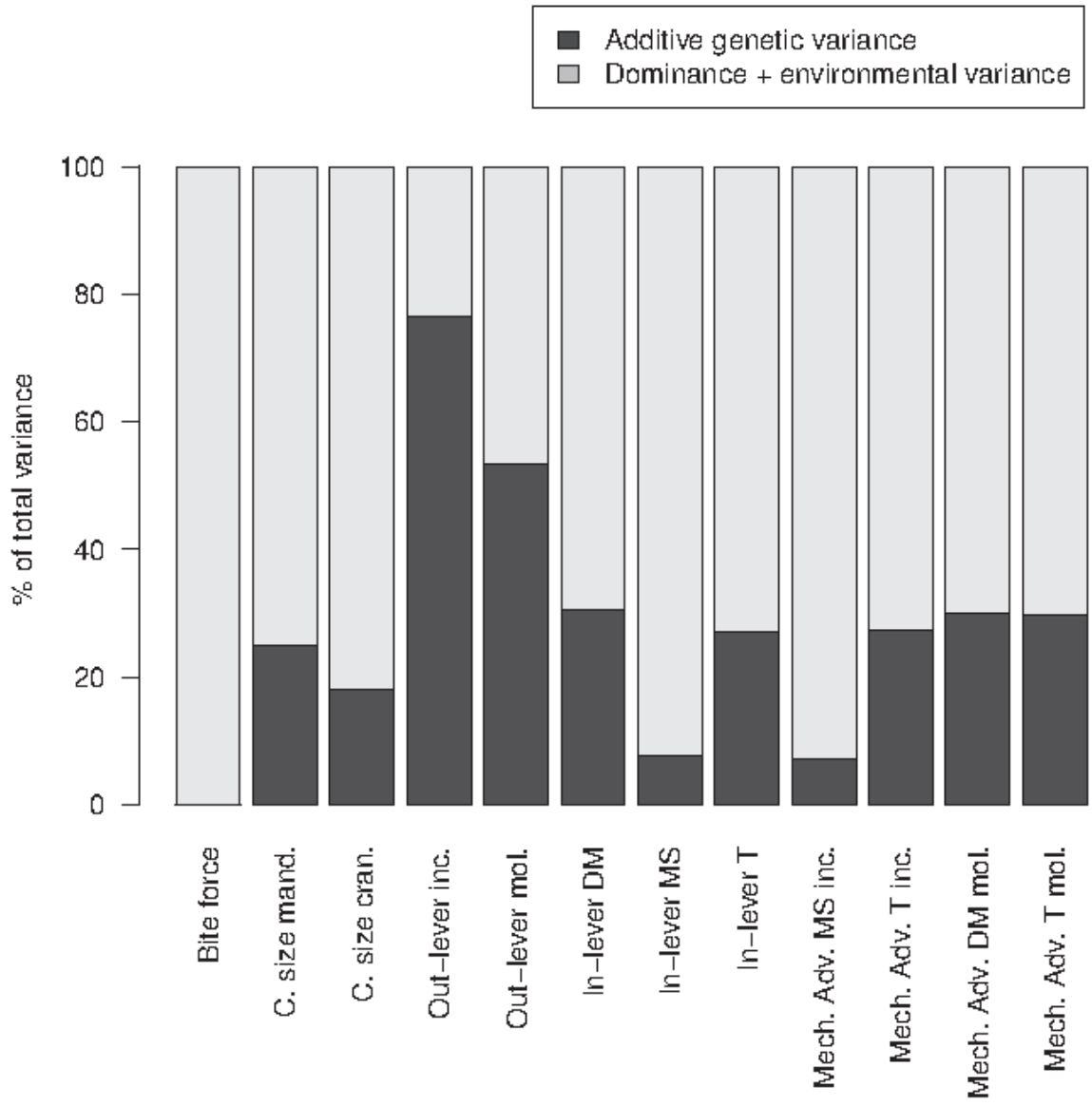

Figure 5. Barplot of phenotypic variance decomposition, in percentage of total variance.

be quantified. For both the cranium and mandible, the RV coefficient between size and shape was > 0.99 with $p < 0.01$, showing the tight genetic relationship uniting size and shape. We also found that the genetic correlation between cranium and mandible shapes was very strong with RV = 0.78 and $p < 0.0001$.

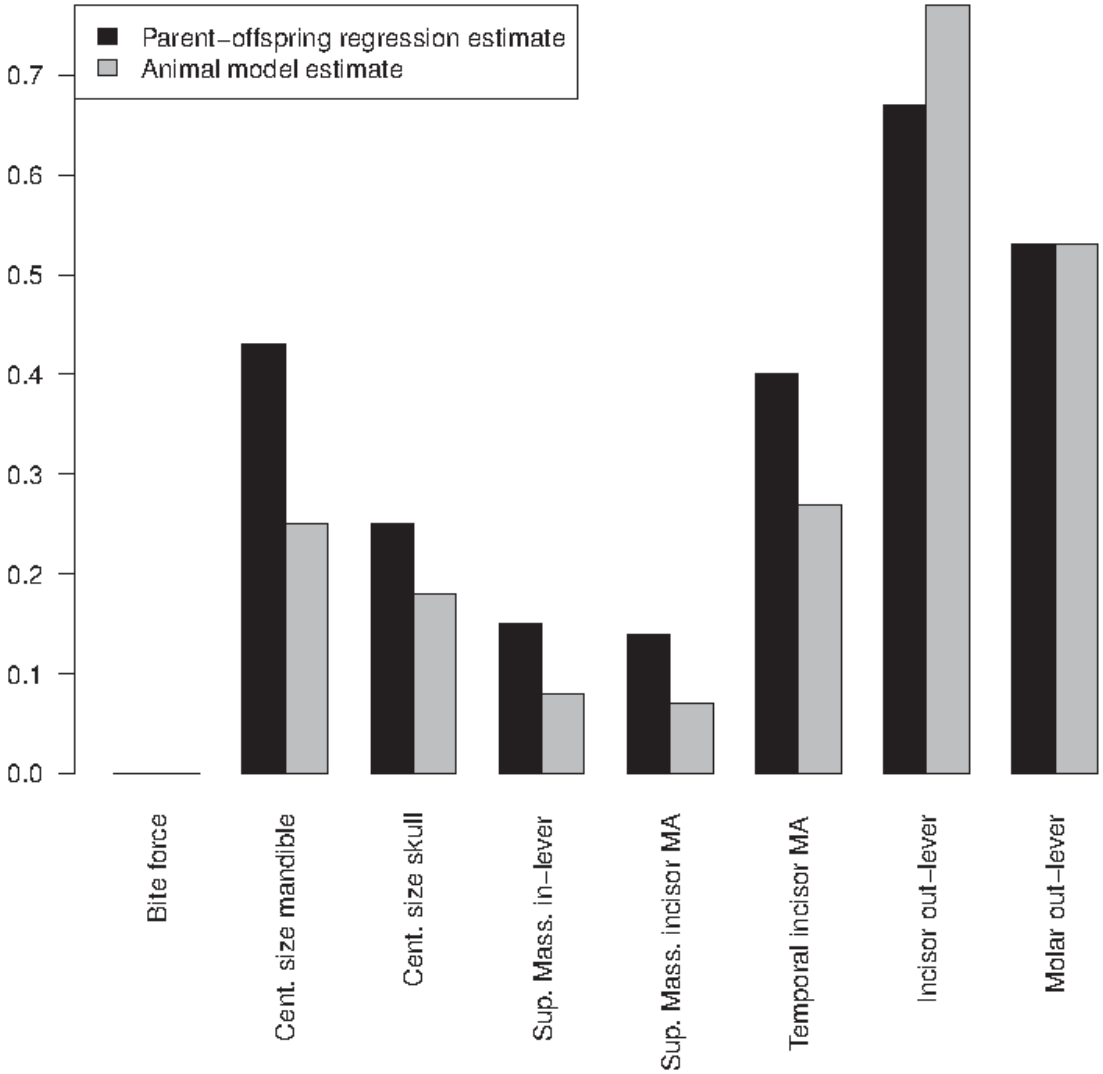

Figure 6. Barplot of narrow-sense heritabilities of bite force related univariate traits, estimated via either parent-offspring regressions or linear mixed models.

Discussion

As expected, we found that morphology and performance are linked at the intra-specific level. Here, the best predictor of bite force is centroid size, with a correlation coefficient of about 0.4 (Fig. 2A & 2B). The selected univariate traits of the mandible related to bite force appear to represent a substantial part of the morphological variation since they are strongly correlated with some of the first

PCs of shape (Fig. 2B and Fig. 3). However, while morphology significantly explains bite force, a large part of bite force performance variation is explained by other factors.

Parent-offspring regressions clearly showed that bite force is not heritable in our case study, while some elements of the skull morphology are (Fig. 4). The half sib analyses showed that the non-significant bite force heritability was not only due to high residual variance (Houle 1992), but also that additive genetic effects were extremely reduced in the variance partition of this trait (Fig. 5). Therefore, evolvability of bite force also appeared to be null (Table 2). On the other hand, morphological characters displayed various levels of additive genetic variance. As expected, heritability and evolvability of the characters studied show divergent results (Houle 1992). It appears that the out-levers, centroid sizes and temporal mechanical advantage have high heritabilities, while only the latter has high evolvability. Despite this, it appears that both indexes suggest that bite force can be expected to show a lack of response to selection, while morphological traits will show various levels of response.

The absence of additive genetic variance for bite force suggests strong stabilizing selection on this fitness-related character, and is coherent with theoretical expectations and empirical studies (Fisher 1958, Mousseau & Roff 1987, Hoffman 2016). Due to its quasi-absent genetic variance, bite force is genetically uncorrelated with morphology, despite being phenotypically dependent on it. Morphological variation, on the other hand, is partly due to additive genetic effects, and there appears to be very significant genetic covariation between size and shape of the cranium and mandible. A strong genetic correlation was also retrieved between cranial and mandibular morphologies, showing that the two parts of the skull are at least in part genetically integrated.

Because the amount of additive genetic variance for one trait is associated with its evolvability (Fisher 1958, Houle 1992), our results suggest that selection on bite force in itself should not have important effects. However, since variation in morphology is partly genetically determined, selection should be able to act more easily on it, especially because of the genetic integration of the cranium and

mandible, which would entail conjunct changes in both structures (both genetically and phenotypically). Since bite force is phenotypically related to skull morphology, changes in the skull morphology and size may create a "genetic line of least resistance" (e.g. Schluter 1996) to direct functional changes in bite force, which are potentially associated with changes in diet for example. These lines of least resistance are expected to follow the axis of greatest additive genetic variance, which in our case is in the functional morphological traits: size, out-levers of the mandible and mechanical advantage of the temporal muscle.

When comparing our results with interspecific patterns, two main elements of discussion can emerge. Firstly, we found weaker correlates between bite force and skull morphology than in interspecific comparisons (e.g. Aguirre et al. 2002, Herrel et al. 2008, Freeman & Lemen 2008). This can probably be explained by the fact that morphological variation is reduced intraspecifically, and even more so in our lab population raised in stable conditions, with controlled age. These particular conditions may reveal the important amount of dominance and environmental effects that can influence bite force variation.

Secondly, the most heritable morphological traits are size and the out-lever lengths of the mandible, both at the incisor and molar, while the most evolvable trait is the mechanical advantage of the temporal muscle. These traits broadly correspond to a general lengthening (incisor out-lever) or heightening (molar out-lever) of the mandible, and changes in the condyloid and coronoid process (temporal mechanical advantage). More importantly, hey can have important functional consequences, by modifying the mechanical advantage of the mandible, and thereby impacting the amount of force produced and the speed of the jaw closure (e.g. Hiiemae 1971, Hiiemae & Houston 1971, Satoh 1997). Comparative morpho-functional studies at the interspecific level in rodents have often noted changes in the length and height of the mandible, as well as in the coronoid and condyloid proecesses, associated with changes in muscular insertions and tooth morphology (e.g. Michaux et al. 2007, Samuels 2009,

Hautier et al. 2012, Maestri et al. 2016). These trends were linked to ecological aspects at different scales, within (Ctenohystrica, Hautier et al. 2012; Sigmodontinae, Maestri et al. 2016) and between (Samuels 2009) various groups of rodents. These morphological changes therefore have been repeatedly selected during their evolutionary history. Our data suggest that size, as well as the lengthening and heightening of the mandible, associated with lever arm changes in the masticatory apparatus, are highly evolvable characters, which may constitute one of the adaptive pathways for rodents to modify their diets or mode of life.

References

Aerts, P., Van Damme, R., Vanhooydonck, B., Zaaf, A., & Herrel, A. (2000). Lizard locomotion: how morphology meets ecology. *Netherlands Journal of Zoology*, 50(2), 261-277.

Aguirre, L. F., Herrel, A., Van Damme, R., & Matthysen, E. (2002). Ecomorphological analysis of trophic niche partitioning in a tropical savannah bat community. *Proceedings of the Royal Society of London B: Biological Sciences*, 269(1497), 1271-1278.

Arnold, S. J. (1983). Morphology, performance and fitness. *American Zoologist*, 23(2), 347-361.

Bates D, Maechler M, Bolker BM and Walker S (2015). "Fitting Linear Mixed-Effects Models using lme4."ArXiv e-print; in press, *Journal of Statistical Software*, <URL:http://arxiv.org/abs/1406.5823>.

Becerra, F., Echeverría, A., Vassallo, A. I., & Casinos, A. (2011). Bite force and jaw biomechanics in the subterranean rodent Talas tuco-tuco (*Ctenomys talarum*) (Caviomorpha: Octodontoidea). *Canadian Journal of Zoology*, 89(4), 334-342.

Claude, J. (2008). Morphometrics with R. Springer Science & Business Media.

Fisher, R. A. (1958). The genetical theory of natural selection.

Freeman, P. W., & Lemen, C. A. (2008). A simple morphological predictor of bite force in rodents. *Journal of Zoology*, 275(4), 418-422.

Ginot, S., Claude, J., Perez, J., & Veyrunes, F. (2017). Sex reversal induces size and performance differences among females of the African pygmy mouse, *Mus minutoides*. *Journal of Experimental Biology*, 220(11), 1947-1951.

Hautier, L., Lebrun, R., & Cox, P. G. (2012). Patterns of covariation in the masticatory apparatus of hystricognathous rodents: implications for evolution and diversification. *Journal of Morphology*, 273(12), 1319-1337.

Herrel, A., De Smet, A., Aguirre, L. F., & Aerts, P. (2008). Morphological and mechanical

determinants of bite force in bats: do muscles matter?. *Journal of Experimental Biology*, 211(1), 86-91.

Herrel, A., Podos, J., Huber, S. K., & Hendry, A. P. (2005). Bite performance and morphology in a population of Darwin's finches: implications for the evolution of beak shape. *Functional Ecology*, 19(1), 43-48.

Herrel, A., Spithoven, L., Van Damme, R., & De Vree, F. (1999). Sexual dimorphism of head size in *Gallotia galloti*: testing the niche divergence hypothesis by functional analyses. *Functional Ecology*, 13(3), 289-297.

Hiiemae, K. (1971). The structure and function of the jaw muscles in the rat (*Rattus norvegicus* L.). *Zoological Journal of the Linnean Society*, 50(1), 111-132.

Hiiemae, K., & Houston, W. J. B. (1971). The structure and function of the jaw muscles in the rat (*Rattus norvegicus* L.) I. Their anatomy and internal architecture. *Zoological Journal of the Linnean Society*, 50(1), 75-99.

Hoffmann, A. A., Merilä, J., & Kristensen, T. N. (2016). Heritability and evolvability of fitness and nonfitness traits: lessons from livestock. *Evolution*, 70(8), 1770-1779.

Houle, D. (1992). Comparing evolvability and variability of quantitative traits. *Genetics*, 130(1), 195-204.

Maestri, R., Patterson, B. D., Fornel, R., Monteiro, L. R., & Freitas, T. R. O. (2016). Diet, bite force and skull morphology in the generalist rodent morphotype. *Journal of evolutionary biology*, 29(11), 2191-2204.

Michaux, J., Chevret, P., & Renaud, S. (2007). Morphological diversity of Old World rats and mice (Rodentia, Muridae) mandible in relation with phylogeny and adaptation. *Journal of Zoological Systematics and Evolutionary Research*, 45(3), 263-279.

Mousseau, T. A., & Roff, D. A. (1987). Natural selection and the heritability of fitness components.

Heredity, 59(Pt 2), 181-197.

Radinsky, L. B. (1981). Evolution of skull shape in carnivores: 1. Representative modern carnivores. *Biological journal of the linnean society*, 15(4), 369-388.

R Core Team (2015). R: A language and environment for statistical computing. R Foundation for Statistical Computing, Vienna, Austria. URL https://www.R-project.org/.

Robert, P., & Escoufier, Y. (1976). A unifying tool for linear multivariate statistical methods: the RV-coefficient. *Applied statistics*, 257-265.

Rohlf, F. J. (2010). tpsDig v2. 16. Department of Ecology and Evolution, State University of New York, Stony Brook, New York.

Samuels, J. X. (2009). Cranial morphology and dietary habits of rodents. *Zoological Journal of the Linnean Society*, 156(4), 864-888.

Satoh, K. (1997). Comparative functional morphology of mandibular forward movement during mastication of two murid rodents, *Apodemus speciosus* (Murinae) and *Clethrionomys rufocanus* (Arvicolinae). *Journal of Morphology*, 231(2), 131-142.

Schluter, D. (1996). Adaptive radiation along genetic lines of least resistance. *Evolution*, 50(5), 1766-1774.

Van Daele, P. A. A. G., Herrel, A., & Adriaens, D. (2008). Biting performance in teeth-digging African mole-rats (*Fukomys*, Bathyergidae, Rodentia). *Physiological and Biochemical Zoology*, 82(1), 40-50.

Vanhooydonck, B., & Van Damme, R. (2001). Evolutionary trade-offs in locomotor capacities in lacertid lizards: are splendid sprinters clumsy climbers?. *Journal of Evolutionary Biology*, 14(1), 46-54.

Table 1. Results of the parent-offspring regressions for bite force, size and morphometric traits in our pedigree of wild-strain *Mus musculus*.

	Estimate	Std.Error	t value	Pr(>|t|)
BF offspring ~ BF dam * sex offspring)				
(Intercept)	13.77563	1.15076	11.971	<2e-16***
BF dam	0.25937	0.04624	5.609	4.4e-08***
Sex offspring	3.23767	1.65297	1.959	0.051.
BF dam : Sex offspring	-0.04261	0.06567	-0.649	0.517

BF offspring ~ BF sire * sex offspring)				
(Intercept)	20.220662	1.224866	16.51	<2e-16***
BF sire	-0.006004	0.046295	-0.13	0.8969
Sex offspring	3.144052	1.786026	1.76	0.0793.
BF sire : Sex offspring	-0.030707	0.066689	-0.46	0.6455

Out-lever incisor offspring ~ Out-lever incisor sire * sex offspring				
(Intercept)	0.3931	0.0727	5.407	1.23e-07***
Out-lever incisor sire	0.4517	0.1008	4.483	1.02e-05***
Sex offspring	0.1602	0.1001	1.601	0.110
Out-lever incisor sire : Sex offspring	-0.2254	0.1387	-1.625	0.105

Out-lever incisor offspring ~ Out-lever incisor dam * sex offspring				
(Intercept)	0.53846	0.05806	9.275	<2e-16***
Out-lever incisor dam	0.25051	0.08045	3.114	0.00202**
Sex offspring	0.1116	0.08218	1.358	0.17541
Out-lever incisor dam : Sex offspring	-0.15837	0.11391	-1.390	0.16540

Centroid size offspring ~ Centroid size dam * sex offspring)				
(Intercept)	1.13019	0.15784	7.16	5.68e-12***
Dam size	0.40019	0.07403	5.405	1.28e-07***
Sex offspring	0.18956	0.22679	0.836	0.404
Dam size : Sex offspring	-0.06865	0.10646	-0.645	0.52

Centroid size offspring ~ Centroid size sire * sex offspring				
(Intercept)	1.47232	0.12687	11.605	<2e-16***
Sire size	0.23483	0.05837	4.024	7.11e-05***
Sex offspring	0.08816	0.19609	0.45	0.653
Sire size : Sex offspring	-0.01965	0.0903	-0.218	0.828

In-lever MS offspring ~ In-lever MS sire * sex offspring				
(Intercept)	0.191029	0.012363	15.452	<2e-16***
In-lever MS sire	0.053393	0.061022	0.875	0.382
Sex offspring	-0.001221	0.018226	-0.067	0.947
In-lever MS sire : sex offspring	0.016989	0.089296	0.190	0.849

In-lever MS offspring ~ In-lever MS dam * sex offspring				
(Intercept)	0.172328	0.018211	9.463	<2e-16***
In-lever MS dam	0.145298	0.089329	1.627	0.105
Sex offspring	-0.001477	0.025153	-0.059	0.953
In-lever MS dam : sex offspring	0.016980	0.123147	0.138	0.890

Mechanical advantage MS/inc offspring ~ Mechanical advantage MS/inc sire * sex offspring				
(Intercept)	0.266857	0.017531	15.222	<2e-16***
Mechanical advantage sire	0.049657	0.062403	0.796	0.427
Sex offspring	-0.004298	0.025717	-0.167	0.867
Mechanical advantage sire : sex offspring	0.029765	0.0985	0.328	0.743

Mechanical advantage MS/inc offspring ~ Mechanical advantage MS/inc dam * sex offspring				
(Intercept)	0.232134	0.025315	9.170	<2e-16***
Mechanical advantage dam	0.17242	0.089571	1.925	0.0551.
Sex offspring	0.006261	0.034577	0.181	0.8564
Mechanical advantage dam : sex offspring	-0.008645	0.12208	-0.071	0.9436

Mechanical advantage T/inc offspring ~ Mechanical advantage T/inc sire * sex offspring				
(Intercept)	0.18719	0.017691	10.581	<2e-16***
Mechanical advantage sire	0.2125	0.073602	2.887	0.00414**

Sex offspring	0.008273	0.026871	0.308	0.75835
Mechanical advantage sire : sex offspring	-0.027717	0.11155	-0.248	0.80392

Mechanical advantage T/inc offspring ~ Mechanical advantage T/inc dam * sex offspring				
(Intercept)	0.16707	0.02357	7.089	8.88e-12***
Mechanical advantage dam	0.29587	0.09785	3.024	0.0027**
Sex offspring	0.03278	0.03352	0.978	0.3289
Mechanical advantage dam: sex offspring	-0.13218	0.13891	-0.952	0.3420

Mechanical advantage T/mol offspring ~ Mechanical advantage T/mol sire * sex offspring				
(Intercept)	0.30593	0.03002	10.193	<2e-16***
Mechanical advantage sire	0.23043	0.07518	3.065	0.00236**
Sex offspring	0.02757	0.045	0.613	0.54048
Mechanical advantage sire : sex offspring	-0.0612	0.11232	-0.545	0.58621

Mechanical advantage T/mol offspring ~ Mechanical advantage T/mol dam * sex offspring				
(Intercept)	0.25574	0.04059	6.301	9.9e-10***
Mechanical advantage dam	0.35402	0.10087	3.51	0.000514***
Sex offspring	0.0858	0.05762	1.489	0.137488
Mechanical advantage dam: sex offspring	-0.20758	0.14319	-1.450	0.148142

Table 2. Results of the quantitative genetic analyses ran in this study for traits correlated with bite force. Abbreviations : Cent. Size. : Centroid size ; Mass. Sup : Superficial masseter muscle ; Inc. : Incisor ; MA : Mechanical advantage.

	Va	Vd+Ve	h^2 (regression)	h^2 (mixed model)	Evolvability (I_A)
Bite force	0	33.23856707	0	0	0
Cent. Size mandible	0.00086599	0.00261647	0.43	0.25	0.00021542
Cent. Size cranium	0.00140929	0.00641219	0.25	0.18	0.00012496
In-lever Mass. Sup.	0.00000697	0.00008322	0.15	0.08	0.00016903
MA Mass. Sup./Inc.	0.00001494	0.00019214	0.14	0.07	0.00018664
MA Temp./inc	0.0000852	0.00022675	0.4	0.27	0.00149183
Out-lever incisor	0.00005746	0.00001765	0.67	0.77	0.00011152
Out-lever molar	0.00001625	0.00001424	0.53	0.53	0.00008815

Partie 2 – Conclusion

Cette partie s'est focalisée sur différents aspects génotypiques et génétiques, de manière à estimer leur effet sur la performance et la morphologie. Il a d'abord été montré que, chez la souris naine *M. minutoides*, les trois génotypes sexuels (mâles, femelles, et mâles féminisés), qui montrent des différences dans leurs agressivité (comportement), diffèrent également dans leur force de morsure. Les mâles féminisés mordent plus fort que les autres souris naines, et cette différence est principalement expliquée par une augmentation de la taille de leur crâne et de leur mandibule. Dans ce cas, ni l'effet direct du sexe (génotype), ni un effet de l'agressivité ne sont à l'origine de cette meilleure performance. L'effet du génotype s'exprime ici sur la morphologie (en particulier la taille), et influence donc seulement indirectement la performance.

La seconde section, avait pour objectif de déterminer si la perte de diversité génétique, qui produit généralement une dépression de consanguinité, pouvait aussi causer une baisse de performance. Il s'est avéré que la consanguinité chez les souches de laboratoire étudiées ne cause pas de baisse de performance. De plus, il n'est pas non plus apparu d'augmentation de l'asymétrie chez ces souris, ce qui aurait permis de démontrer la présence de stress développementaux plus forts chez les plus consanguines. La perte de diversité génétique n'est donc pas dans notre cas une source de variation majeure de la performance et de la morphologie, qui sont certainement plus influencées par la variation d'origine des fondateurs de nos lignées. Il semble donc que des processus développementaux assurent une certaine stabilité à la morphologie mandibulaire, malgré les perturbations génétiques.

Enfin, la dernière section a montré que la force de morsure n'était pas héritable, en raison d'une très faible variation génétique additive, suggérant une stabilisation du trait par sélection. Il est aussi apparu que les traits morphologiques du crâne et de la mandibule, en particulier certains traits fonctionnels comme la longueur de la mandibule, étaient fortement héritables. Il semble donc que la variation de force de morsure n'est pas liée à une variation sous-jacente génétique, et que ses changements au cours de l'évolution sont probablement amenés par les effets de la sélection sur la morphologie. Ici encore, le lien entre génétique et performance semble indirect, nécessitant une étape intermédiaire de changements morphologiques.

Il apparaît donc que les effets directs des gènes sur la force de morsure sont faibles, ou tout du moins réduits proportionnellement aux effets de la morphologie, du développement et de la plasticité. Il

est possible que les changements de performance soient principalement associés à la variation morphologique au cours de l'évolution. Le reste de la variation de force de morsure est donc probablement associée à des effets développementaux et à la plasticité phénotypique de la musculature, ou du comportement, pouvant être induites par les changements de régime alimentaire, l'état de santé des individus, leur statut hormonal ou leur état de stress par exemple. Malgré cette plasticité, nos résultats montrent que l'étude des changements morphologiques, autant que celle des changements de performance, permet de réaliser des inférences sur la fitness des individus, l'évolution de leur niche et la divergence des populations d'une même espèce, qui seront les sujets abordés dans la troisième partie.

Partie 3 – Évolution de la morphologie crânienne et de la force de morsure dans les communautés de rongeurs sauvages.

La première partie a démontré le lien existant entre la morpho-anatomie crânienne et la force de morsure chez diverses espèces de Murinae. La morphologie osseuse, la musculature et la taille jouent toutes un rôle dans la production de la force de morsure. Dans la seconde partie, les effets génétiques et génotypiques ont été testés. Bien que n'ayant pas de lien direct avec la performance, leur influence sur la morphologie est néanmoins susceptible d'affecter la performance.

On s'intéresse dans cette partie à l'évolution des populations en réponse aux pressions

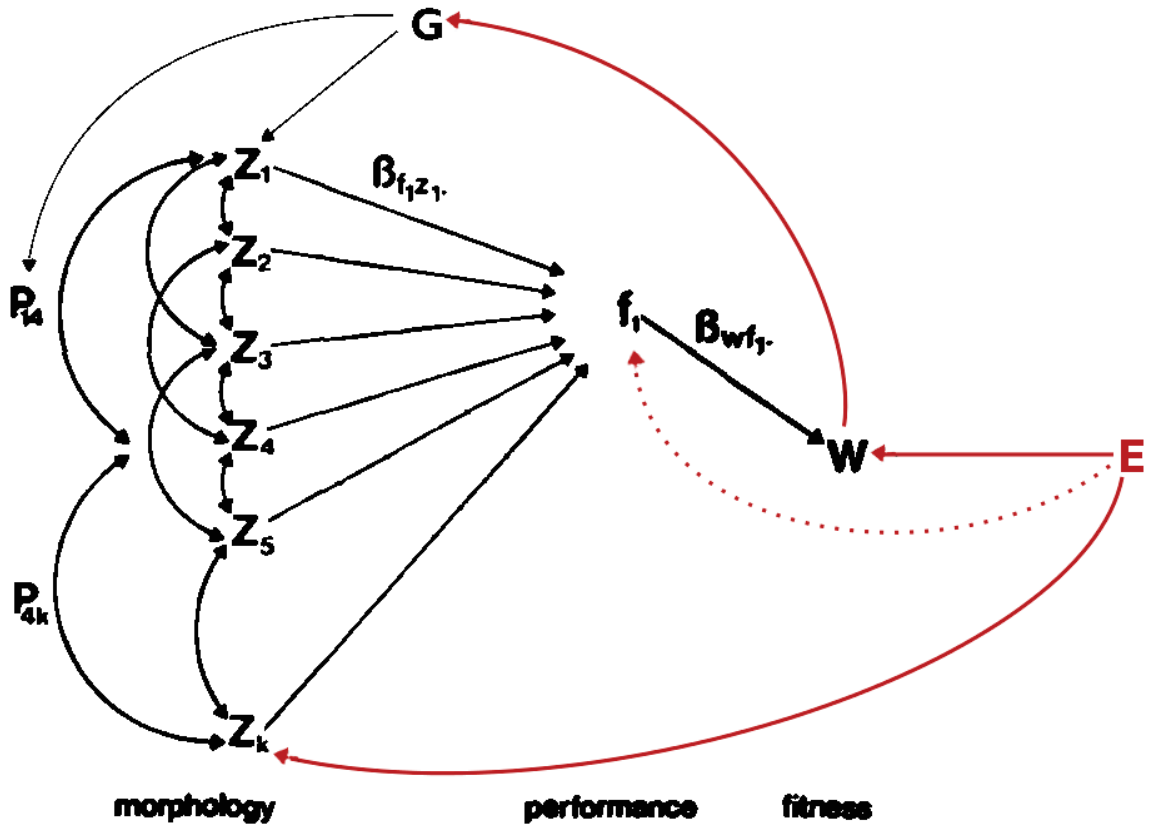

Figure 3.1. Diagramme des chemins reprenant le schéma de Arnold (1983). La partie 2 a permis de montrer que la variation génétique n'avait pas d'effet direct sur la force de morsure (cf. Fig. 2.1), mais qu'elle était liée à la variation morphologique, qui à son tour modifie la performance. Cette partie se focalise sur la réponse morphologique et fonctionnelle des populations sous l'influence de l'environnement (E). Ce dernier modifie la distribution des valeurs sélectives individuelles (W) dans la population, modifiant donc les fréquences alléliques (G). De plus l'environnement a un effet direct sur la morphologie et la performance (plasticité).

environnementales (Fig. 3.1). Celles-ci peuvent faire évoluer la morphologie et la performance des populations en fonction de gradients environnementaux ou bien générer des normes de réactions similaires (plasticité phénotypique).

3.1 – Comparaison de la force de morsure et de la taille chez deux espèces de Murinae syntopiques (article publié dans le *Canadian Journal of Zoology*).

Le mulot sylvestre (*Apodemus sylvaticus*) et la souris à queue courte (*Mus spretus*) sont deux espèces syntopiques dans les garrigues du Sud de la France. Bien qu'étant présentes dans les mêmes localités, et utilisant toutes les deux les même ressources alimentaires (i.e. des glands dans le contexte de la garrigue), il semble que les populations puissent subsister en coexistant. La différence de taille pourrait cependant réduire la compétition entre les deux espèces, en permettant au mulot sylvestre (plus grand) de se nourrir d'objets plus durs et plus gros. L'étude de la force de morsure chez ces deux espèces permettra de vérifier cette hypothèse, ou au contraire de montrer qu'en présence d'une ressource très abondante, la compétition réduite permet aux deux espèces de cohabiter.

Comparative bite force in two syntopic murids (Rodentia) suggests lack of competition for food resources.

Authors : Samuel Ginot* (1), Camille Le Noëne (1), Jaques Cassaing (1)

(1) Institut des Sciences de l'Evolution de Montpellier – UMR 5554. Université Montpellier 2, CNRS, IRD, EPHE – cc 064. F 34095 Montpellier cedex 05.

samuel.ginot@univ-montp2.fr

camille.le-noene@univ-montp2.fr

jacques.cassaing@univ-montp2.fr

*Corresponding author: samuel.ginot@umontpellier.fr.

Ginot, S., Le Noëne, C., Cassaing, J. "Comparative bite force and competition in two syntopic murids (Rodentia)."

Abstract

Closely related syntopic species have been shown to avoid competition by differentiating in the type of food they process. This can be achieved by changes in size or in the masticatory apparatus that produce modifications in bite force. The wood mouse (*Apodemus sylvaticus* L., 1758) and short-tailed mouse (*Mus spretus* Lataste, 1883) are two murid rodent species found in syntopy in the south of France. We measured bite force in wild specimens of both species to test for differences in performance. Despite its greater body mass, the wood mouse showed only slightly higher bite force than the short-tailed mouse. We found no clear sexual dimorphism in either species, however among the males of the short-tailed mouse, two groups appeared in terms of bite force. This bite force difference may correspond to a hierarchical organisation of these males. Overall, it seems that both species have similar bite forces and accordingly overlap in the resources they use. Other factors may exist that create a niche differentiation between the wood mouse and the short-tailed mouse. Another explanation may be a great abundance of food, which would cancel competition for this resource in these species.

Résumé

Il a été montré que les espèces proches vivant en syntopie évitent la competition en différenciant le type de nourriture qu'elles utilisent. Cela peut être permis par des changements de taille ou dans l'appareil masticateur qui sont à l'origine de différences dans la force de morsure. Le mulot

sylvestre (*Apodemus sylvaticus* L. 1758) et la souris à queue courte (*Mus spretus* Lataste 1883) sont deux espèces de rongeurs muridés trouvés en syntopie dans le sud de la France. Nous avons mesuré la force de morsure chez des specimens sauvages des deux espèces pour tester de potentielles différences de performance. Bien que le mulot sylvestre soit plus gros, sa force de morsure n'est que légèrement plus haute que celle de la souris à queue courte. Nous n'avons pas détecté de dimorphisme sexuel marqué au sein des deux espèces, cependant parmi les souris à queue courte mâles, il apparaît deux groupes en termes de force de morsure. Ceux à la morsure plus forte pourraient représenter des mâles dominants, tandis que ceux à la morsure plus faible seraient des subordonnés. Généralement, les deux espèces ont des forces de morsures similaires, et par conséquent montrent un grand chevauchement dans les ressources qu'elles peuvent utiliser. D'autres facteurs pourraient exister qui créeraient une différenciation de niche entre le mulot sylvestre et la souris à queue courte. Une explication alternative pourrait être la présence de nourriture en abondance, qui supprimerait la compétition entre les deux espèces à ce niveau.

Keywords

Performance ; short-tailed mouse (*Mus spretus*) ; wood mouse (*Apodemus sylvaticus*) ; niche overlap ; coexistence ; sex dimorphism

Introduction

Syntopic species (*sensu* Rivas 1964), i.e. species sharing the micro-habitats, have long been known to differentiate in their ability to cope with food types and hardnesses to reduce competition (e.g. Grant 1968 ; Grant 1972 ; Verwaijen et al. 2002 ; Yamashita et al. 2009). Grant (1972) particularly highlighted that there was often significant disparities in size among coexistent species with similar needs and that this was probably due to ecological and evolutionary factors. His synthesis ended by the hypothesis that the advantage to the larger species may be the free access to food, due to dominance, and the ability to deal with larger and/or harder seeds; while the smaller species might have a greater efficiency in energy extraction from the foods it exploits, and being better at avoiding predators. Such a dichotomy can be achieved either by evolution toward a greater body size, or by changes in the masticatory apparatus (e.g.Van Daele et al. 2009). Therefore, comparing pairs of syntopic species at their natural localities can be very fruitful in highlighting ecological performance differences and niche separation. Thus, Verwaijen et al. (2002) correlated bite force and prey hardness in two species of lacertid lizards, and proposed that differences in bite force are an important factor in prey handling efficiency and also influence prey selection in nature. In a large set of turtle species, Herrel et al. (2002) demonstrated that *in vivo* bite force was correlated with trophic ecology, as well as head height. Similar results were found in large Neotropical cats (Kiltie et al. 1984) which differenciate from each other in terms of skull morphology, gape and bite force under the influence of ecological character displacement. In Neotropical bats, the amazing diversity of skull shapes among the phyllostomid radiation was also explained in terms of bite force and dietary niche (Aguirre et al. 2002). Yamashita and colleagues (2009) found that

sympatric (living in the same national park, but not necessarily syntopic) lemurs from Madagascar, all feeding on bamboo, specialized on different part of the plant and accordingly segregated in their feeding behaviours. Finally, comparing two Cricetidae rodent species with different sizes and diets Williams et al. (2009) highlighted the importance of gape in the biting performance. They showed that the larger species, which is also carnivorous, could maintain a large proportion of its maximal bite force at wide gape angles due to a more derived and advantageous condition of the jaw muscles (notably a lower stretch factor).

According to the various studies cited above, the measure of bite force appears to be a great tool to address the evolution of food niche dimension and separation. The wood mouse *Apodemus sylvaticus* (L., 1758) and the short-tailed mouse *Mus spretus* (Lataste, 1883)–two murid species often found in syntopy (*i.e.* caught in the same trap lines) in southern France– are good candidates to run such a study. The two species share several habitats and most food items (Bauduin et al. 2013; Cassaing et al. 2013). Therefore, they may be considered to be in a situation of competition for food, yet they seem to coexist at least since the Holocene period. The wood mouse is about 1.5 times larger than the short-tailed mouse. In an experimental setting in the wild, it has been shown that these rodents can carry and eat larger seeds than equivalent individuals of the short-tailed mouse (Muñoz and Bonal 2008). The question remains as whether it also displays differences in terms of ingestion and comminution of food items. For its part, the short-tailed mouse demonstrates great skills to retrieve food sources. Notably, this species appears to use inadvertent information released by others (Valone 1989; Doligez et al. 2003; Danchin et al. 2004; Parejo et al. 2004), even heterospecifics (Cassaing et al. 2013). This may be highly expensive for the wood mouse if it gets its food caches used by the short-tailed

93 mouse. To our knowledge, there has been no evidence so far that the short-tailed mouse does not
94 achieve the second part of Grant's (1972) prediction mentioned above (*i.e.* that it is better at
95 energy extraction and predator avoidance).

96 We will focus here on the first step of ingestion by measuring the bite force of both species
97 in the wild. This measure, which notably depends on the biomechanics of the skull and
98 associated muscles, is a good proxy of the diet- and competition-related ecological performance,
99 at the inter- and intraspecific levels (Davis et al. 2010; Santana et al. 2010). Myomorphous
100 rodents, such as the species studied here, have been hypothesized to be "high-performance
101 generalists", according to Cox et al. (2012). If this holds true, we may expect strong bite forces
102 in the two murids studied here, compared to values reported in the literature for non-murid
103 rodents. Among them, we expect bite force to correlate body size, both at the interspecific
104 (Freeman and Lemen 2008 ; Ginot et al. 2018), and intraspecific level (Becerra et al. 2011).
105 Within species, we may find sex dimorphism in bite force, associated with intra-sex
106 competition, as reported by Becerra and colleagues (2011) in another species of rodent
107 (*Ctenomys talarum*). Interspecifically, the wood mouse is much larger than the short-tailed
108 mouse and it should display much stronger bites. Because both species occur in syntopy -and
109 feed mostly on the same items (Bauduin et al. 2013; Cassaing et al. 2013)- the difference in bite
110 force may be expected to be large, reducing competition for food (*i.e.* by giving access to harder
111 and larger items to the largest species). On the other hand, the difference may be reduced if
112 resources are widely available, therefore producing no competition between both species, and if
113 other factors (e.g. behaviour differences, intra-specific competition) do not influence bite force.

114

115 **Materials & methods**

116 Individuals of both species were first sampled in a garrigue near Montpellier (43° 34’ 38”
117 N, 03° 43’ 06” W) , with a mix of custom-built multi-catch traps (described in Cassaing 1986)
118 and Victor® Tin Cat® traps set up in a 7 x 7 grid. The traps were 25 m apart, so the grid covered
119 2.25 ha. An exhaustive description of the site can be found in Cassaing et al. (2013). At this site,
120 we captured 45 specimens of wood mice and 27 short-tailed mice. Additional samplings (wood
121 mouse n = 49 ; short-tailed mouse n = 8) were carried out at the Lunaret zoo in Montpellier in a
122 large mixed wood (Holm oak, Aleppo pines) with dense underneath vegetation, setting the same
123 traps every 10 meters along a 100 meter-long line. Although caught within the zoo area, these
124 specimens were wild, living in unkept spaces between the enclosures. Six specimens of wood
125 mice were also captured in the Caroux moutain range (Hérault, France) near the village of
126 Douch (altitude 700m), using the same trap density as for the zoo samples. Wood mice and
127 short-tailed mice were caught in the same trap lines (sometimes even in the same traps), except
128 in the Douch locality, where only wood mice were caught, probably because it is at the limits of
129 the short-tailed mouse's range.

130 We determined the rodents’ age on the basis of their weight, which is known to have a good
131 correlation with genuine age (Pearson's correlation: male R^2=0.88, female R^2=0.79, with p<0.05
132 for both sexes according to Frynta and Zižková 1992). Broad age categories were defined as
133 follows: for the short-tailed mouse, juveniles <10g ; subadults 10 to 13g ; adults >13g; for the
134 wood mouse, juveniles <15g ; subadults 15 to 20g ; adults >20g. We recorded their sex and their
135 apparent reproductive status by morphological features (e.g. testis position, opening of the
136 vagina, nipple condition, suspected gestation).

137 Shortly after capture we measured the animals' voluntary bite force at the incisors using a
138 piezoelectric force transducer (Kistler, type 9203, range 0-500 N, accuracy 0.01–0.1 N;
139 Amherst, NY, USA ; calibrated by the constructor at 25 °C and 36% humidity) attached to a
140 handheld charge amplifier (Kistler, type 5995, Amherst, NY, USA ; Herrel et al. 1999). The
141 force transducer was mounted between two steel bite plates as described in Herrel et al. (1999).
142 We adjusted the distance between the bite plates by measuring it with a caliper, and by
143 increasing or decreasing it via the micrometer head, so that each individual had a gape angle of
144 approximately 30° (Dumont and Herrel 2003), at which we found the rodents bit most
145 consistently. All animals bit directly onto steel at the same spot on the plates (*i.e.* at the tip), to
146 ensure a consistent out-lever length. We recorded three trials in a row for each individual, and
147 the maximal score was used in the analyses. Body mass (g) was recorded using a Pesola®
148 LightLine tubular weighing scale. Bite force over body weight ratios were also computed (Bite
149 Force Quotient, or BFQ, Table 1), after converting mass (g) to weight (N), by dividing it by
150 1000 g/kg and multiplying by 9.8 m/s².
151 All field procedures were under the Approval No. A34-172-042 (Hérault Prefecture). The
152 animals were gently handled, and when necessary, marked by toe-tattooing (e.g. Leclercq and
153 Rozenfeld 2001) to avoid duplicated measurements. All individuals were released at the location
154 of their capture after manipulations.
155 Difference in mean bite forces, mass and BFQ between species, as well as differences in
156 bite force between sexes were tested using two-tailed Student's t-tests. Correlations between bite
157 force and weight were assessed by fitting least-squares linear regressions, and differences
158 between the slopes and intercepts were tested using an ANCOVA. Allometric trajectories of log
159 bite force against log body mass were tested against the expected slope of 2/3 for isometric

160 scaling by linear regressions. Distribution of bite forces within sexes were visually inspected
161 and tested for multimodality using Hartigan's dip test. All analyses were run in R (R Core Team
162 2017).
163
164 **Results**
165 Both species have a similar bite force, barely higher for the wood mouse than for the short-
166 tailed mouse (mean=9.08, max=12.66, min=3.50 for the wood mouse; mean=8.31, max=11.20,
167 min=5.13 for the short-tailed mouse, Table 1). Although apparently negligible, the difference
168 between mean absolute bite force values was significant (Student's t-test: t=2.13, df=64,
169 p<0.05). When comparing only adult specimens with sexes pooled between both species
170 (mean=9.73 ± 2.01 for adult wood mouse ; mean=8.93 ± 1.75 for adult short-tailed mouse), the
171 difference was not significant (Student's t-test: t=1.59, df=30, p=0.123). On the other hand,
172 interspecific differences of mean body mass (g) values were significant either when looking at
173 the whole dataset (Student's t-test: t=10.60, df=81, p<0.01) or only at adults (Student's t-test:
174 t=11.30, df=33, p<0.01). In accordance with the literature, the wood mouse was almost 1.5
175 times bigger than the short-tailed mouse (20.42 g and 13.72 g respectively on average).
176 Therefore, BFQ mean value was significantly higher for the short-tailed mouse than the wood
177 mouse (Student's t-test: t=5.70, df=43, p<0.01).
178 When body mass was plotted against bite force (Fig. 1), both species showed similar ranges
179 in bite force and body mass. Both linear regressions showed a significant relationship, however
180 with fairly low coefficients of determination (short-tailed mouse: R^2=0.14, df=32, p<0.05 ;
181 wood mouse: R^2=0.24, df=99, p<0.01). The ANCOVA run on both species showed that as a

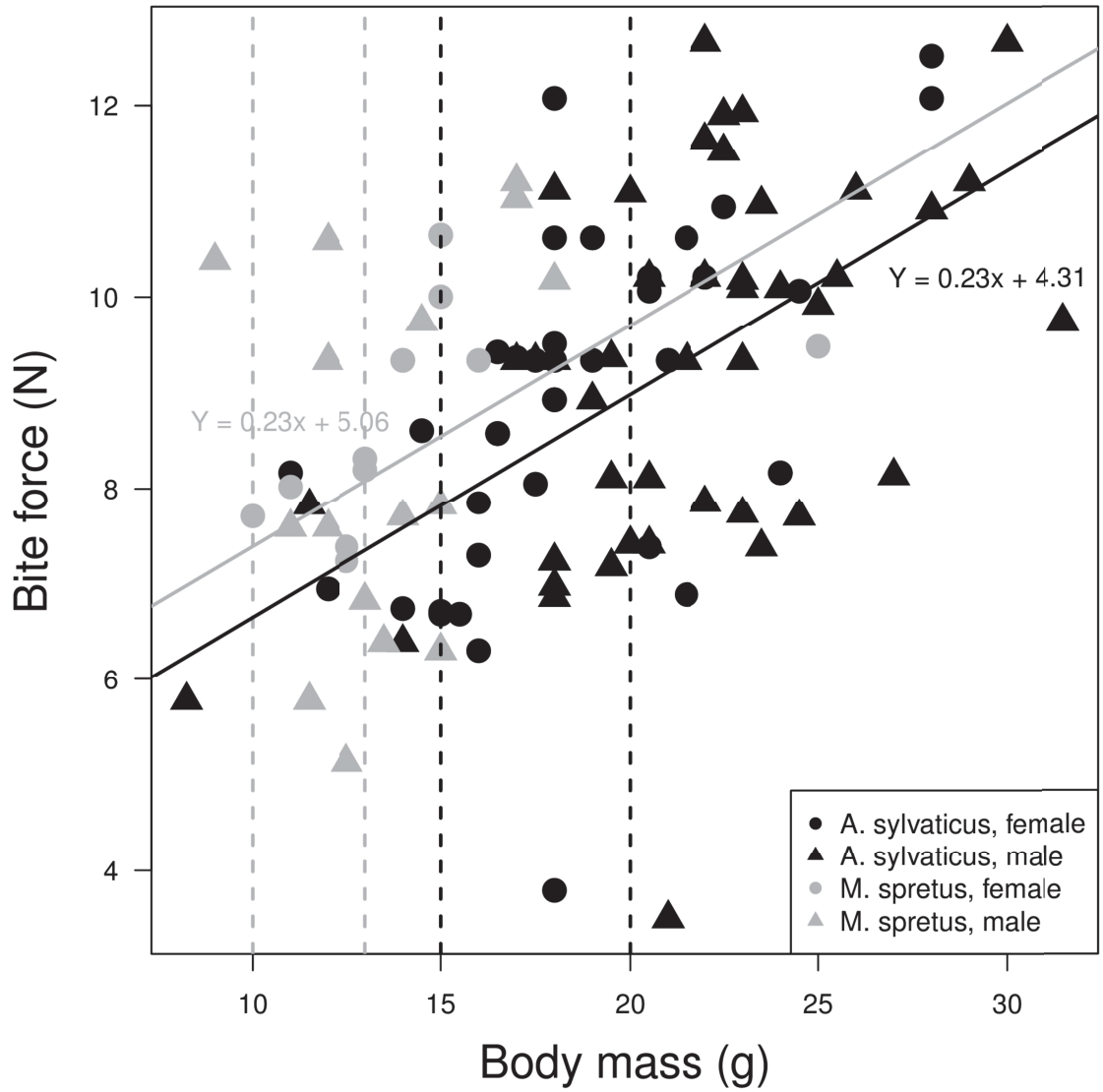

Figure 1. Bite force plotted against body mass in two syntopic murids of the south of France, *Apodemus sylvaticus* and *Mus spretus*. Solid lines are the least-square regression lines for each species. Dashed lines represent the limits of the age categories based on body mass for each species (to the left of the line are juveniles, in the middle are subadults, and to the right are adults).

182 whole, body mass had a significant effect on bite force (F=39.22, df=1, p<0.001) and that the
183 slopes were almost exactly identical to each other (F=0.00, df=1, p=0.988, *i.e.* the relationship
184 between bite force and body mass is the same for both species). Furthermore, the intercepts
185 were not significantly different between both species (F=2.90, df=1, p=0.091), although the

regression line for the short-tailed mouse was slightly higher than that of the wood mouse. Tests of the slopes of log bite force against log body mass showed no significant deviation from isometry (p=0.096 for the wood mouse, p=0.202 for the short-tailed mouse).

Looking at adults within species, we found that the female short-tailed mice did not bite significantly harder than males (Student's t-test: t=1.96, df=14, p=0.069). No sex dimorphism was found in terms of body mass (Student's t-test: t=0.66, df=7.37, p=0.526). Likewise, in the wood mouse there was no difference in either bite force (Student's t-test: t=-0.35, df=36.67, p=0.725), or body mass (Student's t-test: t=-1.38, df=30.10, p=0.176) between sexes.

Visual inspection (Fig. 2) of the distribution of bite forces in short-tailed subadult and adult males reveals two groups, the first one with 14 individuals (11 subadults and 3 adults), had a mean of 6.59 N, and a range from 5.13 N to 7.82 N. The other group, with 7 individuals (2 subadults and 5 adults), had a mean of 10.38 N, with a range from 9.33 N to 11.20 N. Despite the large gap between both groups, Hartigan's dip test for multimodality showed that the distribution was not significantly different from unimodality (D=0.10, p=0.33). Comparing short-tailed mouse adult and subadult males with the higher bite forces to conspecific adult and subadult females, we found a significant difference in mean bite force (Student's t-test: t=3.61, df=18, p<0.01).

Discussion

The two murids we studied showed a consistent bite force compared with published data on murid rodents. Cox et al. (2012) for example, reported an average *in vivo* bite force of 31.1 ±

		***Apodemus sylvaticus* (n=103)**					
		Females (n=42)			Males (n=61)		
		Juveniles (n=4)	Subadults (n=22)	Adults (n=16)	Juveniles (n=3)	Subadults (n=19)	Adults (n=39)
Bite force (N)	Sex(Age class) mean	7.63 ± 0.91	8.57 ± 1.83	9.6 ± 1.65	6.67 ± 1.05	8.28 ± 1.26	9.79 ± 2.17
	Sex mean	8.87 ± 1.78				9.24 ± 2.10	
	Species mean	**9.09 ± 1.97**					
Body mass (g)	Sex(Age class) mean	12.88 ± 1.65	17.18 ± 1.25	22.63 ± 2.47	11.25 ± 2.88	18.61 ± 0.99	23.67 ± 2.67
	Sex mean	18.85 ± 3.71				21.50 ± 3.99	
	Species mean	**20.42 ± 4.07**					
BFQ (Bite force/weight)	Sex(Age class) mean	61.11 ± 11.00	50.72 ± 9.02	43.34 ± 6.26	62.45 ± 13.80	46.25 ± 8.34	42.40 ± 9.75
	Sex mean	48.90 ± 9.66				44.53 ± 10.42	
	Species mean	**46.35 ± 10.29**					

		Mus spretus (n=35)					
		Females (n=13)			Males (n=22)		
		Juveniles (n=0)	Subadults (n=6)	Adults (n=7)	Juveniles (n=1)	Subadults (n=10)	Adults (n=10)
Bite force (N)	Sex(Age class) mean	NA	7.81 ± 0.44	9.83 ± 0.61	10.38 ± NA	7.13 ± 1.80	8.30 ± 2.03
	Sex mean	8.89 ± 1.17				7.97 ± 2.074	
	Species mean	**8.31 ± 1.80**					
Body mass (g)	Sex(Age class) mean	NA	12.00 ± 1.22	16.29 ± 3.90	9 ± NA	11.90 ± 0.66	15.25 ± 1.57
	Sex mean	13.16 ± 3.61				13.36 ± 2.26	
	Species mean	**13.72 ± 2.85**					
BFQ (Bite force/weight)	Sex(Age class) mean	NA	66.97 ± 7.85	63.88 ± 11.91	117.72 ± NA	61.44 ± 16.12	55.12 ± 9.75
	Sex mean	65.31 ± 9.96				61.11 ± 18.38	
	Species mean	**62.72 ± 15.66**					

Table 1. Bite force, body mass, and bite force quotient (bite force/weight ratio) measured in two syntopic species of murine rodents, the short-tailed mouse *Mus spretus* and the woodmouse *Apodemus sylvaticus.* Values shown in the table represent the mean ± standard deviation for each subset. Sex was recorded based on the presence of testicles or nipples, age class is based on body mass (for *M. spretus* : juveniles < 10g ; 10g < subadults < 13g ; > 13g adults. For *A. sylvaticus* : juveniles < 15g ; 15g < subadults < 20g ; > 20g adults).

208 10.75 N in laboratory *R. norvegicus*, which is much bigger than the species studied here.
209 Between our species, the difference in bite force appeared to be small compared to the
210 difference in body mass, and was not signicant in adults. As shown by its greater average BFQ
211 (Table 1), the short-tailed mouse *M. spretus* had a greater bite force relative to its size, compared
212 to the wood mouse *A. sylvaticus*. Within species, a significant positive relationship was found
213 between bite force and size (represented here by body mass), as was found other vertebrates
214 (Herrel and Gibb 2006). Indeed, the lightest individuals, likely the youngest, showed an absolute
215 bite force lower than that of the heavier ones (Fig. 1). Furthermore, we found that bite force
216 scaled isometrically with body mass in both our species, showing that, relative to their mass, the
217 lighter individuals do not have lower bite force than heavier individuals.

218 Short-tailed mouse adult females bit on average harder than males, although not
219 significantly. Furtermore, adult males in this species appeared to be split in two groups in terms
220 of bite force (Fig. 2). However, the distribution was not significantly different from unimodality,
221 perhaps due to small sample size. Still, this result is in line with those of staged dyadic
222 encounters reported by Cassaing (1984). That study suggested some behavioural differences in
223 males due to social hierarchy, and this may influence bite force as well. The adult males with the
224 weaker bite forces could be the subordinate ones, while the other group would comprise the
225 more dominant males. The mean bite force of the latter group is significantly higher than the
226 one of subadult and adult females. So the potentially more dominant males appear to bite harder
227 than the females, in accord with to previous results on rodents (e.g. Becerra et al. 2011). Altough
228 our data may fit with Cassaing's (1984) and Hurst's (1994) hypotheses that male short-tailed
229 mice display hierarchical relationships (with dominant or subordinate status), it is not sufficent
230 to explain or quantify them, and it was not the goal of this study. One way to assess how bite

231 force and social status may be linked to each other in the short-tailed mouse would be by
232 measuring bite force in dominant and defeated individuals of male-male encounters (e.g. Husak
233 et al. 2006).

234 Our results show a suprisingly close bite force for the two syntopic murines studied here. As
235 far as bite force is concerned, their abilities to break down hard seeds seem to be similar. Even if
236 the wood mouse could handle larger acorns thanks to its greater body size -as showed by Muñoz
237 and Bonal (2008) in Central Spain- it should be noted that the higher range of acorns occurring
238 in Spain is missing in garrigues in southern France where animals were captured. It seems that

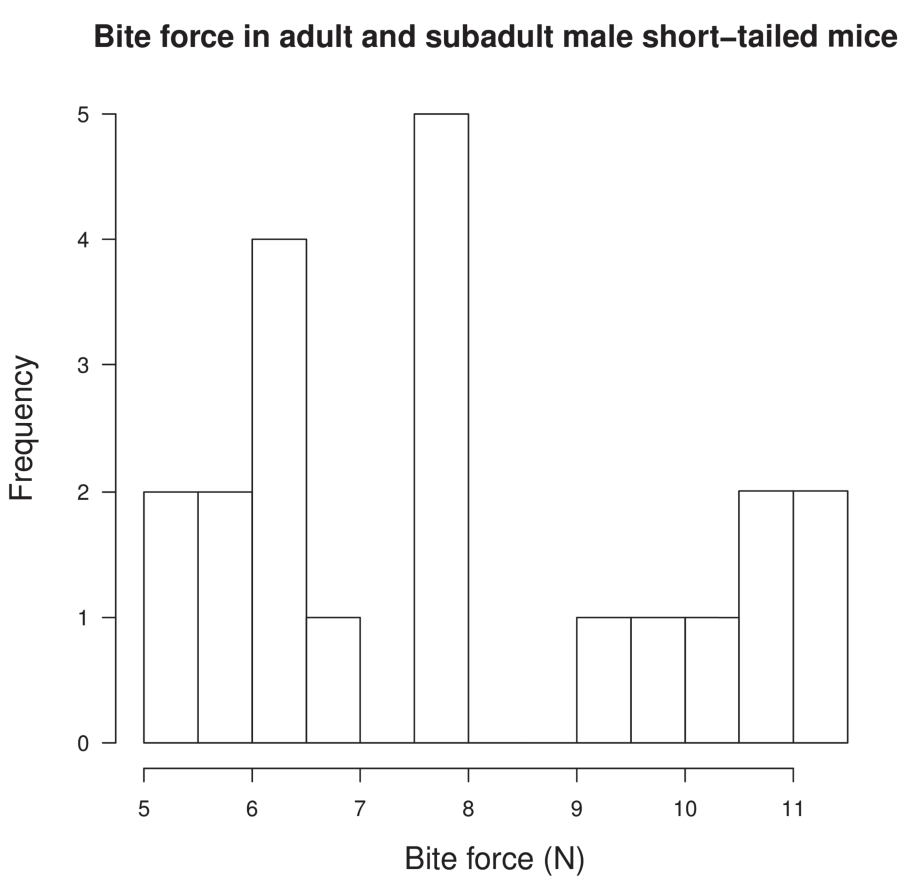

Figure 2. Histogram of bite force in adult and subadult males of Mus spretus, representing the two groups of potentially dominant and subordinate individuals.

239 in our case both species eat the same seeds (Bauduin et al. 2013) and share the same habitat
240 (Cassaing et al. 2013), therefore displaying a great niche overlap, despite their important size
241 differences. This would suggest that, in the areas we studied, the competition for food is not a
242 limiting factor. This may partially explain why the wood mouse seems to show no attempt of
243 pushing the short-tailed mouse aside, despite being used by the latter as a cue to resource
244 abundance.

245 It seems that niche partitioning between our species, if any, does not occur through a
246 qualitative difference in the access to harder foods. Resource partitioning may be produced by
247 other factors such as the level of the habitat being exploited (strictly on the ground, or at least
248 partially above and partially below it), the proportion of the animal parts in the diet, and the
249 metabolic assimilation rate of both species. However, our data, as well as those of Bauduin and
250 colleagues (2013) seem to point toward a lack of competition for resources, perhaps due to a
251 great abundance of food in the localities studied rather than toward niche partitioning.

Acknowledgements

The authors are grateful to workers of the Zoo de Lunaret in Montpellier, as well as François Catzeflis, who allowed us to collect data during the trapping sessions at the zoo. We also thank Pierre-Henri Fabre who organized fieldwork in the Caroux moutains and Thomas Tixier, who helped during fieldwork at the zoo as well as in Murviel-les-Montpellier. We are very grateful to two anonymous reviewers for their exhaustive and in depth comments and corrections, which greatly improved the quality of the manuscript. The authors received no funding for this study. This publication is a contribution of the Institut des Sciences de l'Evolution de Montpellier (UMR5554 – UM2 + CNRS + IRD) No. ISEM 2017-255.

References

Aguirre, L. F., Herrel, A., Van Damme, R., and Matthysen, E., 2002. Ecomorphological analysis of trophic niche partitioning in a tropical savannah bat community. Proc. of the R. Soc. of Lond. B: Biol. Sci. 269(1497); 1271-1278.

Anderson, R.A., Mcbrayer, L.D. and Herrel, A., 2008. Bite force in vertebrates: opportunities and caveats for use of a nonpareil whole-animal performance measure. Biol. J. Linn. Soc. 93; 709-720.

Bauduin, S., Cassaing, J, Moussa, I., Martin and C., 2013. Interactions between the short-tailed mouse *Mus spretus* and the wood mouse *Apodemus sylvaticus:* diet overlap revealed by stable isotopes. Can. J. Zool. 91; 102–109.

Becerra, F., Echeverría, A., Vassallo, A.I., and Casinos, A., 2011. Bite force and jaw biomechanics in the subterranean rodent Talas tuco-tuco (*Ctenomys talarum*) (Caviomorpha: Octodontoidea). Can. J. Zool. 89; 334–342.

Booth, W., Montgomery, W.I., and Prodöhl, P. A., 2007. Polyandry by wood mice in natural populations. J. Zool. (Lond.) 273; 176-182.

Bryja, J., Patzenhauerová, H., Albrecht, T., Mošanský, L., Stanko, M., and Stopka, P., 2008. Varying levels of female promiscuity in four *Apodemus* mice species. Behav. Ecol. Sociobiol. 63; 251–260.

Cassaing, J., 1984. Interactions intra- et inter-spécifiques chez les souris sauvages du Midi de la France, *Mus musculus domesticus* et *M. spretus*: conséquences sur la compétition entre les espèces. Biol. Behav. 9; 281-293.

283 Cassaing, J., 1986. Les captures multiples chez les Rongeurs : fait du hasard ou phénomène
284 social ? Acta Theriol. 31; 239-248.
285 Cassaing, J., Cervera, S., and Isaac, F., 2010. Laboratory and field evidence of paternal care in
286 the Algerian mouse (*Mus spretus*). J. Ethol. 28; 7-13.
287 Cassaing, J, Le Proux de la Rivière, B, de Donno, F, Martinez Garcia, E and Thomas, C., 2013.
288 Interactions between two Mediterranean rodent species: habitat overlap and use of
289 heterospecific cues. Ecoscience, 20; 137−147.
290 Cox, P.G., Rayfield, E.J., Fagan, M.J., Herrel, A, Pataky, T.C., and Jeffery, N., 2012. Functional
291 Evolution of the Feeding System in Rodents. PLoS ONE, 7(4): e36299.
292 doi:10.1371/journal.pone.0036299
293 Danchin, E., Giraldeau, L.-A., Valone, T.J., and Wagner, R.H., 2004. Public Information: From
294 Nosy Neighbors to Cultural Evolution. Science 305; 487-491.
295 Davis, J.L., Santana, S.E., Dumont, E.R., and Grosse, I.R., 2010. Predicting bite force in
296 mammals: two-dimensional versus three-dimensional lever models. J. Exp. Biol. 213;
297 1844-1851
298 Doligez, B., Cadet, C., Danchin, E., and Boulinier, T., 2003. When to use public information for
299 breeding habitat selection? The role of environmental predictability and density
300 dependence. Anim. Behav. 66; 973–988.
301 Dumont, E., and Herrel, A., 2003 The effects of gape angle and bite point on bite force in bats. J.
302 Exp. Biol. 206; 2117-23.
303 Fons, R., Grabulosa, I., Saint Girons, M.-C., Galan-Puchades, M.T., and Feliu, C., 1988.
304 Incendie et cicatrisation des écosystèmes méditerranéens: Dynamique du repeuplement
305 en micromammifères. Vie Milieu, 38; 259-280.

306 Freeman, P.W., and Lemen, C., 2008. Measuring bite force in small mammals with a piezo-
307 resistive sensor. J. Mammal. 89; 513–517.
308 Frynta, D., and Zizkova, M., 1992. Postnatal growth of Wood mouse (*Apodemus sylvaticus*) in
309 captivity. *In* Prague Studies in Mammalogy. *Edited by* I. Horáček and V. Vohralík.
310 Praha. Charles University Press pp. 57-69.
311 Ginot, S., Herrel, A., Claude, J., and Hautier, L., 2018. Skull size and biomechanics are good
312 estimators of *in vivo* bite force in murid rodents. Anat. Rec. 301(2); 256-266.
313 Grant, P. R., 1968. Bill size, body size, and the ecological adaptations of bird species to
314 competitive situations on islands. Syst. Biol. 17(3); 319-333.
315 Grant, P.R., 1972. Interspecific competition in rodents. Annu. Rev. Ecol. Syst. 3; 79-106.
316 Herrel, A., and Gibb, A.C., 2006. Ontogeny of performance in vertebrates. Physiol. Biochem.
317 Zool. 79; 1-6.
318 Herrel, A., and O'Reilly, J. C., 2005. Ontogenetic scaling of bite force in lizards and turtles.
319 Physiol. Biochem. Zool. 79(1); 31-42.
320 Herrel, A., Spithoven, L., Van Damme, and R., De Vree, F., 1999. Sexual dimorphism of head
321 size in *Gallotia galloti*: testing the niche divergence hypothesis by functional analyses.
322 Funct. Ecol. 13; 289–297.
323 Hurst, J. L., Hall, S., Roberts, R. and Christian, C., 1996. Social organization in the aboriginal
324 house mouse *Mus spretus* Lataste: behavioural mechanisms underlying the spatial
325 dispersion of competitors. Anim. Behav. 51; 327-344.
326 Husak, J.F., Lappin, A.K., Fox, S.F., and Lemos-Espinal, J.A., 2006. Bite-Force Performance
327 Predicts Dominance in Male Venerable Collared Lizards (*Crotaphytus antiquus*). Copeia
328 2; 301-306 DOI: 10.1643/0045-8511(2006)6[301:BPPDIM]2.0.CO;2

329 Khidas, K., Khammes, N., Kelloufi, S., and Aulagnier, S., 2002. Abundance of the wood mouse
330 *Apodemus sylvaticus* and the Algerian mouse *Mus spretus* (Rodentia, Muridae) in
331 different habitats of Northern Algeria. Mammal. Biol. 67; 34-41.
332 Kiltie, R. A., 1984. Size ratios among sympatric Neotropical cats. Oecologia, 61(3); 411-416.
333 Leclercq, G. C., and Rozenfeld, F. M., 2001. A permanent marking method to identify individual
334 small rodents from birth to sexual maturity. J. Zool. (Lond.) 254(2); 203-206.
335 Muñoz, A., and Bonal, R., 2008. Are you strong enough to carry that seed? Seed size/body size
336 ratios influence seed choices by rodents. Anim. Behav. 76; 709–715
337 Parejo, D., Danchin, E., and Aviles, J.M., 2004. The heterospecific habitat copying hypothesis:
338 can competitors indicate habitat quality? Behav. Ecol. 16; 96–105.
339 Rivas, L. R., 1964. A reinterpretation or the concepts “Sympatric” and “Allopatric” with
340 proposal or the additional terms “Syntopic” and “Allotopic”. Syst. Zool. 13(1); 42-43.
341 Santana, S.E., Dumont, E.R., and Davis, J.L., 2010. Mechanics of bite force production and its
342 relationship to diet in bats. Funct. Ecol. 24; 776-784 doi: 10.1111/j.1365-
343 2435.2010.01703.x
344 Valone, T., 1989. Group foraging, public information and patch estimation. Oikos, 56; 357–363.
345 Van Daele, P.A.A.G., Herrel, A., and Adriaens, D., 2009. Biting Performance in Teeth-Digging
346 African Mole-Rats (*Fukomys*, Bathyergidae, Rodentia). Physiol. Biochem. Zool. 82; 40–
347 50.
348 Verwaijen, D., Van Damme, R., and Herrel, A., 2002. Relationships between head size, bite
349 force, prey handling efficiency and diet in two sympatric lacertid lizards. Funct. Ecol.
350 16; 842-850.

351 Williams, S.H., Peiffer, E., and Ford, S., 2009. Gape and Bite Force in the Rodents *Onychomys*
352 *leucogaster* and *Peromyscus maniculatus*: Does Jaw-Muscle Anatomy Predict
353 Performance? J. Morphol. 270; 1338-47. Doi: 10.1002/jmor.1076
354 Yamashita, N., Vinyard, C. J., and Tan, C. L., 2009. Food mechanical properties in three
355 sympatric species of *Hapalemur* in Ranomafana National Park, Madagascar. Am. J.
356 Phys. Anthropol. 139(3); 368-381.

3.2 – Variation de morphologie cranio-mandibulaire et de force de morsure chez des communautés de murinés Sud-Est asiatiques soumis aux changements environnementaux anthropiques (article en préparation).

L'Asie du Sud-Est subit actuellement de fortes pressions environnementales d'origine anthropique, telles que la déforestation, l'urbanisation, ou l'expansion des terres agricoles. Par les changements impliqués ou la destruction de milieux naturels, de nombreuses espèces sont menacées. Cependant, certaines espèces semblent s'adapter et profiter de cette expansion humaine. C'est notamment le cas de certains rongeurs murinés en Asie du Sud-Est. Cette section a pour but de montrer comment l'apparition de ces modes de vie plus ou moins commensaux de l'homme influence la variation morpho-fonctionnelle chez ces rongeurs. L'étude s'intéresse à plusieurs échelles de variation : inter- et intra-population, mais aussi à des comparaisons inter-spécifiques des réponses morphologiques afin d'identifier de potentielles convergences et modification anatomiques liées à l’action de l'homme sur l’environnement.

Intra- and interspecific comparisons of the skull morphological variation in Southeast Asian murine rodent communities shed light on morpho-functional responses to anthropized environments.

Abstract

Southeast Asia is a hotspot of animal and plant diversity, which is currently experiencing major and global environmental changes, notably due to the anthropization of habitats (e.g. deforestation, agriculture, and urbanization). A large number of murine rodents originated and/or evolved in South and Southeast Asia. Among them, several murine rodents are tolerant to, or more or less dependent on human activities. We used the cranial and mandibular morphology variation in five species of mice and rats as a proxy to assess how these synanthropic to commensal animals may face the recent globalized anthropization of habitats. We captured specimens in localities in mainland Southeast Asia (Thailand, Lao PDR, Cambodia and Vietnam), with a particular focus on localities where two or more species are sympatric. Our results show that the degree of synanthropy between humans and murines influences the amount of morphological variation within localities, as well as the amount of morphological divergence between localities. Murine communities do not evolve convergently in their shared localities, but rather display divergent morphological responses to local environments. If the mice studied here potentially show adaptive morpho-functional changes, our data suggest that the skull variation in the forest-dwelling rat species cannot be explained by changes of bite force. Overall, we propose that close relationships with humans may limit divergence between localities via long-distance migration, but may also limit morphological variation within localities by a lack of tendency to disperse. We show that cases of morphological parallel changes can be found mainly between the two closely related species of rats, which are also the most commensal species in our sample. Furthermore, there are also cases of similar morphological changes between the synanthropic mice and these two

25 rats. We suggest that some of these cases may be linked to local adaptations to anthropized habitats.

26

Introduction

Southeast Asia hosts a major biodiversity hotspot, with particularly high rates of endemism, which are explained by its unique geographical and geological contexts (Sodhi et al. 2004; Claude 2017). Meanwhile, this region is experiencing one of the most rapid socio-economical and environmental changes (Sodhi et al. 2004, 2009, 2010, Wilcove et al. 2013). Anthropogenic activities induced an extremely fast decrease of primary forest areas, so that pristine environments have all but disappeared (Sodhi et al. 2004, 2009, 2010, Wilcove et al. 2013). Aside from major conservation issues (notably in terms of extinctions), these rapid and drastic environmental changes might also represent important drivers of phenotypic evolution within and between communities (Walther 2010).

Southeast Asia is also home to a very diverse murid rodent fauna, and likely constitutes the area of origin and diversification for most of these species (Marshall 1977, Boonsong & McNeely 1977, Pagès et al. 2010, Fabre et al. 2013). Rodents are of particular interest in the study of anthropogenic changes due to their apparent abilities to adapt quickly, notably through usage of human productions, and to achieve various degrees of commensalism (i.e. tendency for a species to be found within and around houses) or synanthropy (i.e. tendency for a species to tolerate human presence and anthropization of habitats ; Hulm-Beaman et al. 2016), repeatedly and independently (e.g. Auffray et al. 1988, Brouat et al. 2007, Aplin et al. 2011, Thomson et al. 2014). Southeast Asian murid rodent communities often include species that display a large ecological spectrum, which is especially well suited to human modified ecosystems (Morand et al. 2015). Since most environmental components of the area are anthropized, most rodent populations can be considered as synanthropic to some extent (as defined in Hulm-Beaman et al. 2016), while some species may be occasionally or fully commensal.

The consequences of the current environmental changes are often looked through the lens of conservation biology, especially in the cases of extinction, habitat shrinkage or fragmentation, or loss

of genetic diversity (Sodhi et al. 2004, 2009, 2010, Wilcove et al. 2013). Startlingly, less attention has been paid to the phenotypical variation induced by these changes, especially in mammals, although more attention has been paid to birds (e.g. Francis and Chadwick 2011). In rodents, despite the existence of several independant occurrences of commensal evolution, not much is known about morphological changes linked to human densities and urbanisation (but see Pergrams and Lawler 2009). Studying phenotypic evolution in this context is of particular interest, since the use of niches made available by anthroposystems produces changes in feeding resources, predator presence, migratory patterns, reproduction strategies and social behaviours (Hulm-Beaman et al. 2016, Sanchez-Villagra et al. 2016). Therefore, important differences in selective pressures can be expected between species depending on their capacity to evolve quickly in concert with the ecosystem modifications induced by humans. Here, we seek to understand how murid rodents differentiate among communities with respect to their degree of dependency on human resources. More specifically, our goal is to assess the main drivers of morphological variation between and within populations, as well as to estimate whether or not different species have identical morphological responses to environmental variations across scattered communities.

This work will focus on the shape variation of the skull, which represents a highly integrated morphological structure. While the link between its interspecific variation and dietary or ecological adaptation has attracted attention (e.g. Hautier et al. 2008, 2009, Michaux et al. 2007, Samuels 2009), intraspecific differences in morphology were more rarely assessed. In mice, several studies have related skull variation to geographical distances, differences in diet, or a combination of these factors (e.g. Renaud & Michaux 2007, Renaud & Auffray 2010, Valenzuela-Lamas et al. 2011, Renaud et al. 2015). In our case, the use of urban or agricultural food resources, and more generally the changes in the biology of species, are expected to entail morphological and functional variations on the skull. Fully commensal species may be expected to vary less morphologically between localities, due to the

homogeneity of their habitat over their geographical range (use of human resources would reduce the need for local adaptations), and potential long-distance transport via human vehicles (e.g. Varudkar and Ramakrishnan 2015). Within localities, if morphological patterns follow molecular evolution patterns, commensal species may show less variability due to less tendency to disperse (e.g. Brouat et al. 2007). Occasional commensal species can be considered generalists since they are able to thrive in both anthropic and non-anthropic habitats, and such generalist species are known to display slower rates of morphological evolution (e.g. in rodents Renaud et al. 2007), but may be more plastic. Therefore we may find reduced morphological variation in such species due to polyvalent morphologies and slow morphological evolution, or higher variation if the generalist ecology is due to higher phenotypic plasticity. On the other hand more specialized species are expected to show less variable morphologies between localities, due to their limited habitat range. Finally, non-commensal species are exposed to more variable conditions, and human activities are expected to increase their habitats' patchiness. Therefore, these species may show larger and / or more geographically driven divergence between populations due to evolution in isolation. Clearly, influence of human activities on a species' habitat should vary, especially with regard to the various degrees of tolerance to human presence.

To test these predictions, we will look at five southeast asian murine rodents more or less closely associated to humans: *Rattus exulans*, a small commensal rat ; *Rattus tanezumi*, a large, opportunistic rat which can thrive around and in urban areas ; *Mus caroli*, a small mouse found in association with flooded rice cultures ; *Mus cookii*, a more mountainous mouse, which is found in sloped agricultural areas ; and *Maxomys surifer* a forest-dwelling rat which is less tolerant to human presence and influence on habitats (Morand et al. 2015). In recent times, the evolution of these species has been influenced by human activities, either through habitat loss, gain in food resources, or passive transportation. In this study, we will try to understand how these changes can be related with morphological variation in this sample of species. To do so, we will use a morphometric geometric

approach on the cranium and mandible. We will aim at revealing how various degrees of synanthropy and ecological specialization may modify the amount of morphological variation of a species, within and between localities. We will then compare these variations to geographical distances and migratory pathways (either limited or improved by human activities). We will also assess if the observed morphological differences can be translated into functional changes by estimating bite force from morphology. Finally we will compare the inter-locality patterns of morphological changes between species, to highlight potential similar responses to human-mediated environmental changes at the community level. We expect that species that are phylogenetically and/or ecologically closer may show more cases of similar morphologies, due to similar habitats and/or similar morphological constraints.

Materials and Methods.

Specimens and localities sampled.

For this study, we used in total 590 crania, and 593 mandibles of rodents, captured over several years of fieldwork across continental Southeast Asia in the framework of the CERoPath project (www.ceropath.org). Specimens for this study come from a total of 16 localities (Fig. 1), of which nine are Thai, three are Cambodian, two are Laotian, and one is Vietnamese. The species used include two mice, *Mus cookii* (sampled in 4 localities) and *Mus caroli* (sampled in 6 localities), the forest-dwelling rat *Maxomys surifer* (sampled in 6 localities), the partially commensal rat *Rattus tanezumi* (sampled in 11 localities), and the fully commensal rat *Rattus exulans* (sampled in 13 localities). All localities are affected by some level of human-mediated changes, including the forested areas, which are secondary forests. Table 1 shows a synthesis of the ecological characteristics of the five species studied here.

The animals were caught using live-traps, and euthanized by CO2 inhalation. They were then dissected for various soft tissue and parasite samples. Following this, the head was cut off, and kept in

70% ethanol to be brought back to the lab. All head were cleaned of their soft tissues manually, then the skulls were dried, to be added to the collection, which is kept at the faculty of Veterinary Technology in Kasetsart University (Thailand).

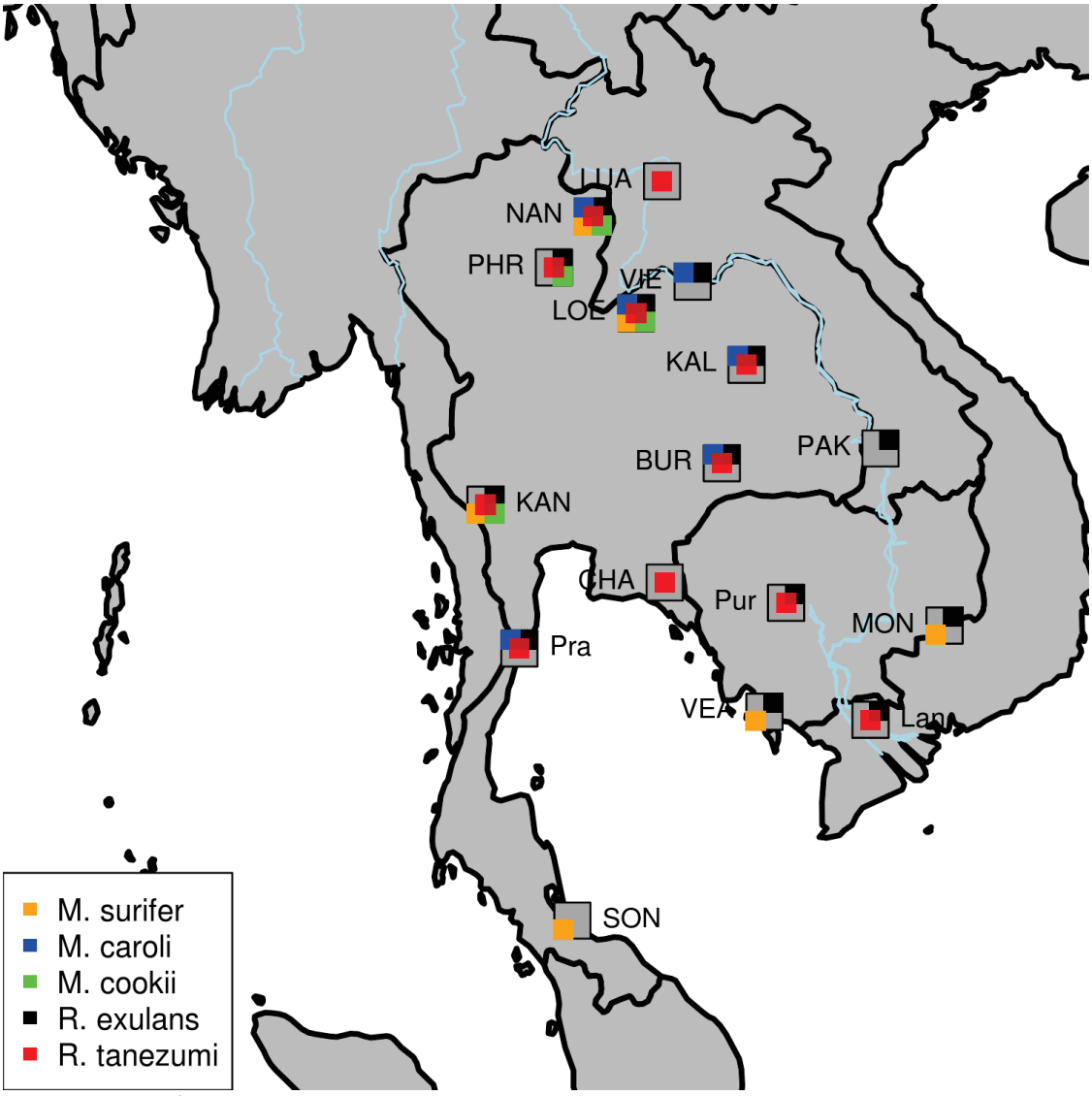

Figure 1. Map of continental South-east Asia, showing the localities sampled in this study, and the species caught in each. Abbreviations : CHA, Chantaburi (Thailand) ; KAL, Kalasin (Thailand) ; KAN, Kanchanaburi (Thailand) ; Lan, Cao Lanh (Vietnam) ; LOE, Loei (Thailand) ; LUA, Luang Prabang (Lao PDR) ; MON, Mondolkiri (Cambodia) ; NAN, Nan (Thailand) ; PAK, Pakse (Lao PDR) ; PHR, Phrae (Thailand) ; Pra, Prachuap (Thailand) ; Pur, Pursat (Cambodi) ; SON, Songklah (Thailand) ; VEA, Veal Renh (Cambodia) ; VIE, Vientiane (Lao PDR).

Geometric morphometric analysis.

The palatal side of the cranium and lateral side of the mandible were photographed in a standardized way, using a Pentax K200D reflex camera in a fixed position, with a 45mm focal distance. The left mandible was preferentially considered. When it was broken or absent, we used a mirrored photograph of the right mandible. Twenty-two landmarks were selected on the cranium, and 16 on the mandible (Fig. 2), and were digitized using the tpsDig2 software (Rohlf 2010). Landmark coordinates

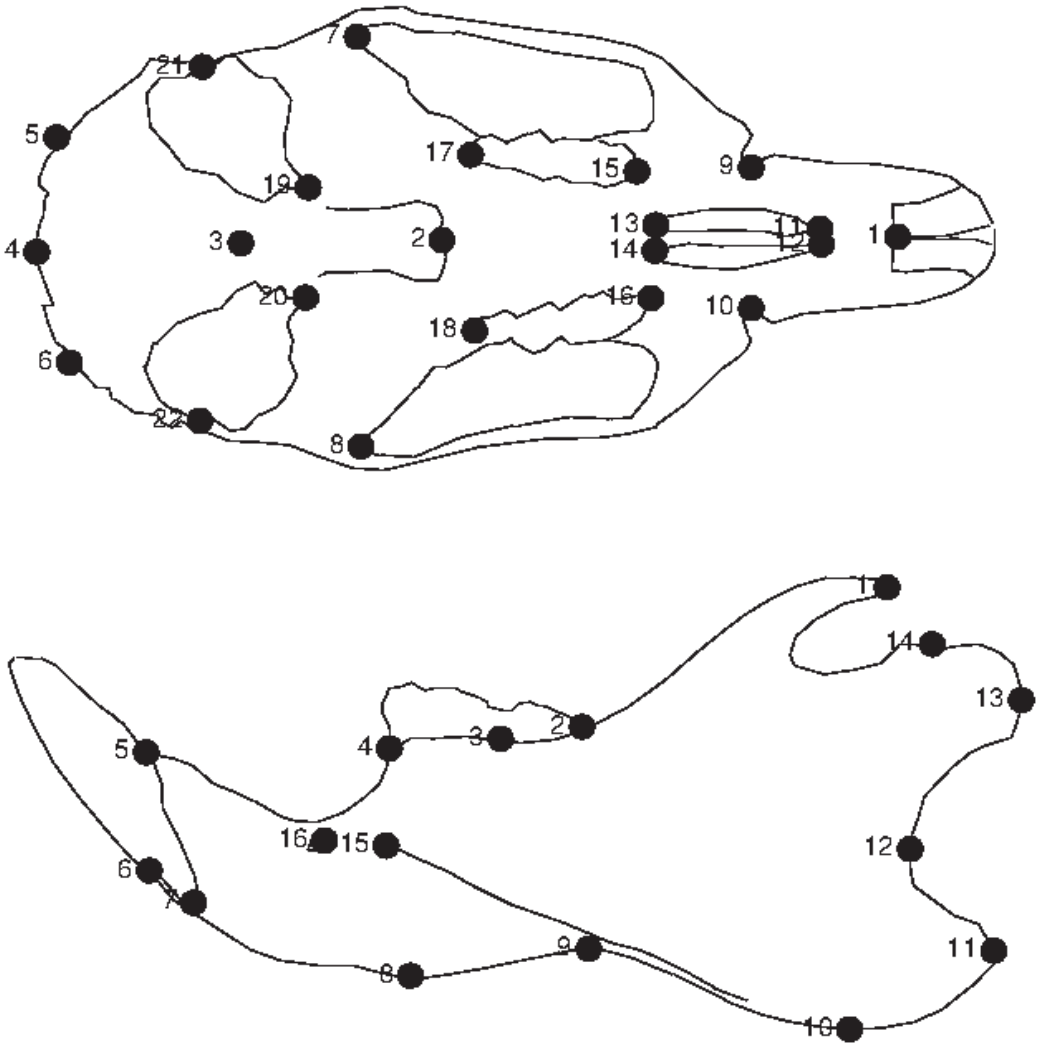

Figure 2. Outlines of the palatal view of the cranium, and lateral view of the mandible of *Rattus tanezumi*, displaying the landmarks used in this study.

data were then imported in R (R Core Team 2017) to be scaled, centered, and superimposed using Procrustes analyses functions from Claude (2008).

Interspecific shape variation among localities.

We perfomed a canonical analysis using the 'lda' function of package 'MASS' (Venables & Ripley 2002) on the whole dataset, with species and localities as grouping variables in order to assess the relative role of interspecific and locality effect in explaining some of the observed morphological differences.

Intraspecific shape analysis and morphological divergence between localities.

We ran series of linear discriminant analyses for each species, with the localities as the grouping variable, to reveal the structure of morphological variation at an inter-populational level (*i.e.* compare intra- and inter-population morphological distances and find the extent to which populations differ from each other). From these analyses, we computed the Mahalanobis distances between each pair of centroid of the discriminant space of each population, using the 'dist' function of package 'stats' (R Core Team 2017), which resulted in a morphological discrimination distance matrix. These distances were used as a proxy for the morphological divergence between populations in all species.

Within-locality morphological variation analyses.

To compute the average within-locality morphological variation, we fitted for each species a linear model of shape with locality as the explanatory factor (shape ~ locality). The intra-locality variation was assessed from the residuals of this linear model: we calculated the cross-product of the residual matrix divided by the number of individuals minus the number of localities for this species. We then used the trace of the resulting matrix as an index of average within-locality morphological

158 variation.

159

160 *Geographic distances calculations vs intraspecific morphological divergences.*

161 Latitude and longitude of each trapping sites were recorded by GPS during fieldwork. From
162 these, we were able to compute the shortest geographic distances between pairs of localities using the
163 'geosphere' package in R (Hijmans 2016). The result is a geographical distance matrix expressed in
164 meters, which was converted into kilometers (Table 2).

165 Both this matrix and the morphological discrimination distance matrix enable us to test the
166 correlation between morphological similarity and geographical distance. We did so by using a Mantel
167 test, with function 'mantel.test' from the package 'ape' version 4.1 (Paradis et al. 2004). We also used
168 Procrustes test (function 'protest' from the package 'vegan'; Oksanen 2017), which is less prone to false
169 positive errors (Peres Neto & Jackson 2001). Since we obtained the same results using both methods,
170 only results from the Mantel tests will be reported here.

171

172 *Comparison divergences and variation among species.*

173 To check whether species showed similar amount of morphological divergence across
174 sampling localities, we computed their respective ratio of the sum of Mahalanobis distances over the
175 sum of geographic distances across localities. To estimate the significance of differences among
176 species, we bootstrapped localities within species and re-computed the distance ratio 1000 times, to
177 obtain 95% confidence intervals.

178 The calculation of within-locality morphological variance (see above) was also bootstrapped
179 1000 times by resampling individuals and the corresponding localities. 95% confidence intervals were
180 obtained to check for significant differences of average intra-locality variation between species.

181

Functional differences in bite force.

During the two last fieldwork sessions, we were able to measure the rodents' *in vivo* bite force at the incisors, using a Kistler force transducer linked to a charge amplifier, similar to the set-up presented in Herrel et al. (1999) and Aguirre et al. (2002). After capture, we performed three consecutive trials for each animal. The maximal bite force recorded across the three trials was retained and used in subsequent analyses. In this study, we use bite force data of 92 individuals, including 30 specimens of *Rattus tanezumi*, 42 specimens of *Rattus exulans*, 13 specimens of *Mus caroli*, and seven specimens of *Mus cookii*.

We cleaned the crania and mandibles of these individuals as previously described, and digitized the same landmarks as shown in Fig. 2 on the mandibles. We then merged this geometric morphometric data with that of other specimens included in this study. These individuals were used as the training set to create several linear model of bite force. We fitted models with size, shape, and size+shape as explanatory variables. To assess the quality of estimates from these various models, we designed a leave-one-out cross validation approach. The process requires excluding one of the individuals from the training set, fitting the model on the 91 other individuals, then estimating the bite force of the excluded individual. Once this was done for each member of the training set, we could compare the estimated and *in vivo* bite forces by least-square linear regression to test the quality of estimates. Results from size, shape and size+shape models are presented in Supp. Mat. 1. Within the text, we only present the model including size as the only explanatory variable as it gave the best estimation of *in vivo* bite force (higher R^2 and correlation closer to 1). Then, the bite forces of the 593 other specimens included in this study were estimated by using the previously constructed model. To do so, we used the function 'predict' in R, which allowed estimation of bite force for these individuals based on their mandibular centroid sizes.

This estimated bite force dataset allowed us to test for performance differences between

populations within species. This was done by using a Tukey's HSD test to compare the mean estimated bite force all pairs of populations within one species.

Shared patterns of morphological responses.

To test whether our species showed similar morphological responses in their shared localities, we computed ANOVAs (for estimated bite force) and MANOVAs (for shape) on all pairs of localities in all pairs of species. Only individuals from shared localities between two species were included in the analyses. The tested models included shape, or bite force as the response variable(s), with species, localities and species:locality interaction as the explanatory variables. A significant effect of locality but a non-significant interaction represents similar morphological or functional responses in both species of the pair, between the pair of localities studied.

Results.

Interspecific linear discriminant analyses.

Overall, interspecific LDA from the cranial morphology (Fig. 3A) shows very good discrimination between species overall (99% of correct assignations with cross validations). However, discrimination between localities is not as good, with only 43% of correct assignations. Fig. 3A shows the separation of *Maxomys surifer* against all other species on the first discriminant axis, while the second discriminant axis separates mice from the rat species. The LDA based on mandibular shape (Fig. 3B) also shows very good discrimination between the five species (97% of correct assignations). The first axis appears to separate the three genera (*Maxomys*, *Rattus*, and *Mus*), as well as partly discriminates both *Rattus* and *Mus* species. This axis also shows a size ordination from *M. surifer* (largest) to *M. caroli* (smallest). The second axis discriminates *M. surifer* from other rats, as well as *M.*

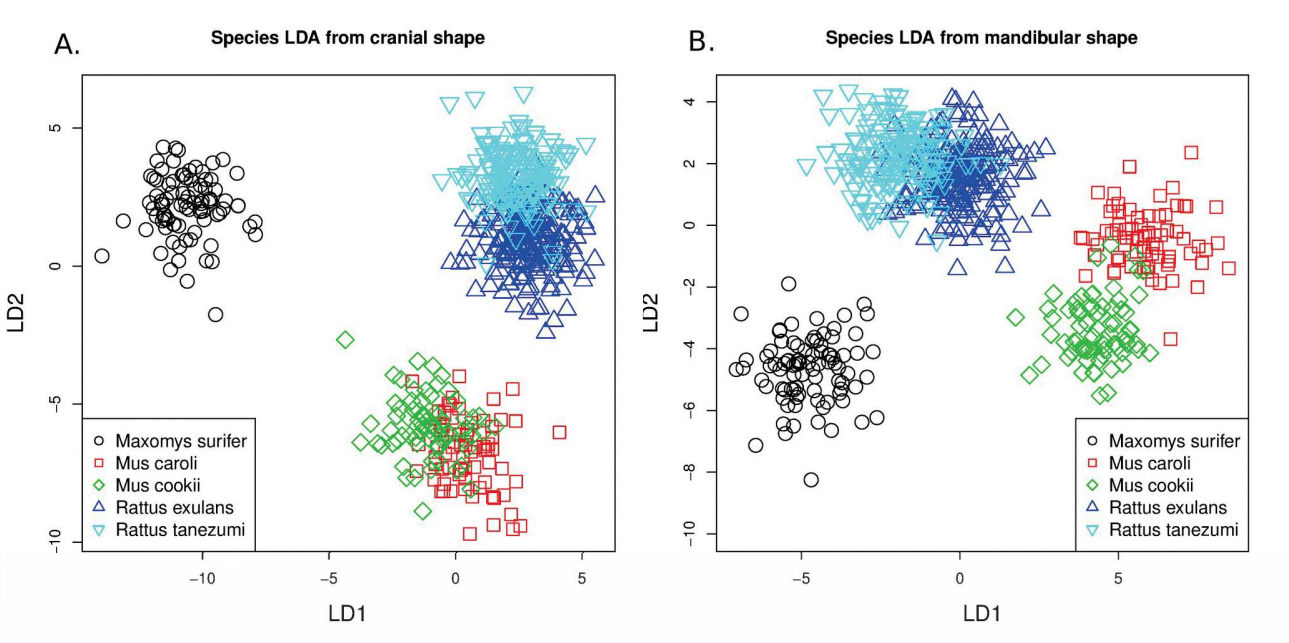

Figure 3. Linear discriminant analyses of skull shape with species and localities as the grouping variables. Only species differences are visible in these analyses.

cookii from *M. caroli*. Here as well, separation between localities within species is not good with 47% of correct assignations.

Intraspecific discriminant analyses and geographic divergence.

Mus caroli.

In this species, significant morphological differences were detected between localities both for the cranium (MANOVA: Pillai = 2.158 ; F = 1.375 ; df = 200, 155 ; $P < 0.05$) and the mandible (MANOVA : Pillai = 2.969 ; F = 2.246 ; df = 140, 215 ; $P < 0.001$). Along the LD1 (Fig. 4A), two clusters are visible, one containing populations from Kalasin (KAL), Buriram (BUR) and Loei (LOE), the other with those from Nan (NAN), Vientiane (VIE), and Prachuap (Pra); on LD2 Buriram is well discriminated from all other localities. However, the cross-validated correct assignation rate of this LDA only reaches 35% of good classifications. Mandible morphology discrimination (Fig. 4B) is

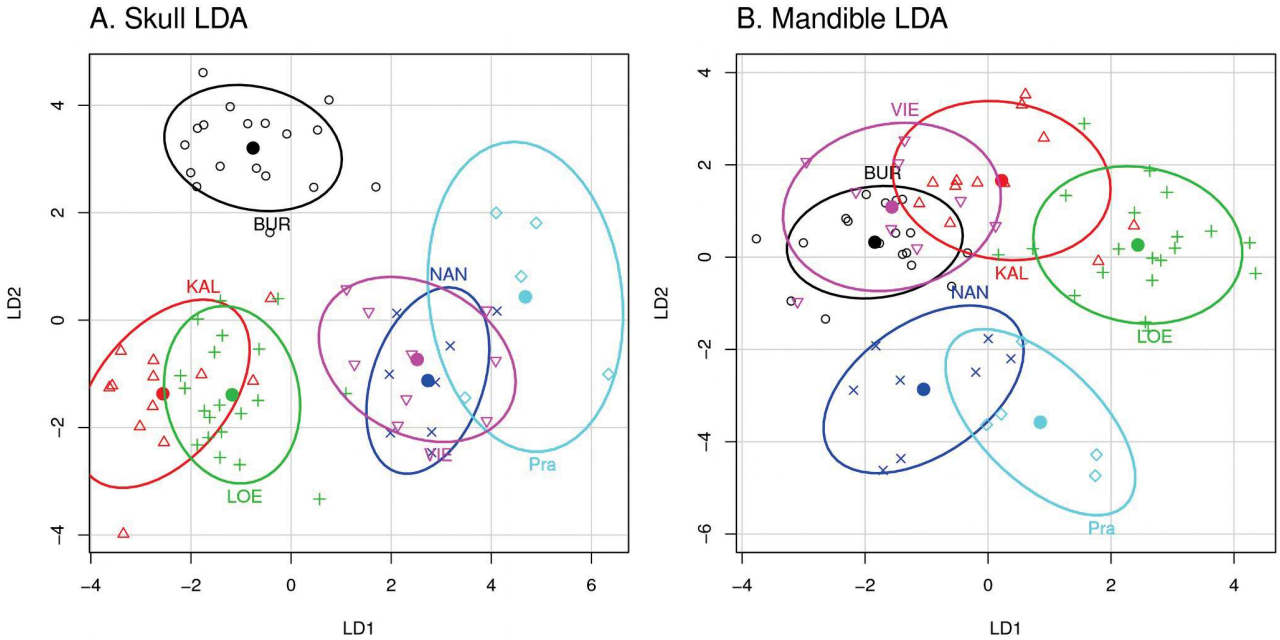

Figure 4. Linear discriminant analyses of the A) palatal cranium shape and B) mandible shape of *Mus caroli*, with localities as the grouping variable. Ellipses represent the 70% intervals for each group. Abbreviations: BUR, Buriram ; KAL, Kalasin ; LOE, Loei ; NAN, Nan ; Pra, Prachuap ; VIE, Vientiane.

better, with 54% of correct assignations. The Buriram and Vientiane populations can be separated from the Kalasin and Loei ones along LD1, while Nan and Prachuap can be differentiated t from other localities on LD2.

Mahalanobis distances from both the cranium and mandible analyses are not significantly correlated to geographic distances between localities (Mantel test: p = 0.12 and 0.08, respectively).

Mus cookii.

In *M. cookii*, as in *M. caroli*, morphological differences between localities are significant for both the cranium (MANOVA: Pillai = 2.231; F = 2.176; df = 120, 90, P < 0.001) and the mandible (MANOVA: Pillai = 1.661; F = 1.860; df = 84, 126; P < 0.001). The cranial morphology allows very good discrimination of the Kanchanaburi population against all others (LD1 on Fig. 5A), while the three other localities can also be separated along the second discriminant axis. In total, this analysis

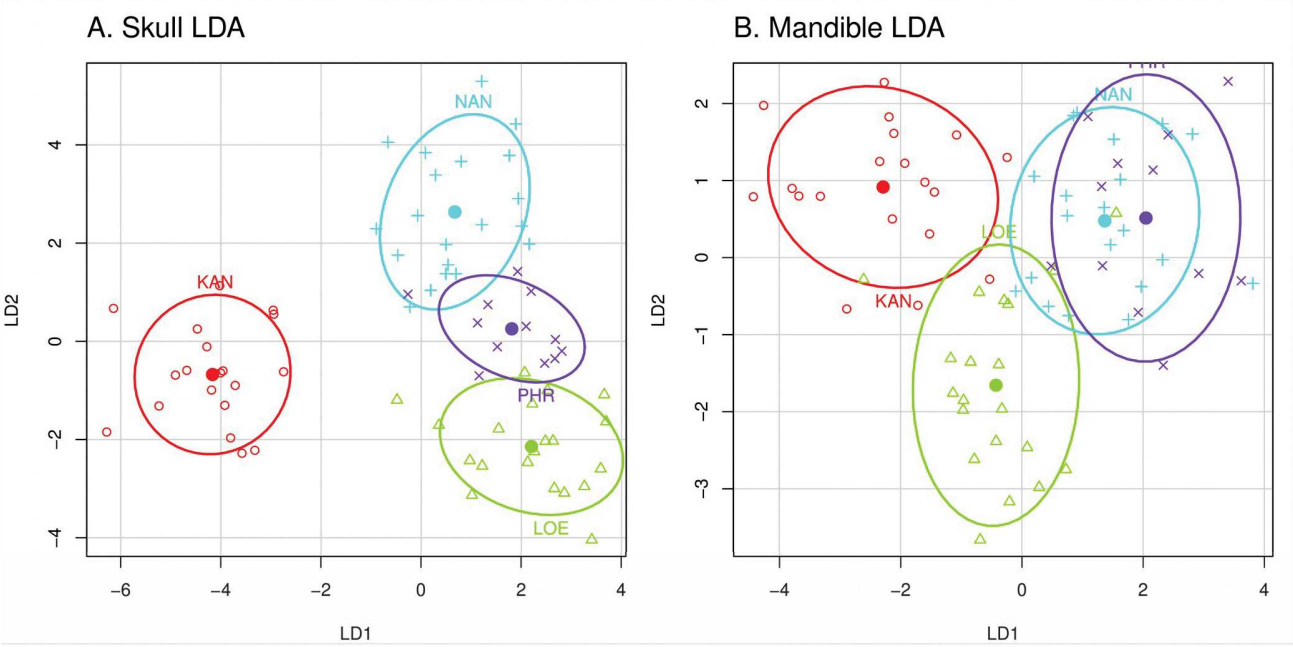

Figure 5. Linear discriminant analyses of the A) palatal cranium shape and B) mandible shape of *Mus cookii*, with localities as the grouping variable. Ellipses represent the 70% intervals for each group. Abbreviations: KAN, Kanchanaburi ; NAN, Nan ; LOE, Loei ; PHR, Phrae.

allows a correct classification in 49% of the cases. A slightly different pattern is observed when looking at mandibular morphology (Fig. 5B). The Kanchanaburi population is still discriminated on the first axis (although less clearly than with the cranium), but the second axis separates the Loei population from all others. The Phrae and Nan populations greatly overlap, although. Here, 46% of correct assignations are obtained after cross validation.

As in *M. caroli*, morphological distances are uncorrelated to geographic distance, both for the cranium and mandible (both $p > 0.2$).

Maxomys surifer.

Morphological differences between localities are significant for both the cranium (MANOVA: Pillai = 3.615; F = 2.937; df = 200, 225; $P < 0.001$) and the mandible (MANOVA: Pillai = 3.165; F = 3.573; df = 140, 290; $P < 0.001$). In the cranium discriminant analysis (Fig. 6A, 55% of correct

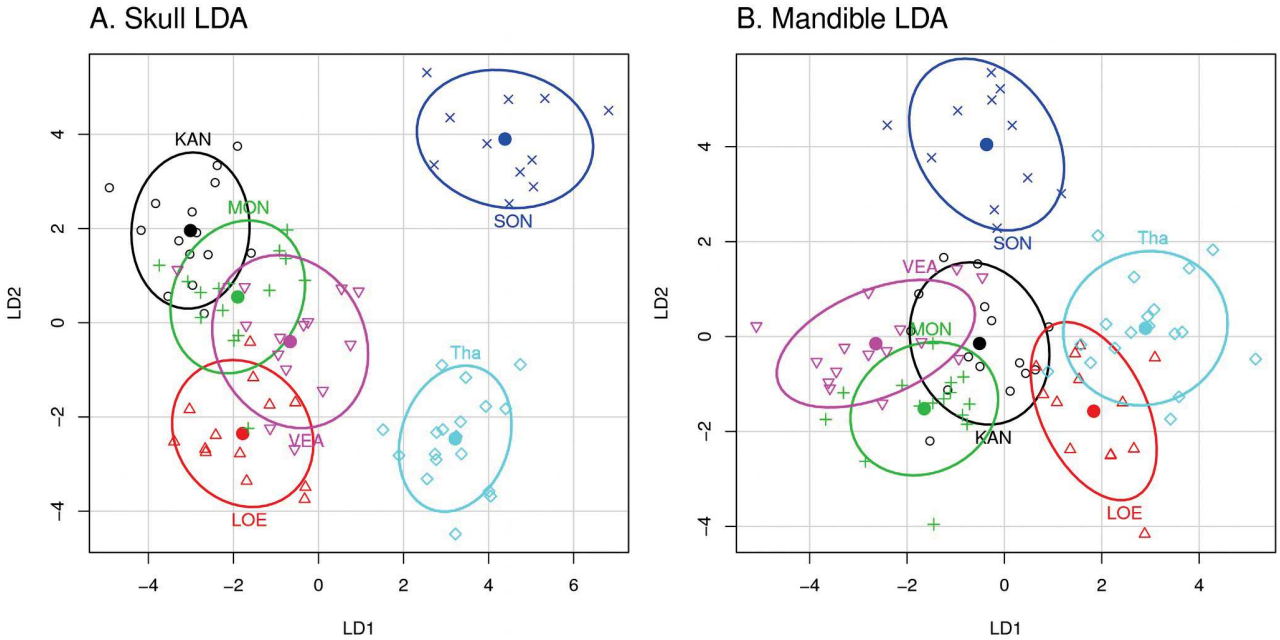

Figure 6. Linear discriminant analyses of the A) palatal cranium shape and B) mandible shape of *Maxomys surifer*, with localities as the grouping variable. Ellipses represent the 70% intervals for each group. Abbreviations: KAN, Kanchanaburi ; LOE, Loei ; MON, Mondolkiri ; NAN, Nan ; SON, Songklah ; VEA, Veal Renh.

classifications), the Songklah (SON) and Nan (Tha) populations are clearly discriminated from all others on the first discriminant axis, while they are widely separated from each other on the second axis. Other localities congregate in the negative values of the first discriminant axis, and are partly separated along the second axis. Mandibular morphology (Fig. 6B, 63% of correct assignations) discriminates Songklah from all other localities, while the latter are split into two clusters (Nan + Loei and Veal Renh (VEA) + Mondolkiri (MON)) along the first axis. Kanchanaburi appears intermediate between both of these clusters.

Morphological distances from the cranium do not correlate to geographic distances (Mantel test: $p = 0.28$). However, distances from the mandibular morphology are significantly related to the distance between pairs of localities (Mantel test: $z = 58628.3$, $p < 0.001$).

Rattus exulans.

In *R. exulans*, we retrieved significant morphological differences between localities in both the cranium (MANOVA: Pillai = 4.063; F = 1.997; df = 480, 1872; P < 0.001) and the mandible (MANOVA: Pillai = 3.450; F = 2.436; df = 336, 2028; P < 0.001). Despite this, both the cranium and mandible LDA show important overlap of most localities (Fig. 7A and B, 32% and 41% of correct classifications, respectively). However, both analyses also reveal two fairly well separated clusters along the first discriminant axis. These clusters comprise the Mondolkiri, Kanchanaburi, Loei, Kalasin, Buriram, Nan and Phrae populations on the one hand, and the Pursat, Vientiane, Caoh Lanh, Paksé, and Prachuap populations on the other hand.

Morphological distances for both the cranium and mandible are not significantly correlated to geographic distances (Mantel test: both p > 0.1).

Rattus tanezumi.

Significant differences between localities are found in the cranium (MANOVA: Pillai = 3.285; F

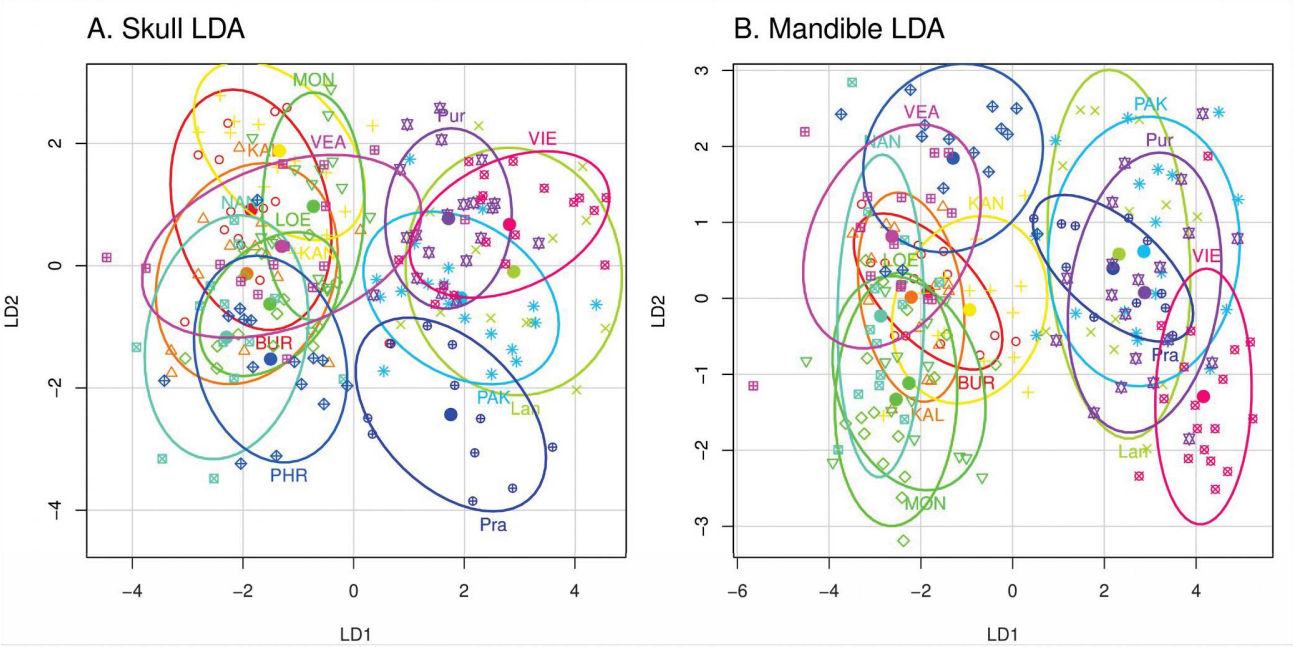

Figure 7. Linear discriminant analyses of the A) palatal cranium shape and B) mandible shape of *Rattus exulans*, with localities as the grouping variable. Ellipses represent the 70% intervals for each group. Abbreviations: BUR, Buriram ; KAL, Kalasin ; KAN, Kanchanaburi ; Lan, Cao Lanh ; LOE, Loei ; MON, Mondolkiri ; NAN, Nan ; PAK, Pakse ; PHR, Phrae ; Pra, Prachuap ; Pur, Pursat ; VEA, Veal Renh ; VIE, Vientiane.

= 1.504; df = 400, 1230; P < 0.001) and the mandible (MANOVA: Pillai = 3.140; F = 2.223; df = 280, 1360; P < 0.001). As in *R. exulans*, populations of *R. tanezumi* appear to show important morphological overlap, especially for the cranium (Fig. 8A, 27% of correct classifications). However, in the mandible discriminant analysis, two clusters can be distinguished along LD1 (Fig. 8B, 42% of correct classifications): one including the Nan, Kanchanaburi, Loei, Kalasin, Buriram and Phrae populations, and the other comprising the Chantaburi, Luang Prabang, Caoh Lanh, Prachuap and Pursat populations. A similar pattern can be seen in the cranium analysis, but the separation between the two clusters is weaker.

Like for *R. exulans*, morphological distances are uncorrelated to geographic distances (Mantel test : both p > 0.3) in *R. tanezumi*.

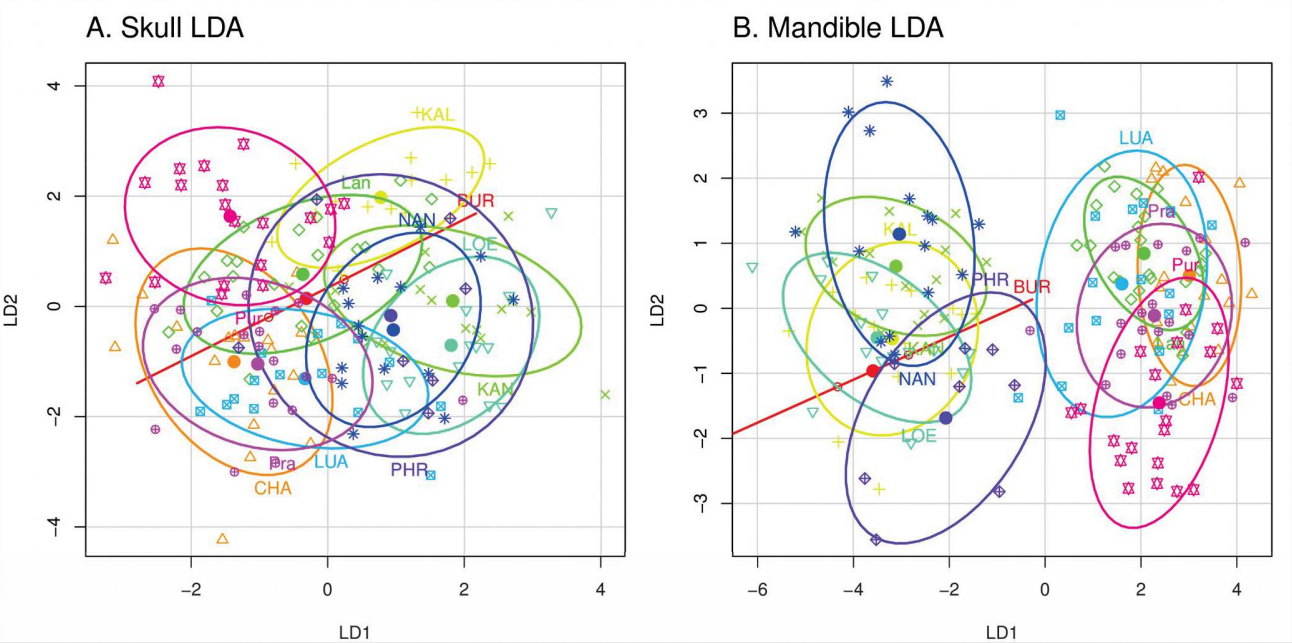

Figure 8. Linear discriminant analyses of the A) palatal cranium shape and B) mandible shape of *Rattus tanezumi*, with localities as the grouping variable. Ellipses represent the 70% intervals for each group. Abbreviations: BUR, Buriram ; CHA, Chantaburi ; KAL, Kalasin ; KAN, Kanchanaburi ; Lan, Cao Lanh ; LOE, Loei ; LUA, Luang Prabang ; NAN, Nan ; PHR, Phrae ; Pra, Prachuap ; Pur, Pursat.

Interspecific comparison of between-locality divergences and within-locality variances.

Our bootstrapped estimates for mean between-locality distance ratios within species showed that rats were overall less morphologically divergent than mice (Fig. 9). Based on mandibular morphology, *M. surifer* has particularly low ratio values (Fig. 9A), while the three rat species show equivalent values when looking at cranial morphology. However, the 95 % intervals overlap in all

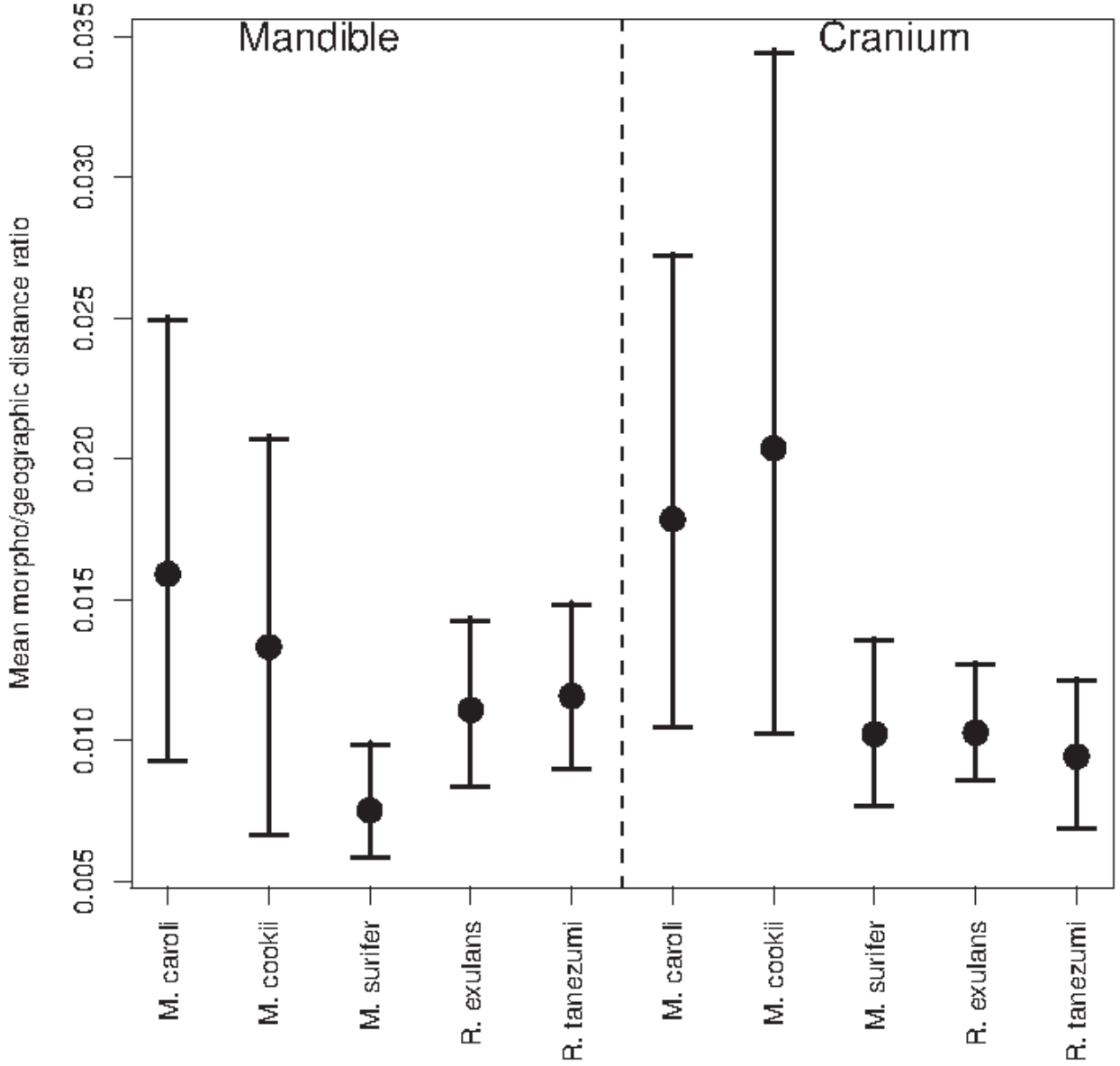

Figure 9. Mean morphological divergence between localities, within species (computed as the mean Mahalanobis distance / Mean geographical distance ratios for each species). Error bars represent the 95% confidence intervals obtained by 1000 bootstraps of the localities.

310 cases, therefore interspecific differences are not significant in the amount of mean morphological
311 divergence between-locality.

312 Interspecific differences in mean within-locality variation show a different pattern (Fig. 10).
313 Here, both *Rattus* species show lower intra-locality morphological variation, while *M. surifer* is closer
314 to the mice species. The 95% confidence intervals show that the difference between *Rattus* versus other

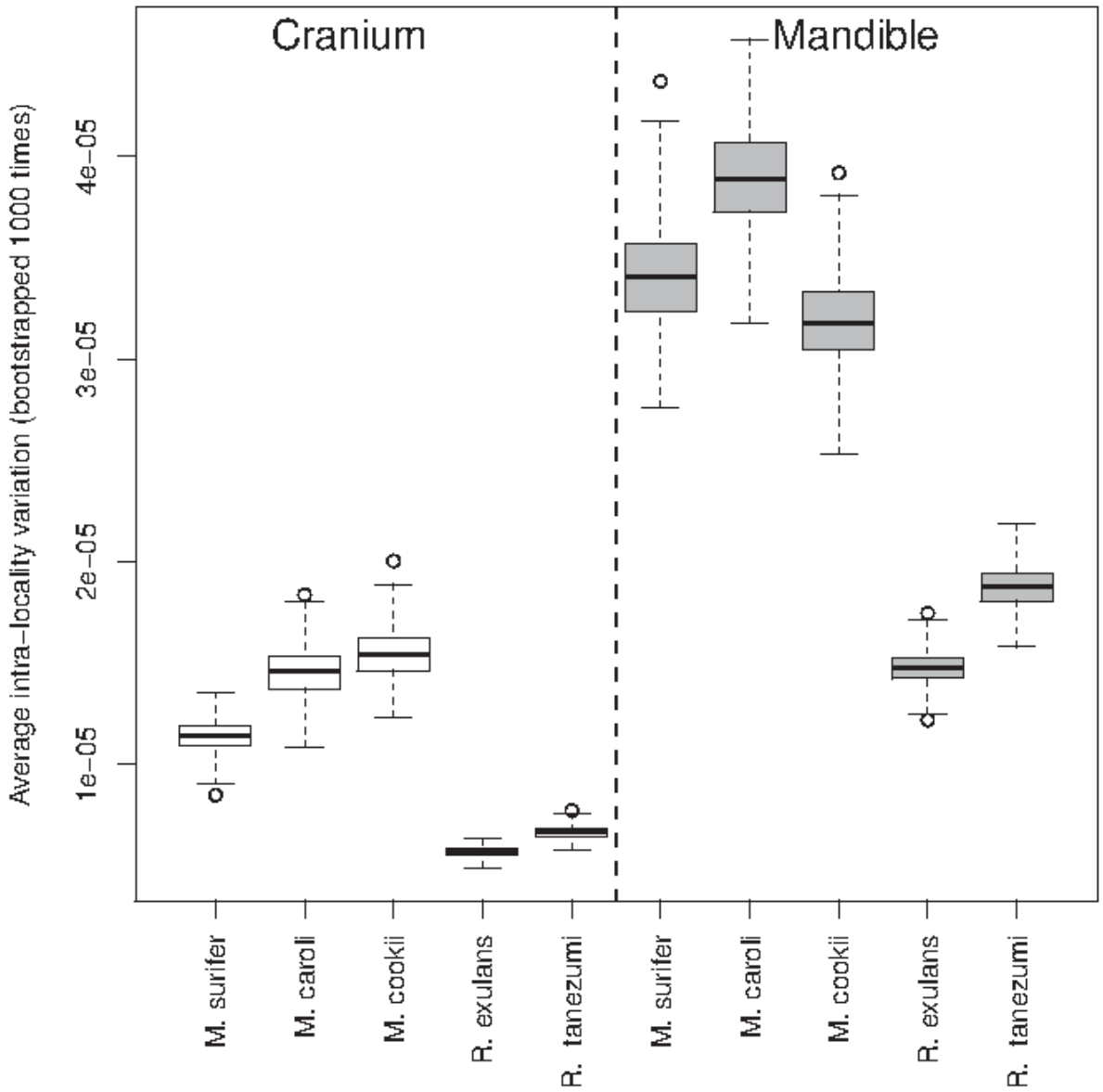

Figure 10. Boxplots of the average morphological variation (based on distances in the discriminant space) within locality and within species, with error bars showing 95% intervals obtained by bootstrapping individuals 1000 times.

315 species is significant. Differences were not significant between the two *Rattus* species, nor between the
316 mice and *M. surifer*. Whatever the species, the mandible is always significantly more variable than the
317 cranium.
318
319 *Bite force differences among populations*
320 Among the 92 individuals for which both *in vivo* and estimated bite force values were available,
321 the correlation between them was significant (Estimate = 0.78, R^2 = 0.77, df = 90, $p<0.001$). The
322 residual variation remains large (see Supp. Mat. 1), and individual estimations are therefore imprecise
323 (Fig. 11), but we expect that this correlation is sufficiently robust to reveal potential between-
324 population differences. Residuals of the model were normally distributed (Shapiro-Wilk normality test :
325 W = 0.98, p = 0.17).
326 We therefore used the model to estimate bite force in individuals for which *in vivo* values were
327 lacking, to see if variation in size could be linked to performance differences between localities.
328
329 *Mus caroli.*
330 This species displayed significant between-population variation in bite force (Fig. 12, Table
331 3A). However, no population had significantly higher or lower mean bite force than the others
332
333 *Mus cookii.*
334 The Kanchanaburi population displays higher estimated bite force than the others. Indeed, the
335 KAN individuals have significantly higher mean bite force than those from Phrae (PHR), Loei (LOE)
336 and Nan (all differences > 3; all P < 0.001). On the other hand, no significant difference appeared
337 among these three localities (Table 3B).
338

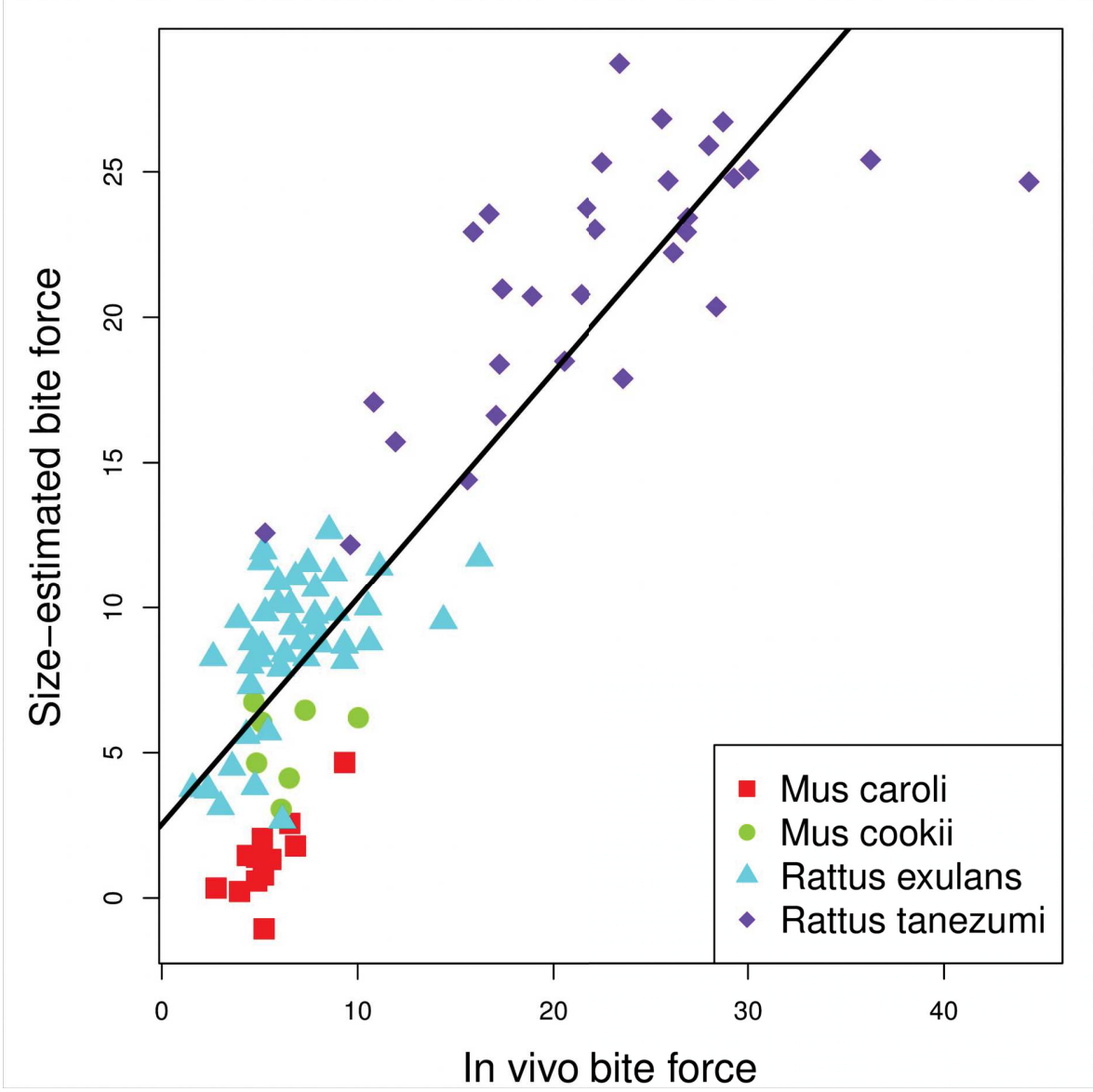

Figure 11. Scatterplot of size-estimated bite force against *in vivo* bite force showing the good correlation between both. The black line represents the least-squares linear regression line.

Maxomys surifer.

In this species, the Mondolokiri (MON) and Songklah (SON) populations show significant differences in estimated bite force from other localities (Fig. 12, Table 3C). The Mondolkiri population displays higher mean bite force than all other populations except Veal Renh (VEA). On the other hand, the Songklah population has a smaller mean bite force than all other localities. The Veal Renh population also has high mean bite force, but it is only significantly higher than the Songklah and Nan

populations.

Rattus exulans.

Significant differences in mean bite force are found between *R. exulans* population (Fig. 12, Table 3D). In particular, the Buriram population has significantly lower mean bite force than the Kanchanaburi, Cao Lanh, Mondolkiri, and Nan populations. The Nan, Cao Lanh, and Mondolkiri, on the other hand, have higher mean bite force than the other localities, sometimes significantly so (Table 3D). The differences in mean bite force do not parallel the separation between groups from the discriminant analysis (Fig. 7B).

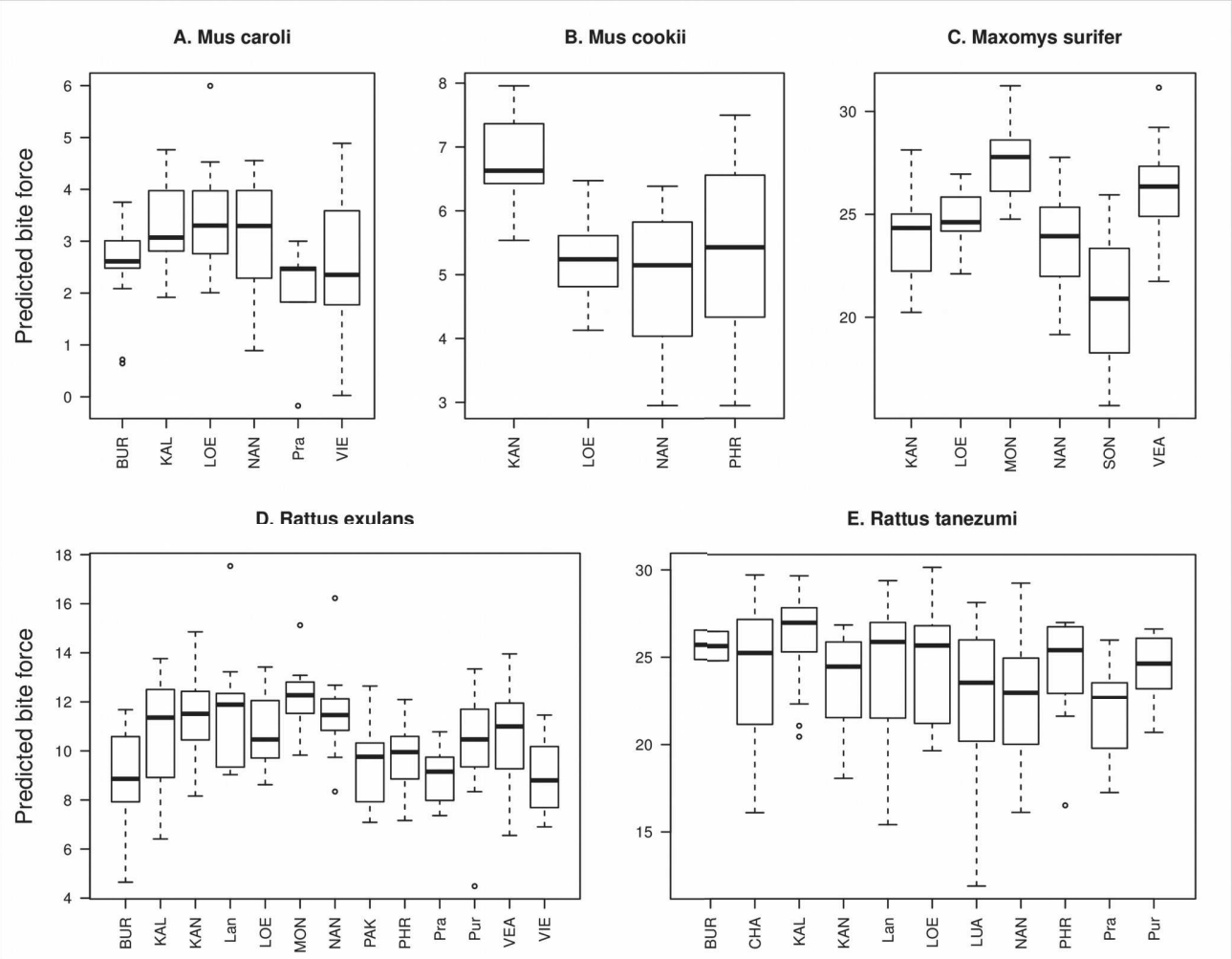

Figure 12. Boxplots of estimated bite force within localities for each species.

355 *Rattus tanezumi.*

356 In this species, inter-population variation is present (Fig. 12, Table 3E), but difference in mean
357 bite force is only significantly higher in Kalasin (KAL) compared to Prachuap (Pra).

358

359 *Tests of morpho-functional responses in pairs of species.*

360 Species pairwise MANOVAs comparing shape variation between pairs of shared localities
361 revealed morphological parallel changes in overall 22% of the cases (Table 4). Pairs of species that
362 mostly had similar responses were *M. caroli* and *R. tanezumi* (40% of cases), *M. cookii* and *R. exulans*
363 (50% of cases), *M. cookii* and *R. tanezumi* (50% of cases), and *R. exulans* and *R. tanezumi* (22.2% of
364 cases).

365 Regarding bite force (estimated from centroid size of the mandible), pairwise ANOVAs also
366 showed parallel responses in 22% of the cases (Table 4). Again, *M. surifer* did not show similar
367 responses with the other species, but *M. caroli* did with *R. exulans* (40% of cases) and *R. tanezumi*
368 (20% of cases), *M. cookii* with *R. exulans* (33.3% of cases) and *R. tanezumi* (16.7% of cases), and *R.*
369 *exulans* with *R. tanezumi* (22.2% of cases).

370 Surprisingly, shape changes and bite force changes were not always conjunct. Although this is
371 certainly explained by the fact that bite force was estimated through size, it still suggests that evolution
372 of bite force through size and shape may be achieved separately. However, it should also be noted that,
373 overall, species pairs showing similar morphological responses were the same for bite force and shape.

374

375 **Discussion.**

376

377 *Interspecific identification and intraspecific locality discrimination.*

378 Our analyses showed very good discrimination between species, even for closely related ones,

379 both using the mandibular and cranial shape. Within species, the discrimination between localities was
380 not as good despite significant differences. *Rattus* species in particular showed only 27 to 42% of
381 assignations to the correct locality, while the *Mus* species had between 35 and 54%, and *Maxomys*
382 *surifer* between 55 to 63% whether we considered crania or mandibles.

383 The Mahalanobis distances computed from these LDAs showed no significant correlation with
384 geographical distance, except for *M. surifer*. This supports a lack of a morphological isolation-by-
385 distance except in the latter species. In most species, differences are not accumulating according to the
386 geographical distance (at least partially), but may reflect a more complex structuring with local
387 particularities (this could reflect particular environmental condition and local adaptations or phenotypic
388 plasticity responses). For instance, the two clusters recognized in *R. exulans* (Fig. 7A and 7B) likely
389 separate one group containing populations from the Mekong river basin from all other localities. For *R.*
390 *tanezumi*, a similar clustering was found (Fig. 8A and 8B), this time separating northern localities
391 (except Luang Prabang) from southern ones (plus Luang Prabang).

392

393 *Average between-locality morphological divergence.*

394 The ratio of morphological divergence over geographical distance was higher for the mice
395 species than for the rats, including *M. surifer.* It suggests that mice tend to diverge morphologically
396 more than rats in localities located at an equal distance. However, 95% confidence intervals showed
397 that these differences were not significant. The non-significance of these results may be due to the fact
398 that we bootstrapped localities, and that in some species we sampled only four or six localities.
399 Therefore this test may be overly conservative. This analysis complements the results of the LDAs, and
400 shows that the discrimination of *M. surifer* populations is likely explained by the large distance
401 between the studied localities (rather than a particular tendency to morphologically diverge) since its
402 morphological divergence over distance ratio is low. This brings evidence in favor of a morphological

isolation-by-distance for this species, by slow, random morphological change rather than by major local adaptations (Renaud et al. 2007), probably linked to its limited habitat range.

Within-locality morphological variation.

The mice species and *M. surifer* show significantly larger variation within localities than the *Rattus* species. Furthermore, the variation in the mandible is much higher than in the cranium in all species. Reduced variation was expected in *R. exulans* due to its fully commensal lifestyle, producing a homogeneous environment and reducing the propensity to disperse locally (Brouat et al. 2007, Hulme-Beaman 2016). A similar low within-population variance was found for *R. tanezumi*, which may be due to its very generalist lifestyle. Such a low variance suggests that the morphology of its masticatory apparatus is polyvalent enough to cope with various functional demands (as proposed for *R. norvegicus* by Cox et al. 2012), without requiring major adaptive or plastic changes. The difference in variation between the mandible and cranium may be explained by a larger plasticity or evolvability of the mandible, while the palatal side of the cranium may be more phylogenetically and developmentally constrained (e.g. Caumul and Polly 2005).

Morpho-functional local morphological responses.

Our pairwise analyses of shape and bite force clearly show fairly frequent similar morphological responses, notably between *Rattus tanezumi* and *Rattus exulans*, but also between these rats and *Mus caroli* or *Mus cookii*. While the first result was expected due to the close relationship between the two rats, both phylogenetically and ecologically, the latter results were more unexpected. Indeed, *Mus caroli* and *Mus cookii* have fairly divergent ecologies from both *Rattus* species. *Maxomys surifer,* on the other hand has almost no case of identical response except one with *R. exulans*. Although this latter case is intriguing, the overall lack of similarities is coherent with the more specialized, and

non-synanthropic lifestyle of this species compared to the others.

Looking more closely at the cases of similar responses between the *Mus* and *Rattus* species, trapping data shows that, in the same locality, the mice and rats were usually caught in different places, in accordance with their average ecology (Table 1). This suggest that the morphology of the species does not respond to similar species ecological displacements in the pair of localities studied, but rather to regional differences, affecting all the niches in at a time.

Drivers of morphological divergence and variation.

The species studied here display various modes of morphological diversification, potentially linked to their relationship with humans. *Maxomys surifer* is the only species in which morphological divergence is significantly correlated to geographic distances between localities. This particular species is a forest-dwelling rat, and the rampant deforestation of Southeast Asia (Sodhi et al. 2004, 2009) probably constitutes a very limiting factor to the dispersal of individuals. Yet, our results also suggest that the *M. surifer* populations did not diverge greatly in proportion to their geographic separation, compared to other species. These results taken together suggest that the skull morphology of *M. surifer* has only slightly evolved, and probably through evolutionary drift linked to isolation-by-distance at longer timescales than human-mediated changes, rather than through local adaptations.

In the mice species, distance is not significantly correlated to morphological changes. In *M. cookii*, the Kanchanaburi population differs from the others both morphologically (Fig. 5A and 5B) and functionally (Fig. 12). The presence of this species in this region has never been reported yet (Marshall 1977, Aplin et al. 2016), and it may represent a population (or subspecies) isolated in a refugia during climatic extremes. If it is the case, the isolation of the population, coupled with the local environmental conditions, may have driven the observed morpho-functional changes. In *M. caroli*, the Buriram population is separated from the others only by its cranial morphology (Fig. 4A), and is grouped with

451 the Kalasin and Loei populations by its mandibular morphology. Distance does not drive morphological
452 change in this species, as some very distant populations are grouped in the LDA (e.g. Prachuap and
453 Nan). However, we did not find any significant bite force difference between the populations either. In
454 this species, morphological changes may be linked to more subtle functional differences than just
455 maximal bite force at the incisors (e.g. gape, molar bite force, speed of jaw movements). Furthermore,
456 since this species relies almost exclusively on agricultural resources (Shimada et al. 2007), its diet
457 might be more homogeneous across the localities, which may limit the need for local adaptations in
458 terms of bite force.

459 Both mice species show similar patterns in term of average divergence, with higher divergence
460 over distance ratios (although not significantly) than all rat species. This may suggest that mice show a
461 greater tendency for local morphological evolution (regardless of the driver) than rats. It may also be
462 linked to differences in migratory patterns with mice showing a lower tendency to disperse than rats or
463 being less passively transported via human movements. Additionally, the mice, as well as *M. surifer*,
464 show much higher intra-locality variation than *R. exulans* and *R. tanezumi*. This suggests that the
465 commensal and generalist lifestyles have a significant influence on morphological variance and tend to
466 stabilize it (however human environments may not be as stable as sometimes thought, see Hulme-
467 Beaman et al. 2016).

468 In *R. exulans*, the main morphological divergence involved a "Mekong subgroup", which may
469 suggest that populations along this river are being permanently admixed via boat transportation. These
470 populations may also represent a more historical picture of ancestral populations that came from insular
471 Southeast Asia (Thomson et al. 2014) and colonized mainland Southeast Asia via the coast and rivers.
472 In both cases, the Mekong river seems to represent a major migratory pathway, and suggests that *R.*
473 *exulans* also has important long-distance dispersal capacities despite showing uniform populations at
474 the locality level.

475 *R. tanezumi* also shows little divergence between localities. The two clusters found in the LDA
476 seem to broadly separate northern from southern localities, which may represent historically isolated
477 refugia populations. This was previously suggested by Pagès and colleagues (2013) and, although the
478 localities sampled do not match perfectly, there seems to be some congruence between their 'R3
479 lineage' and *R. tanezumi* distributions and our two clusters. Pagès et al. (2013) confirmed that the R3
480 lineage was included within *R. tanezumi* and suggested that it was a previously isolated population.
481 They also showed that genetic fluxes were fully reestablished between the two populations nowadays.
482 Our results support this hypothesis, since both clusters are now morphologically overlapping However,
483 the locality of Luang Prabang does not match the pattern observed by Pagès et al. (2013), because it
484 would be expected to cluster with the northern localities.

485 Results from the paired morphological response analyses (Table 4) show that when looking
486 more closely at cases of similarities, *Mus* and *Rattus* species often experience parallel changes between
487 pairs of localities. This suggests that, despite the previously described historical or migratory patterns
488 observed in the *Rattus* genus, regional adaptation also participates (perhaps to a lesser extent) to
489 differences between localities.

490

491 **Conclusion**

492 As expected, interactions between Southeast Asian murine rodents and humans have important
493 consequences on morphological variation of their skulls. The morphology of the two rat species that
494 may be found in settlements and cities (*R. exulans* and *R. tanezumi*) is indicative of frequent passive
495 long-distance dispersal between localities, or of historical population splits. Although the mice species
496 studied here (*M. caroli* and *M. cookii*) are dependent on agriculture as a food source, they
497 morphologically diverge among localities more than rats. This may be due to less frequent long-
498 distance relocation (although examples exist, e.g. Shimada et al. 2007), or to a greater skull evolvability

499 (or adaptive phenotypic plasticity). Thes latter possibility is supported by the fact that *M. surifer*
500 populations do not show great morphological divergence in proportion to their distances. In this
501 species, the isolation created by deforestation is probably the main limiting factor to migration, since
502 *M. surifer* is ecologically restricted to forests.

503 At the community level, anthropized environments still offer variable niches within different
504 levels of anthorpization to murine rodents, including secondary and/or logged forests, agricultural
505 fields, gardens or houses, which when combined form a new adaptive landscape with multiple peaks.
506 Thanks to their adaptability, murine rodents are able to sustain or even take advantage of these changes,
507 making these communities a great model to look at the effects and evolution of synanthropy and
508 commensalism (Hulme-Beaman et al. 2016).

509

510 **References**

511 Achmadi, A. S., Esselstyn, J. A., Rowe, K. C., Maryanto, I., & Abdullah, M. T. (2013). Phylogeny,
512 diversity, and biogeography of Southeast Asian spiny rats (Maxomys). *Journal of*
513 *Mammalogy*, *94*(6), 1412-1423.

514 Aplin, K. P., Suzuki, H., Chinen, A. A., Chesser, R. T., Ten Have, J., Donnellan, S. C., ... &
515 Catzeflis, F. (2011). Multiple geographic origins of commensalism and complex dispersal
516 history of black rats. *PloS one*, *6*(11), e26357.

517 Claude, J. (2008). *Morphometrics with R*. Springer Science & Business Media.

518 Claude, J.(2017). The continental fossil record and the history of biodiversity in Southeast Asia. In:
519 *Biodiversity Conservation in Southeast Asia: Challenges in a Changing Environment*. Eds.
520 Serge Morand, Claire Lajaunie, Rojchai Satrawaha.

521 Cox, P. G., Rayfield, E. J., Fagan, M. J., Herrel, A., Pataky, T. C., & Jeffery, N. (2012). Functional
522 evolution of the feeding system in rodents. *PLoS One*, *7*(4), e36299.

523 Blasdell, K., Bordes, F., Chaisiri, K., Chaval, Y., Claude, J., Cosson, J. F., ... & Tran, A. (2015).
524 Progress on research on rodents and rodent-borne zoonoses in South-east Asia. *Wildlife*
525 *Research*, *42*(2), 98-107.

526 Boonsong, L., & McNeely, J. A. (1977). Mammals of Thailand. *Mammals of Thailand.*

527 Brouat, C., Loiseau, A., Kane, M., Bâ, K., & DUPLANTIER, J. M. (2007). Population genetic
528 structure of two ecologically distinct multimammate rats: the commensal *Mastomys*
529 *natalensis* and the wild *Mastomys erythroleucus* in southeastern Senegal. *Molecular*
530 *ecology*, *16*(14), 2985-2997.

531 Caumul, R., & Polly, P. D. (2005). Phylogenetic and environmental components of morphological
532 variation: skull, mandible, and molar shape in marmots (Marmota,
533 Rodentia). *Evolution*, *59*(11), 2460-2472.

534 Fabre, P. H., Pages, M., Musser, G. G., Fitriana, Y. S., Fjeldså, J., Jennings, A., ... & Supriatna, N.
535 (2013). A new genus of rodent from Wallacea (Rodentia: Muridae: Murinae: Rattini), and its
536 implication for biogeography and Indo-Pacific Rattini systematics. *Zoological Journal of*
537 *the Linnean Society*, *169*(2), 408-447.
538 Francis, R. A., & Chadwick, M. A. (2012). What makes a species synurbic?. *Applied*
539 *Geography*, *32*(2), 514-521.
540 Gorog, A. J., Sinaga, M. H., & Engstrom, M. D. (2004). Vicariance or dispersal? Historical
541 biogeography of three Sunda shelf murine rodents (*Maxomys surifer*, *Leopoldamys sabanus*
542 and *Maxomys whiteheadi*). *Biological Journal of the Linnean Society*, *81*(1), 91-109.
543 Hautier, L., Bover, P., Alcover, J. A., & Michaux, J. (2009). Mandible morphometrics, dental
544 microwear pattern, and paleobiology of the extinct Balearic Dormouse *Hypnomys*
545 *morpheus*. *Acta Palaeontologica Polonica*, *54*(2), 181-194.
546 Hulme-Beaman, A., Dobney, K., Cucchi, T., & Searle, J. B. (2016). An ecological and evolutionary
547 framework for commensalism in anthropogenic environments. *Trends in ecology &*
548 *evolution*, *31*(8), 633-645.
549 Marshall, J. T. (1977). A synopsis of Asian species of *Mus* (Rodentia, Muridae). Bulletin of the
550 AMNH; v. 158, article 3.
551 Matisoo-Smith, E., & Robins, J. H. (2004). Origins and dispersals of Pacific peoples: evidence from
552 mtDNA phylogenies of the Pacific rat. *Proceedings of the National Academy of Sciences of*
553 *the United States of America*, *101*(24), 9167-9172.
554 Michaux, J., Chevret, P., & Renaud, S. (2007). Morphological diversity of Old World rats and mice
555 (Rodentia, Muridae) mandible in relation with phylogeny and adaptation. *Journal of*
556 *Zoological Systematics and Evolutionary Research*, *45*(3), 263-279.
557 Morand, S., Bordes, F., Blasdell, K., Pilosof, S., Cornu, J. F., Chaisiri, K., ... & Herbreteau, V. (2015).

558 Assessing the distribution of disease-bearing rodents in human-modified tropical
559 landscapes. *Journal of Applied Ecology*, *52*(3), 784-794.
560 Pagès, M., Bazin, E., Galan, M., Chaval, Y., Claude, J., Michaux, J., Piry, S., ... & Cosson, J. F. (2013).
561 Cytonuclear discordance among Southeast Asian black rats (*Rattus rattus* complex). *Molecular*
562 *Ecology*, *22*(4), 1019-1034.
563 Pagès, M., Chaval, Y., Herbreteau, V., Waengsothorn, S., Cosson, J. F., Hugot, J. P., ... & Michaux,
564 J. (2010). Revisiting the taxonomy of the Rattini tribe: a phylogeny-based delimitation of
565 species boundaries. *BMC evolutionary Biology*, *10*(1), 184.
566 Peres-Neto, P. R., & Jackson, D. A. (2001). How well do multivariate data sets match? The
567 advantages of a Procrustean superimposition approach over the Mantel
568 test. *Oecologia*, *129*(2), 169-178.
569 Pergams, O. R., & Lawler, J. J. (2009). Recent and widespread rapid morphological change in
570 rodents. *PLoS One*, *4*(7), e6452.
571 Renaud, S., & Auffray, J. C. (2010). Adaptation and plasticity in insular evolution of the house mouse
572 mandible. *Journal of Zoological Systematics and Evolutionary Research*, *48*(2), 138- 150.
573 Renaud, S., Chevret, P., & Michaux, J. (2007). Morphological vs. molecular evolution: ecology and
574 phylogeny both shape the mandible of rodents. *Zoologica scripta*, *36*(5), 525-535.
575 Renaud, S., Gomes Rodrigues, H., Ledevin, R., Pisanu, B., Chapuis, J. L., & Hardouin, E. A. (2015).
576 Fast evolutionary response of house mice to anthropogenic disturbance on a Sub- Antarctic
577 island. *Biological journal of the Linnean Society*, *114*(3), 513-526.
578 Renaud, S., & Michaux, J. R. (2007). Mandibles and molars of the wood mouse, *Apodemus*
579 *sylvaticus* (L.): integrated latitudinal pattern and mosaic insular evolution. *Journal of*
580 *biogeography*, *34*(2), 339-355.
581 Samuels, J. X. (2009). Cranial morphology and dietary habits of rodents. *Zoological Journal of the*

582 *Linnean Society*, *156*(4), 864-888.
583 Sánchez-Villagra, M. R., Geiger, M., & Schneider, R. A. (2016). The taming of the neural crest: a
584 developmental perspective on the origins of morphological covariation in domesticated
585 mammals. *Open Science*, *3*(6), 160107.
586 Shimada, T., Aplin, K. P., Jogahara, T., Lin, L. K., Herbreteau, V., Gonzalez, J. P., & Suzuki, H. (2007).
587 Complex phylogeographic structuring in a continental small mammal from East Asia, the rice field
588 mouse, *Mus caroli* (Rodentia, Muridae). *Mammal Study*, *32*(2), 49-62.
589 Sodhi, N. S., Koh, L. P., Brook, B. W., & Ng, P. K. (2004). Southeast Asian biodiversity: an
590 impending disaster. *Trends in Ecology & Evolution*, *19*(12), 654-660.
591 Sodhi, N. S., Lee, T. M., Koh, L. P., & Brook, B. W. (2009). A meta-analysis of the impact of
592 anthropogenic forest disturbance on Southeast Asia's Biotas. *Biotropica*, *41*(1), 103-109.
593 Sodhi, N. S., Posa, M. R. C., Lee, T. M., Bickford, D., Koh, L. P., & Brook, B. W. (2010). The state
594 and conservation of Southeast Asian biodiversity. *Biodiversity and Conservation*, *19*(2), 317-
595 328.
596 Suzuki, H., Shimada, T., Terashima, M., Tsuchiya, K., & Aplin, K. (2004). Temporal, spatial, and
597 ecological modes of evolution of Eurasian *Mus* based on mitochondrial and nuclear gene
598 sequences. *Molecular phylogenetics and evolution*, *33*(3), 626-646.
599 Thomson, V., Aplin, K. P., Cooper, A., Hisheh, S., Suzuki, H., Maryanto, I., ... & Donnellan, S. C.
600 (2014). Molecular genetic evidence for the place of origin of the Pacific rat, *Rattus*
601 *exulans*. *PloS one*, *9*(3), e91356.
602 Valenzuela-Lamas, S., Baylac, M., Cucchi, T., & Vigne, J. D. (2011). House mouse dispersal in Iron
603 Age Spain: a geometric morphometrics appraisal. *Biological Journal of the Linnean*
604 *Society*, *102*(3), 483-497.
605 Walther, G. R. (2010). Community and ecosystem responses to recent climate change. *Philosophical*

606 *Transactions of the Royal Society of London B: Biological Sciences*, *365*(1549), 2019-2024.
607 Wilcove, D. S., Giam, X., Edwards, D. P., Fisher, B., & Koh, L. P. (2013). Navjot's nightmare
608 revisited: logging, agriculture, and biodiversity in Southeast Asia. *Trends in ecology &*
609 *evolution*, *28*(9), 531-540.
610

Tables

Table 1. Synthetic table of the ecologies of the species studied here, based on conclusion from Morand et al. (2015).

	Specialist/generalist	**Habitat**	**Synanthropy**	**Commensalism**
M. surifer	Specialist	Forest	no	no
M. cookii	mid	Agricultural fields (sloped)	yes	no
M. caroli	mid	Flooded agricultural fields	yes	no
R. tanezumi	Generalist	Human settlements	yes	yes
R. exulans	Specialist	Human settlements	yes	yes

615

616 **Table 2.** Geographical distances between the localities sampled. Abbreviations : CHA, Chantaburi (Thailand) ;
617 KAL, Kalasin (Thailand) ; KAN, Kanchanaburi (Thailand) ; Lan, Cao Lanh (Vietnam) ; LOE, Loei (Thailand) ;
618 LUA, Luang Prabang (Lao PDR) ; MON, Mondolkiri (Cambodia) ; NAN, Nan (Thailand) ; PAK, Pakse (Lao
619 PDR) ; PHR, Phrae (Thailand) ; Pra, Prachuap (Thailand) ; Pur, Pursat (Cambodi) ; SON, Songklah (Thailand) ;
620 VEA, Veal Renh (Cambodia) ; VIE, Vientiane (Lao PDR).

	BUR	CHA	KAL	KAN	Lan	LOE	LUA	MON	NAN	PAK	PHR	Pra	Pur	SON	VEA
CHA	247														
KAL	189	434													
KAN	437	359	541												
Lan	552	458	702	814											
LOE	320	507	221	450	872										
LUA	538	751	375	683	1076	251									
MON	508	520	607	871	223	810	975								
NAN	517	697	391	573	1068	197	139	996							
PAK	290	467	289	727	508	509	635	351	675						
PHR	475	623	391	461	1024	170	251	975	118	679					
Pra	507	294	673	276	662	662	911	784	819	759	715				
Pur	286	226	451	580	268	606	820	294	803	336	755	498			
SON	899	655	1088	794	669	1142	1392	883	1317	1050	1222	518	714		
VEA	471	304	650	642	197	781	1009	369	977	536	915	468	207	529	
VIE	343	565	183	560	881	117	196	789	216	461	250	755	624	1215	815

621

622 **Table 3.** Results of the Tukey HSD tests for differences in mean bite force between localities within
623 species. Abbreviations as in Table 2 and diff: difference between mean values ; lwr: lower interval ;
624 upr: upper interval ; p adj: adjusted p-value.

A. *Mus caroli*				
	diff	lwr	upr	p adj
KAL-BUR	1.84	-0.91	4.58	0.37
LOE-BUR	2.03	-0.36	4.42	0.14
NAN-BUR	1.17	-1.96	4.30	0.88
Pra-BUR	-1.58	-5.31	2.14	0.81
VIE-BUR	-0.24	-3.25	2.77	1.00
LOE-KAL	0.19	-2.50	2.88	1.00
NAN-KAL	-0.67	-4.03	2.70	0.99
Pra-KAL	-3.42	-7.34	0.50	0.12
VIE-KAL	-2.08	-5.32	1.17	0.43
NAN-LOE	-0.86	-3.94	2.22	0.96
Pra-LOE	-3.61	-7.30	0.07	0.06
VIE-LOE	-2.27	-5.23	0.69	0.23
Pra-NAN	-2.75	-6.95	1.45	0.40
VIE-NAN	-1.41	-4.99	2.17	0.86
VIE-Pra	1.34	-2.77	5.45	0.93
B. *Mus cookii*				
	diff	lwr	upr	p adj
LOE-KAN	**-3.8**	**-5.64**	**-1.96**	**0**
NAN-KAN	**-4.38**	**-6.23**	**-2.54**	**0**
PHR-KAN	**-3.32**	**-5.45**	**-1.2**	**0**
NAN-LOE	-0.58	-2.4	1.24	0.83
PHR-LOE	0.48	-1.63	2.58	0.93
PHR-NAN	1.06	-1.04	3.16	0.55
C. *Maxomys surifer*				
	diff	lwr	upr	p adj
LOE-KAN	2.15	-3.74	8.04	0.89

MON-KAN	**8.83**	**3.15**	**14.5**	**0**
NAN-KAN	-0.42	-5.86	5.01	1
SON-KAN	**-7.05**	**-13.22**	**-0.88**	**0.02**
VEA-KAN	5.59	-0.09	11.26	0.06
MON-LOE	**6.68**	**0.79**	**12.57**	**0.02**
NAN-LOE	-2.57	-8.23	3.09	0.77
SON-LOE	**-9.2**	**-15.57**	**-2.83**	**0**
VEA-LOE	3.44	-2.45	9.33	0.53
NAN-MON	**-9.25**	**-14.69**	**-3.82**	**0**
SON-MON	**-15.87**	**-22.05**	**-9.7**	**0**
VEA-MON	-3.24	-8.92	2.44	0.56
SON-NAN	**-6.62**	**-12.57**	**-0.68**	**0.02**
VEA-NAN	**6.01**	**0.58**	**11.45**	**0.02**
VEA-SON	**12.64**	**6.47**	**18.81**	**0**
D. *Rattus exulans*				
	diff	lwr	upr	p adj
KAL-BUR	4.32	-1.12	9.76	0.28
KAN-BUR	**5.46**	**0.11**	**10.81**	**0.04**
Lan-BUR	**6.49**	**0.94**	**12.03**	**0.01**
LOE-BUR	4.19	-1.07	9.46	0.28
MON-BUR	**7.53**	**2.19**	**12.88**	**0**
NAN-BUR	**5.97**	**0.42**	**11.51**	**0.02**
PAK-BUR	1.26	-3.81	6.33	1
PHR-BUR	1.38	-3.97	6.72	1
Pra-BUR	-0.17	-5.97	5.63	1
Pur-BUR	3.15	-1.86	8.17	0.66
VEA-BUR	3.77	-1.57	9.12	0.47
VIE-BUR	-0.12	-5.25	5.01	1
KAN-KAL	1.14	-4.2	6.49	1
Lan-KAL	2.17	-3.37	7.71	0.98
LOE-KAL	-0.12	-5.39	5.14	1
MON-KAL	3.22	-2.13	8.57	0.72

NAN-KAL	1.65	-3.89	7.19	1
PAK-KAL	-3.06	-8.13	2.01	0.72
PHR-KAL	-2.94	-8.29	2.41	0.82
Pra-KAL	-4.49	-10.29	1.31	0.32
Pur-KAL	-1.16	-6.18	3.85	1
VEA-KAL	-0.54	-5.89	4.81	1
VIE-KAL	-4.44	-9.57	0.69	0.17
Lan-KAN	1.03	-4.43	6.48	1
LOE-KAN	-1.27	-6.44	3.91	1
MON-KAN	2.07	-3.18	7.33	0.98
NAN-KAN	0.51	-4.95	5.96	1
PAK-KAN	-4.2	-9.17	0.77	0.19
PHR-KAN	-4.09	-9.34	1.17	0.31
Pra-KAN	-5.63	-11.35	0.08	0.06
Pur-KAN	-2.31	-7.23	2.61	0.93
VEA-KAN	-1.69	-6.94	3.57	1
VIE-KAN	**-5.59**	**-10.62**	**-0.55**	**0.02**
LOE-Lan	-2.29	-7.67	3.08	0.97
MON-Lan	1.05	-4.41	6.5	1
NAN-Lan	-0.52	-6.17	5.13	1
PAK-Lan	**-5.23**	**-10.41**	**-0.05**	**0.05**
PHR-Lan	-5.11	-10.57	0.34	0.09
Pra-Lan	**-6.66**	**-12.56**	**-0.76**	**0.01**
Pur-Lan	-3.33	-8.46	1.79	0.6
VEA-Lan	-2.71	-8.17	2.74	0.9
VIE-Lan	**-6.61**	**-11.85**	**-1.37**	**0**
MON-LOE	3.34	-1.83	8.51	0.62
NAN-LOE	1.77	-3.6	7.15	1
PAK-LOE	-2.93	-7.82	1.95	0.72
PHR-LOE	-2.82	-7.99	2.35	0.83
Pra-LOE	-4.36	-10	1.27	0.32
Pur-LOE	-1.04	-5.87	3.79	1
VEA-LOE	-0.42	-5.59	4.75	1

VIE-LOE	-4.32	-9.26	0.63	0.16
NAN-MON	-1.57	-7.02	3.89	1
PAK-MON	**-6.27**	**-11.25**	**-1.3**	**0**
PHR-MON	**-6.16**	**-11.42**	**-0.9**	**0.01**
Pra-MON	**-7.7**	**-13.42**	**-1.99**	**0**
Pur-MON	-4.38	-9.3	0.54	0.14
VEA-MON	-3.76	-9.02	1.5	0.45
VIE-MON	**-7.66**	**-12.69**	**-2.63**	**0**
PAK-NAN	-4.71	-9.89	0.47	0.12
PHR-NAN	-4.59	-10.05	0.86	0.2
Pra-NAN	**-6.14**	**-12.03**	**-0.24**	**0.03**
Pur-NAN	-2.81	-7.94	2.31	0.83
VEA-NAN	-2.19	-7.65	3.26	0.98
VIE-NAN	**-6.09**	**-11.33**	**-0.85**	**0.01**
PHR-PAK	0.12	-4.86	5.09	1
Pra-PAK	-1.43	-6.88	4.02	1
Pur-PAK	1.89	-2.72	6.5	0.98
VEA-PAK	2.51	-2.46	7.49	0.89
VIE-PAK	-1.38	-6.12	3.35	1
Pra-PHR	-1.54	-7.26	4.17	1
Pur-PHR	1.78	-3.14	6.7	0.99
VEA-PHR	2.4	-2.86	7.66	0.95
VIE-PHR	-1.5	-6.53	3.53	1
Pur-Pra	3.32	-2.08	8.73	0.69
VEA-Pra	3.94	-1.77	9.66	0.51
VIE-Pra	0.05	-5.46	5.56	1
VEA-Pur	0.62	-4.3	5.54	1
VIE-Pur	-3.28	-7.95	1.4	0.48
VIE-VEA	-3.9	-8.93	1.13	0.32
E. *Rattus tanezumi*				
	diff	lwr	upr	p adj
CHA-BUR	-4.1	-23.69	15.49	1

KAL-BUR	1	-18.78	20.78	1
KAN-BUR	-4.7	-24.48	15.08	1
Lan-BUR	-3.79	-23.2	15.62	1
LOE-BUR	-2.62	-22.4	17.16	1
LUA-BUR	-7.32	-27.03	12.39	0.98
NAN-BUR	-7.2	-26.99	12.58	0.98
PHR-BUR	-3.47	-24.24	17.31	1
Pra-BUR	-9.27	-28.81	10.26	0.9
Pur-BUR	-2.87	-22.36	16.62	1
KAL-CHA	5.1	-4.09	14.28	0.77
KAN-CHA	-0.6	-9.79	8.58	1
Lan-CHA	0.31	-8.05	8.66	1
LOE-CHA	1.48	-7.71	10.67	1
LUA-CHA	-3.22	-12.25	5.81	0.99
NAN-CHA	-3.11	-12.29	6.08	0.99
PHR-CHA	0.63	-10.53	11.8	1
Pra-CHA	-5.18	-13.82	3.47	0.68
Pur-CHA	1.23	-7.31	9.76	1
KAN-KAL	-5.7	-15.3	3.89	0.69
Lan-KAL	-4.79	-13.59	4.01	0.79
LOE-KAL	-3.62	-13.21	5.98	0.98
LUA-KAL	-8.32	-17.76	1.13	0.14
NAN-KAL	-8.2	-17.8	1.39	0.17
PHR-KAL	-4.46	-15.97	7.04	0.97
Pra-KAL	**-10.27**	**-19.35**	**-1.2**	**0.01**
Pur-KAL	-3.87	-12.85	5.1	0.94
Lan-KAN	0.91	-7.89	9.71	1
LOE-KAN	2.08	-7.51	11.68	1
LUA-KAN	-2.61	-12.06	6.83	1
NAN-KAN	-2.5	-12.1	7.1	1
PHR-KAN	1.24	-10.27	12.74	1
Pra-KAN	-4.57	-13.65	4.51	0.86
Pur-KAN	1.83	-7.15	10.81	1

LOE-Lan	1.17	-7.63	9.97	1
LUA-Lan	-3.53	-12.16	5.11	0.96
NAN-Lan	-3.41	-12.21	5.39	0.97
PHR-Lan	0.33	-10.52	11.18	1
Pra-Lan	-5.48	-13.71	2.75	0.52
Pur-Lan	0.92	-7.2	9.04	1
LUA-LOE	-4.7	-14.14	4.75	0.87
NAN-LOE	-4.59	-14.18	5.01	0.9
PHR-LOE	-0.85	-12.35	10.66	1
Pra-LOE	-6.66	-15.73	2.42	0.38
Pur-LOE	-0.25	-9.23	8.72	1
NAN-LUA	0.11	-9.33	9.56	1
PHR-LUA	3.85	-7.53	15.23	0.99
Pra-LUA	-1.96	-10.87	6.96	1
Pur-LUA	4.44	-4.37	13.26	0.86
PHR-NAN	3.74	-7.77	15.24	0.99
Pra-NAN	-2.07	-11.15	7.01	1
Pur-NAN	4.33	-4.65	13.31	0.89
Pra-PHR	-5.81	-16.88	5.27	0.83
Pur-PHR	0.59	-10.4	11.59	1
Pur-Pra	6.4	-2.02	14.82	0.32

625

Table 4. Summary of the species x localities pairwise MANOVAs and ANOVAs ran to assess the similarity of morphological responses. Numbers left of the slash bar correspond to shape MANOVAs (0: no convergence, 1: cranium convergence, 2: mandible convergence, 3: cranium+mandible convergence) ; numbers right of the slash bar correspond to estimated bite force ANOVAs (0: no convergence, 1: convergence). Grayed out cells are inexistent species pair x locality pair combinations.

Locality combo	*M. surifer x M. caroli*	*M. surifer x M. cookii*	*M. surifer x R. exulans*	*M. surifer x R. tanezumi*	*M. caroli x M. cookii*	*M. caroli x R. exulans*	*M. caroli x R. tanezumi*	*M. cookii x R. exulans*	*M. cookii x R. tanezumi*	*R. exulans x R. tanezumi*	
BUR KAL						2 / 1	1 / 0			3 / 0	
BUR KAN										1 / 0	
BUR Lan										0 / 0	
BUR LOE						0 / 1	0 / 0			2 / 0	
BUR NAN						0 / 0	1 / 0			0 / 0	
BUR PHR										0 / 0	
BUR Pra						0 / 0	1 / 1			0 / 0	
BUR Pur										0 / 0	
BUR VIE						0 / 0					
KAL KAN										0 / 0	
KAL Lan										0 / 0	
KAL LOE						0 / 0	1 / 0			0 / 0	
KAL NAN						0 / 0	0 / 0			1 / 0	
KAL PHR										0 / 1	
KAL Pra						0 / 1	0 / 0			0 / 1	
KAL Pur										0 / 0	
KAL VIE						0 / 1					
KAN Lan										0 / 0	
KAN LOE		0 / 0	0 / 0	0 / 0				0 / 1	0 / 0	0 / 0	
KAN MON			0 / 0								
KAN NAN		0 / 0	0 / 0	0 / 0				0 / 0	2 / 1	1 / 0	
KAN PHR								0 / 1	0 / 0	0 / 0	
KAN Pra										0 / 1	
KAN Pur										0 / 0	
KAN VEA			0 / 0								
Lan LOE										0 / 0	
Lan NAN										0 / 0	

Lan PHR										0 / 0	
Lan Pra										0 / 1	
Lan Pur										0 / 0	
LOE MON			0 / 1								
LOE NAN	0 / 0	0 / 0	0 / 0	0 / 0	0 / 0	0 / 0	0 / 0	1 / 0	1 / 0	1 / 0	
LOE PHR								1 / 0	2 / 0	0 / 0	
LOE Pra						0 / 1	0 / 1			2 / 1	
LOE Pur										0 / 0	
LOE VEA			0 / 0			0 / 0					
MON NAN			0 / 0								
MON VEA			2 / 1								
NAN PHR								2 / 0	0 / 0	0 / 0	
NAN Pra						0 / 1	0 / 0			0 / 1	
NAN Pur										0 / 0	
NAN VEA			0 / 0								
NAN VIE						0 / 0					
PHR Pra										2 / 1	
PHR Pur										0 / 0	
Pra Pur										0 / 1	
Pra VIE						0 / 0					
											Grand total
Total combo	1	3	10	3	1	15	10	6	6	36	91
Convergence shape	0	0	1	0	0	1	4	3	3	8	20
Convergence BF	0	0	2	0	0	6	2	2	1	8	21
Percentage shape	0	0	10	0	0	6,67	40	50	50	22,22	21,98
Percentage BF	0	0	20	0	0	40	20	33,33	16,67	22,22	23,08

631

CONCLUSION GENERALE

Le cadre "Morphologie-Performance-*Fitness*" proposé par SJ Arnold (1983) a permis d'inclure la morphologie fonctionnelle dans un cadre adaptationiste (ou évolutioniste). La variation de performance, formant le noyau des différences de capacité de survie et de reproduction des individus, est au centre des problématiques de sélection et d'adaptation. L'inclusion de ce paradigme dans un ensemble plus large, le rapprochant des domaines de la génétique quantitative et de la biologie des populations, permet de s'intéresser directement aux processus évolutifs mis en œuvre (Irschick et al. 2008).

La première partie de cette thèse s'est d'abord focalisée sur la variation morpho-anatomique du crâne chez les Murinae, en étudiant les conformations de musculatures chez plusieurs souris. Puis le lien entre morphologie et performance a pu être directement testé grâce à des mesures *in vivo* de force de morsure. Les estimations de force de morsure basées sur l'anatomie crânienne étant corrélées aux mesures *in vivo*, le lien performance-morphologie a pu être confirmé dans notre cas. Cependant, cette partie a aussi permis de révéler une importante variation résiduelle de performance, en particulier au niveau intraspécifique. Bien que l'ontogénie et la plasticité de performance intra-individuelle expliquent certainement une partie de cette variation, l'existence d'une variation génétique sous-jacente pouvait également être un facteur important. En effet, dans sa plus stricte définition, le paradigme "Morphologie-Performance-*Fitness*", n'inclut pas la prise en compte des potentiels "gènes de la performance" pouvant avoir un effet plus ou moins direct sur cette dernière (des exemples de tels gènes sont connus chez l'homme ; e.g. Montgomery et al. 1998, Yang et al. 2003, Bray et al. 2009). Il n'inclut pas non plus l'étude de l'influence de la génétique sur la morphologie. En revanche, le champ de la génétique quantitative s'est largement intéressé à ces relations, et son utilisation est l'une des voies proposées pour compléter le cadre "Morphologie-Performance-*Fitness*" dans l'étude des processus évolutifs (Garland 1994).

Dans la seconde partie de la thèse, les effets de la variation génétique et du stress génétique sur la performance et la morphologie ont été testés. Les sources de variation/stress génétiques étudiées ont porté sur le déterminisme génétique du sexe, la mise en consanguinité et finalement la variation génétique additive elle même. La consanguinité n'est pas apparue comme une source de changements significatifs de performance ou de morphologie. En revanche, le déterminisme sexuel a pu être associé

à des variations de taille et de force de morsure. L'analyse approfondie de ce résultat a montré que la variation de force de morsure était dans sa majorité expliquée par la variation de taille, elle-même induite par les différences génotypiques. L'étude de la variation génétique additive dans une population de laboratoire a quant à elle permis de montrer que l'héritabilité de la force de morsure *in vivo* était extrêmement faible, tandis que celle de la morphologie était souvent élevée, avec des variations selon les caractères étudiés. Il semble donc que la variabilité génétique qui sous-tend les variations de formes de l'appareil masticateur n'impacte pas de manière directe la performance non-morphologique chez les muridés. La variation génétique de la performance serait donc faible. Malgré cela, les variations génétiques de la morphologie peuvent permettre de la faire évoluer. En d'autres termes, il semble que les "gènes de performance" des souris, s'ils existent, ne présentent pas ou peu de variation génétique additive. Cette hypothèse est conforme au postulat, découlant du théorème de Fisher (1958), qui prévoit que la variabilité génétique des traits associés à la valeur sélective soit faible, par l'action uniformisatrice de la sélection stabilisante. La variation de performance, tout du moins celle concernant la force de morsure, est donc expliquée par la variation morpho-anatomique, ontogénétique, plastique et d'autres facteurs héritables ou non. À l'inverse, la forte héritabilité et variance génétique de certains traits de la mandibule, connus pour leur variabilité aux niveaux interspécifiques ou inter-populationnels, font de ces traits des lignes de moindre résistance évolutive qui permettent des changements adaptatifs de la performance. Lors du processus de différenciation, la sélection pourrait donc s'être porté sur des traits anatomiques associés à la force de morsure (e.g. taille, musculature et bras de levier), pour donner l'actuelle diversité morpho-fonctionnelle.

Dans la dernière partie, les réponses des populations de rongeurs sauvages aux pressions environnementales ont été étudiées. La première étude a révélé que deux espèces de murinés de tailles très différentes et vivant en syntopie pouvaient produire des forces de morsure équivalentes. Ceci suggère que la compétition interspécifique n'affecte pas la valeur de ce trait. Il est également possible que la morphologie crânienne de la plus petite espèce ait évolué, via la sélection naturelle des individus pouvant accéder à une ressource particulièrement importante dans les localités étudiées. Cet exemple pourrait donc refléter une convergence du point de vue de la performance, malgré une divergence en terme de taille. L'étude des communautés de muridés d'Asie du Sud-Est a montré l'existence de différences inter-populationnelles dans la morphologie du crâne et de la mandibule. Au niveau intraspécifique, les différences morphologiques entre populations sont parfois expliquées par une structuration géographique dont les origines peuvent être directement associées avec le degré de

synanthropie des espèces. De plus, il apparaît que les espèces synanthropiques ont fréquemment des réponses morpho-fonctionnelles convergentes, malgré des niches différentes et leur éloignement phylogénétique. L'adaptabilité des Murinae aux changements environnementaux liés à l'homme semble donc pouvoir suivre des trajectoires communes entre espèces.

Bien que les axes de recherche développés dans cette thèse aient permis de vérifier ou d'établir des liens entre génétique, morphologie, performance et adaptation, certaines relations n'ont pas pu être testées (Fig. 9). Notamment, l'importance de la plasticité phénotypique sur la force de morsure doit être testée de manière directe. Ceci pourrait être réalisé en milieu naturel grâce au marquage des individus, par des mesures de performances répétées (par exemple pendant différentes saisons). En laboratoire, le

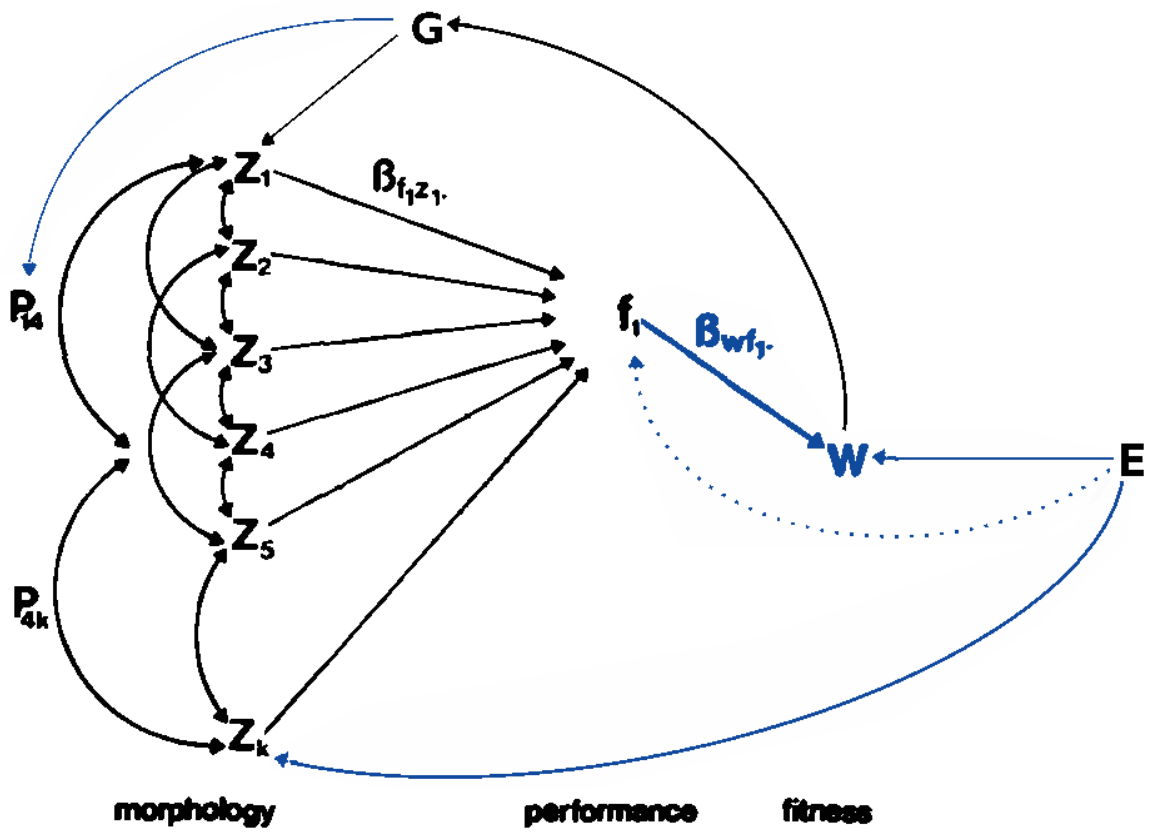

Figure 9. Diagramme des chemins élargi à partir de Arnold (1983). Les relations en bleu n'ont pas été étudiées dans cette thèse : lien performance-valeur sélective ; plasticité phénotypique de la morphologie et de la performance ; effets génétiques sur l'intégration morphologique. P : corrélations entre caractères morphologiques (intégration) ; Z : caractères morphologiques ; f : performance ; W : valeur sélective ; E : contraintes environnementales ; G : structure génétique de la population ; β_{fz} : gradient de performance ; β_{wf} : gradient de valeur sélective.

même type de mesures répétées pourrait être effectué, en ayant un contrôle instantané et précis sur les conditions environnementales et le stress. De plus, cette dernière approche permettrait en théorie de séparer les effets de la plasticité et de la variance génétique additive.

L'étude de la génétique quantitative de la morphologie et de la performance peut être améliorée par le développement d'outils permettant de mesurer l'héritabilité de manière multivariée (Claude et al. in prep.). Ceci permettrait aussi d'ajouter les aspects d'intégration des caractères morphologiques qui n'ont pas pu être abordés ici. En effet, l'intégration constitue probablement une des voies facilitatrices de l'évolution des caractères morphologiques, reliés ou non à la performance, et il est également possible que l'évolution de traits liés à la performance entraîne des changements associés dans d'autres traits.

Enfin, le lien entre performance et valeur sélective ("Performance-*Fitness*") doit encore être éclairci. En effet, il constitue la connexion majeure entre phénotype et sélection. Cependant, ce lien est soumis à des variations locales, dépendantes notamment des conditions environnementales mais aussi de la variation génétique présente dans les populations, ce qui rend difficiles les généralisations. Ce lien doit donc être étudié au cas par cas en testant l'évolution de la distribution des valeurs sélectives dans une population. Par exemple, l'utilisation adéquate des ressources alimentaires disponibles ne requière pas toujours une grande puissance musculaire. Dans certains cas, l'utilisation des ressources peut plutôt nécessiter une plus grande vitesse et précision d'incision, ou une largeur d'ouverture de la bouche plus grande, ce qui peut réduire la force musculaire disponible, ou modifier les bras de leviers au niveau mandibulaire. Enfin l'étude des différences d'origines comportementales entre performance réalisable et réalisée semble être nécessaire à la compréhension du lien performance-*fitness* dans les populations naturelles.

D'un point de vue plus général, la combinaison d'approches, telle que proposée dans cette thèse, élargit les connexions de la morphologie fonctionnelle avec d'autres disciplines au sein de la biologie de l'évolution. L'ajout de la génétique quantitative au cadre "Morphologie-Performance-*Fitness*" permet d'améliorer la compréhension de l'action de la sélection sur la performance et sur la morphologie. De même, l'étude *a posteriori* des modifications de performance et de morphologie face aux pressions environnementales nous renseignent sur les voies d'adaptation locale possibles et réalisées dans la nature. Inversement, la morphologie fonctionnelle permet de quantifier la variation de performance induite par les changements phénotypiques observés.

Le potentiel du cadre "Morphologie-Performance-*Fitness*" a été largement reconnu et utilisé depuis sa formalisation dans les années 80. Le nombre d'études citant explicitement Arnold (1983), ou s'inscrivant dans ce paradigme, a depuis lors été en constante augmentation (Kingslover & Huey 2003, Irschick et al. 2008). L'élargissement de ce cadre (Fig. 9) est actuellement applicable dans l'étude de l'évolution à une échelle populationnelle. Cet élargissement permet de changer la vision linéaire morphologie → performance → valeur sélective en une boucle incluant l'effet de la sélection sur la performance et ses conséquences sur la variabilité génétique, qui à leur tour modifient la variation phénotypique liée à la performance. Dans cette boucle, le paradigme originel reste central, et la nécessité de tester formellement les liens entre morphologie et performance, et entre performance et valeur sélective subsiste. Ce cadre élargi permet de comprendre la totalité du phénomène d'évolution phénotypique en milieu naturel, en incluant les mouvements du paysage adaptatif et les réponses phénotypiques possibles (lignes de moindre résistance, héritabilité) et réalisées des populations (convergences, divergences). Cette thèse s'inscrit dans ce cadre, en associant des études en laboratoire et en populations naturelles, à différentes échelles et sur différentes espèces. Cette variété d'approches montre que l'étude du cadre "génétique-morphologie-performance-*fitness*-évolution" dans son ensemble n'est pas uniquement possible par le suivi à long terme de populations ou de communautés, mais aussi en combinant l'utilisation de différentes espèces proches dans différents environnements.

Références bibliographiques

Aguilar, J. P. (1982). Contributions à létude des micromammifères du gisement Miocène supérieur de Montredon (Hérault). 2. Les rongeurs. *Palaeovertebrata*, 12(3), 81.

Ameur, R. (1984). Découverte de nouveaux rongeurs dans la formation Miocène de Bou Hanifia (Algérie occidentale). *Geobios*, 17(2), 167-175.

Anderson, R. A., McBrayer, L. D., & Herrel, A. (2008). Bite force in vertebrates: opportunities and caveats for use of a nonpareil whole-animal performance measure. *Biological Journal of the Linnean Society*, 93(4), 709-720.

Aplin, K. P., Suzuki, H., Chinen, A. A., Chesser, R. T., Ten Have, J., Donnellan, S. C., ... & Catzeflis, F. (2011). Multiple geographic origins of commensalism and complex dispersal history of black rats. *PloS one*, *6*(11), e26357

Arnold, S. J. (1983). Morphology, performance and fitness. *American Zoologist*, 23(2), 347-361.

Auffray, J. C., & Britton-Davidian, J. (2012). The house mouse and its relatives: systematics and taxonomy. *Evolution of the House Mouse*. *Cambridge University Press, Cambridge*, 3, 1-34.

Auffray, J. C., Orth, A., Catalan, J., Gonzalez, J. P., Desmarais, E., & Bonhomme, F. (2003). Phylogenetic position and description of a new species of subgenus *Mus* (Rodentia, Mammalia) from Thailand. *Zoologica Scripta*, 32(2), 119-127.

Auffray, J. C., Vanlerberghe, F., & Britton-Davidian, J. (1990). The house mouse progression in Eurasia: a palaeontological and archaeozoological approach. *Biological Journal of the Linnean Society*, 41(1-3), 13-25.

Badyaev, A. V., Foresman, K. R., & Fernandes, M. V. (2000). Stress and developmental stability: vegetation removal causes increased fluctuating asymmetry in shrews. *Ecology*, 81(2), 336-345.

Baverstock, H., Jeffery, N. S., & Cobb, S. N. (2013). The morphology of the mouse masticatory musculature. *Journal of Anatomy*, 223(1), 46-60.

Becerra, F., Echeverría, A., Vassallo, A. I., & Casinos, A. (2011). Bite force and jaw biomechanics in the subterranean rodent Talas tuco-tuco (*Ctenomys talarum*)(Caviomorpha: Octodontoidea). *Canadian Journal of Zoology*, 89(4), 334-342.

Brandt, J. F. (1855). Beiträge zur näheren Kenntniss der Säuge-Thiere Russlands: Mit 19 Tafeln. (Aus den Mém. Mathémat., phys. Et nat., Tom. VII. Besonders abgedruckt.). Kaiserl.

Academ. d. Wiss.

Bray, M. S., Hagberg, J. M., Perusse, L., Rankinen, T., Roth, S. M., Wolfarth, B., & Bouchard, C. (2009). The human gene map for performance and health-related fitness phenotypes: the 2006-2007 update. *Medicine & Science in Sports & Exercise*, 41(1), 34-72.

Carleton, M. D., & Musser, G. G. (2005). Order rodentia. *Mammal species of the world: a taxonomic and geographic reference. JHU Press, Baltimore*, 2, 745-2142.

Carter, A. J. R., Weier, T. M., & Houle, D. (2009). The effect of inbreeding on fluctuating asymmetry of wing veins in two laboratory strains of *Drosophila melanogaster*. *Heredity*, 102(6), 563.

Chaimanee, Y., & Jaeger, J. J. (2001). Evolution of *Rattus* (mammalia, Rodentia) during the plio-pleistocene in Thailand. *Historical Biology*, 15(1-2), 181-191.

Chevret, P., Granjon, L., Duplantier, J., Denys, C., & Catzeflis, F. M. (1994). Molecular phylogeny of the *Praomys* complex (Rodentia: Murinae): a study based on DNA/DNA hybridization experiments. *Zoological Journal of the Linnean Society*, 112(4), 425-442.

Chevret, P., Jenkins, P., & Catzeflis, F. (2003). Evolutionary systematics of the Indian mouse *Mus famulus* Bonhote, 1898: molecular (DNA/DNA hybridization and 12S rRNA sequences) and morphological evidence. *Zoological Journal of the Linnean Society*, 137(3), 385-401.

Chevret, P., Veyrunes, F., & Britton-Davidan, J. (2005). Molecular phylogeny of the genus *Mus* (Rodentia: Murinae) based on mitochondrial and nuclear data. *Biological Journal of the Linnean Society*, 84(3), 417-427.

Claude, J. (2008). *Morphometrics with R. Springer Science & Business Media, Berlin*.

Cook, M. J. (1965). *The anatomy of the laboratory mouse*. *Academic Press, London*.

Cox, P. G., & Jeffery, N. (2011). Reviewing the morphology of the jaw-closing musculature in squirrels, rats, and guinea pigs with contrast-enhanced microCT. *The Anatomical Record*, 294(6), 915-928.

Cox, P. G., Rayfield, E. J., Fagan, M. J., Herrel, A., Pataky, T. C., & Jeffery, N. (2012). Functional evolution of the feeding system in rodents. *PLoS One*, 7(4), e36299.

Darwin, C. (1859). *On the origin of the species by natural selection*. *John Murray, London*.

Druzinsky, R. E., Doherty, A. H., & De Vree, F. L. (2011). Mammalian masticatory muscles: homology, nomenclature, and diversification. *Integrative and comparative biology*, 51(2), 224-234.

Emerson, S. B., & Bramble, D. M. (1993). Scaling, allometry, and skull design. In : *The skull. The University of Chicago Press, Chicago and London*, 3, 384-421.

Fabre, P. H., Hautier, L., Dimitrov, D., & Douzery, E. J. (2012). A glimpse on the pattern of rodent diversification: a phylogenetic approach. *BMC evolutionary biology*, 12(1), 88.

Fabre, P. H., Hautier, L., & Douzery, E. (2015). A synopsis of rodent molecular phylogenetics, systematics and biogeography. *Evolution of the Rodents. Advances in Phylogeny, Functional Morphology and Development. Cambridge University Press, Cambridge*, 5, 19-69.

Fabre, P. H., Herrel, A., Fitriana, Y., Meslin, L., & Hautier, L. (2017). Masticatory muscle architecture in a water-rat from Australasia (Murinae, *Hydromys*) and its implication for the evolution of carnivory in rodents. *Journal of Anatomy, in press*.

Fabre, P. H., Pages, M., Musser, G. G., Fitriana, Y. S., Fjeldså, J., Jennings, A., ... & Supriatna, N. (2013). A new genus of rodent from Wallacea (Rodentia: Muridae: Murinae: Rattini), and its implication for biogeography and Indo-Pacific Rattini systematics. *Zoological Journal of the Linnean Society*, 169(2), 408-447.

Falconer, D. S. (1947). Milk production in mice. *The Journal of Agricultural Science*, *37*(3), 224-235.

Fénichel, P., Paris, F., Philibert, P., Hiéronimus, S., Gaspari, L., Kurzenne, J. Y., ... & Sultan, C. (2013). Molecular diagnosis of 5α-reductase deficiency in 4 elite young female athletes through hormonal screening for hyperandrogenism. *The Journal of Clinical Endocrinology & Metabolism*, 98(6), E1055-E1059.

Fisher, R. A. (1958). *The genetic theory of natural selection*. *Dover publications*.

Freeman, P. W., & Lemen, C. A. (2008). A simple morphological predictor of bite force in rodents. *Journal of Zoology*, 275(4), 418-422.

Freeman, P. W., & Lemen, C. A. (2008). Measuring bite force in small mammals with a piezo-resistive sensor. *Journal of Mammalogy*, 89(2), 513-517.

Gans, C., & Northcutt, R. G. (1983). Neural crest and the origin of vertebrates: a new head. *Science*, 220(4594), 268-273.

Garland Jr, T. (1994). Quantitative genetics of locomotor behavior and physiology in a garter snake. *Quantitative genetic studies of behavioral evolution. University of Chicago Press, Chicago*, 251-277.

Gendron-Maguire, M., Mallo, M., Zhang, M., & Gridley, T. (1993). Hoxa-2 mutant mice exhibit homeotic transformation of skeletal elements derived from cranial neural crest. *Cell*, 75(7),

1317-1331.

Gould, S. J. (1966). Allometry and size in ontogeny and phylogeny. *Biological Reviews*, 41(4), 587-638.

Greene, E. C. (1955). *Anatomy of the Rat. Hafner Publishing Co., New York and London.*

Hanken, J., & Thorogood, P. (1993). Evolution and development of the vertebrate skull: the role of pattern formation. *Trends in Ecology & Evolution*, 8(1), 9-15.

Hautier, L., Lebrun, R., & Cox, P. G. (2012). Patterns of covariation in the masticatory apparatus of hystricognathous rodents: implications for evolution and diversification. *Journal of Morphology*, 273(12), 1319-1337.

Hautier, L., & Saksiri, S. (2009). Masticatory muscle architecture in the Laotian rock rat *Laonastes aenigmamus* (Mammalia, Rodentia): new insights into the evolution of hystricognathy. *Journal of Anatomy*, 215(4), 401-410.

Heaney, L. R., Piper, P. J., & Mijares, A. S. (2011). The first fossil record of endemic murid rodents from the Philippines: A late Pleistocene cave fauna from northern Luzon. *Proceedings of the Biological Society of Washington*, 124(3), 234-247.

Herrel, A., Moore, J. A., Bredeweg, E. M., & Nelson, N. J. (2010). Sexual dimorphism, body size, bite force and male mating success in tuatara. *Biological Journal of the Linnean Society*, 100(2), 287-292.

Herrel, A., O'Reilly, J. C. (2005). Ontogenetic scaling of bite force in lizards and turtles. *Physiological and Biochemical Zoology,* 79(1), 31-42.

Herrel, A., Spithoven, L., Van Damme, R., & De Vree, F. (1999). Sexual dimorphism of head size in *Gallotia galloti*: testing the niche divergence hypothesis by functional analyses. *Functional Ecology*, 13(3), 289-297.

Herrel, A., Van Damme, R., & De Vree, F. (1995). Sexual dimorphism of head size in *Podarcis hispanica atrata*: testing the dietary divergence hypothesis by bite force analysis. *Netherlands Journal of Zoology*, 46(3), 253-262.

Herrel, A., Van Damme, R., Vanhooydonck, B., & Vree, F. D. (2001). The implications of bite performance for diet in two species of lacertid lizards. *Canadian Journal of Zoology*, 79(4), 662-670.

Herrel, A., Vanhooydonck, B., & Van Damme, R. (2004). Omnivory in lacertid lizards: adaptive evolution or constraint?. *Journal of evolutionary biology*, 17(5), 974-984.

Herzog, W. (1994). Muscle. In: B.M. NIGG & W. HERZOG (Eds.): *Biomechanics of the musculoskeletal system*. *John Wiley & Sons, Chichester*, 154-187.

Hiiemae, K. (1971). The structure and function of the jaw muscles in the rat (*Rattus norvegicus* L.). *Zoological Journal of the Linnean Society*, 50(1), 111-132.

Hiiemae, K., & Houston, W. J. B. (1971). The structure and function of the jaw muscles in the rat (*Rattus norvegicus* L.) I. Their anatomy and internal architecture. *Zoological Journal of the Linnean Society*, 50(1), 75-99.

Huchon, D., Madsen, O., Sibbald, M. J., Ament, K., Stanhope, M. J., Catzeflis, F., ... & Douzery, E. J. (2002). Rodent phylogeny and a timescale for the evolution of Glires: evidence from an extensive taxon sampling using three nuclear genes. *Molecular Biology and Evolution*, 19(7), 1053-1065.

Huyghe, K., Vanhooydonck, B., Scheers, H., Molina-Borja, M., & Van Damme, R. (2005). Morphology, performance and fighting capacity in male lizards, *Gallotia galloti*. *Functional Ecology*, 19(5), 800-807.

Irschick, D. J., Meyers, J. J., Husak, J. F., & Le Galliard, J. F. (2008). How does selection operate on whole-organism functional performance capacities? A review and synthesis. *Evolutionary Ecology Research*, 10(2), 177-196.

Jacobs, L. L., & Downs, W. R. (1994). The evolution of murine rodents in Asia. *National Science Museum Monographs*, 8, 149-156.

Jacobs, L. L., & Flynn, L. J. (2005). Of mice… again: the Siwalik rodent record, murine distribution, and molecular clocks. *Interpreting the past: essays on human, primate, and mammal evolution in honor of David Pilbeam. Brill Academic Publishers, Leiden*, 63-80.

Jansa, S. A., Barker, F. K., & Heaney, L. R. (2006). The pattern and timing of diversification of Philippine endemic rodents: evidence from mitochondrial and nuclear gene sequences. *Systematic Biology*, 55(1), 73-88.

Jones, E. P., Skirnisson, K., McGovern, T. H., Gilbert, M. T. P., Willerslev, E., & Searle, J. B. (2012). Fellow travellers: a concordance of colonization patterns between mice and men in the North Atlantic region. *BMC Evolutionary Biology*, 12(1), 35.

Kesner, M. H. (1980). Functional morphology of the masticatory musculature of the rodent subfamily Microtinae. *Journal of morphology*, 165(2), 205-222.

Kimura, Y., Hawkins, M. T., McDonough, M. M., Jacobs, L. L., & Flynn, L. J. (2015). Corrected

placement of *Mus-Rattus* fossil calibration forces precision in the molecular tree of rodents. *Scientific reports*, 5.

Kingsolver, J. G., & Huey, R. B. (2003). Introduction: The Evolution of Morphology, Performance, and Fitness. *Integrative and Comparative Biology*, 43(3), 361-366.

Klingenberg, C. P., & Leamy, L. J. (2001). Quantitative genetics of geometric shape in the mouse mandible. *Evolution*, 55(11), 2342-2352.

Klingenberg, C. P., Leamy, L. J., Routman, E. J., & Cheverud, J. M. (2001). Genetic architecture of mandible shape in mice: effects of quantitative trait loci analyzed by geometric morphometrics. *Genetics*, 157(2), 785-802.

Lailvaux, S. P., Herrel, A., VanHooydonck, B., Meyers, J. J., & Irschick, D. J. (2004). Performance capacity, fighting tactics and the evolution of life–stage male morphs in the green anole lizard (*Anolis carolinensis*). *Proceedings of the Royal Society of London B: Biological Sciences*, 271(1556), 2501-2508.

Landry Jr, S. O. (1970). The Rodentia as omnivores. *The Quarterly Review of Biology*, 45(4), 351-372.

Lecompte, E., Aplin, K., Denys, C., Catzeflis, F., Chades, M., & Chevret, P. (2008). Phylogeny and biogeography of African Murinae based on mitochondrial and nuclear gene sequences, with a new tribal classification of the subfamily. *BMC evolutionary Biology*, 8(1), 199.

Maestri, R., Patterson, B. D., Fornel, R., Monteiro, L. R., & Freitas, T. R. O. (2016). Diet, bite force and skull morphology in the generalist rodent morphotype. *Journal of evolutionary biology*, 29(11), 2191-2204.

Martín, J., & López, P. (2001). Hindlimb asymmetry reduces escape performance in the lizard *Psammodromus algirus*. *Physiological and Biochemical Zoology*, 74(5), 619-624.

Matsuo, I., Kuratani, S., Kimura, C., Takeda, N., & Aizawa, S. (1995). Mouse Otx2 functions in the formation and patterning of rostral head. *Genes & development*, 9(21), 2646-2658.

Méndez, J., Keys, A. (1960). Density and composition of mammalian muscle. *Metabolism*, 9, 184-188.

Merilä, J., & Sheldon, B. C. (1999). Genetic architecture of fitness and nonfitness traits: empirical patterns and development of ideas. *Heredity*, 83(2), 103-109.

Michaux, J., Chevret, P., & Renaud, S. (2007). Morphological diversity of Old World rats and mice (Rodentia, Muridae) mandible in relation with phylogeny and adaptation. *Journal of*

Zoological Systematics and Evolutionary Research, 45(3), 263-279.

Montgomery, H. E., Marshall, R., Hemingway, H., Myerson, S., Clarkson, P., Dollery, C., ... & Brynes, A. E. (1998). Human gene for physical performance. *Nature*, 393(6682), 221.

Nedbal, M. A., Honeycutt, R. L., & Schilitter, D. A. (1996). Higher-level systematics of rodents (Mammalia, Rodentia): evidence from the mitochondrial 12S rRNA gene. *Journal of Mammalian Evolution*, 3(3), 201-237.

Nies, M., & Ro, J. Y. (2004). Bite force measurement in awake rats. *Brain research protocols*, 12(3), 180-185.

Pagès, M., Chaval, Y., Herbreteau, V., Waengsothorn, S., Cosson, J. F., Hugot, J. P., ... & Michaux, J. (2010). Revisiting the taxonomy of the Rattini tribe: a phylogeny-based delimitation of species boundaries. *BMC evolutionary Biology*, 10(1), 184.

Patel, N. G. (1978). Functional morphology of the masticatory muscles of *Mus musculus* L. *Proceedings of the Indian Academy of Sciences-Section B, Animal Sciences*, 87(3), 51-57.

Patnaik, R. (2000). Siwalik murid rodents: Origin and dispersal. *Himalayan Geol*, 21(1/2), 145-151.

Patnaik, R. (2013). Indian Neogene Siwalik mammalian biostratigraphy: an overview. *Fossil Mammals of Asia: Neogene Biostratigraphy and Chronology. Columbia University Press, New York*, 423-444.

Patnaik, R. (2014). Phylogeny of Siwalik murine rodents: Implications for *Mus-Rattus* divergence time. *Journal of the Palaeontological Society of India*, 59(1), 15-28.

Rahmoun, M., Perez, J., Saunders, P. A., Boizet-Bonhoure, B., Wilhelm, D., Poulat, F., & Veyrunes, F. (2014). Anatomical and molecular analyses of XY ovaries from the African pygmy mouse *Mus minutoides*. *Sexual Development*, 8(6), 356-363.

R Core Team (2017). R: A language and environment for statistical computing. Vienna, Austria; 2014.

Renaud, S., & Auffray, J. C. (2010). Adaptation and plasticity in insular evolution of the house mouse mandible. *Journal of Zoological Systematics and Evolutionary Research*, *48*(2), 138-150.

Renaud, S., Auffray, J. C., & De la Porte, S. (2010). Epigenetic effects on the mouse mandible: common features and discrepancies in remodeling due to muscular dystrophy and response to food consistency. *BMC Evolutionary Biology*, 10(1), 28.

Renaud, S., & Michaux, J. R. (2007). Mandibles and molars of the wood mouse, *Apodemus sylvaticus* (L.): integrated latitudinal pattern and mosaic insular evolution. *Journal of biogeography*, *34*(2),

339-355.

Rinker, G. C. (1954). The comparative myology of the mammalian genera *Sigmodon*, *Oryzomys*, *Neotoma*, and *Peromyscus* (Cricetinae), with remarks on their intergeneric relationships. *Miscellaneous Publications Museum of Zoology, University of Michigan Press, Ann Arbor,* 83.

Rivera, G., & Claude, J. (2008). Environmental media and shape asymmetry: a case study on turtle shells. *Biological journal of the Linnean Society*, 94(3), 483-489.

Rohlf, F. J. (2010). tpsDig v2. 16. *Department of Ecology and Evolution, State University of New York, Stony Brook, New York*.

Roldan, E. R. S., Cassinello, J., Abaigar, T., & Gomendio, M. (1998). Inbreeding, fluctuating asymmetry, and ejaculate quality in an endangered ungulate. *Proceedings of the Royal Society of London B: Biological Sciences*, 265(1392), 243-248.

Rowe, K. C., Achmadi, A. S., & Esselstyn, J. A. (2016). Repeated evolution of carnivory among Indo-Australian rodents. *Evolution*, 70(3), 653-665.

Rowe, K. C., Aplin, K. P., Baverstock, P. R., & Moritz, C. (2011). Recent and rapid speciation with limited morphological disparity in the genus *Rattus*. *Systematic Biology*, 60(2), 188-203.

Rowe, K. C., Reno, M. L., Richmond, D. M., Adkins, R. M., & Steppan, S. J. (2008). Pliocene colonization and adaptive radiations in Australia and New Guinea (Sahul): multilocus systematics of the old endemic rodents (Muroidea: Murinae). *Molecular phylogenetics and evolution*, 47(1), 84-101.

Ruedas, L. A., & Kirsch, J. A. (1997). Systematics of *Maxomys* Sody, 1936 (Rodentia: Muridae: Murinae): DNA/DNA hybridization studies of some Borneo-Javan species and allied Sundaic and Australo-Papuan genera. *Biological Journal of the Linnean Society*, 61(3), 385-408.

Sahai, H., & Ojeda, M. M. (2005). Analysis of Variance for Random Models, Unbalanced Data. *Birkhuser, Boston*, 2.

Samuels, J. X. (2009). Cranial morphology and dietary habits of rodents. *Zoological Journal of the Linnean Society*, 156(4), 864-888.

Santana, S. E., Dumont, E. R., & Davis, J. L. (2010). Mechanics of bite force production and its relationship to diet in bats. *Functional Ecology*, 24(4), 776-784.

Satoh, K. (1997). Comparative functional morphology of mandibular forward movement during mastication of two murid rodents, *Apodemus speciosus* (Murinae) and *Clethrionomys*

rufocanus (Arvicolinae). *Journal of Morphology*, 231(2), 131-142.

Satoh, K. (1998). Balancing function of the masticatory muscles during incisal biting in two murid rodents, *Apodemus speciosus* and *Clethrionomys rufocanus*. *Journal of morphology*, 236(1), 49-56.

Satoh, K. (1999). Mechanical advantage of area of origin for the external pterygoid muscle in two murid rodents, *Apodemus speciosus* and *Clethrionomys rufocanus*. *Journal of morphology*, 240(1), 1-14.

Satoh, K., & Iwaku, F. (2004). Internal architecture, origin-insertion site, and mass of jaw muscles in Old World hamsters. *Journal of Morphology*, 260(1), 101-116.

Satoh, K., & Iwaku, F. (2006). Jaw muscle functional anatomy in northern grasshopper mouse, *Onychomys leucogaster*, a carnivorous murid. *Journal of Morphology*, 267(8), 987-999.

Satoh, K., & Iwaku, F. (2008). Masticatory muscle architecture in a murine murid, *Rattus rattus*, and its functional significance. *Mammal Study*, 33(1), 35-42.

Satoh, K., & Iwaku, F. (2009). Structure and direction of jaw adductor muscles as herbivorous adaptations in *Neotoma mexicana* (Muridae, Rodentia). *Zoomorphology*, 128(4), 339-348.

Saunders, P. A., Franco, T., Sottas, C., Maurice, T., Ganem, G., & Veyrunes, F. (2016). Masculinised behaviour of XY females in a mammal with naturally occurring sex reversal. *Scientific reports*, 6, 22881.

Schenk, J. J., Rowe, K. C., & Steppan, S. J. (2013). Ecological opportunity and incumbency in the diversification of repeated continental colonizations by muroid rodents. *Systematic Biology*, 62(6), 837-864.

Schluter, D. (2000). *The ecology of adaptive radiation*. *OUP, Oxford*.

Sehgal, R. K., & Patnaik, R. (2012). New muroid rodent and *Sivapithecus* dental remains from the Lower Siwalik deposits of Ramnagar (J&K, India): Age implication. *Quaternary international*, 269, 69-73.

Siahsarvie, R. (2012). Comparaison de la divergence morphologique et génétique chez la souris domestique au cours de son expansion géographique. D*octoral dissertation, Université Montpellier 2, Montpellier*.

Simpson, G. G., & Roe, A. (1939). *Quantitative zoology: Numerical concepts and methods in the study of recent and fossil animals*. *McGraw-Hill publications in the zoological sciences, New York*.

Simpson, G. G. (1945). The principles of classification and a classification of mammals. *Bull. Amer. Museum Nat. History*., 85.

Singleton, G. R., Hinds, L. A., Krebs, C. J., & Spratt, D. M. (2002*). Rats, mice and people: rodent biology and management*. *ACIAR, Camberra*.

Steppan, S. J., Adkins, R. M., Spinks, P. Q., & Hale, C. (2005). Multigene phylogeny of the Old World mice, Murinae, reveals distinct geographic lineages and the declining utility of mitochondrial genes compared to nuclear genes. *Molecular phylogenetics and evolution*, 37(2), 370-388.

Steppan, S. J., & Schenk, J. J. (2017). Muroid rodent phylogenetics: 900-species tree reveals increasing diversification rates. *PloS one*, *12*(8), e0183070.

Suzuki, H., & Aplin, K. P. (2012). Phylogeny and biogeography of the genus *Mus* in Eurasia. *Evolution of the House Mouse (Cambridge series in morphology and molecules)(eds.: M. Macholán, SJE Baird, P. Munclinger, and J. Piálek)*, 35-64.

Suzuki, H., Shimada, T., Terashima, M., Tsuchiya, K., & Aplin, K. (2004). Temporal, spatial, and ecological modes of evolution of Eurasian *Mus* based on mitochondrial and nuclear gene sequences. *Molecular phylogenetics and evolution*, 33(3), 626-646.

Tullberg, T. (1899). Ueber das System der Nagethiere: eine phylogenetische Studie. *Akademische Buchdruckerei*.

Turnbull, W. D. (1970). Mammalian masticatory apparatus. *Fieldiana Geol.*, 18, 149-356.

Valenzuela-Lamas, S., Baylac, M., Cucchi, T., & Vigne, J. D. (2011). House mouse dispersal in Iron Age Spain: a geometric morphometrics appraisal. *Biological Journal of the Linnean Society*, 102(3), 483-497.

Van Daele, P. A. A. G., Herrel, A., & Adriaens, D. (2008). Biting performance in teeth-digging African mole-rats (*Fukomys*, Bathyergidae, Rodentia). *Physiological and Biochemical Zoology*, 82(1), 40-50.

Van De Weerd, A. (1976). Rodent faunas of the Mio-Pliocene continental sediments of the Teruel-Alfambra region, Spain. *Doctoral dissertation, Utrecht University, Utrecht*.

Verneau, O., Catzeflis, F., & Furano, A. V. (1998). Determining and dating recent rodent speciation events by using L1 (LINE-1) retrotransposons. *Proceedings of the National Academy of Sciences*, 95(19), 11284-11289.

Vervust, B., Van Dongen, S., Grbac, I., & Van Damme, R. (2008). Fluctuating asymmetry,

physiological performance, and stress in island populations of the Italian Wall Lizard (*Podarcis sicula*). *Journal of Herpetology*, 42(2), 369-377.

Verwaijen, D., Van Damme, R., & Herrel, A. (2002). Relationships between head size, bite force, prey handling efficiency and diet in two sympatric lacertid lizards. *Functional Ecology*, 16(6), 842-850.

Veyrunes, F., Britton-Davidian, J., Robinson, T. J., Calvet, E., Denys, C., & Chevret, P. (2005). Molecular phylogeny of the African pygmy mice, subgenus *Nannomys* (Rodentia, Murinae, *Mus*): implications for chromosomal evolution. *Molecular phylogenetics and evolution*, 36(2), 358-369.

Veyrunes, F., Chevret, P., Catalan, J., Castiglia, R., Watson, J., Dobigny, G., ... & Britton-Davidian, J. (2010). A novel sex determination system in a close relative of the house mouse. *Proceedings of the Royal Society of London B: Biological Sciences*, 277(1684), 1049-1056.

Waterhouse, G. R. (1839). *The Zoology Of The Voyage Of HMS Beagle, Under The Command Of Captain Fitzroy, RN, During The Years 1832 To 1836: Mammalia*. *Smith, Elder & Company, London*.

Wessels, W. (2009). Miocene rodent evolution and migration Muroidea from Pakistan, Turkey and Northern Africa. *Geologica Ultraiectina*, 307, 1-290.

Weijs, W. A., & Dantuma, R. (1975). Electromyography and mechanics of mastication in the albino rat. *Journal of Morphology*, 146(1), 1-33.

Wood, A. E. (1965). Grades and clades among rodents. *Evolution*, 19(1), 115-130.

Woods, C. A. (1972). Comparative myology of jaw, hyoid, and pectoral appendicular regions of New and Old World hystricomorph rodents. *Bulletin of the AMNH*; v. 147, article 3.

Yang, N., MacArthur, D. G., Gulbin, J. P., Hahn, A. G., Beggs, A. H., Easteal, S., & North, K. (2003). ACTN3 genotype is associated with human elite athletic performance. *The American Journal of human genetics*, 73(3), 627-631.

Remerciements

Je remercie infiniment Julien et Lionel qui ont partagé avec moi leurs expériences, leurs conseils et qui m'ont surtout offert leur amitié. Merci de m'avoir permis de découvrir la recherche dans d'aussi bonnes conditions, avec de bonnes rigolades et en me laissant une indépendance plus qu'appréciable tout en maintenant le cap. Merci à Camille et Mélanie pour le super esprit d'équipe de Macroévolution et Développement, et bien sûr à Sylvie pour sa présence, son aide, sa gentillesse et sa bonne humeur inaltérables pendant ces trois ans, partager un bureau (ou une salle d'animalerie) ne sera plus jamais aussi facile, ni aussi agréable.

Merci encore à Julien de m'avoir initié au sein de l'univers qu'est la Thaïlande et de m'avoir fait rencontrer tous les gens adorables que l'on a pu côtoyer là-bas. Il me faut au passage remercier aussi Madame Songkran Claude et toute sa famille pour leur hospitalité absolument incroyable, et tous les moments que nous avons partagé malgré certaines limitations linguistiques. Merci aussi à tous les étudiants et enseignants-chercheurs de l'Université de Mahasarakham que j'ai eu le plaisir de rencontrer, ainsi qu'à Serge Morand, Anamika Karnchanabanthoeng et Noppawan Thaprathom pour toute leur précieuse aide pratique, pour le terrain, et pour les innombrables découvertes culinaires.

Toute ma gratitude va à l'ensemble des gens de l'ISEM qui font de ce laboratoire un lieu de rencontre, où il fait bon être thésard, et où la convivialité est fructueuse autant en science qu'en amitiés. Je remercie particulièrement toutes les personnes qui m'ont amené jusqu'à la thèse par leur aide, leurs contacts, et leurs enseignements, durant la licence et le master : en particulier Monique, PierrO, Rodolphe, Lionel, Laurent, et d'une manière plus générale tous les enseignants-chercheurs du master de paléontologie Poitiers / Montpellier. Ce fut également pour moi un plaisir et une réussite de pouvoir collaborer avec plusieurs personnes d'autres équipes : Fred (Veyrunes), Julie, Camille, Jacques, PH, entres autres ; cela m'a ouvert sur beaucoup d'horizons, et j'espère réciproquement. Un grand merci aussi à tous et toutes les thésard-e-s et post-doc de l'ISEM pour les nombreuses et mémorables "discussions scientifiques" apéritives et festives, durant lesquelles l'inspiration, l'intelligence et la finesse n'ont jamais manqué.

Je remercie également les personnes qui m'ont suivi durant ma thèse notamment au cours des comités (mais pas seulement), ainsi que les membres de mon jury, dont les conseils, les collaborations, et les critiques furent précieux : Anthony Herrel, Luis-Miguel Chevin, Sabrina Renaud, Christiane Denys, Leandro Monteiro, et Alexandra Houssaye.

Une salve spéciale de remerciements va à tous les copains/llègues, de plus ou moins longue date, et qui forment une constellation magnifique de gens brillants, beaux et drôles, dans le désordre : tous les Boyz (et affiliées), les Saint-Pierres, Lulu, Super Yoyo, Myriam, Marty, Alice, Chaton, Andréas, Anne, les Scalateux, les South Attack et leur monde, la Mourlam family, Quentin, Jules, Seb Camille, Alex, et aussi les Moreno-ettes, les Chanuels, les Moloz, les Ceveracs, Fredo, et compagnie…

Je voudrais dédier cette thèse à toute ma famille, et d'abord à mes parents et à mes grand-parents, qui m'ont toujours poussé sur la voie de la recherche, que j'ai choisie depuis tout petit, et qui m'ont permis d'arriver au bout de cette longue bambée (et au début de la suivante), avec leurs encouragements et leur curiosité. Durant ma thèse, ma famille s'est quelque peu élargie, et je dois donc remercier également Bernadette, Guy, Martin et les Rengard-Gourdin de m'avoir accepté en leur sein, de l'aide qu'ils m'ont donné dans l'organisation des grands évènements ayant marqué ces trois ans, et de l'intérêt qu'il portent à mon travail et à moi-même. Et je les remercie bien sûr d'avoir mis sur ma route Florette, dont la rencontre à tout changé pour moi, et qui a rempli ces trois années des moments les plus intenses et les plus beaux de ma vie. Enfin, je la dédie à Loulou et Élo, qui ont été des sources intarissables de bonheur et de fierté depuis qu'elles sont arrivées dans ma vie.

Summary: The theme of this thesis is the anatomy and morphology of the cranio-mandibular complex in various species of murine rodents. The main objectives are to describe the morpho-functional link between the skull and bite force as a measure of performance, to identify the genetic sources of morphological and performance variation, and finally to understand how morpho-functional variation depends on a species diet and lifestyle.

The first part describes the anatomy of the masticatory apparatus in the genus *Mus*. Differences were found, which could be interpreted functionally and linked to variation in diets. The first part also investigates the links between morpho-anatomy and function, and various morphological proxies used for estimating bite force. This is done by building a biomechanical model of masticatory muscles. The bite force estimates obtained match the *in vivo* measurements at the inter-specific level, but are less precise at the intra-specific level. Then, two osseous mandibular proxies of bite force are compared (lever arms and their mechanical advantage, and its shape data). *In vivo* and estimated bite force were well related at the inter-specific level, but less at the intra-specific level, depending on the species. To explain these imprecisions, the ontogenetic variation of bite force and mandibular morphology is described. Under controlled age, the bony development is slowing down earlier than bite force, which can partly explain the inconsistencies of estimated bite force.

The second part focuses on the genetics of morphological and functional variation. In *Mus minutoides*, changes in the sexual chromosomes entail size and performance changes. The feminized males found in this species are known to be more aggressive than other individuals, and they produce a higher bite force, mainly due to an increase in skull size. The feminizing gene(s) therefore drive whole-organism-scale changes. Then, the links between inbreeding, asymmetry and performance are investigated in the house mouse. The most inbred mice do not experience an increase in the asymmetry of their mandibles. Contrary to expectations, the performance of the most inbred or most asymmetric mice do not decrease and differences in asymmetry levels have no influence on biting performance. The last section estimates the heritabilities of bite force and morphology. *In vivo* bite force is not heritable, but some morphological characters are. Given the functional link between morpho-anatomy and bite force shown in the first part, these results suggest that morphological changes represent evolutionary pathways of least resistance, and drive changes in performance rather than behavioral or related traits.

The last part took morphology and performance as linked to a species' niche. The first section explores the differences between *Apodemus sylvaticus* and *Mus spretus*. Both share their habitat and food resources, in spite of a marked size difference. Results show great overlap between their bite force distributions supporting the hypothesis of a shared diet. The absence of shift in a trait related to resource use may be due to a large abundance of the food resources where both species are found in syntopy. In the final section the morphological variation in several rodents from Southeast Asia was quantified. Less morphological variability is found in generalist and commensal rats by comparison to other species. At the community level, synanthropic species show frequent convergent responses between localities in terms of bite force and morphology. These common patterns in response suggest that synanthropic species tend to be very adaptable to regional environmental differences.

The approaches used in this thesis enable us to show the link between genetic, phenotypic and ecological variation. This link, sometimes difficult to describe, is nevertheless at the root of the appearance of new forms and species, and constitutes a crucial aspect of evolutionary biology.

Résumé: Cette thèse porte sur l'anatomie et la morphologie du complexe crânien chez les murinés. Ses objectifs sont de démontrer et de décrire le lien morpho-fonctionnel entre le crâne et la force de morsure, représentant la performance, d'identifier les sources génétiques de la variation de la performance et de la morphologie, et de comprendre comment la variation morpho-fonctionnelle dépend du mode de vie d'une espèce.

La première partie décrit l'anatomie de l'appreil masticateur dans le genre *Mus*. Des différences fonctionnelles et liées au régime alimentaire sont montrées. Puis, on s'intéresse au lien entre morphologie et fonction, et aux proxies morpho-anatomiques permettant d'estimer la force de morsure. Un modèle biomécanique des muscles masticateurs est d'abord utilisé. Les estimations obtenues sont proches des mesures *in vivo* au niveau interspécifique, mais moins précises au niveau intraspécifique. L'avantage mécanique et la forme de la mandibule sont ensuite utilisés comme proxies. La force de morsure estimée et réelle sont corrélées au niveau interspécifique, mais moins au niveau intraspécifique, avec des différences selon les espèces. Pour expliquer ces imprécisions, la variation ontogénétique de la force de morsure et de la forme de la mandibule sont décrites. Lorsque l'âge est contrôlé, le développement osseux ralentit plus tôt que celui de la force de morsure, ce qui peut expliquer les biais trouvés dans les estimations de la force de morsure.

La deuxième partie se concentre sur les sources génétiques des variations morpho-fonctionnelles. Chez *Mus minutoides*, des changements sur les chromosomes sexuels produisent des différences de taille et de force de morsure. Les mâles féminisés de cette espèces sont plus agressifs que les autres individus, et montrent une force de morsure plus puissante, principalement grâce à un plus gros crâne. Le(s) gène(s) féminisant produis(ent) donc des changements à l'échelle de l'organisme tout entier. La section suivante s'intéresse aux liens entre consanguinité, asymétrie et performance chez la souris domestique. Les souris les plus consanguines ne montrent pas d'augmentation de l'asymétrie de leurs mandibules, et la performance des souris les plus consanguines ou les plus asymétriques n'est pas affectée. Enfin, l'héritabilité de la force de morsure et de la morphologie est estimée. La force de morsure *in vivo* n'est pas héritable, bien que la morphologie le soit. Etant donné le lien entre morpho-anatomie et force de morsure, ces résultats suggèrent que les changements morphologiques sont des voies de moindre résistance évolutive, et qu'ils peuvent être à l'origine de changements de performance.

La dernière partie utilise la morphologie et la performance en tant que caractères liés à l'écologie des espèces. La première section s'intéresse aux différences de performance entre *Apodemus sylvaticus* et *Mus spretus*, qui partagent leur habitat et leurs ressources alimentaires, malgré une différence de taille marquée. Nos résultats montrent un recouvrement des distributions des forces de morsures, soutenant l'hypothèse d'un régime alimentaire commun. Cette coexistence pourrait être due à une abondance de ressources là où ces espèces sont syntopiques. Enfin, la variation morphologique est quantifiée chez plusieurs murinés d'Asie du Sud-Est. Les espèces de rats commensaux et généralistes sont moins variables que les autres espèces. Les espèces synanthropiques montrent des réponses morpho-fonctionnelles convergentes entre localités qui suggèrent qu'elles partagent des patrons communs de réponse et donc qu’elles peuvent s'adapter aux variations environnementales régionales induites par l’homme.

L'approche utilisée dans cette thèse nous a permis de montrer le lien entre variation génétique, phénotypique et écologique. Ce lien parfois difficile à décrire, est cependant à la base de l'apparition de nouvelles formes et espèces, et constitue un aspect crucial de la biologie de l'évolution.